Title

Incorporation of a Photo-Crosslinking Unnatural Amino Acid for In Vivo Capture and Identification of 26S Proteasome Substrates

Author

Yori Restrepo, Santiago

Publication Date

2024

Peer reviewed|Thesis/dissertation

Incorporation of a Photo-Crosslinking Unnatural Amino Acid for In Vivo Capture and Identification of 26S Proteasome Substrates

By

Santiago Yori Restrepo

A dissertation submitted in partial satisfaction of the

requirements for the degree of

Doctor of Philosophy

in

Molecular and Cell Biology

in the

Graduate Division

of the

University of California, Berkeley

Committee in charge:

Professor Andreas Martin, Chair
Professor Nicholas Ingolia
Professor James Olzmann
Professor Michael Rapé

Fall 2024

Abstract

Incorporation of a Photo-Crosslinking Unnatural Amino Acid for *In Vivo* Capture and Identification of 26S Proteasome Substrates

by

Santiago Yori Restrepo

Doctor of Philosophy in Molecular and Cell Biology

University of California, Berkeley

Professor Andreas Martin, Chair

Degradation of proteins is an essential biological process. As is the case for protein synthesis, degradation equally represents an intricate and tightly regulated process which is coordinated by a large macromolecular assembly. Compartmentalized proteases have been an evolutionary solution to the need of the cell to selectively remove proteins and are seen in all membrane-bound organisms, from the ClpXP complex in bacteria to the 26S proteasome in eukaryotes. An astounding 80% of all proteins are believed to be shipped into this degradation machine. In eukaryotes, this fate is largely determined by a protein's post or co-translational modification with the small signaling protein ubiquitin by a network of ubiquitin ligases. Together, protease and signal form the cell's ubiquitin-proteasome system (UPS). Protein clearance can be as specific as the removal of a single copy protein in a sea of thousands or as broad as remodeling the entire proteome. The UPS has critical roles in every aspect of cell biology from the regulation of gene transcription to quality control of translation, and protein import across membranes. Despite this, methods to profile the pool of substrates of the proteasome have not developed as robustly as methods to profile the entire pool of translated mRNAs as has been done with the proteasome's counterpart, the ribosome.

The second chapter of this thesis describes the theory and application of genetic code expansion for the introduction of chemical tools to trap substrates in the act of translocation into the proteasome. Taking a structure-guided approach in addition to leveraging a suite of chemical biology tools available, I describe the construction of a system for the incorporation of a light-activated crosslinking

unnatural amino acid (UAA) into recombinantly expressed proteasomes. Systematic testing of UAA-containing variants allowed me to find a position within the substrate pore of the AAA+ motor of the proteasome base subcomplex that resulted in proteasomes which were capable of still engaging and degrading a substrate. Using crosslinking assays, I could show that these proteasomes are crosslinking competent in a UV-dependent manner and that they cross-link specifically to substrates with a *bona fide* initiation region. Using this biochemical information, a system for the incorporation of UAA in live cells was developed and shown to also result in proteasome crosslinking to substrate.

Having set up systems for recombinant and live-cell crosslinking and found a permissible crosslinking position on the proteasome motor, In the third chapter of this work, I focus on then optimizing a workflow for the purification of proteasome-substrate crosslinks and their preparation and identification through mass spectrometry (MS). By using a denaturing IMAC approach, I was able to purify proteasome-substrate crosslinks that I could then analyze using mass spectrometry. My results identified over 900 putative proteasome substrates whose roles in the cell are predictably varied. I show that in log-phase growth cells the proteasome is turning over a large pool of cytosolic enzymes as its primary substrates. Amongst these protein substrates are a large pool of metabolic enzymes, translation associated proteins, either subunits or assembly factors of the ribosome, and stress granule components. Taken together this work demonstrates the power of the use of genetic code expansion as a tool for probing complex biological systems. It also represents the first use of a crosslinker to trap substrates to an actively translocating molecular motor.

Table of Contents

Acknowledgements

I do not know what a normal PhD is supposed to be like, but what I am sure is that this one has been eventful. I moved to California in 2017 not knowing what to expect and I don't think that I could ever have anticipated the wild ride that this ended up being. It has been, at times, euphoric. The thrill of meeting new people and learning new things. Celebrating achievements, like passing a qualifying exam or getting a fellowship. In other times, between a hostile political climate and constantly being worried about being deported, wildfires turning the sky orange, a global pandemic and more, it has represented some of the lowest lows I have ever experienced. In either case, I do not think I could have done this without having a community to celebrate with me, laugh with me, cry with me, and ultimately support me in such a way that I was able to see this journey out to the end.

The first step in graduate school was joining a lab and I could not have asked for better lab mates and so I want to acknowledge the Martinians. Erika, I want to thank you for always listening, for helping me rediscover what it means to be Latin-American, for introducing me to new artists, and for always inspiring me to be a better scientist and human. Te quiero mucho, mi cabrona. Ken, I want to thank you for being an invaluable friend. Having you sitting next to me has been the absolute privilege of being in the lab. I have grown and learned so much from you during this time, both in science and in life. Zaw, you are the wisest and most kind person I know. I will always try to emulate you as much as possible when moving forward in any job. You are quick to put down what you're doing to help people, you're as bright and sharp as you are kind and hilarious. I am so thankful to have you in my life. Diego, you are more than just a lab friend, more than un hermano—you are un broder. I admire your kindness and patience, your diligence towards science and your diligence towards doing the right thing. I have no doubt in my mind that you will be successful moving forward. To Miri, I want to thank you for allowing me to mentor you, it was a privilege. You make me so proud, and I am always so happy to see you grow as a scientist, and I am so happy to call you a friend. Of course, I want to thank my thesis advisor Andy for believing in me and allowing me to be creative in my pursuit of science. Thank you for advocating for me when it was necessary and for your patience throughout these years. I would also like to thank the rest of my thesis committee, Nick, Micha, and James for their thoughtful feedback and encouragement during our meetings.

During this time in graduate school, and in this foreign land called California, I have been blessed with an incredible chosen family. To Fernando & Jess, thank you for always making me feel welcome and loved. Thanks for thinking of me when pho is

involved and for coming to cheer me on while doing stupid things like running half marathons. I love spending time with the two of you—watching you both grow in your love for each other (and Oakland), and your shared life has been a privilege. To God's Perfect Scientist™, Jesse thank you for always being a source of strength. I am always in awe of the finesse with which you achieve things; the way you command a room, whether it's a symposium or a party. I will never forget you being there for me when I needed it the most. To Angel, it's crazy to think about the random course of events that led to us becoming friends and collaborators. I admire you so much and whenever we work together, I feel that anything is possible, even running a lab, which is saying a lot (for me). Thanks for always pushing me to be a better version of myself.

I want to also acknowledge friends from across the country who changed my life before I ever set foot in graduate school. To Matias, Maria, and Robin, thank you for being the best friends I could have ever asked for in Florida. I could write an entire thesis of what I have learned from you and your family. To Alberto, thank you for being an incredible role model. I think about you often, all those times in North Captiva chatting and all the adventures on the water. I think about all the life lessons you taught me. Thank you for giving me a chance and welcoming me into your family, you changed my life, and I miss you.

My Boston family also deserves a shout-out. Lindsey, thank you for being one of the best friends I could ask for. You amaze me each time we talk! I admire you so much for all the work that you do and the intensity with which you love science and mentorship. I watch all your academic and scientific adventures and am constantly in awe. I am so glad that we have remained friends throughout the years. Quique, thank you for always grounding me. You are truly my closest friend, and I am thankful for your friendship, for always listening, and for our ongoing traditions that make me feel like more than friends, but family. Cathy, thank you for being a tireless supporter and for always believing in me. Thank you for pushing me to challenge myself, for thinking of me and checking in with me, and for hyping me up. I am so excited to be able to do science with you in the future.

To my Florida family, Robert, Drew, Carley, Jessica & Paul, Sameer & Bonnie: Living in Florida was difficult, but I loved being with all of you. When it came time to leave you all made it so hard. Despite everything, it was home because of you all and I am so thankful we remain friends.

To my undergraduate mentor, Sharon, you were my first scientific role model, and I am so thankful it was you. If I am a tree, it is because you planted a seed. I can't

say that I admire you as a scientist because that would be selling it so short. I admire the way you approach life as a series of challenges and adventures. You are continually evolving, from chemical engineer, to virologist, to martial artist, to marathon runner, to graphic designer, to actress—how do you do it?! I could not be here if it wasn't for both your inspiration and your help. Thank you for everything.

To my mama, Rocio. Te quiero mucho, mami. Gracias por siempre dejarme correr detrás mis sueños. Desde el momento que me compraste los videos de National Geographic siempre he tenido la curiosidad de nuestro mundo. Por toda mi vida me has empujado a trabajar duro y siempre meterle las ganas a todos mis proyectos. Esta tesis es la culminación de esa curiosidad que cultivaste en mi, estoy muy agradecido que eres mi mama. Sé que a veces ha sido difícil, pero quiero que sepas que te quiero mucho y aprecio todo lo que has hecho por Cami y yo. Siempre has sido mi heroína, la mujer más fuerte que conozco—la tremenda original. To Cami, I know we don't always see eye-to-eye, but I want you to know that your tenacity and strength inspires me. I have always and I continue to admire you. I hope, as we enter these new stages of our lives, that the three of us can spend more time and grow as a family and as friends. To my late abuelita Chechi. I wish you could have been here to see me walk the stage as a PhD. Sometime ago, I was contemplating why I became so interested in science, and as silly as it sounds, I kept thinking back to the person who took me to see all the sci fi movies when I was younger. Jurassic Park, the Matrix, you name it. Often, I find myself thinking about myself at home playing video games with you knitting, watching, and asking questions fully plugged into a game you weren't playing. You were the original nerd, I miss you every day, and so I would like to dedicate my nerdiest undertaking to you.

Finally, I would like to acknowledge undocumented people in the United States and abroad. I hate that man-made borders, arbitrary laws, and the racism that underlies immigration policies continue to attempt to deny us the opportunities we dream of. I have been so fortunate to meet and learn from other members of this incredible community both at Berkeley and at other institutions. I've tried to give back as best as I can, and I promise I will continue to use whatever leverage I have to uplift our community. I hope we continue to persist, ignoring those who insist on telling us we can't do things. I also hope that we eventually understand, as I continually struggle to, that our existence *anywhere* is valid and does not need to be justified by our productivity, our papers, our skin color, or our nationality.

Sí, se puede.

Chapter 1

The Ubiquitin-Proteasome System

1.A. Introduction to protein degradation and the Ubiquitin-Proteasome System

It is truly humbling to think about the decades of research required to decipher their interactions between these chemical building blocks that make life much more than the sum of its parts. The physico-chemical properties of the four major groups of macromolecules and their building blocks (polysaccharides and sugars, lipids and fatty acids, proteins and amino acids, nucleic acids and nucleotides) had been known for decades prior to the condensation of physics, chemistry, and biology into what we now call molecular and cell biology.

The enzyme diastase was the first to be characterized in 1833 cementing the importance of proteins as critical catalytic biomolecules for not only the structure but also the function of life. However, up until the 1930s, it was believed that metabolism was comparable to a combustion engine (Ciechanover, 2005). Some macromolecules constituted a rigid, unchanging body through which other macromolecules would pass as fuel to be spent and expelled. This was the prevailing paradigm until the advent of stable isotopes allowed researchers to track biomolecules with isotopically labeled building blocks. The work of Rudolph Schoenheimer and colleagues demonstrated that rats fed with ^{15}N-labeled tyrosine only excreted approximately half of the input isotope (Schoenheimer et al., 1939; Reviewed in Simoni et al., 2002). This led to the discovery that, unlike an engine burning gasoline, there is a chemical interchange between the structural components of an organism and its ingested fuel. More specifically, it suggested that cellular proteins experienced turnover by a yet-undiscovered regulated mechanism and that this mechanism must be tightly controlled, so as not to degrade the proteins the cell needs.

The first of these mechanisms was discovered in the 1950s by Christian de Duve, with the discovery of the lysosome, an acidic, membrane-bound cellular compartment containing hydrolytic enzymes whose activities are optimal at low pH (de Duve & Wattiaux, 1966). The membrane-enclosed architecture of lysosomal degradation fulfilled the hypothetical requirement that a protein turnover mechanism must be kept separate from the general proteome to prevent uncontrolled degradation. However, while the discovery of the lysosome definitively ended debate on the theory of the dynamic nature of proteins in the cell, it could not explain all the observations associated with protein turnover. Perhaps the biggest of these discrepancies were that the mechanism of lysosomal protein turnover could not account for the wide range of measured half-lives of different proteins (Reviewed in Ciechanover, 2005) and that

general inhibition of the lysosome resulted in only partially lowering protein degradation (Poole, 1978). Additionally, there was no lysosome in prokaryotic cells which still displayed evidence of regulated protein degradation, suggesting that a second mechanism of protein turnover had to exist (Mandelstam, 1958).

The discovery of the second mechanism for protein degradation was discovered when Aaron Ciechanover, Yaacov Hod, and Avram Hershko carried out fractionation of reticulocyte lysate via diethylaminoethyl cellulose (DEAE-C) anion exchange chromatography, which separated the lystate into two fractions (Ciechanover et al., 1978). The flow-through from the resin, Fraction I, contained no degradation activity. A high-salt elution from the column, Fraction II, had mild proteolytic activity which was slightly stimulated in the presence of ATP. However, when the two fractions were combined, ATP-dependent stimulation of degradation was seen. This proteolysis-stimulating activity in Fraction I was purified and shown to be a small (~8.5 kDa), heat-stable protein, which they dubbed the ATP-dependent proteolysis factor 1 (APF-1). With the confirmation that protein degradation was carried out by a multi-component protease system, they showed that the addition of APF-1 to substrates was ATP-dependent, reversible, and, with Irwin Rose, they showed that multiple copies of APF-1 could be appended to substrates prior to degradation (Ciechanover et al., 1980; Hershko et al., 1980).

The identity of the cause of specific degradation arrived later in 1985 with the fractionation and discovery of a large, ATP-dependent protease which could degrade ubiquitin-lysozyme (Hough et al., 1985). Originally called the multicatalytic protease (MCP), Hoffman and colleagues using native gel electrophoresis and biochemistry were the first to clearly delineate the two forms of the MCP, the fast-migrating and slower-migrating 20S and 26S proteases. Since these early studies our understanding of the molecular details of APF-1 and the MCP has exploded. Of course, we now understand APF-1 to be the protein ubiquitin, which can be post-translationally appended to proteins via an extensive enzymatic network of ligases and whose addition then marks a protein as a substrate for degradation by the 26S proteasome. Together, APF-1 and the MCP, form the cellular ubiquitin-proteasome system and represent one of the most intricate and crucial functions of the cell: the programmed removal of nearly all cellular proteins.

1.B. Structure and function of the 26S proteasome

1.B.i. Structure of the 26S proteasome

The proteasome's structural components reflect its task as a cellular machine to recognize and selectively degrade protein substrates. Degradation takes place in a compartmentalized protease, the 20S core peptidase (CP). Structural work has shown that the 20S chamber is composed of 14 distinct proteins, α1-7 and β1-7 (Löwe et al., 1995; Groll et al., 1997; Unno et al., 2002) (**Figure 1.1D**). The α subunits form a heptamer ring which rests atop a β heptamer ring. The complete 20S CP is assembled from two αβ rings in an $\alpha_7\beta_7\beta_7\alpha_7$ layout, highlighting the role of the α rings as axial gatekeepers into the chamber formed by the β subunits. β1, 2, and 5 contain proteolytic active sites with trypsin, chymotrypsin, and caspase-like activities, respectively, which give the 20S chamber a dual set of three proteolytic sites with broad degradation capabilities. While some evidence suggests that unstructured polypeptides may be able to diffuse into the 20S unaided (Sahu et al., 2021), the regulation of protein degradation is carried out by regulatory caps which bind to one or both sides of the 20S— of these, the most prominent is the 19S regulatory particle (RP). The 19S regulatory particle is the best-characterized proteasome cap; it contains the energy-dependent and recognition elements of proteasomal degradation. This complex can be biochemically divided into two subcomplexes, the base and the lid (**Figure 1.1A**).

The base subcomplex is composed of 9 protein subunits. Six of these, Rpt1-6, form a hexameric motor of the AAA+ (ATPases Associated with cellular Activities) family (Beckwith et al., 2013) (**Figure 1.1B**). This unfoldase uses the energy of ATP hydrolysis to undergo conformational changes and generate the mechanical force required to unfold protein substrates and translocate the polypeptide into the 20S. Each Rpt subunit contains an inward-facing pore-loop segment containing a conserved tyrosine residue, which makes physical contact with the substrate to grip and unfold it (de la Peña et al., 2018) (**Figure 1.3B**). The functional link between the base unfoldase and the 20S degradation is also beautifully emphasized by structural and biochemical data showing 20S α gate opening in response to binding of the C-termini of Rpt2, 3, and 5 to pockets on the α ring (**Figure 1.1E**). Two of the remaining base proteins, Rpn1 and Rpn13, act as receptors for the ubiquitin degradation signal (Shi et al., 2016; Husnjak et al., 2008). The remaining subunit, Rpn2, forms a scaffold mediating the binding of Rpn13 to the rest of the base.

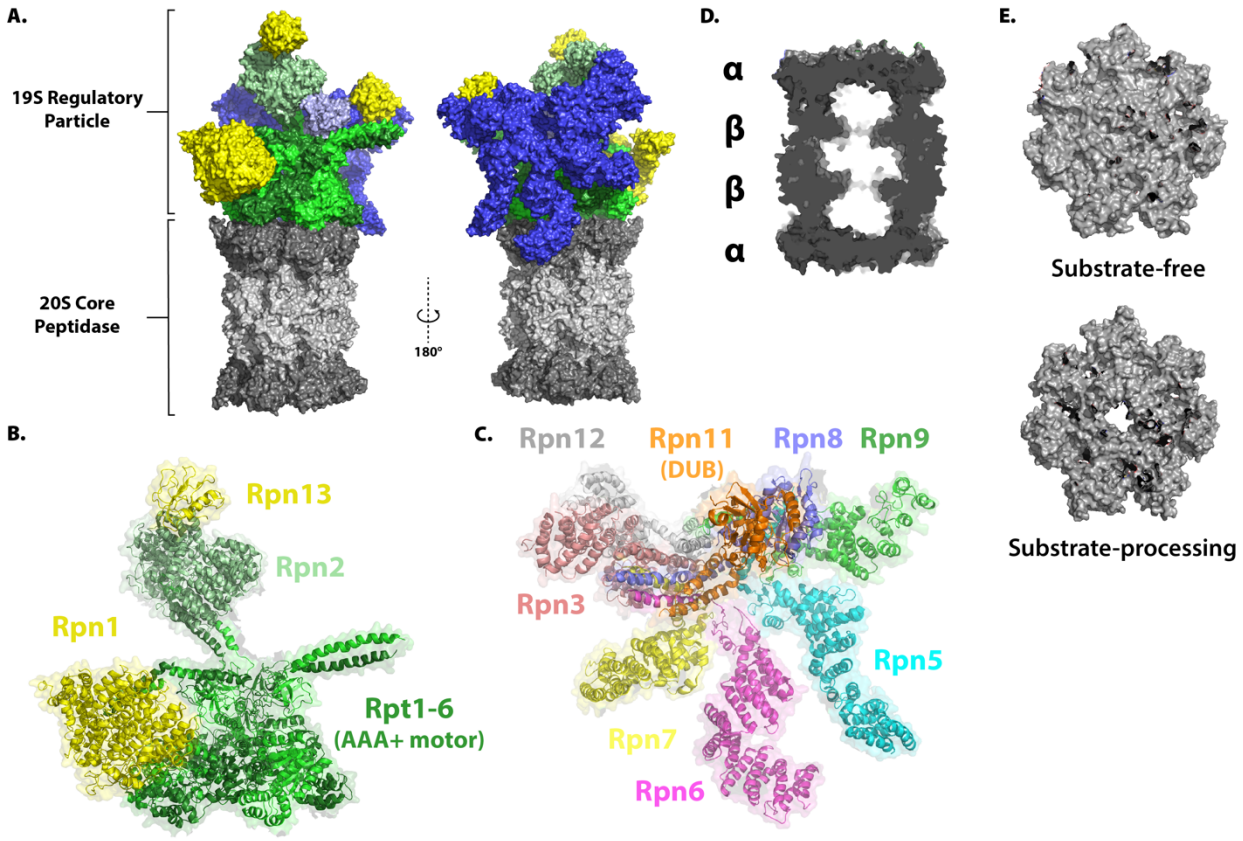

Figure 1.1: Structure of the 26S proteasome and its subcomplexes.

A. Structure of the 26S proteasome (Luan et al., 2016; **PDB**: 3JCP). The proteasome can be biochemically and functionally divided into the 20S core peptidase and the 19S regulatory particle which can cap one or both ends of the 20S CP. **B.** The base subcomplex of the 19S RP contains two of the three ubiquitin receptors (yellow) and the AAA+ motor complex (green). An additional ubiquitin receptor, Rpn10, binds between the lid and base but is not biochemically grouped into either subcomplex. **C.** The lid subcomplex of the 19S lays to the side of the base, mediates many conformational changes and contains the essential deubiquitinase, Rpn11 (orange). **D.** A cross-section through the 20S core peptidase displays the αββα ring layout and the proteolytic chamber enclosed within. **E.** Entry into the proteolytic chamber is gated by the α rings which open in response to 19S substrate engagement (de la Peña et al., 2019; **PDB**: 6EF3).

The lid is also composed of 9 proteins. The main scaffold of the lid is formed by Rpn3, 5, 6, 7, 8, 9, 11, 12, and Sem1, which come together to form a horseshoe-shaped PCI (proteasome-CSM-initiation factor 3) structure (Lander et al., 2012) (**Figure 1.1C**). Embedded within this scaffold is the essential deubiquitinase (DUB), Rpn11. A member of the Zn^{2+}-dependent JAMM/MPN metallo-isopeptidase family, Rpn11 is responsible for the liberating and recycling of ubiquitin from substrates back into the cytosolic ubiquitin pool (Verma et al., 2002; Yao & Cohen, 2002). Upon assembly, the lid docks adjacent to the base and positions the active site of Rpn11 near the unfoldase pore (**Figure 1.3C**). A third ubiquitin receptor, Rpn10, binds between the lid and base within this context as well. Together as the 19S RP, these subcomplexes can cap one or both ends of the 20S to form the 26S or 30S holoenzyme, respectively.

1.B.ii. Substrate degradation by the 26S proteasome

It is estimated that the cellular protein concentration ranges from 20-30% and that an estimated 80% of eukaryotic proteins meet their end via the proteasome. This highlights an incredible feature of the proteasome— its activity must be both selective and general. This is to say, the proteasome must be capable of degrading the bulk of the cellular proteome while also being able to single out proteins with single digit copy numbers out of millions of candidates (Beck et al., 2011). As part of this balance of selectivity versus generality, the prerequisites for degradation are that substrates are recruited to the proteasome and contain a suitable engagement region (Inobe et al., 2011).

Work in the Martin lab has delineated the pathway from substrate to degradation once a substrate finds itself at the 26S (Bard et al., 2019) (**Figure 1.2**). This pathway can be broken down into 5 steps: 1). substrate recruitment, 2). insertion of the engagement region, 3). engagement by the proteasomal motor, 4). translocation dependent deubiquitination of the substrate, and 5). unfolding and degradation by the 20S.

In the cell, substrates are recruited to the proteasome via binding of ubiquitin to one or possibly more than one of the ubiquitin receptors located on the 19S RP. It has been suggested that the proteasome has an inherent preference for certain types of ubiquitin chains with K48 and K11 chains being the preferred signal for proteasomal degradation (Komander & Rape, 2012) (**Figure 1.4A**). However, it has been shown that the proteasome is somewhat agnostic as to how a substrate is recruited. Our lab demonstrated that the proteasome is perfectly capable of degrading substrates with a

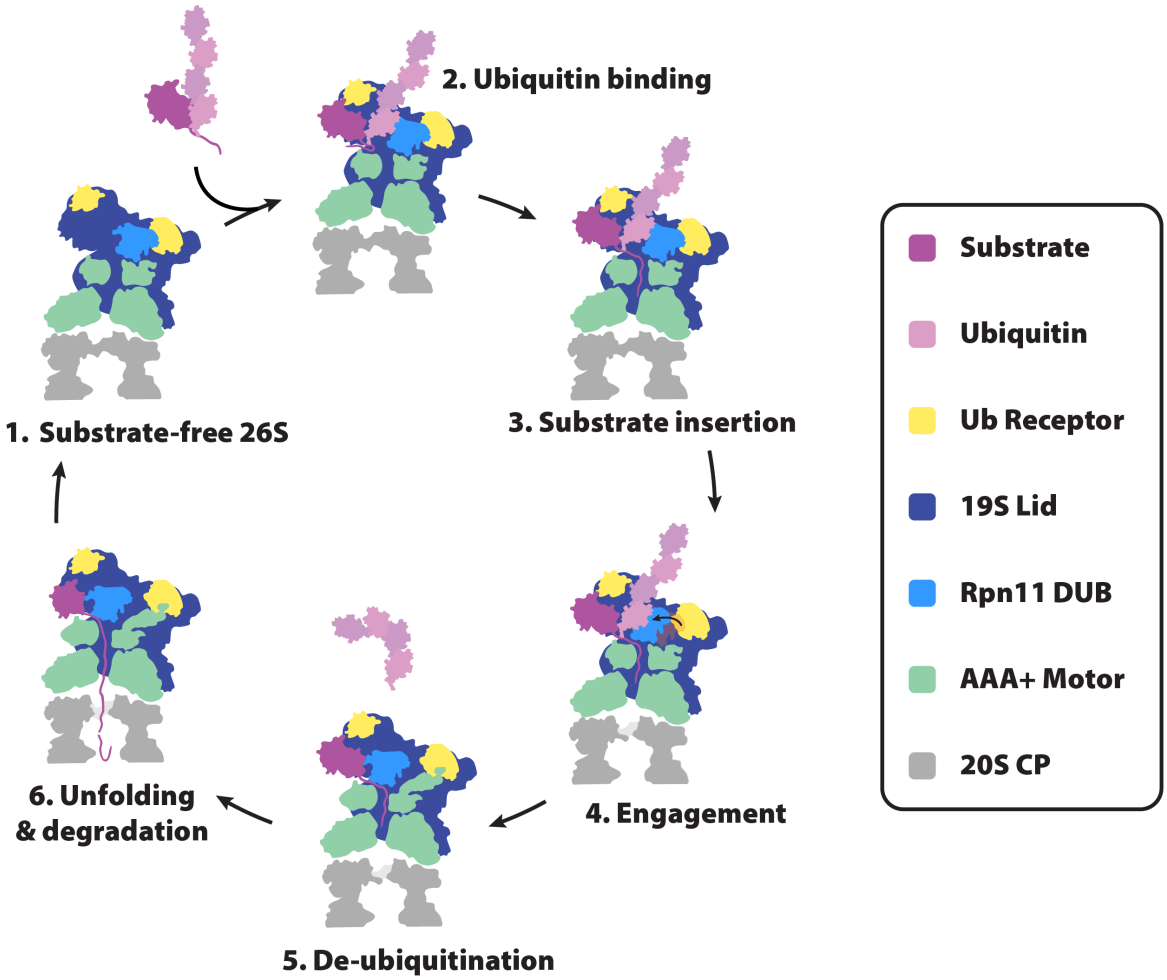

Figure 1.2: Steps in 26S Proteasome Degradation.

1. The 26S proteasome first exists in a substrate-free state in which the entrance into the pore of the proteasome is unobstructed but the axial pores are misaligned. **2.** Substrates are recruited to the 19S RP via binding to one of three ubiquitin receptors. **3.** The substrate must contain a flexible initiation region that can diffuse into the pore of the proteasomal motor. **4.** The motor engages the initiation region which induces a conformational change into the substrate-bound state and the ATP-fueled unfolding of the substrate. **5.** Substrate translocation pulls the ubiquitin-substrate isopeptide bond into the active site of Rpn11 for de-ubiquitination. **6.** The substrate is unfolded and threaded into the 20S core peptidase for degradation.

K63 linkage and, even more interestingly, that it is possible to recruit a substrate to the proteasome in a ubiquitin-independent manner (Bashore et al., 2015). By fusing the bacterial protein $SspB_2$ to the base subunit Rpt2, substrates containing the 11 amino acid ssrA tag are artificially delivered to the proteasome and degraded. The SspB/ssrA binding interaction normally recruits proteins to the AAA+ unfoldase of the bacterial compartmentalized protease ClpXP. In agreement with *in vitro* reconstituted ubiquitin-independent degradation, several proteins have been found to meet their end by the proteasome in a ubiquitin-independent manner in the cell.

Three prominent examples of this are the degradation of the enzyme ornithine decarboxylase (ODC), the turnover of proteins—primarily certain transcription factors—by the Midnolin-proteasome pathway, and the degradation of FAT10 and FAT10 conjugates via its interactions with Nub1 and the proteasome. In all cases, a protein adaptor that binds the substrate and the proteasome presents an engagement region to the 19S base to begin unfolding. In the case of Midnolin, substrate disordered regions which form a β-strand are thus “caught” by Midnolin’s Catch domains (Gu et al., 2023). Midnolin contains a Ubl domain that then binds the proteasome and delivers the substrates to the proteasome. FAT10 is an 18 kDa ubiquitin-like protein with two Ubl domains which, similar to ubiquitin, can be added via its C-terminus as a modification on proteins. Unlike Midnolin or ubiquitin-dependent degradation, FAT10 is itself targeted for degradation along with the substrate. Work in our lab has now shown that FAT10 itself acts as an initiation region for the proteasome via its interactions with Nub1, while Nub1 binding the 19S receptor Rpn1 mediates delivery to the proteasome (Arkinson et al., 2024). The degradation of ODC by the proteasome is the first demonstrated case of ubiquitin-independent degradation (Murakami et al., 1992). In this work, it was shown that ODC is degraded in a 26S, but not ubiquitin, dependent manner and is dependent on the action of the ODC antizyme OAZ1 and the exposure of the N-terminus of ODC (Gödders et al., 2011). While the exact molecular detail of this interaction remains to be described, the dependence of the degradation on OAZ1 suggests a similar mechanism to Midnolin and Nub1’s generation of an engagement region and delivery to the proteasome.

Cryogenic electron microscopy (Cryo-EM) work carried out by several groups has shown us that the proteasome exists in a continuum of conformational states, for the sake of simplicity these can be simplified into engagement-competent and post-engagement states (Matyskela et al., 2013; Wehmer et al., 2016). An engagement-competent state, as the name suggests, presents the optimal configuration for a substrate to engage with the proteasome. In this state, entry into the substrate channel of the 19S base is unrestricted. However, the 19S and 20S channels are unaligned, the

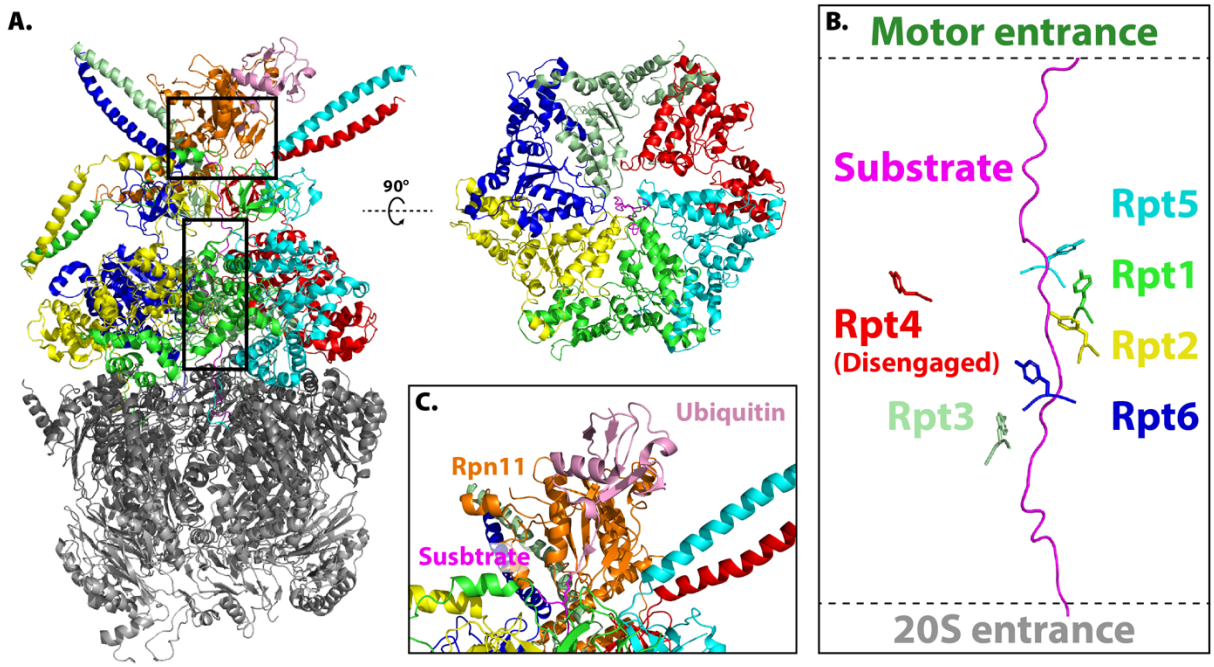

Figure 1.3: Structure of a Substrate-Bound 26S Proteasome.

A. Right, cryo-EM structure (de la Peña et al., 2018, **PDB**: 6EF3.) of 26S stalled on a model substrate. Left, top-down view of the ATPase domains of the motor. **B.** Pore loop tyrosine residues take on a characteristic “spiral staircase” arrangement to make physical contact with the substrate polypeptide during translocation. **C.** Active site of the essential DUB Rpn11 showing the substrate-ubiquitin isopeptide bond.

gate to the 20S is closed, and the base ATPase subunits arrange themselves in a defined order. Recruitment of the substrate serves to place the engagement region of the substrate into proximity to the accessible pore of the base unfoldase in an engagement-competent 26S proteasome. Once a substrate's disordered engagement region enters the pore of the proteasome, the proteasome undergoes a global conformational change into the post-engagement conformation in which the base AAA+ motor engages the substrate. This conformational change results in the rotation of the 19S to position the Rpn11 DUB active site into position over the pore of the motor. In this post-engagement state, the base motor then undergoes an ATP hydrolysis cycle that results in a hand-over-hand motion to unfold and translocate the substrate through its central pore. As the substrate is translocated, the isopeptide bond of the ubiquitinated substrate is pulled into the active site of the Rpn11 deubiquitinase, which removes the ubiquitin from the substrate (Worden et al., 2017). Ubiquitin removal is an essential step, it not only allows the ubiquitin chain to be recycled, but proteasomes with catalytically-dead Rpn11 mutations ($Rpn11^{AXA}$) will stall on substrate ubiquitin chains, preventing degradation. It was this stalling phenomenon that allowed our lab to capture a substrate bound proteasome structure using cryo-EM (de la Peña et al., 2018) (**Figure 1.3C**). In this post-engagement state the axial pore formed by the seven α subunits of the 20S is also opened to allow the substrate to enter the chamber formed by the β subunits.

1.C. The cell biology of the 26S proteasome

From a cellular logic point of view, the function of the proteasome is to end the functional cycle of other proteins. As a protein complex, it can be functionally simplified into “protease + unfoldase + receptor”. Since the ubiquitin receptors of the proteasome do not appear to display any strong preference for ubiquitin chains, the standalone 26S complex can be abstracted to being indifferent to substrates it encounters provided that those substrates have the correct signal for recruitment and engagement as previously described above. What I mean is that there is little distinction between a substrate that has been signaled for degradation after days of being in the cell and a protein which has misfolded as it exits the ribosome— both present the same features to the proteasome, a ubiquitin (or some other ub-independent) signal and an initiation region. The regulation and selectivity of the degradation is carried out by different layers of “filters” that screen proteins prior to them meeting their end at the pore-loops of the proteasome.

The first of these filters is the post-translational modification of potential substrates with ubiquitin or ubiquitin-like proteins, such as SUMO or FAT10, by a complex network of ligases which read and write functions onto protein substrates (Komander & Rape, 2012; Dikic & Schulman, 2022). Generally, these ligases all follow a similar architecture: 1). The first step is an energy-dependent process and primes the modifier protein (ubiquitin, SUMO, etc.) for conjugation, 2). The second step temporarily accepts the high-energy modifier protein 3). The third step recognizes both the substrate protein and the product of the second step and mediates the transfer to the substrate. I refer to these as steps and not enzymes because, especially in the case of step three, these steps can involve multiple proteins. Some have catalytic functions and some which serve as interchangeable adaptors that can be dependent on cell state, subcellular localization, or even on the type of tissue in which degradation is needed. In the classical example of this cascade, adenylation at the C-terminus glycine residue of ubiquitin is first catalyzed by the E1 ubiquitin-activating enzyme, UBA1 in both budding yeast and humans. The ubiquitin-adenylate first reacts via a transthiolation reaction with a cysteine residue on the E1. The E1 then binds a ubiquitin conjugating enzyme, E2, and positions the ubiquitin thioester within reach of an active site cysteine to mediate the formation of a ubiquitin-E2 thioester (Kochańczyk et al., 2024). The ubiquitin-E2 and substrate are recognized by a ubiquitin ligase, E3, which then catalyzes a transfer of ubiquitin onto a substrate lysine residue via the formation of an isopeptide bond (**Figure 1.4B**). As mentioned above, this third step in the pathway can occur in three different ways depending on the family of E3 ligase. In the

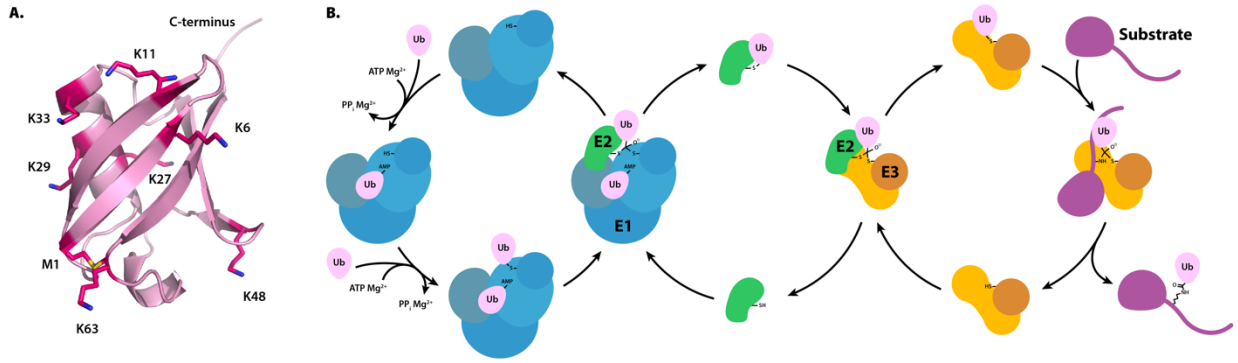

Figure 1.4: Ubiquitin is a Protein Post-Translational Modification Signal for Degradation.

A. Structure of ubiquitin (**PDB**: 1UBQ) highlighting the 8 possible conjugation sites for different chain varieties. **B.** Ubiquitin activation and transfer, as shown by Kochańczyk and colleagues, is first carried out by the ubiquitin-activating enzyme, E1, which first adenylates ubiquitin and then mediates transfer to the ubiquitin-conjugating enzyme, E2 . The E3 enzyme binds the ubiquitin-charged E2 enzyme and is then either ubiquitinated and then directly transfers the ubiquitin to the substrate or positions the substrate from direct transfer from the E2 (not shown).

HECT family of E3 ligases, the transfer of ubiquitin occurs first from the E2 to the E3, and then the E3 will transfer the ubiquitin to the substrate. In the case of the RING family of E3 ligases, the E3 will bring substrate and an E2 and serve as a scaffold for the transfer of ubiquitin from the E2 to the substrate. A third modality is a hybrid of the two and is seen in RING-between-RING (RBR) E3 ligases, which bind an E2 and substrate and ubiquitin is transferred from E2 to the E3 and then to the substrate.

In addition to these ligases, the second filter to degradation is the presence of additional interacting protein factors which can modify the original signal, (either by adding or subtracting to signals), or even aid in degradation by shuttling or pre-processing substrates prior to their degradation. For example, the cells contain many cellular deubiquitinating enzymes which can either trim or remove ubiquitin chains from the substrates. One such enzyme is Ubp6, or Usp14 in humans, which binds the 26S proteasome and has been shown to stabilize the substrate-engaged conformation of the proteasome (Bashore et al., 2015). Another example is the pre-unfolding of substrates lacking an engagement region by the AAA+ motor Cdc48, or p97 in humans, (Bodnar & Rapoport, 2017; Olszewski et al., 2019) which we now understand to be able to engage ubiquitin itself as a universal initiation region (Twomey et al., 2019). As with ubiquitination, expression and differential activities of these protein factors can change in response to various cell conditions, which ultimately change which proteins, and thus their functions, are terminated by the proteasome.

Since the role of the proteasome is to effectively press the “quit” button on a function in the cell, it makes sense that the scope of its degradation is nearly every function in the cell (Livneh et al., 2006). While a comprehensive review of all the roles of the proteasome is a monumental task, I will attempt to briefly outline the roles of the proteasome in cellular functions in major compartments of the cell which I will divide into three broad categories: the nucleus, the cytosol, and at the lipid bilayer boundaries of organelles.

1.C.i. Degradation in the nucleus

The nucleus is the location of the cellular blueprints and is therefore arguably the most important and dynamic organelle of the cell. The functions of the nucleus are centered around its major component: approximately two meters length of DNA which must be read, decoded, and replicated for the cell to function and divide. This massive genome must be efficiently condensed around protein histones to fit inside the nuclear

membrane and be selectively unpackaged so that it can be accessed for transcription. It's been estimated that 80% of cellular proteasomes are localized to the nucleus in actively dividing budding yeast (Pack et al., 2014) and global protein localization studies using fluorescent protein tags have also confirmed that many proteasome subunits appear to be primarily nuclearly localized (Huh et al., 2003). Decades of research have provided evidence that the proteasome plays a role in many aspects of nuclear biology.

In budding yeast, it has been shown that either 20S or singly-capped 26S proteasome are imported into the nucleus by the action of the protein Sts1 in collaboration with the importin system of the nuclear pore complex (NPC) (Breckel et al., 2024). Sts1 reportedly binds the proteasome subunit Rpn11. It contains two tandem nuclear localization signal (NLS) sequences, which are recognized by the karyopherin-α protein, Srp1. The karyopherin-α/β/Sts1 complex transport the proteasome through the nuclear pore and into the nucleus, where the karyopherins are dissociated from the complex and Sts1 is turned over by the proteasome. While other protein components of the 20S have been speculated to have putative NLS it remains unclear if these signals are actually used for transport once they are assembled into a complex. In higher eukaryotes there exists an analogous process with different proteins. Human AKIRIN2 carries out the function of yeast Sts1 with AKIRIN2 similarly binding the proteasome and a nuclear import protein, IPO9, which results in proteasome import into the nucleus (de Almeida et al., 2021). As in yeast, AKIRIN2 is ultimately turned over by the proteasome.

One of the first (Glotzer et al., 1991) and most well-known examples of nuclear proteasomal degradation is the turnover of proteins involved in progression of the cell cycle (Dang et al., 2021). Specifically, the activity of cyclin-dependent kinases (CDKs), the master regulators of cell cycle progression, is modulated by the activity of their cyclin binding partners and inhibitory proteins (CDKIs). These regulators of the CDKs are themselves regulated by their ubiquitination and removal by the proteasome. In addition to being essential to cell division, the proteasome is also involved in gene expression through the degradation of histones (Shmueli et al., 2021). Histones may be turned over for a variety of factors which can range from control of gene expression via selective degradation on specifically modified histones (Fatima et al., 2020), to the re-initiation of transcription and establishment of cell plasticity (Oh et al., 2020), to the control of supernumerary histone proteins which may become toxic to the cell (Singh et al., 2010). Another aspect of nuclear proteasome degradation is the removal of transcription factors. Perhaps the most apt example of this is the proteasome's negative regulation of its own expression through the action of the transcription factor

NRF1. NRF1 is synthesized in the endoplasmic reticulum (ER), where it is retrotranlocated and degraded by ER-associated degradation (ERAD, see below). In a cell with abundant proteasome populations, NRF1 is successfully degraded upon translocation, but if the cell is proteasome-depleted NRF1 escapes degradation and folds into a transcription factor which travels to the nucleus to promote expression of proteasome genes (Northrop et al. 2020). When it comes to regulating transcription, the proteasome may directly degrade a transcription factor, or it may degrade a transcription factors inhibitor to allow for gene activation as is the case of NF-kB and its inhibitor IkB in response to inflammatory cytokines (Taniguchi & Karin, 2018). In this case, the NFkB transcription factor composed of a dimer of p50 and p65 is bound and inactivated by IkB protein. The cell's response to inflammation is to phosphorylate IkB, which promotes its ubiquitination and degradation, freeing NF-kB to activate genes in response to the inflammation.

One important function of the nucleus is the transcription of rRNA and the formation of ribosomal precursors from nuclear imported ribosome proteins. In actively proliferating cells the ribosome is amongst the most produced protein complexes (Lewis et al., 2000), and its correct assembly is important for timely translation during growth. While degradation of the ribosome has been largely attributed to autophagy in a process known as ribophagy (An & Harper, 2019), degradation by the 26S proteasome has also been implicated in the control of ribosomal function. Through the use of microscopy and quantitative mass spectrometry, it was first shown that there was a significant difference in the quantity of ribosomal proteins imported into the nucleus following translation and the ribosomal proteins which are end up assembled into functional ribosomal precursors, implicating the proteasome in the degradation of a large pool of ribosomal proteins (Lam et al., 2007). This was further verified with genetic and biochemical studies to confirm that ribosomal proteins failed to overexpress, their integration into ribosome complexes required removal of the endogenous ribosomal protein gene, and that proteasome inhibition, but not autophagy inhibition, resulted in accumulation of poly-ubiquitinated ribosomal proteins (Sung et al., 2016a). Follow-up work by the same group named this pathway ERISQ, for excess ribosomal protein quality control and identified the yeast protein Tom1 as the E3 ligase involved in this degradation of supernumerary ribosomal proteins in the nucleus, (Sung et al., 2016b). This work also showed that the Tom1 ligase recognized contacts in excess ribosomal proteins which are normally hidden in assembled ribosomes, mirroring a paradigm in translation quality control (see below), and that this pathway was conserved in mammals through the E3 ligase HUWE1. Additional work has shown that excess ribosomal proteins which fail to import to the nucleus are also ubiquitinated and degraded by the proteasome in the cytosol through the action of

protein quality control mechanism for orphan proteins of multiprotein complexes (Yangitani et al., 2017). This highlights the versatility and redundancy of the UPS system in degrading proteins in different contexts in different compartments of the cell.

1.C.ii. Degradation in the cytosol

The cytosol is the volume of the cell not contained within a membrane. Composing an estimated 70% of the volume of the cell, it is a crowded solution of proteins and the location of the cytoskeleton, translation, and basal metabolic processes such as glycolysis. Proteasomal degradation in the cytosol is, unsurprisingly, composed of a diverse repertoire of molecular functions but perhaps the most notable molecular event which takes place in the cytosol is the synthesis of proteins via translation of mRNA by the ribosome. It is not surprising that the proteasome and the ribosome are intimately involved in protein quality control in the cytosol and at the organelle membranes (see section 1.C.iii below). In fact, early evidence in both yeast (Turner & Varashavsky, 2000) and mammalian cells (Schubert et al., 2000) suggested that a significant percent, up to 30%, of the translation occurring in the cytosol terminates in degradation by the proteasome. These translation events were termed defective ribosomal products (DRiPs) and were initially hypothesized to be a major source of peptides for antigen presentation via MHC I complexes in higher eukaryotes. Indeed, the proteasome has been extensively implicated as the generator of peptides for MHC presentation (Rock et al., 1994) and there is even a cellular proteasome variant termed the immunoproteasome (Eshof et al., 2021). While the extent of DRiPs and their role in antigen presentation is contentious (Rock et al., 2014), it is clear quality control of protein folding does indeed begin with folding surveillance at the ribosome and ends with degradation by the proteasome.

Since the proposal of DRiPs we now know that there is an extensive network of quality control pathways that screens proteins as they come out of the ribosome. Many of these are chaperones which mediate folding of nascent chains, some of these involve the co-translational ubiquitination of nascent chains and are dependent on the nascent chain itself (Duttler et al., 2013; Wang et al., 2013), and some monitor the state of translation itself regardless of the nascent chain. This quality control pathway, which has been termed ribosome-associated quality control (RQC), represents the intersection of mRNA quality control and protein synthesis quality control. Defects in mRNA may cause stalls in translation for reasons ranging from truncated mRNA, excessive secondary structure, or shortages in translation components such as appropriate tRNAs (Brandman & Hegde, 2016). In each of these cases the result is a

stalled ribosome complex with a partially translated protein and the cellular response is to disassemble the stalled complex, recycle the ribosome, degrade the faulty mRNA, and degrade the potentially problematic faulty protein.

Disassembly of the stalled complex occurs through the recognition of the stalled ribosome-mRNA complex by the proteins Dom34, Hbs1, (Doma & Parker, 2006;) and Rli1 (Shoemaker & Green, 2011) (Pelota, Hbs1, ABCE1 in mammals) (Pisavera et al., 2011) which recognize and split the ribosome large and small subunits (Shoemaker et al., 2010). Following splitting the large subunit bound to a tRNA-nascent chain is recognized by the protein Rqc2 (NEMF in mammals), which recognizes the now exposed small subunit binding interface. With Rqc2p bound then the E3 ligase Ltn1 (Listerin in mammals) can bind the large subunit complex and ubiquitinated the nascent chain (Brandman et al., 2012; Shao et al., 2013). One interesting aspect of RQC is the generation of C-terminal alanine-threonine tails (CAT tails) on the nascent chain (Shen et al., 2015). It has been shown that the structure of Rqc2p favors interactions with Ala- and Thr-tRNAs which can enter the empty A-site of the large ribosomal subunit. The interactions can position the new tRNAs in close contact with the P-site and, independently of the small subunit, elongate the stalled nascent chain. It has been proposed that these CAT tails may act to extend the nascent chain for the presentation of a lysine residue to Listerin for ubiquitination (Shen et al., 2015). Following ubiquitination, the ubiquitinated nascent chain follows a path similar to many protein quality control mechanisms, the extraction of the ubiquitinated protein from the complex via the action of the unfoldase Cdc48 and subsequent degradation by the proteasome (Brandman & Hegde, 2016).

In addition to maintaining protein homeostasis at the earliest possible moment via cotranslational ubiquitination and RQC, the ribosome itself is controlled in some measure by the UPS in the cytosol. This is mediated by the action of the protein UBE2O, which is responsible for the recognition and ubiquitination of orphan proteins of multiprotein complexes (Yanagitani et al., 2017). Interestingly, UBE2O was also implicated in the proteome-wide remodeling of erythrocyte precursors during their terminal differentiation into mature erythrocytes (red blood cells) (Nguyen et al., 2017). This work demonstrated the role of UBE2O as a hybrid E2-E3 not only in the recognition, ubiquitination, and degradation of ribosomal proteins, but also in a wide variety of non-ribosomal substrates and in the generation of amino acids for protein synthesis in late differentiation. Given that ribosomal proteins: 1). Play such an important role in cell growth and 2). exist in different compartments during their synthesis and assembly into the final ribosome complex, it is not surprising that there

are mechanisms in both compartments to ensure that only properly assembled RPs remain in the cell.

Another cytosolic phenomenon in which proteasomal degradation plays an important part is in the clearance of stress granules. When proteotoxic stress results in an overwhelming amount of damaged or misfolded proteins, the cell can collect and sequester these proteins into membrane-less compartments: aggresomes (Kopito, 2000) and stress granules (Nollen et al., 2001). The two compartments are distinct; the former is recalcitrant to degradation while the latter is resolvable with a functioning UPS (Xu et al., 2022). This segregation of potentially toxic proteins provides temporary relief to normal cell functions, prevents the propagation of damage from one protein to the other, and affords the cell time to weather out a stressful condition or perhaps clear the misfolded proteins. Stress granules represent another intersection of RNA quality control and proteolysis, since they are formed through the interactions of mRNA and mRNA binding proteins when translation is impaired due to stressors including heat, starvation (Reviewed in Grousl et al., 2021). It is worth mentioning that this same process occurs in the nucleus within the nucleolus (Nollen et al., 2001; Frottin et al., 2019) and it has been shown that cytosolic stress granules appear to relieve the UPS in the nucleolus (Xu et al., 2023). In either case it has been shown that in addition to mRNA, damaged proteins, and the various proteins involved in the formation of stress granules, the proteasome is also a constitutive resident of these membraneless compartments, and its function is critical in their clearance (Xie et al., 2024).

1.C.iii. Degradation at membrane-bound organelles

Organelles are characterized by a membrane which separates their contents from the general cytosol. Proteasomes, except for the case of the nucleus which contains nuclear pores, do not localize in the interior of organelles, thus proteasomal degradation at and around organelles is synonymous with degradation at membranes and in the context of protein transport across membranes. Regardless of the organelle, membrane-associated quality control pathways share a common architecture: protein degrons are recognized by membrane-integrated ubiquitin ligase complexes which ubiquitinate the protein, then the proteins are extracted from the membrane by the molecular motor Cdc48 and associated cofactors, and finally degraded by the proteasome. Protein substrates can either be membrane-anchored proteins which aggregate on the membrane surface or are mislocalized to the wrong membrane, misfolded proteins in the interior space (lumen) of the membrane, or proteins which experience some form of defect when translocated across the membrane. There are four well-characterized systems of quality control, and they are named after the

organelles they survey: endoplasmic reticulum associated degradation (ERAD) and its related inner nuclear membrane associated degradation (INMAD), endosome and Golgi associated degradation (EGAD), and mitochondria associated degradation (MAD).

The endoplasmic reticulum is composed of an extensive network of membranes which is continuous with the nuclear membrane. A major site for translation, ribosomes associate with ER via protein-conducting channels known as translocons, which translocate nascent peptides into the membrane or lumen of the ER. The ER translocon is the first step in the secretory pathway that ensures that ER-membrane or luminal proteins take on the correct fold and are modified correctly and are then shuttled to their proper locations in the cell or secreted. The magnitude of translation that takes place at the ER requires that strict quality control of ER proteins take place. As a consequence of its significance in the cell, the molecular mechanisms of ERAD have been extensively studied and have revealed variations in common principles of quality control that are mirrored in other organelles, as described below.

In yeast there are three E3 ubiquitin ligase complexes which mediate quality control of ER proteins: Hrd1, Doa10, and Asi. All three complexes are capable of degrading membrane and soluble membrane-associated proteins; however, the Hrd1 complex is unique for its role in the recognition, retrotranslocation, ubiquitination, and degradation of soluble proteins in the ER lumen, termed ERAD-L. The Hrd1 complex is composed of a core of integral membrane proteins, the eponymous RING-type E3 ligase Hrd1, Hrd3, Der1, Usa1, and various associated proteins. Substrates are recruited to the complex via interactions with Hrd3 and a glycan-binding protein, Yos9. They are then retrotanslocated from the ER lumen to the cytosolic side via a channel formed by a Hrd1/Der1 dimer mediated by Usa1. On the cytosolic side, the protein Cue1 recruits the E2 Ubc7 which mediates substrate ubiquitination by the RING domain of Hrd1. Ubiquitinated species are recognized by the Cdc48-Ufd1-Npl4 complex for extraction from the membrane and degraded by the proteasome. Doa10 and Asi contain a similar architecture of a central integral membrane complex containing a RING-type E3 that associates with various factors to recruit substrates and E2 enzymes. Since the ER membrane is continuous with the nuclear membrane, ERAD and INMAD share the Doa10 complex, while the Asi complex is exclusive to the INMAD.

In post-ER membrane compartments, such as the Golgi, the most well-characterized method of protein quality control is carried out by the endosomal sorting complexes required for transport (ESCRT) machinery, which results in degradation by the lysosome. However, in addition to the ESCRT system, there exists an ERAD-like

mechanism for protein degradation in the Golgi. Endosome and Golgi associated degradation has been shown to be carried out by the Dsc complex, which contains the integral membrane E3 ligase, Tul1 (Schmidt et al., 2019). Similar to ERAD, the Dsc complex recognizes substrates and recruits them to Tul1 for ubiquitination, after which Cdc48 extracts the proteins out of the membrane for degradation by the 26S proteasome. The EGAD substrate discovered in this work, Orm2, is an inhibitor of the ceramide biosynthesis SPOTS enzyme complex. This implicates EGAD in the positive regulation of lipid biosynthesis. This is not surprising considering that ERAD itself has long been implicated in the regulation of lipid biosynthesis with the discovery that 3-Hydroxy-3-methylglutaryl coenzyme A reductase (HMGR) is dependent on its integral membrane domain for its sterol-dependent degradation (Gil et al., 1985) and that this degradation is ultimately carried out by the 26S proteasome (Hampton et al., 1996). The degradation of HMGR via ERAD and of Orm2 by EGAD, emphasizes that these degradation systems can serve regulatory roles in addition to their more commonly cited protein quality control functions.

Mitochondria present an interesting case for protein quality control for several reasons. For one, while mitochondria have their own genome and a separate central dogma, the bulk of mitochondrial proteins are encoded in the nucleus, synthesized in the cytoplasm, and must be imported into the mitochondria. This presents the second challenge to mito protein quality control: the mitochondrion is a double-membraned organelle. Mitochondrial proteins can exist as membrane-integral in the outer or inner membrane, or soluble in the intermembrane space or in the matrix. This means that some mitochondrial proteins need to be transported across two membranes and fold into their correct shape and function. The third challenge is that, due to their proximity to or involvement in energy production, mitochondrial proteins are liable to be exposed to damage from byproducts of energy production, such as reactive oxygen species (ROS). The role of ubiquitin at the mitochondria has been primarily understood to be a signal for membrane potential and for the need to remove faulty, depolarized mitochondria through mitophagy, a specialized form of autophagy (Ng et al., 2021), however there do exist examples where ubiquitin serves as a signal for the degradation of mitochondrial proteins and even in the regulation of global mitochondrial phenotypes.

One such example of a ubiquitination and proteasomal degradation event at the mitochondria is the degradation of the mitofusin Fzo1 (Cohen et al., 2008). While degradation of Fzo1 had been previously established, Cohen and colleagues showed that its degradation was dependent on ubiquitination by the F-box protein Mdm30, which serves to recognize Fzo1 and form an E3 ligase of the Skp1-Cullin-F-box (SCF)

family for ubiquitination. Subsequent work by the same group showed that, like ERAD, the degradation of Fzo1 was dependent on its post-ubiquitination extraction from the mitochondrial outer membrane by Cdc48 which was recruited by the protein Vms1 (Heo et al., 2010). This work shows that the UPS certainly acts in the regulation of mitochondrial proteins to some extent, in fact, defects in the degradation of Fzo1 appear to have effects on the morphology of the mitochondria and its function. With that being said, while it is clear that the UPS plays a role in mitochondrial quality control (Livtnat-Levanon & Glickman, 2011), the extent of mitochondria associated degradation is not as well understood as ERAD or EGAD. For example, even though Fzo1 degradation requires extraction via Cdc48 as in ERAD, there has not been a Hrd1-like integral membrane E3 complex discovered at either mitochondrial membrane.

1.D. Identification of proteasome substrates

As with the original discovery of the UPS, substrates are usually discovered when researchers working on a particular protein or pathway discover that their protein of interest is either ubiquitinated or directly removed from the cell in a proteasome dependent way. Given the diversity of processes that the proteasome is essential in, a complete understanding of the substrate pool of the proteasome is necessary. The aim of this thesis work is to develop a method to identify proteins degraded by the proteasome in a 19S mediated manner in live cells using a chemical biology cross-linking approach. Here I will provide a brief review on the efforts and approaches of other groups in answering the same question: Can we understand the scope of proteasome degradation at a systems level?

1.D.i. Mass spectrometry identification of the ubiquitinome

The first of such approaches was developed in the early 2000's by Steve Gygi and Dan Finley's groups at Harvard Medical School, described in their 2003 publication in *Nature Biotechnology* (Peng et al., 2003). Aiming to understand protein ubiquitination in cells, Peng, Schwartz, and colleagues utilized a yeast strain with ubiquitin fused to a six-histidine tag for affinity purification. With this his-tagged ubiquitin strain they were able to purify ubiquitin conjugates from cells and, by comparison with a wild-type ubiquitin strain, identify 1,075 candidate substrates for ubiquitination.

In addition to the identification of new ubiquitin substrates, this paper is notable for the inception of di-glycine (diGly) proteomics. Peng, Schwartz, and colleagues recognized that a tryptic digest of a ubiquitin-protein conjugate results in a branch point with two glycines from the ubiquitin modification on peptides of the modified protein. This diGLY modification corresponds to a mass shift of 114.1 Da, which can be searched for when performing the database search for peptide-spectral matches. Using this approach, they were able to identify 110 ubiquitination sites within 72 of their candidate ubiquitin substrates list. Most notably, was their confirmation of the ubiquitination of ubiquitin itself. While ubiquitination at ubiquitin Lys48 and Lys63 had been confirmed at the time, modification of ubiquitin at Lys6, Lys11, Lys27, and Lys33 were confirmed for the first time in this paper (**Figure 1.4A**). Lys11, in particular, was shown to be as abundant in this dataset as the traditional Lys48 modification signal and has since been confirmed to be a signal for proteasomal degradation (Matsumoto et al., 2010).

The ubiquitinome approach is powerful for its simplicity, which is often a key component of a robust mass spectrometry workflow, but the technique itself is not necessarily proteasome specific. Many ubiquitination signals, such as Lys63 ubiquitin chains, are not degradation signals. Thus, the approach really is really centered around identifying all proteins which are ubiquitylated, some of which may end up at the proteasome. The simplicity of the technique allowed other labs to modify the approach to make it more proteasome centered. For example, in a pair of papers Mayor and colleagues employed the same ubiquitin conjugate purification approach paired with mass spectrometry to determine which subset of proteasome substrates are shuttled to the proteasome by the Rpn10 ubiquitin receptor (Mayor et al., 2005). By comparing an RPN10Δ yeast strain to wild-type and determining which ubiquitin conjugates are stabilized in the deletion strain, they identified a subset of ubiquitinated substrates which are candidates for shuttling to the proteasome in an Rpn10-dependent manner. They iterate on this approach with the use of isotope labels to provide a more detailed and quantitative look at the same question in a follow up paper in which they estimate that a quarter of substrates may be shuttled through the Rpn10 receptor (Mayor et al., 2007). However, one drawback to this approach is the recent discovery of proteins whose degradation is 19S-dependent but ubiquitin-independent, as reviewed previously.

1.D.ii. Mass spectrometry analysis of proteasome-cleaved peptides

One of the more recent approaches to identify proteasome substrates was work carried out by Yifat Merbl's group at the Weizmann Institute, described in their 2018 publication in *Nature Biotechnology* (Wolf-Levy et al., 2018). Taking an alternative approach to ubiquitination-based identification of substrates, Wolf-Levy and colleagues instead aimed to directly sequence the peptides that are generated by the 20S core peptidase in a method they call mass spectrometry analysis of proteasome-cleaved peptides (MAPP). MAPP employs a reversible cross-linker to broadly cross-link cell lysates followed by immunoprecipitation of 20S with an anti 20S antibody. This approach assumes that nascent peptides either inside the 20S or exiting the 20S from the axial pores would then be cross-linked to the proteasome. They could then undo the cross-linking and separate the peptides from the 20S protein complex using reverse-phase chromatography and sequence the peptides using mass spectrometry. They identified 1,004 proteins from this technique in HEK293 cells and show that the generation of peptides and subsequent identification of proteins is proteasome-dependent. As a proof of principle, they were able to identify an exogenously

expressed model substrate only in samples where it is expressed and in the absence of proteasome inhibition. At a peptide level, their technique results in the detection of peptides longer in length and with a wide diversity of amino acids at the proteolytic cleavage sites when compared to peptides generated from traditional proteomic preparation via trypsin digestion. They are however unable to see the specificity of the catalytic site of the β7 subunit of the 20S.

One of the strengths of this approach is that it does not rely on recombinant molecular biology techniques, which allows it to be used on clinical samples. Indeed, Wolf-Levy et al. demonstrate the application of MAPP in peripheral blood mononuclear cells (PBMCs) derived from patients with systemic lupus erythematosus (SLE) and compare substrates from healthy PMBCs. From this comparison they can distinguish SLE and healthy cells from their degradation profiles and identify histone variants as strongly changing across the two conditions. However, this approach has a major drawback which is that the cells are lysed prior to their cross-linking and subsequent purification of 20S. Since the technique is dependent on sequencing of free peptides in the cell, the process of cell lysis removes any form of spatio-temporal information about the substrates while almost certainly introducing artifacts. Additionally, MAPP relies on analyzing peptides that are presumably produced or near the 20S and 20S can degrade substrates independent of the 19S RP, thus MAPP may also misrepresent the substrate pool.

1.E. Discussion

The 26S proteasome is the cellular hub for regulated protein degradation. Its evolutionary design as a compartmentalized protease with accompanying ubiquitin receptors, paired with the ubiquitin signaling protein and a complex network of ubiquitin ligases and deubiquitinating enzymes, ensures that cellular proteins are turned over selectively in a tightly regulated manner. Much work has been carried out in the structure and biochemical function of the proteasome, ubiquitin, and the ubiquitin ligases but most of the identification of proteasome substrates has occurred on a case-by-case basis. Some work has been done to identify proteasome substrates more globally, primarily through the identification of ubiquitinated proteins and through the sequencing of proteasome-derived peptides from cells. In this work I aim to develop a new method for identifying proteasome substrates. To do this, I hypothesized that it might be possible to trap substrates as they are being translocated through the central pore of the proteasome. In this method, one would induce cross-linking of proteasome to the substrate and then use an affinity tag on the cross-linker to enrich the trapped substrate for identification.

In the following chapter of this thesis, I describe the biochemistry of site-specifically introducing a photo-cross-linking unnatural amino acid (UAA) *p*-benzoyl-L-phenylalanine into the proteasomal AAA+ motor. Through the use of a reconstitution system, I screen for proteasome base variants that remain functional with the UAA and verify that these bases are able to engage and trap ubiquitinated substrates. I also show that this UAA incorporation is feasible in live cells and results in cross-linking nearly identical to my in vitro results. This method results in trapping of proteasome substrates without the requirement for lysis, using a relatively low-energy irradiation with 365 nm light, which is minimally disturbing to the cell. In this way, the UAA trapping approach retains the spatio-temporal information of the proteasome substrate in a way that lysis prior to cross-linking loses. Additionally, the position of the cross-linker in addition to an enrichment step for the cross-linking subunit ensures that proteins trapped are *bona fide* substrates. In chapter 3 of this thesis, I describe the affinity purification of trapped substrates from live cells and the optimization of their identification using mass spectrometry. Following crosslinking in live cells, I use a denaturing immobilized metal affinity chromatography (IMAC) purification to purify out proteasome-substrate conjugates. Using high-resolution mass spectrometry and label-free quantification, I was able to identify over 700 putative proteasome substrates which represent the broad diversity of proteasome substrates.

Chapter 2

Engineering of a Photocrosslinking 26S Proteasome

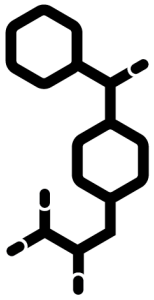

2.A. Unnatural amino acids as chemical biology tools

Proteins are the workhorses of the cell and carry out all the important processes of life. Proteins are built using instructions encoded in the genetic code and interpreted by the ribosome which assembles proteins using the 20 canonical amino acids as building blocks. Each of these amino acids has a distinct side chain with different chemical properties. Almost every protein function, such as binding or catalysis, can be described as the consequence of amino acid side chain chemistry. It is remarkable to think that so much diversity of function can be generated from a 20 amino acid palette. It should be mentioned that this palette expanded in the cell by post-translational modifications—phosphorylation, acetylation, or myristoylation, to name a few, can be enzymatically appended on certain amino acid side chains. With that being said, the amino acid side chain chemical toolbox is relatively limited, but several groups have sought to expand it via expansion of the genetic code for the incorporation of unnatural amino acids (UAAs) into proteins. This expanded palette of amino acids allows for the site-specific modification of proteins with new functionalities for labeling, crosslinking, and more. Here, I will briefly summarize the theory of genetic code expansion for UAA incorporation and review some of the developments in the field relevant to my applications for this work.

2.A.i. Genetic code expansion

The general premise of genetic code expansion is simple: how can the instructions of life be modified to encode additional amino acids with desired chemical properties. To achieve this, you must first understand the central dogma of molecular biology. Instructions for the assembly of proteins are encoded in specific sequences of nucleotides, genes, in the DNA of a cell. The process of transcription reads the instructions on the DNA and makes a working copy of a protein-coding sequence, messenger RNA or mRNA. The mRNA sequence is bound by the ribosome and its sequence decoded, or translated, from nucleic acid to amino acid. Three nucleotides compose a codon, which is interpreted by the complementary anticodon of a transfer RNA (tRNA). Prior to translation, amino acids are enzymatically charged onto a tRNA by an aminoacyl-tRNA synthetase, and as the tRNA binds to its corresponding codon the ribosome catalyzes the transfer of the amino acid from the tRNA onto the nascent polypeptide. One by one, tRNAs bring the next amino acid in the protein instructions by reading the codon on the mRNA until the mRNA sequence reaches what is known as a stop codon, upon which translation is terminated.

Given the four nucleotide bases (A, T/U, C, G) and codons composed of a trio of bases, there are a possible 64 codons (**Figure 2.1A**). Some codons only code for one specific thing, for example the codon UGG is the only codon for the amino acid tryptophan. Some codons have double meanings—the AUG codon codes for methionine, but also acts as a signal for the initiation of protein translation. Some amino acids are coded for by multiple codons, such as arginine, which is encoded by 6 different codons. Another example of this is termination of translation, which is encoded by the three named "stop" codons: UAA (ochre), UGA (opal), and UAG (amber). These codons highlight another property of the degeneracy of the genetic code: not every codon is used with the same frequency. In fact, the amber stop codon is only used 9% of the time in the genetic code of *E. coli* and only 24% of the time in the genetic code of *S. cerevisiae*, and they rarely code for essential genes (**Figure 2.1B**). The built-in degeneracy of the genetic code hints at the potential for restructuring the codons for the incorporation of something other than the 20 canonical amino acids. Hypothetically, to reprogram the genetic code you would either need to repurpose an existing codon or build a new codon. This means that you would have to have a tRNA which is charged with your non-canonical amino acid by a tRNA synthetase, which can then read out a repurposed or modified codon and incorporate your desired amino acid into the polypeptide. Then, you should be able to introduce a UAA with a desired chemical function into the repurposed codon in your protein of interest.

However, there are three considerations. First, the codon you repurpose cannot also code for something else. This eliminates the start codon, but it also largely eliminates all other amino acid codons. Stop codons do not code for any amino acid and are instead read out by translation termination factors. This fact paired with the differences in codon frequency across the three stop codons made them a logical starting point for genetic code expansion. Other approaches have gone further and developed tRNAs which are able to read out four-base codons in an RNA message. Second, the tRNA and tRNA synthetase used must be orthogonal to the host organism's machinery; that is, the new tRNA should not be able to be charged with a normal amino acid by the host synthetases and likewise the new synthetase must not charge normal tRNAs with non-canonical amino acids. This is overcome by the expression of tRNA/tRNA synthetase pairs from organisms in different domains, so that their machinery does not interfere with host machinery. Finally, the unnatural amino acid must be bioavailable to the organism, either supplemented in the growth media or synthesized by the organism itself.

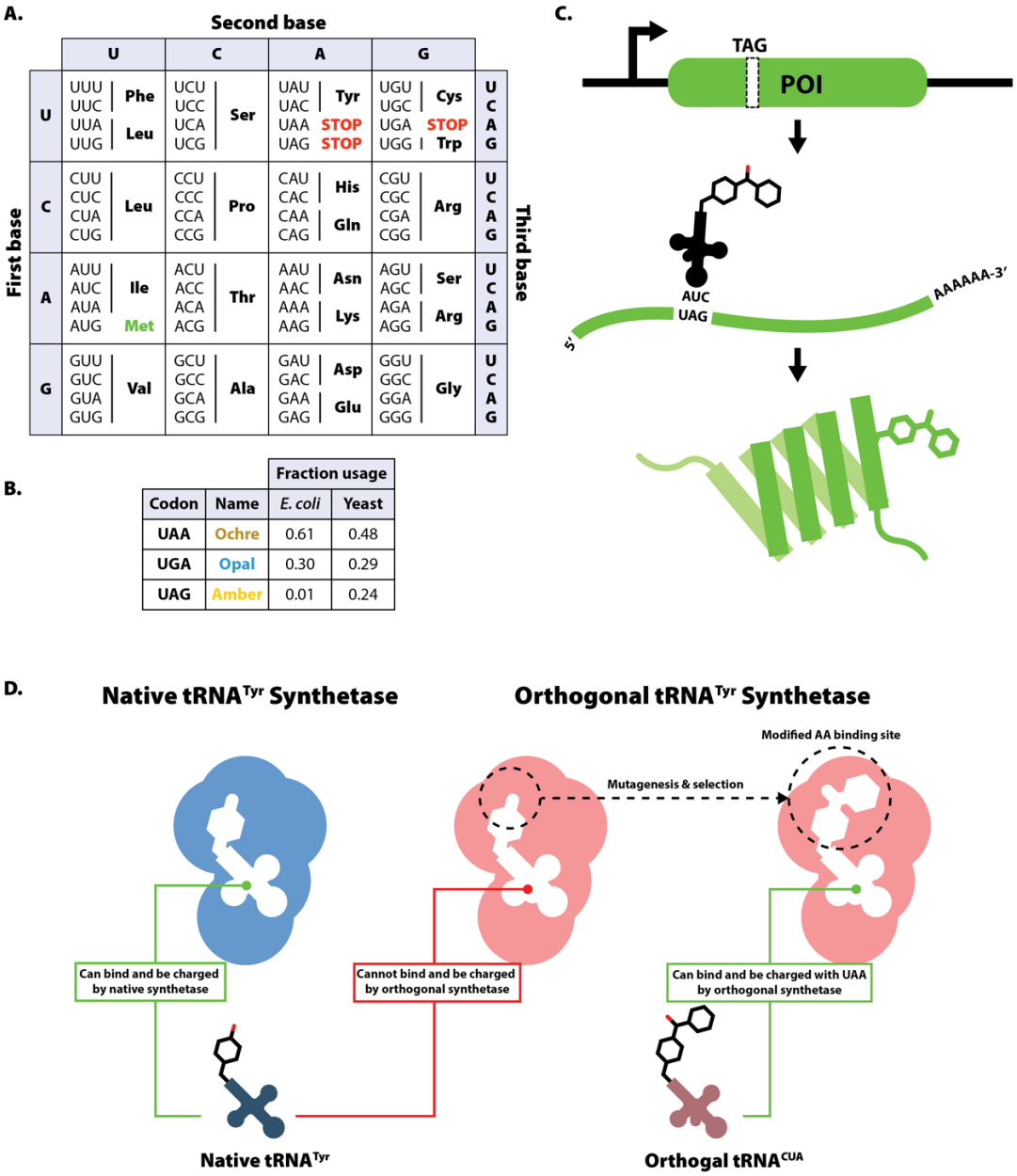

Figure 2.1: Principles of Genetic Code Expansion.

A. Codon table shows the three codons which encode translation termination. **B.** The three "stop" codons, Ochre, Opal, and Amber, are listed in order of their fractional appearance in the genomes of *E. coli* and *S. cerevisiae*. **C.** Through the use of a tRNA with a modified anticodon loop, it is possible to "suppress" a stop codon. Suppressor tRNAs can be used to genetically and site-specifically incorporate new chemical modalities in proteins. **D.** Via directed evolution, tRNA synthetases can be modified to accept cognate amber suppressor tRNAs and charge new, unnatural amino acids (UAAs). Their introduction into different, or orthogonal, organisms results in translation without interference of the host organism's native tRNA and tRNA synthetase pairs.

2.A.ii. Tools for unnatural amino acid incorporation in *E. coli*

One of the first examples of this concept of genetic code expansion was carried out by Peter Schultz's group at the Scripps Institute through the mutation of the *E. coli* GlnRS/tRNA^{GLN} pair and the yeast AspRS/tRNA^{ASP} pair for the incorporation into *E. coli* (Liu et al., 1999). Follow up work then determined that the archaean *Methanocaldococcus jannaschii* had a TyrRS and tRNA^{TYR} pair that was suitable for amber codon suppression in E. coli. This tRNA-synthetase pair was less orthogonal in E. coli than the previously used *Ec*GlnRS and *Sc*AspRS, but resulted in more aminoacylation of the tRNA, suggesting that its further modification could result in better orthogonality.

Indeed, in a hallmark 2001 paper, the Schultz lab built on their previous work to show the use of *M. jannaschii* in the genetic code expansion in the prokaryote *E. coli* (Wang et al., 2001). The *M. jannaschii* tyrosyl-tRNA synthetase had been shown to have features that made it a promising candidate for orthogonal use in bacteria. For one, it has no proof-reading activity and would therefore not correct the loading of the tRNA with a non-canonical amino acid. Secondly, its anticodon recognition loop of the Tyr-tRNA-RS was minimal and amenable to mutations and the synthetase had been shown to be able to charge its amber codon cognate tRNA. A structure of the homologous TyrRS from a *Bacillus* species allowed the group to use error-prone PCR mutagenesis to vary residues within 6.5Å of the *para* position of the ring of the synthetase-bound tyrosine. By transforming a library of TyrRS mutants into *E. coli* with an amber codon-containing antibiotic resistance gene and selecting with antibiotics, they could positively select for amber codon-suppressing variants. They would then follow this selection by plating the cells in media without the unnatural amino acid. Cells that then did not grow were therefore UAA-dependent and were selected from a replica plate. With rounds of selection, Wang and colleagues showed that they could select for a system that allowed for the specific incorporation of the UAA O-methyl-L-tyrosine.

The development of that original mutated *M. jannaschii* TyrRS/tRNA^{TYR} pair represented a starting point for the development of many derivatives of the system for the incorporation of UAA tyrosine analogs, most notably *p*-azido-L-phenylalanine (Azf) (Chin et al., 2002a) and *p*-benzoyl-L-phenylalanine (Bpa) (Chin et al., 2002b) which are relevant to my goals of crosslinking within the proteasome. In a series of publications, Jason Chin of the Schultz lab was able to generate variants for the introduction of Azf and Bpa into *E. coli* proteins by using the same structure-guided mutagenesis followed

by selection strategy. In this case, mutant RS libraries were initially positively selected for their suppression of an amber codon in an antibiotic resistance gene. Surviving variants underwent a negative selection for the suppression of an amber codon-containing gene toxic to *E. coli* in the absence of the UAA. This second round of selection resulted in variants that would only incorporate the UAA and not tyrosine. These new tRNA/synthetase pairs were then used to show incorporation into myoglobin as well as UV-dependent crosslinking of GST dimers, in both the AzF and Bpa systems.

2.A.iii. Tools for unnatural amino acid incorporation in eukaryotes

Interestingly, the strategy described above was also the same employed by Jason Chin for the early work on genetic code expansion in eukaryotes in a publication in *Science* in 2003 (Chin et al., 2003). An amber codon-suppressing tRNA had been described in *E. coli* as early as 1968 and it was known that this amber-suppressor tRNA was not recognized by yeast synthetases, but when charged it could be used in translation. Similar to the *M. jannaschii* TyrRS, the *E. coli* TyrRS also did not contain any proof-reading activity and would not edit a non-canonical amino acid from the tRNA. Once again using the structure of the homologous *Bacillus* TyrRS, Chin and colleagues were able to mutate residues in close proximity to the para position of the aryl ring of the tyrosine in the synthetase active site and transform the library of variants into yeast for a selection process similar to their approach for *E. coli*, that is positive selection followed by negative selection to filter for variants that incorporate only the desired UAA. Using this approach, synthetase/tRNA pairs were generated for five unnatural amino acids: *p*-acetyl-L-phenylalanine, *p*-benzoyl-L-phenylalanine, *p*-azido-L-phenylalanine, O-methyl-L-tyrosine, and *p*-iodo-L-tyrosine.

While this initial publication represented the first expansion of the genetic code in eukaryotes, the incorporation was less efficient than the equivalent system in *E. coli*. Reportedly, a one-liter growth from *E. coli* produced milligram quantities of UAA-containing protein while the yeast system produced microgram quantities. It was hypothesized that the differences in expression of UAA-containing protein were due to the efficiency in the transcription of the suppressor tRNA. Qian Wang and Lei Wang noted that transcription of yeast tRNAs is dependent on promoters within the tRNA gene itself, which are known as the A-box and B-box, and that the genes are transcribed without a 3' CCA sequence which is enzymatically added post transcription (Wang & Wang, 2008). To avoid adversely modifying the suppressor tRNA to include these promoter elements, they utilized the promoter sequence of the yeast

SNR52 gene, which contains an A- and B-box sequence, to drive expression of a suppressor tRNA sequence lacking the 3' CCA trinucleotide. Their results showed a 9-fold increase in suppression as measured by expression of a GFP with an internal amber stop codon. Surprisingly, a northern blot showed that while the tRNA is greatly more expressed with just a normal yeast 5' and 3' tRNA sequence, their modified expression system led to correctly processed tRNA and therefore better amber codon suppression.

The development of these tools makes it possible for me to carry out crosslinking in live yeast cells following screening of the Bpa position within the 19S in an established recombinant system. It is worth mentioning that the Wang lab's approach of using a modified *E. coli* TyrRS and a hybrid promoter for the expression of the bacterial $tRNA^{CUA}$ in an orthogonal organism has been used to express UAAs in *C. elegans* (Parrish et al., 2012), stem cells (Shen et al., 2011), and neuronal cells (Wang et al., 2007). Given this incorporation of UAAs in higher eukaryotes one thing that could also be of interest in future work is that, in theory, crosslinking 19S to substrates could be modified to be carried out in mammalian cells.

2.A.iv. Bpa as a photocrosslinking UAA

Aryl ketone photo-probes, such as benzophenone, were first described in the 70s and were immediately noted for their photo-chemical properties when compared to other photo-activated crosslinkers, such as aryl azides and diazirines (Galardy et al., 1973). Aryl ketones are chemically stable, allowing them to be manipulated in ambient light (see section 2Bii), they can be excited into a diradical triplet state with low-energy UV light (>350 nm), they do not readily react with water in solution, and the probe can be reactivated repeatedly if no initial crosslinking occurs (Dormán & Prestwich, 1994) (**Figure 2.2**). The first reported application was the incorporation of acetophenone into a peptide fragment binder of albumin. The synthesis of the benzophenone probe into the amino acid *p*-Benzoyl-L-phenylalanine (Bpa), then allowed more site-specific probing, initially through the solid-phase synthesis incorporation of Bpa into peptide fragments such as with calmodulin and a calmodulin-binding peptide (Kauer et al., 1986).

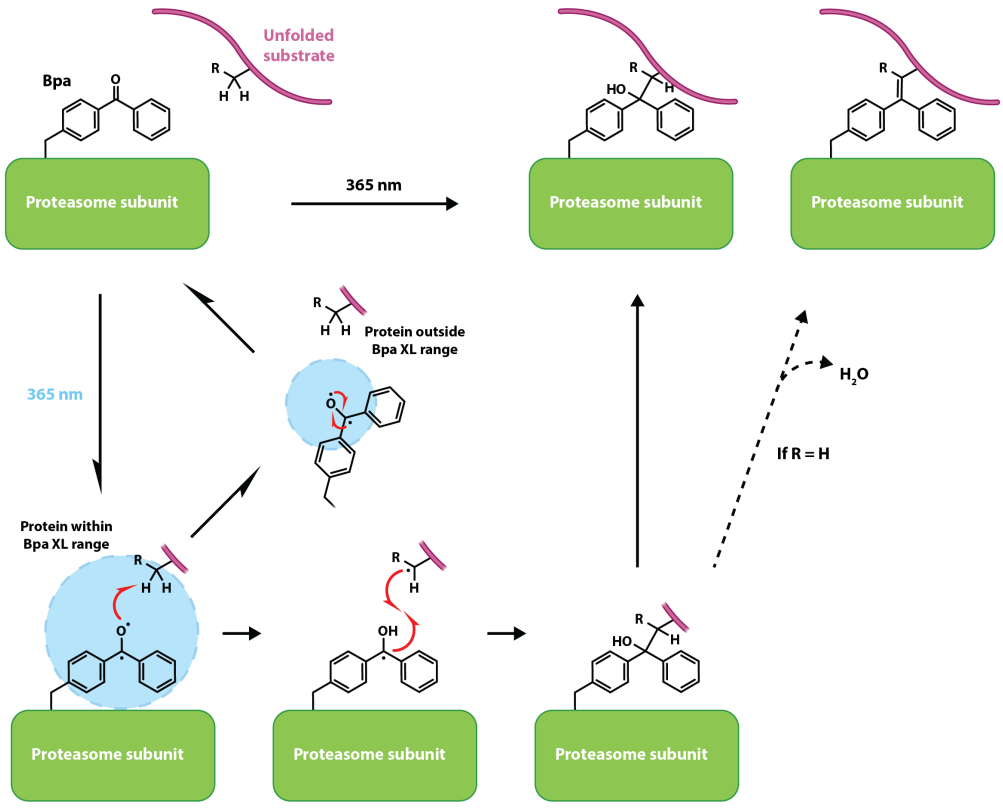

Figure 2.2: Photochemistry of 4-benzoyl-L-phenylalanine (Bpa).

Bpa (p-benzoyl-L-phenylalanine) is a cross-linking unnatural amino acid. Upon irradiation by 365 nm light, the ketone of the benzophenone sidechain is excited to a triplet state which allows it to react with carbon-hydrogen bonds within its cross-linking range. If there is no suitable cross-linking position within range, the triplet state collapses and reforms the Bpa, which can undergo subsequent rounds of excitation and cross-linking. C-H bonds within the radius will undergo hydrogen abstraction and then bond-formation between the carbonyl carbon of the Bpa and the target to form a benzopinacol-like covalent adduct. If the sidechain is a glycine, the newly formed covalent adduct can undergo rearrangement and loss of water to form an alkene.

2.B. Development of recombinant 26S proteasome with photocrosslinking UAA

The 26S proteasome is a large multi-subunit complex and it is essential for function in the cell. Instead of attempting to infer UAA-modified proteasome function from live cell experiments, which would be difficult to carry out and interpret, my approach was to try recombinant expression of 19S regulatory particle (RP) in *E. coli* for assays to screen for positions where the incorporation of a crosslinking UAA would result in a functional reconstituted proteasome. My strategy was to choose a position which made close or direct contact with the substrate and to preferably pick a residue which was already hydrophobic or aromatic. Two pieces of information guided the positioning of the UAA. First, a cryogenic electron microscopy (Cryo-EM) structure of substrate-bound 26S published by our lab in 2018 revealed the path of the substrate from the isopeptide bond of ubiquitin up until its entrance into the 20S (de la Peña et al., 2018). It revealed a wide central channel through the 19S base, with the pore loop tyrosine residues of each Rpt arranged in a spiral staircase around the substrate. Second, prior biochemical data from the lab had shown that each Rpt motor subunit had a different contribution to substrate degradation (Beckwith et al., 2013). In particular, Rpt1 was shown to be dispensable for proteasome activity. I hypothesized that substituting the pore loop tyrosines with either AzF or Bpa might result in a functional, yet crosslinking-competent, AAA+ motor.

2.B.i. Building system for recombinant incorporation of a crosslinking UAA in 26S proteasome.

Currently, our lab expresses 19S RP from *S. cerevisiae* in *E. coli* through the use of two sets of plasmids for the base and lid subcomplexes of the 19S (Beckwith et al., 2013). For expression of the base a pCOLA-Duet plasmid encodes six open reading frames for Rpt1-6. This plasmid contains a FLAG-tag on Rpt1 and a 6xHis tag on Rpt3 for affinity purification. A pET-Duet plasmid encodes the ubiquitin receptors Rpn1, Rpn13 and the structural subunit Rpn2. The final plasmid, a pACYC-Duet, contains the chaperones that template proper base assembly, Nas2, Nas6, Hsm3, and Rpn14. For expression of the lid the pCOLA plasmid codes for Rpn3,7, and 12. The pET plasmid encodes Rpn5,6,8,9, and 11. The pACYC for the lid encodes Hsp70 and Sem1. For either subcomplex, the addition of an UAA for the introduction of p-azido-L-phenylalanine (AzF) a fourth plasmid encoding for a AzF tRNA synthetase/tRNA pair was developed in a fourth pULTRA expression plasmid (Bard et al., 2019). Using this

19S expression system, our lab was able to reconstitute functional 26S proteasome using natively purified yeast 20S core peptidase. The benefit of this reconstituted system is that it allows for the introduction of mutations into 26S holoenzyme which may not be permissible in yeast due to their lethal effects on the cell. This benefit extends to the ability to screen positions for the introduction of unnatural amino acids which could yield functional proteasomes.

As described in a previous section in this chapter, while AzF has been used in the literature for crosslinking studies, its primary purpose is for bioconjugation using click chemistry to an alkyne-containing molecule. In contrast, Bpa was developed for the purpose of crosslinking and has reportedly better crosslinking chemistry. Its incorporation would require the cloning of a new plasmid for recombinant expression. To clone this plasmid, I modified the pEVOL-Bpa plasmid developed by the Schultz lab (Chin et al., 2002) by subcloning the tRNA-synthetase pair into a pULTRA backbone for IPTG-inducible expression compatible for recombinant proteasome expression. This new plasmid, pULTRA-Bpa, resulted in IPTG-inducible expression of the tRNA-synthetase pair to complement the existing recombinant proteasome expression plasmids (**Figure 2.3A**).

2.B.ii. Expression and purification of UAA proteasome bases.

A typical recombinant expression system in *E. coli* employs a strong overexpression of a protein of interest by co-opting the biology of infection of the T7 bacteriophage. E. coli strains, such as BL21 cells, are engineered for protein expression by having the T7 DNA polymerase integrated into their chromosome. Introduction of a plasmid containing the T7 promoter sequence results in the strong expression of mRNA of the open reading frame downstream of the promoter. The T7 polymerase is placed under control of the *E. coli Lac* operon and its expression is then induced by the addition of the allolactose analog isopropyl β-D-1-thiogalactopyranoside (IPTG). Cells are grown until they reach an exponential growth phase—at this point in growth cellular energy and nutrient conditions are optimal and the cell is poised for the optimal expression of protein. The addition of IPTG results in mimicking the process of bacteriophage infection, that is, to hijack the translation machinery of the bacteria to highly express its own protein products. The bacteria is allowed to express the protein of interest for some optimized amount of time, then harvested, lysed, and the protein is purified from the *E. coli* lysate by leveraging the properties of the target protein. This can be the charge, hydrophobicity, or even a genetically encoded affinity tag on the recombinant protein.

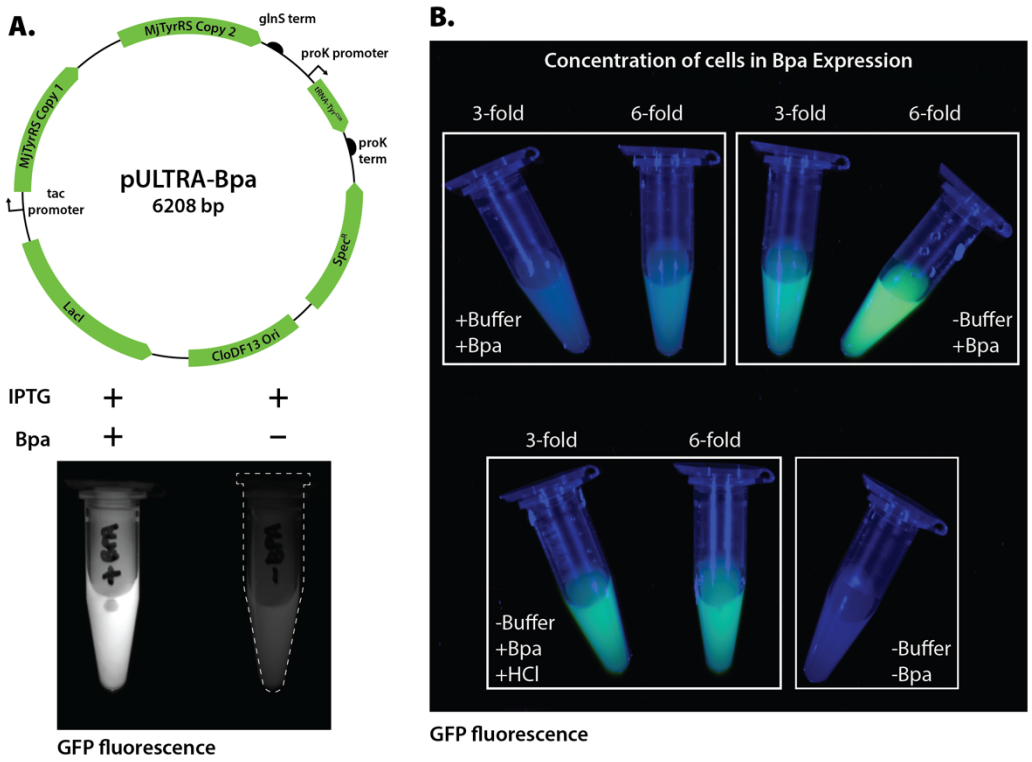

Figure 2.3: A pULTRA-Bpa plasmid for the expression of Bpa containing proteins.

Bpa can be site-specifically introduced into a protein using amber stop codon suppression. **A.** Top, plasmid map for the pULTRA-Bpa plasmid used in this protocol shows the tac promoter expression of two copies of the tRNA synthetase for Bpa incorporation. Bottom, expression test with a GFP amber codon test construct of the IPTG-inducible expression of Bpa incorporation machinery. Amber suppression is also shown to be Bpa-dependent. **B.** Bpa incorporation is dependent on its availability to the cell. Expression tests using the same GFP reporter construct show that concentrating cells 6-fold allows better exposure to the Bpa for incorporation. Conversely, addition of a buffering agent to the Terrific Broth media resulted in precipitation of the Bpa and poor-incorporation. Bpa is dissolved in 1 M NaOH, neutralization of the media with 1 M HCl after addition of the Bpa also results in reduced incorporation. Culture ODs were normalized to the -Buffer -Bpa control. Cell GFP fluorescence images were captured on a ChemiDoc MP using the fluorescein 532/30 filter set and automatic exposure.

Incorporation of the UAA AzF had been established in the Martin lab by a previous graduate student who had employed the azide functional group of the unnatural amino acid for a reaction with a dibenzocyclooctyne (DBCO) fluorophore via copper-free click-chemistry reaction to generate specific labeling of the proteasome. This technique was used first in bulk assays to decipher the kinetic pathways of the proteasome (Bard et al., 2019) and is now additionally used in single molecule experiments (Jonsson et al., 2022; López-Alfonzo et al., 2023; Htet et al., 2024). For both AzF and Bpa, the most expensive and limiting reagent in the expression is the UAA itself, which is typically added to a final concentration of 2 mM. To maximize delivery of the UAA into cells, the typical T7 expression experiment is modified. First, a large volume of cells is grown in a sufficiently complete media until they reach approximately mid-log phase, they are then harvested by centrifugation and resuspended a smaller volume of a very rich media such as Terrific Broth (TB) supplemented with the UAA. Concentrating the cells results in more cells in the same concentration of UAA, which maximizes the use of the UAA reagent. After concentration the cells are briefly incubated in the new media to allow the adjustment to the new media and absorption of the UAA. Expression of recombinant proteasome subcomplex is then induced by the addition of IPTG and the protein complex is allowed to express for four hours at 30 °C and then left overnight at 18 °C. The complex was then purified first by running the lysate through a Ni-NTA column and then through an anti-FLAG M2 Antibody resin in the presence of ATP. The resulting FLAG elution was concentrated down to 500 uL and then further cleaned up and buffer exchanged into gel filtration/assay buffer by running it on a pre-equilibrated Superose 6 Increase SEC column.

Previous work with AzF incorporation used a six-fold concentration of cells into buffered TB media (Bard et al., 2018). Due to the insolubility of the Bpa UAA, systematic testing was carried out to determine the ideal conditions for expression. My method requires dissolving the Bpa in sodium hydroxide to effectively salt-in the UAA. In order to rapidly optimize conditions for growth, I used a GFP reporter assay with an amber TAG codon positioned so that the fluorescence only evolves upon proper incorporation of Bpa. I confirmed that a 6-fold concentration of cells results in robust Bpa incorporation. However, unlike with AzF incorporation, the addition of a buffering component into the TB resulted in precipitation of the Bpa, making it unavailable to the *E. coli* resulting in poor incorporation as assayed by suppression of an amber codon-containing GFP construct (**Figure 2.3B**). Additionally, other groups have reported neutralizing the NaOH after dissolving the Bpa through the addition of an equivalent amount of HCl (Kolhe et al., 2023), which I found to also reduce Bpa incorporation

through the eventual precipitation of the UAA. Using this information, I proceeded to express recombinant 19S base with Bpa incorporation.

As previously mentioned, in order to select a position of incorporation of the UAA, two pieces of information were taken into consideration. Previous biochemical data from the Martin lab had shown that the motor subunits of the base subcomplex had different contributions to unfolding (Beckwith et al., 2013). This data showed that when the pore-1 loop tyrosine residue of Rpt1 was mutated to an alanine it still retained near 100% activity. In fact, both Rpt6 and Rpt5 also showed minimal defects when these mutations were made. I hypothesized that since removal of the bulk of Tyr seemed to have no effect in the unfolding and degradation of proteasomes, therefore the substitution of the pore-1 loop residue with a residue with similar properties, such as Bpa, would result in a functional unfoldase. Second, a structure of the proteasome in the process of translocating a substrate showed the path that a polypeptide takes through the central channel of the complex (de la Peña et al., 2018). It suggested several points at which the substrate either comes into physical contact or close proximity with the motor subunits (**Figure 2.4A**). From the entrance of the proteasome, the substrate first comes into proximity with an N-terminal ring made up by the oligosaccharide-binding (OB-fold) domains of Rpt1-6. However, this region is fairly wide and solvent exposed and there were few residues which could be mutated to either AzF or Bpa. Next, the substrate makes physical contact with the pore-1 loop of the Rpt large ATPase domain. This loop's sequence is fairly conserved in every Rpt and bears a Tyrosine residue which acts as the teeth on a gear to grip and pull on the substrate. Given the sequence conservation and role of the aromatic residue the pore-1 loop position seemed the best location to place a Tyrosine UAA analog. Next, the substrate came into proximity with the pore-2 loop, whose sequence was less conserved but largely was Glycine-rich.

Of the Rpt-TAG mutants that expressed and purified, SDS-PAGE showed a marked difference in the amounts of purified recombinant base, which was used as an initial measure of the functionality of the variants (**Figure 2.4B**). Rpt1-P1L (Y283TAG) and Rpt2-P1L (Y257TAG) expressed robustly, while the Rpt1-N-ring (Y181TAG) variant had modest expression. Most P2L variants I generated resulted in empty gels and size-exclusion traces with big voids. Two were able to be weakly seen via PAGE, Rpt1-P2L-1 (A323TAG) and P2L-2 (G325TAG). Rpt1-P1L and Rpt2-P2L size exclusion traces showed a similar elution volume to a wild-type control (**Figure 2.4C**).

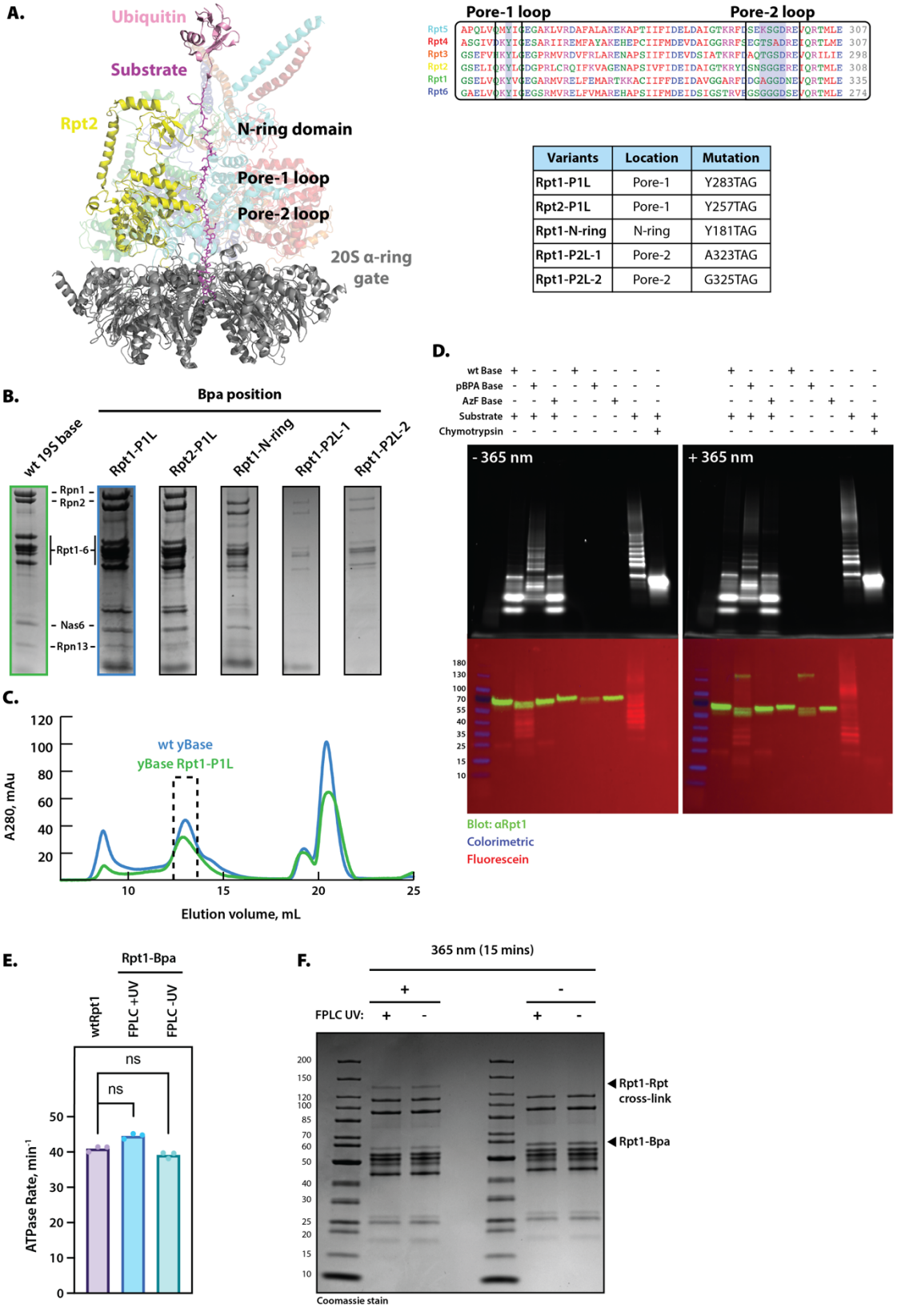

Variants	Location	Mutation
Rpt1-P1L	Pore-1	Y283TAG
Rpt2-P1L	Pore-1	Y257TAG
Rpt1-N-ring	N-ring	Y181TAG
Rpt1-P2L-1	Pore-2	A323TAG
Rpt1-P2L-2	Pore-2	G325TAG

Figure 2.4: Introduction of Bpa into the 19S base subcomplex of the proteasome

A. Structure of substrate path shows three points of close proximity with Rpt subunits, Rpt2 shown as an example (de la Peña et al., 2018, **PDB**: 6EF3.). Sequence alignment on the right shows Rpt proteins composition and conservation at pore-1 and pore-2 loop positions. **B.** SDS-PAGE gels of purifications of Bpa base variants. **C.** Representative size exclusion trace of Rpt1-P1L-Bpa compared to normal 19S base. **D.** Preliminary cross-linking experiment shows that Bpa base variants, but not AzF, crosslink in response to 365 nm light. **E.** ATPase rate of recombinant wt and Bpa-containing 19S base are comparable. Bpa-containing base was purified as described and cleaned up via size-exclusion with the 280 nm UV detector activated or deactivated to ensure that clean up by SEC did not induce unwanted crosslinking. **F.** Cross-linking assay visualized by SDS-PAGE demonstrates that Bpa-19S base crosslinks only upon irradiation by 365 nm light and not from the 280 nm detector of the FPLC.

To verify that the FPLC 280 nm UV detector does not affect the stability of the Bpa during purification, the SEC step was carried out with and without the UV detector and found that the detector did not induce unwanted crosslinking. We further tested whether incorporation of Bpa altered the activity of the proteasome by testing the ATPase rates of the base subcomplex and show that the Bpa-base exhibited similar ATPase rates to the unmodified subcomplex with a rate of about 40 ATP min^{-1} (**Figure 2.4E**). When analyzed by SDS-PAGE, we see that a crosslinking product appeared only after exposure to 365 nm light (**Figure 2.4F**) but not from elution from the SEC column with UV detection. This crosslink product corresponds to an Rpt-Rpt crosslink (see below, **Figures 2.4D** and **2.6B**).

In short, the biochemical and structural information predicted the pore-1 loop position to be the best position. Given the initial purifications, the P1L variants appeared to generate the most biochemically stable base subcomplexes. It is worth mentioning that yields of these recombinant bases were, at best, one-third the yield of a normal recombinant base prep. This was also confirmed by others in the lab who used my Bpa plasmid for their own crosslinking studies, most notably in the expression of ubiquitin which normally expresses quite well. However, the Bpa-incorporation plasmid (pULTRA-Bpa) I cloned for these recombinant expressions is based on the original publication and therefore does not have some of the more optimized plasmid features that some other more modern UAA plasmids contain. It would probably be possible to optimize the Bpa plasmid for better expression, but for my purposes it served its job well.

2.B.iii. Assaying crosslinking proteasomes

The first question was whether to use AzF or Bpa as the crosslinking UAA in my approach. As mentioned earlier, both AzF and Bpa have been reported to cross link when irradiated with UV light at wavelengths of 254 and 365 nm, respectively (Shao et al., 2015; Chin & Schultz, 2002). A lower-energy UV exposure is optimal—it reduces the damage that cells would take during the crosslinking which could theoretically change the proteome being measured, as well as avoiding damage to the proteins themselves. To initially assay crosslinking, reconstituted proteasomes containing wildtype, AzF-, or Bpa-containing Rpt1 were assayed for crosslinking using 365 nm light. Wild type proteasomes and AzF-containing proteasomes did not show any crosslinking, while Bpa containing proteasomes showed a UV-dependent shift to a higher MW weight band (**Figure 2.4D**). UV light at 254 nm has been historically used for experimentally inducing DNA damage, sterilization of lab equipment, and has been

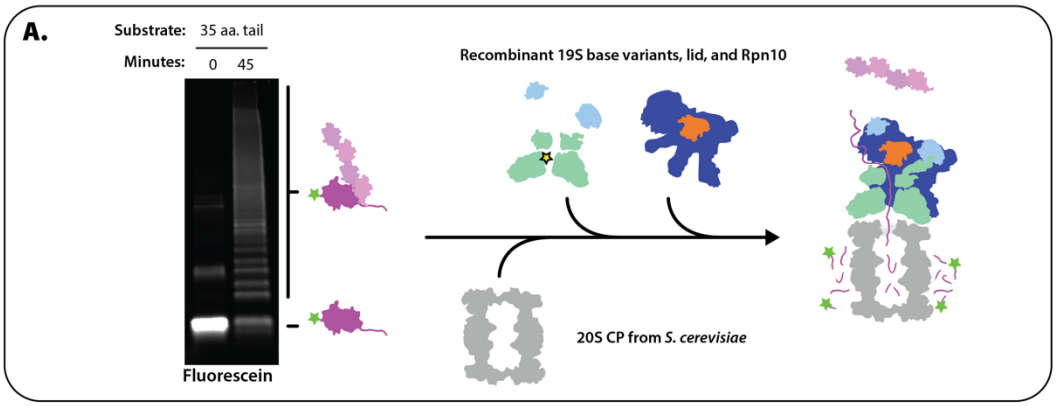
A.
Substrate:
35 aa. tail
Minutes:
0
45
Fluorescein
Recombinant 19S base variants, lid, and Rpn10
20S CP from S. cerevisiae

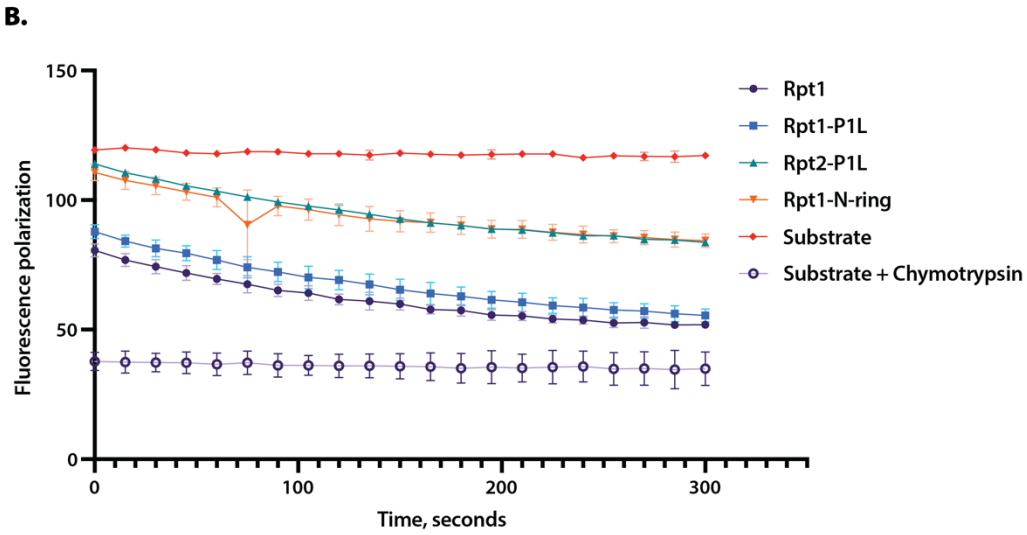
B.
Fluorescence polarization
150
100
50
0
0
100
200
300
Time, seconds
Rpt1
Rpt1-P1L
Rpt2-P1L
Rpt1-N-ring
Substrate
Substrate + Chymotrypsin

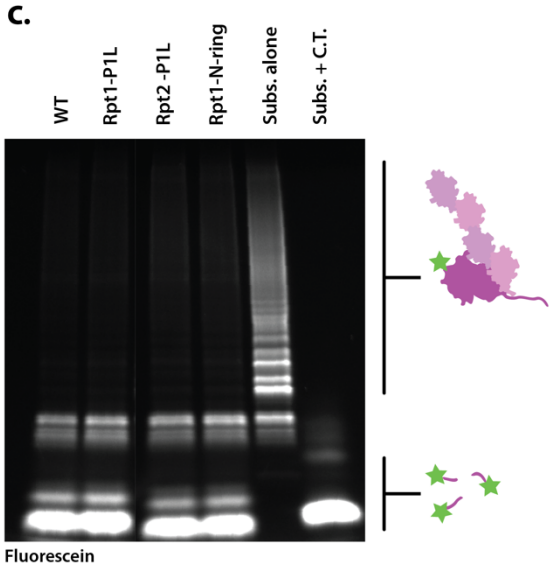
C.
WT
Rpt1-P1L
Rpt2 -P1L
Rpt1-N-ring
Subs. alone
Subs. + C.T.
Fluorescein

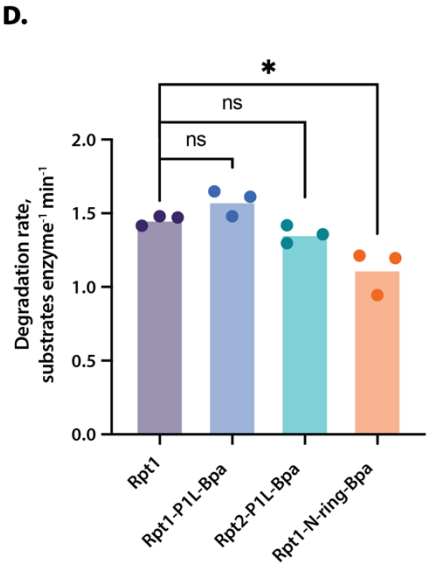
D.
*
ns
ns
Degradation rate, substrates enzyme-1 min-1
2.0
1.5
1.0
0.5
0.0
Rpt1
Rpt1-P1L-Bpa
Rpt2-P1L-Bpa
Rpt1-N-ring-Bpa

Figure 2.5: Reconstitution and substrate degradation by Bpa-variant 26S proteasomes.

A. Bpa-containing 26S proteasome holoenzyme can be reconstituted *in vitro* by incubating recombinant 19S base variants and lid to form 19S and adding 20S CP purified endogenously from yeast. A fluorescently-labeled model substrate composed of a Titin-I27 domain with a 35 amino acid cyclin B tail is *in vitro* ubiquitinated and incubated with 26S holoenzyme to monitor degradation. **B.** Raw traces monitoring the loss of fluorescence polarization of labeled Titin substrate being degraded into peptides. **C.** Gel-based endpoint assay confirms that assembled Bpa proteasome variants indeed degrade ubiquitinated substrates into peptide products. **D.** Multiple-turnover degradation monitored by fluorescence anisotropy of substrates demonstrates that Bpa proteasomes can carry out substrate turnover.

known to result in changes in protein abundance, which are not seen with 365 nm light (Ruskowitz & DeForest, 2019). These experiments, in addition to the literature supporting the robustness of Bpa as a crosslinker over aryl azides (Galardy et al., 1973), eliminated AzF as a viable candidate for crosslinking.

To assay the activity of Bpa-containing base variants, I measured their degradation of a model substrate, a titin-I27 domain fused to a disordered 35-amino acid cyclin-B-derived tail. This model titin substrate is labeled at its N-terminus with a fluorescein dye using sortase chemistry so that degradation can be monitored using a decrease in fluorescence anisotropy (**Figure 2.5B**). To recruit the substrate to 26S, its ubiquitination with reconstituted Uba1 (E1), Ubch7 (E2) and Rsp5 (E3) enzymes. The ubiquitination reaction was optimized so that the substrates had medium-length chains which would migrate well via SDS-PAGE for western blotting (**Figure 2.5A**). Proteasome holoenzyme was then reconstituted by incubating 50 nM 20S core peptidase purified from yeast with 0.4 uM recombinant lid and 0.6 uM wild type or Bpa-variant base. Lid and base complex were added in excess to ensure that 20S was doubly capped. Holoenzyme was mixed with excess ubiquitinated substrate at 2uM to measure the multiple-turnover degradation, as substrate K_M has been previously measured to be approximately 0.22 uM (Bard et al., 2019). Endpoint analysis by in-gel fluorescence of the titin substrate showed that all variants could degrade a poly-ubiquitinated substrate and converting it into peptides, however not at the same rates (**Figure 2.5C**). The Rpt1-P1L-Bpa variant had the most similar degradation to the wildtype rate of 1.45 substrates enzyme^{-1} min^{-1}, with 1.58 substrates enzyme^{-1} min^{-1}, followed by the Rpt2-P1L-Bpa and then Rpt1-N-ring-Bpa variants with rates of 1.35 and 1.11 substrates enzyme^{-1} min^{-1}, respectively (**Figure 2.5D**). It is interesting to note that the base assembly efficiencies correlated well with their degradation rates, although it was surprising to see a slight defect in degradation with the positioning of the Rpt1-N-ring-Bpa variant. Perhaps the positioning of a bigger residue at the entrance to the pore somehow impairs substrate entry, but this was not investigated further.

To assay the UV-dependent crosslinking of reconstituted proteasome to substrate, degradation reactions were prepared as described and allowed to proceed either covered or exposed to 365 nm light. Despite being incubated with a poly-ubiquitinated model substrate, which appears as a laddering smear when run on a gel, the initial crosslinking experiments showed the 56 kDa Rpt1 band shifting to a single band of approximately 120 kDa. The appearance and approximate size of the UV product suggested that Rpt1-Bpa was forming a covalent adduct with another Rpt in the ring of the motor. My initial hypothesis was that proteasomes were processing substrates too

quickly such that upon crosslinking the most-accessible polypeptide was from an adjacent Rpt motor protein. Stalling the substrate would allow the Bpa-base to crosslink to a smear of poly-ubiquitinated substrates. To test this hypothesis, the experiment was repeated with holoenzymes reconstituted with a 19S lid containing a catalytically-dead Rpn11 deubiquitinase, $Rpn11^{AXA}$. The $Rn11^{AXA}$ mutation prevents removal of ubiquitin chains from substrates during translocation and leads to proteasomal stalling on the uncleavable isopeptide bond (**Figure 2.6A**). Analyzing this new set of reconstituted degradations via an endpoint gel assay, I confirmed that $Rpn11^{AXA}$ holoenzymes resulted in impaired degradation and an accumulation of ubiquitinated titin substrate (**Figure 2.6B, AXA lanes**). Western blotting of these stalled reactions against Rpt1 revealed a shift of the Rpt1 band into a smear corresponding to UV-dependent crosslinking to a polyubiquitinated titin substrate (**Figure 2.6B, bottom**).

In addition to the 33 subunits that compose the holoenzyme, the proteasome is a hub for the binding of many proteins, some which interact transiently. To ensure that the crosslinking is a result of translocation and not crosslinking of transient interactors, proteasome crosslinking was assayed with a poly-ubiquitinated substrate with a single amino acid tail which has been previously demonstrated as failing to engage by the proteasome (Bard et al., 2019). Incubation with a standard 35 amino acid tail substrate resulted in the characteristic crosslink smear, while incubation with the 1-mer tailed substrate showed only Rpt-Rpt crosslinking (**Figure 2.6C**). These results show that crosslinking occurs robustly with substrates which are actively being engaged and translocated by the proteasome base, while excluding proteins which may be either transiently bound to the proteasome or are otherwise unengaged by the 19S motor.

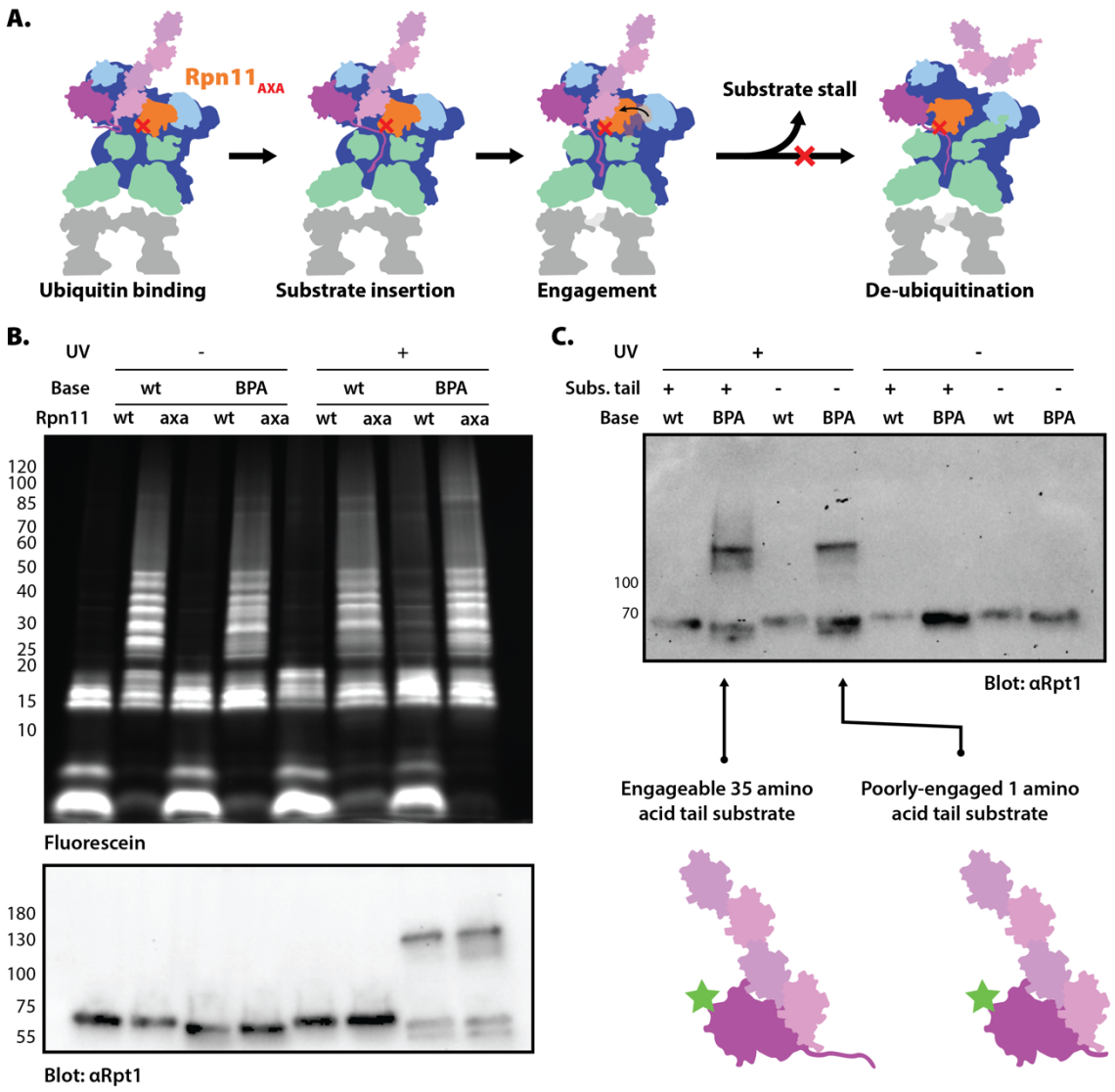

Figure 2.6: Reconstituted Bpa-26S cross-links to substrate in a UV- and engagement-dependent manner.

A. Scheme of modified reconstitution degradation. 26S that is reconstituted with a lid containing a catalytically-dead Rpn11 variant ($Rpn11^{AXA}$) results in no de-ubiquitination and stalling of the substrate. **B.** Western blot analysis of stalled 26S-substrate complexes show a UV-dependent smear corresponding to Rpt1 cross-linking to poly-Ub substrate input. **C.** Bpa-26S incubated with a substrate with a non-engaging 1 amino acid tail results in a disappearance of the Rpt1-substrate smear by blot.

2.C. Expression of cross linking 26S base in live budding yeast cells

Having verified that Bpa incorporation into the 19S base results in a functional holoenzyme which crosslinks to substrates in a UV-dependent manner, I then aimed to implement this crosslinking approach in live cells. My original approach was to express an extra copy of an Rpt with the Bpa incorporated which would be incorporated into holoenzyme and result in a subset of proteasomes in the cells containing the crosslinker. As described in section 2B of this thesis, incorporation of Bpa in *S. cerevisiae* into functional 26S holoenzyme was verified, thus the next step was to settle on a method for expressing the Bpa-containing motor subunit and attempt crosslinking in live cells.

2.C.i Cloning of pSNR-AzF-RS and pSNR-Bpa-RS

As reviewed earlier in this chapter, incorporation of both AzF and Bpa had been described in eukaryotes in work carried out by the legendary Jason Chin and colleagues in Peter Schultz's group as early as 2003. In 2008, Qian Wang and Lei Wang further improved this system by optimizing yeast expression of the amber-suppressor tRNA. What follows below is the saga of how I had to re-engineer these plasmids for my thesis research.

I reached out to Lei Wang's group at UCSF, who kindly provided me with the pSNR tRNA-synthetase pair plasmid and a reporter plasmid with a constitutively expressed green fluorescent protein (GFP) with an amber stop codon insertion at position 39 (pGFP-39-TAG) for testing incorporation in yeast (**Figure 2.7A**). The pSNR-TyrRS plasmid was transformed into XL1 Blue *E. coli* cells to amplify the DNA and make a glycerol stock, but the transformation produced no colonies. Surprised that there were no colonies on the plate, I left the plate growing an extra night. The following day, I was able to see small colonies on the plate which led me to believe that an extra copy of a modified tRNA and tRNA synthetase present in *E. coli* resulted in a growth defect. Indeed, all subsequent transformations of pSNR variants required at least two day's growth following transformation, which was an important, but unmentioned, consideration when cloning variants of the pSNR plasmid. The pSNR UAA system uses a constitutively expressed *E. coli* tyrosine tRNA synthetase (ecTyrRS), which has been mutated to both accommodate the modified Tyr-tRNA and either AzF or Bpa, depending on the mutations present on the ecTyrRS (**Figure 2.7C**).

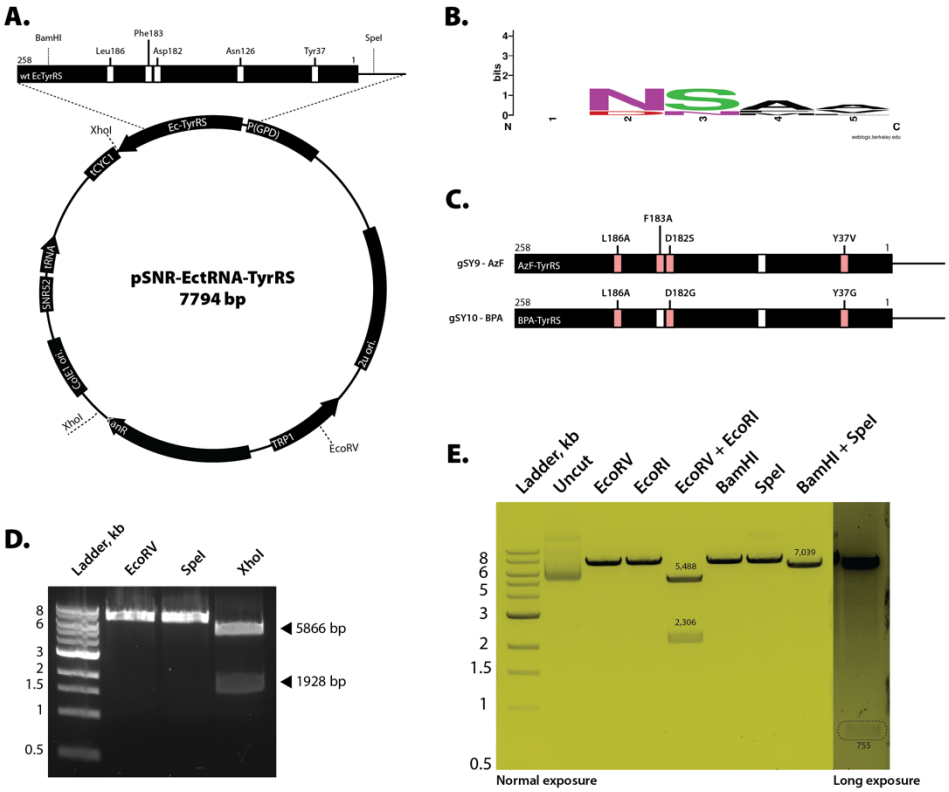
A.
BamHI
Phe183
Leu186
Asp182
Asn126
Tyr37
SpeI
258
wt-EcTyrRS
1
XhoI
Ec-TyrRS
P(GPD)
T(CYC1)
pSNR-EctRNA-TyrRS
7794 bp
tRNA
SNR52
CoIE1 ori
XhoI
ApR
TRP1
EcoRV
2μ ori
B.
bits
4
3
2
1
0
N
C
C.
F183A
L186A
D182S
Y37V
gSY9 - AzF
AzF-TyrRS
L186A
D182G
Y37G
gSY10 - BPA
BPA-TyrRS
D.
Ladder, kb
EcoRV
SpeI
XhoI
8
6
3
2
1.5
1
0.5
5866 bp
1928 bp
E.
Ladder, kb
Uncut
EcoRV
EcoRI
EcoRV + EcoRI
BamHI
SpeI
BamHI + SpeI
8
6
5
3
2
1.5
1
0.5
5,488
2,306
7,039
755
Normal exposure
Long exposure
F.
+ AzF
pSNR-AzfRS
pSNR-BpaRS
pSNR-TyrRS
WT
+ BPA
pSNR-AzfRS
pSNR-BpaRS
pSNR-TyrRS

Figure 2.7: Reconstituted Bpa-26S cross-links to substrate in a UV- and engagement-dependent manner.

A. Plasmid map of the pSNR-ecTyrRS plasmid containing the amber codon suppressor tRNACUA and the wildtype E. coli Tyr tRNA synthetase with relevant amino acid-interacting positions which can be changed to accommodate AzF or Bpa. **B.** Sequence logo of the AzfRS variants. **C.** Mutations made to the TyrRS for incorporation of AzF and Bpa. **D.** Agarose gel of restriction enzyme digest of pSNR-TyrRS showing that a cryptic XhoI cutting site prevented the published cut/paste cloning to generate TyrRS variants. **E.** A new cloning strategy for inserting the RS variants utilized BamHI and SpeI to drop the coding region of the pSNR plasmid and Gibson the correct variant. **F.** Yeast expressing the three pSNR variants (TyrRS, AzfRS, or BpaRS) and a GFP-39-TAG reporter were grown in the presence of the indicated UAA, showing the specificity for the pSNR-BpaRS plasmid. Surprisingly, the AzFRS variant used was unable to incorporate its UAA.

Upon receiving the plasmid and sequencing it, I confirmed that the plasmid was the unmodified pSNR-ecTyrRS. In Supplementary Table 1 within the supplementary material of the original 2003 Science paper, one can find all of the point mutations that can be made on the ecTyrRS to generate various forms of UAA-RS (Chin et al., 2003). For the generation of a pSNR-Bpa-TyrRS plasmid, I was able to find specific variants that had been used experimentally (Wang et al., 2007). However, the pSNR-AzF-TyrRS plasmid was not so straightforward, there were six different variants and the original paper did not indicate which one was used. To try and determine which sequence elements were important for the AzF-Rs, I took all six variant sequences and generated a sequence logo, which indicated that variants 2 or 3 had the most conserved elements from the six variants (**Figure 2.7B**).

Having identified the TyrRS variants, I then set out to recreate the pSNR-AzF-TyrRS and pSNR-Bpa-TyrRS plasmids. Several publications indicated that swapping the TyrRS for a variant could be accomplished using restriction enzyme sites for XhoI and SpeI, which flanked the TyrRS open reading frame (**Figure 2.7A**). However, upon digestion of the plasmid with the indicated enzymes it became clear that there was a second unannotated XhoI site which complicated the cut-paste cloning (**Figure 2.7D**). Despite various attempts at trying to clone this plasmid, including PCR amplification of the backbone for Gibson insertion, it evaded cloning until 2021 when whole-plasmid sequencing via nanopore technology became the standard. With this new technology, the whole plasmid, including all cryptic restriction enzyme cut sites, could be determined. Eventually, I was able to insert the correct variants into the plasmid by cutting within the TyrRS gene using the BamHI and SpeI enzymes (**Figure 7E**). This restriction digest dropped a 755 bp segment of the TyrRS gene and allowed for the insertion of the modified segment of the gene with a Gibson assembly using a synthesized gene portion.

To test out the amber codon suppression of the resulting plasmids, I transformed the pSNR-Bpa and AzF plasmids into yeast containing the pGFP-39-TAG plasmid. Cultures of each pSNR strain were grown in media supplemented with AzF or Bpa (2mM final) and then allowed to grow overnight. Following overnight growth, the cultures were spun down, resuspended with PBS and imaged for GFP fluorescence. The subsequent yeast strains were then grown in media containing either AzF or Bpa. As expected, in the presence of Bpa only the pSNR-Bpa-RS containing yeast were able to suppress the amber stop codon as seen by GFP fluorescence (**Figure 2.7F**). Surprisingly, the pSNR-AzF-RS plasmid did not suppress the amber codon. Perhaps a different set of mutations in the wild type TyrRS results in better suppression of AzF,

but having successfully cloned the desired Bpa RS plasmid, I did not pursue cloning of an AzF construct further.

2.C.ii. Expression of crosslinking Rpt1/Rpt2 using a GAL-inducible system

To first try incorporation of an extra Rpt subunit bearing a Bpa, I generated a galactose-inducible expression plasmid containing the N-terminally HA-tagged versions of Rpt1 and Rpt2 with an amber stop codon at the corresponding pore-1 loop position. These constructs were transformed into yeast containing the pSNR-Bpa-RS plasmid and grown in media with 2% raffinose and 0.1% glucose. After the cells reached mid-log phase, expression of either Rpt1 or Rpt2 was induced by the addition of galactose to 4% final concentration. Cells were harvested after reaching stationary phase, flash frozen, cryo-ground, and proteasome holoenzyme was purified using anti-FLAG antibody resin to pull on the FLAG-tag on the 20S core peptidase subunit PRE1. The concentrated elution of both samples showed that 26S had been purified from both strains. However, blotting for the HA tag on the Bpa-containing subunit showed that only HA-Rpt1-Bpa had been incorporated and purified along with the rest of the proteasome.

These results confirmed that an exogenously expressed copy of Rpt1-Bpa is incorporated into the 26S (**Figure 2.8A**). Surprisingly, the results for the same experiment but with the HA-Rpt2-Bpa variant showed that Rpt2-Bpa was not incorporated into holoenzyme, despite having confirmed that an Rpt2-Bpa base forms a functional motor and holoenzyme with reconstituted proteins. These results highlight that there are still unknown aspects of proteasome assembly in the cell. However, having confirmed the expression and incorporation of Rpt1-Bpa, I decided to move forward with Rpt1 for *in vivo* crosslinking experiments.

2.C.iii. Expression of crosslinking Rpt1 using an orthogonal human hormone receptor system.

The shift from glucose to galactose results in major transcriptional changes in yeast, additionally it induces a major stress known as the diauxic shift, which can ultimately result in the death of many cells. Galactose induction of protein expression leads to strong expression of the target protein but comes with the aforementioned caveats. To avoid perturbing the cells, and thus the proteome, I employed a method for

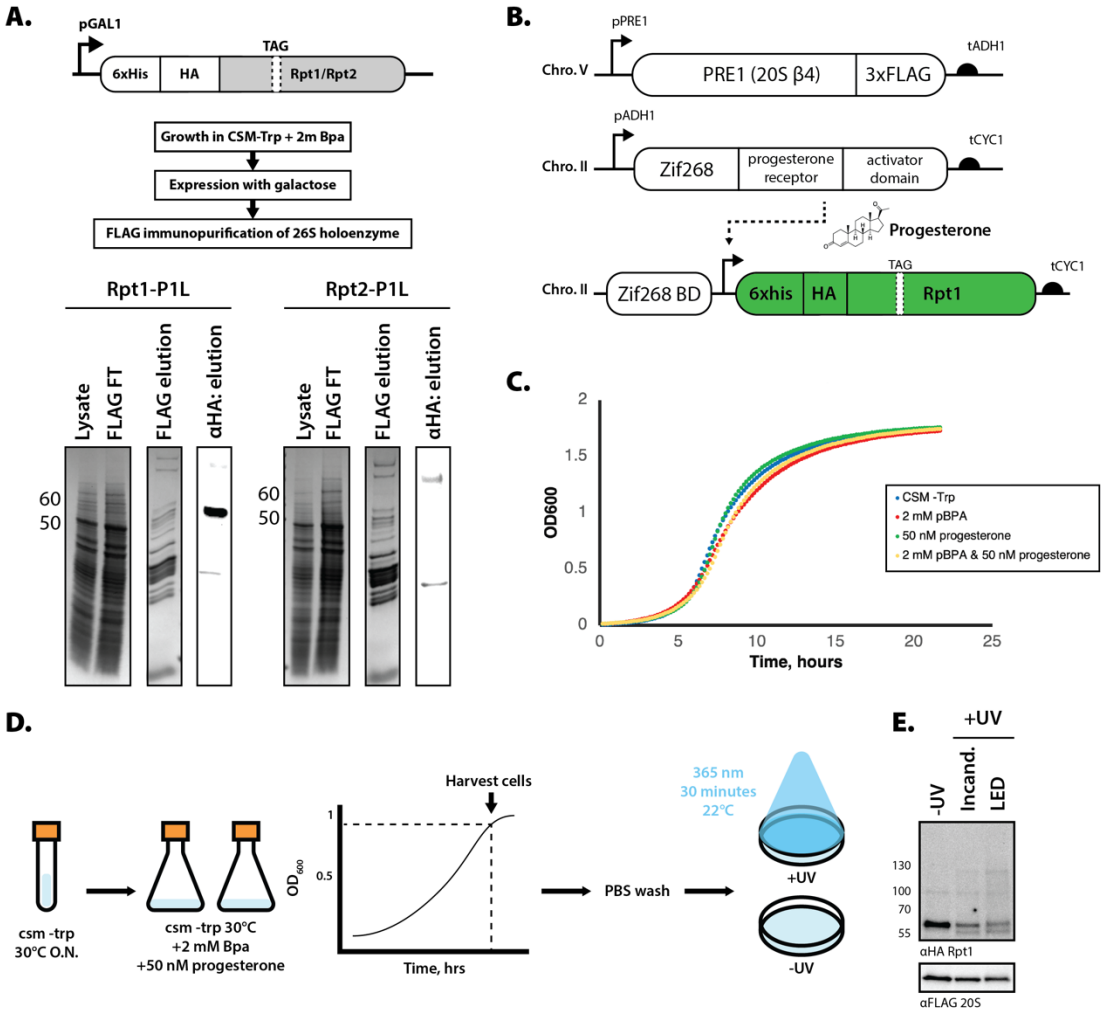

Figure 2.8: In vivo expression of Rpt1-Bpa and cross-linking to substrates.

A. Galactose-induced expression of HA-tagged Bpa-Rpt1 and Bpa-Rpt2 followed by purification of yeast holoenzymes shows that Bpa-Rpt1, but not Bpa-Rpt2, is incorporated into yeast holoenzymes. **B.** Orthogonal expression system of HA- and 6xhis-tagged Bpa-Rpt1 via the addition of the human hormone progesterone. Endogenous locus of 20S subunit PRE1 is 3xFLAG-tagged for purification and western blotting. **C.** Yeast growth is not altered by the presence of Bpa or the expression of Rpt1 via progesterone. **D.** To cross-link, cells were grown in selection media in the presence of 2 mM Bpa and 50 mM progesterone until late log phase, harvested, washed with PBS, and split into two dishes. One dish was exposed to 365 nm light for 30 minutes at 22°C and the other was left in the dark. **E.** Results of in vivo cross-linking using two different 100W 365 nm light sources, an incandescent lamp and an LED lamp. Both show robust cross-linking in vivo comparable to the *in vitro* reconstituted cross-linking reactions.

expressing Rpt1 that was orthogonal to endogenous yeast transcription. This new system, originally developed by Aranda-Diaz and colleagues at UCSF, initiates expression of a protein of interest in yeast through the addition of a human hormone, progesterone (Aranda-Díaz et al., 2016). In short, a human progesterone receptor ligand-binding domain is fused to a ZIF268 DNA-binding domain (DBD) as well as a yeast transcriptional activator (MSN-AD). The hybrid receptor-activator is sequestered in the cytoplasm by molecular chaperones and addition of progesterone displaces the chaperone from the receptor and allows it to be translocated into the nucleus. The protein of interest coding sequence can be downstream of the ZIF268 DNA element, for orthogonal expression of the protein (**Figure 2.8B**).

Progesterone, its receptor, and ZIF268 are all mammalian components and have no effects on normal yeast transcription other than the expression of the introduced protein. To test this, yeast transformed with the Bpa tRNA and tRNA synthetase plasmid under -Trp selection were grown in selection media lacking tryptophan in the presence of 2 mM Bpa, 50 nM progesterone or both to measure any growth defects from the addition of either chemical or the expression of an extra copy of Rpt1. Growth curves from the experiments showed that there was no growth defect in the yeast (**Figure 2.8C**), so in all subsequent experiments cells were grown in the presence of 2 mM Bpa, and 50 nM progesterone from a starting OD_{600} of 0.1. Cells were harvested when they reached late log phase (OD_{600} = 0.7), washed, and resuspended in PBS. The cell suspension was split into two dishes with one placed under a 365 nm lamp for 30 minutes (**Figure 2.8D**). The same number of cells from each plate were then harvested, lysed, and the lysate ran on SDS-PAGE, and transferred onto a PVDF membrane using an iBlot 2.0 system. Blotting against the HA tag on Rpt1 demonstrated a UV-dependent disappearance of HA-Rpt1 accompanied by the appearance of a higher molecular weight smear identical to the results seen with reconstituted 26S with Bpa-containing 19S base and a model substrate (**Figure 2.8E**).

Previous *in vitro* reconstituted experiments were carried out under an incandescent bulb-containing 100W 365 nm lamp. This lamp set up worked well for small-scale crosslinking but had two issues. First, the nature of the spot bulb meant that it had a narrow area for crosslinking and resulted in the lamp and the sample becoming very hot. Second, the cost of the lamp meant that scaling up would be expensive. For the purpose of scaling up crosslinking, a set of four 100W 365 nm LED lamps were acquired, which were available to buy on Amazon and were substantially more affordable than the incandescent lamp. Cell crosslinking was carried out as described above and I confirmed that the LED lamps were just as, if not more, efficient than the traditional incandescent lamp (**Figure 2.8E**).

2.D. Discussion

Incorporation of UAAs is a powerful chemical biology tool. Through mutation, protein machinery which reads and translates the genetic code can be used to add a non-canonical functional group to a protein of interest. Amino acids with new functional groups in their side chains have allowed for the site-specific labeling of proteins, the introduction of post-translational modification mimics, and crosslinking functional groups for the study of protein-protein interactions. While UAA incorporation has been used to site-specifically label recombinantly expressed 19S proteasome regulatory particle subcomplexes, it has never been used for crosslinking mass spectrometry protein-protein interaction studies in the proteasome. Incorporation of a UAA in a live cell is less common, and this approach has certainly not been used within the proteasome before.

Using a structure-guided approach, it was possible to site-specifically incorporate a photo-crosslinking UAA, *p*-benzoyl-L-phenylalanine, into the proteasome with no defect in function. The original 19S base reconstitution showed that a tyrosine to alanine mutation of the pore loop residue of the base resulted in different effects on degradation, with Rpt1 being the least disrupted. In agreement with this, introduction of Bpa into the pore 1 loop position of the base results in a proteasome base with relatively normal degradation. This crosslinking proteasome variant can crosslink to *bona fide* proteasome substrates in a UV-dependent manner. Having found a location and tested the functionality of crosslinking base unfoldase, using Bpa incorporation machinery that has been developed for yeast *in vivo* crosslinking was also tested. An adapted orthogonal expression system allows for the expression of Bpa-containing 19S base in live yeast, which shows a UV-dependent crosslinking to multiple species as with the reconstituted proteasomes. The incorporation of Bpa into the proteasome and subsequent crosslinking to substrates represents the first *in vivo* trapping of 19S-dependent proteasome substrates in live cells. With the affinity tag on the crosslinking subunit, Rpt1, it should be possible to then affinity purify the covalently trapped substrates for mass spectrometry identification, which will be discussed in the next chapter of this thesis.

Chapter 3

Capture and Identification of 26S Proteasome Substrates in Living Cells

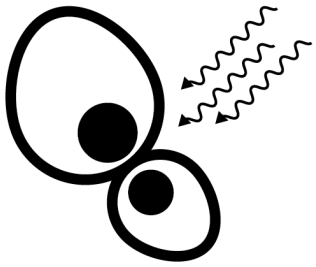

3A. Mass spectrometry as a tool in proteomics

The goal of this thesis was the identification of actively-translocating proteasome substrates—the proteins covalently crosslinked to Rpt1 in live cells after exposure to UV light. The gold standard technique for the sequencing and identification of proteins is mass spectrometry (MS). In this chapter, I will first briefly introduce the technique by outlining the theory of MS, its implementation in the field of proteomics, and its pairing with chemical crosslinkers. Then I will describe my own work in the expression of a crosslinking protein in live cells, *in vivo* crosslinking, and determination of proteasome substrates in live cells by their purification and identification by MS. Because mass spectrometry is an incredibly sensitive technique, I will also spend a considerable amount of time discussing my processing of the data to determine the cut-off for what I will call a putative proteasome substrate.

3.A.i. Mass spectrometry theory

All mass spectrometer instruments ultimately provide a measurement of the mass to charge ratio (m/z) of an ion. An analyte is ionized so that it may be manipulated (accelerated, decelerated, filtered, or trapped) using electric and magnetic fields and its mass to charge ratio is measured by a mass analyzer (Olshina & Sharon, 2016). The exact method by which the analyte mass is analyzed depends on the instrument, and many current MS instruments contain multiple mass analyzers within the same instrument. The analyte may be fragmented into smaller ions, which can be used to further determine the structure or composition of the original molecule. This core MS design is usually paired with digestion of proteins into peptides and an upstream analyte separation step, which in turn makes MS a very precise methodology for measuring complex samples.

3.A.ii. Mass spectrometry for proteomics

Proteomics is the study of the protein complement of the genome and mass spectrometry became the standard technique for analyzing the proteome. A typical mass spec proteomics experiment begins with a protein sample, either whole-cell protein extract or an affinity purified sample from cells or tissues. First the proteins are denatured to linearize the protein sequences, disulfides are reduced and alkylated to prevent reformation, and the linearized sample is digested with a protease to generate peptides. Typically, protein samples are digested with trypsin which is a serine-threonine protease that preferentially cuts after positively charged residues. Digestion

with trypsin does two things in MS sample prep, first it produces peptides which are, on average, 8-15 amino acids long—this mass range is ideal for detection on an MS instrument. Second, its amino acid selectivity ensures that each peptide contains at least two ionic groups, a positively charged amino group and a positively charged residue. This makes sample manipulation by the instrument easier, since MS requires the acceleration of charged analytes. Depending on the sample being analyzed, other proteases may be used such as chymotrypsin which may change the physicochemical properties of the peptides generated and increase coverage of a sample or a particular protein (Giansanti et al., 2016).

To begin with a complex mixture of proteins and end with a protein sequence, a proteomics MS workflow employs a liquid chromatography mass spec-mass spec workflow (LC-MS/MS), meaning that the peptides undergo two rounds of mass analysis. Peptides resulting from a protein sample are separated by size and hydrophobicity by a reverse phase C18 column via a liquid chromatography system (LC). As peptides elute off the column, they are ionized into the instrument which undergoes a series of steps to measure the masses of the peptides in the sample. First, the instrument does a survey scan, or MS1, across a range of m/z to measure the masses and relative abundances of the peptides coming off the LC. It then picks one ion (corresponding to a peptide), typically the most abundant ion within the survey scan, filters for that ion's m/z, and fragments that ion into smaller ions (peptide fragments or peptide fingerprints as they are sometimes called). There are many methods to fragment peptides (precursor or parent ions) into smaller ions (fragment or daughter ions), but most commonly the precursor ion is accelerated into a neutral gas such as nitrogen, which results in its fragmenting. Peptides fragment in characteristic ways, and the masses of the resulting ions are measured to generate an MS2 spectra. Having measured an MS1 and MS2 pair the instrument will then go back to the survey scan and select another ion to fragment and measure. After a given number of scans or a length of time, the instrument will then collect another survey scan and begin the process again. These steps are known as the instrument duty cycle and the speed at which the instrument can cycle through the collection of this data depends on how many mass analyzers and the method by which they carry out the mass analysis and ultimately determine what coverage of the sample the instrument samples.

By the end of a run, the instrument has collected information about the retention time, precursor mass, and fragment masses of as many peptides as the duty cycle allowed it to. To then go from MS to information about the protein content of the original sample, the instrument data (RT, MS1, MS2) must undergo a database search to match the acquired data to proteins from the organism in which the experiment was

performed. Effectively what the database search does is fingerprint the collected spectra against theoretical spectra generated from all the possible peptides of possible protein products of the organism. The result of this database search is a list of all the proteins from the organism database for which spectra in the data were matched, this is known as a peptide-spectra match or PSM.

3.B. Purification of proteasome-substrate crosslinks and 26S holoenzyme MS analysis

Having confirmed that Bpa-Rpt1 is expressed and crosslinks in live cells, I wanted to confirm that I could purify substrate-holoenzyme crosslinks by purifying the proteasome fraction from yeast lysate. From an overnight starter culture, eight liters of complete synthetic media without tryptophan (Csm-Trp), supplemented with 1X Yeast Nitrogen Base (YNB), 2% glucose, and 2 mM Bpa were inoculated to a starting OD_{600} of 0.1 and incubated with shaking at 30 °C for 30 minutes to allow import of Bpa into the cells. After the incubation, expression of Rpt1 was induced by the addition of 50 nM progesterone. Cells were grown until they reached mid-log phase (OD_{600} of 0.7, approximately 13 hrs of growth), and were harvested by centrifugation, washed once with sterile water, and resuspended in 400 mL of PBS, pH 7.4. To crosslink the cells, 50 mL of cell suspension was added to eight 150 x 25 mm tissue culture dishes and four of the dishes were exposed to 365 nm light for 30 minutes and the other half was left in the dark. The 365 nm lamps produce heat and to ensure that the cells did not overheat, the crosslinking exposure was carried out in a 4 °C cold room. There, the lamps heated the benchtop to approximately room temperature (22). Following crosslinking, +UV and -UV cells were harvested from plates into 50 mL conicals, centrifuged, resuspended with protease inhibitors, and drip-frozen with liquid nitrogen. The cell pellets were lysed by cryo-milling and resuspended in a buffer with ATP regeneration to prevent base disassembly and 0.2% NP-40. The lysate was incubated with regenerated FLAG resin in a rotator at 4 °C for 1 hour to bind the 3X FLAG tag on the 20S. The lysate-resin mixture was poured into a glass chromatography column and allowed to flow-through, followed by two washes. The proteasome fraction was eluted by the addition buffer with 0.15 mg/mL FLAG peptide and concentrated using a 30K MWCO spin concentrator.

Analysis of the elution by SDS-PAGE confirmed the purification of holoenzyme from both +UV and -UV conditions, with all components of the 20S and 19S present (**Figure 3.1A**). A western blot against HA-Rpt1-Bpa demonstrated a UV-dependent Rpt1 smear and confirmed that trapped substrates were being pulled down with holoenzyme (**Figure 3.1B, middle**). Since the FLAG affinity tag is located on the 20S core, this also indicates that the proteasome holoenzyme does not disassemble with a substrate stalled in the 19S pore. Interestingly, although the two preparations appeared identical when visualized by stain-free gel, Coomassie staining of the gel resolved the appearance of an additional >10 kDa protein in the +UV holoenzyme prep (**Figure 1A, bottom**). Since ubiquitin cannot be visualized by stain-free gels due to its lack of

tryptophan residues and given the size of the band, I hypothesized that this band might be free ubiquitin removed from crosslinked poly-ubiquitinated substrates.

To test this hypothesis, I blotted the +/-UV preparations for ubiquitin. Surprisingly, the anti-ubiquitin blot revealed a ubiquitin smear in both +UV and -UV samples. This indicates that, despite extensive washing, ubiquitin conjugates co-purify with proteasome holoenzymes. Additionally, the ubiquitin smear from +UV holoenzyme preps was significantly diminished in size. To further verify these results, the +/-UV samples were methanol precipitated, reduced, alkylated, trypsin digested, and the peptides were analyzed by mass spectrometry for protein identification. While this preliminary MS analysis confirmed the presence of all 33 proteasome components in both the +UV and -UV samples, it also confirmed that many proteins co-purify with 26S in these preparations. In total, MS analysis identified 627 different proteins across the +UV and -UV FLAG elutions (see **Appendix Tables 2.1 & 2.2**). While 51 proteins were identified in only the +UV samples, there were 108 proteins identified in only the -UV samples, and 468 proteins were shared across the two conditions. Amongst these co-purifying proteins were several deubiquitinating enzymes, including the proteasome associated DUB Ubp6, which is proposed to trim chains on the proteasome. The presence of this DUB in the proximity of a crosslinked and stalled poly-ubiquitinated substrate could explain the UV-dependent appearance of monoubiquitin via gel.

Taken together, this system allows Bpa-Rpt1 to be expressed and incorporated into 26S proteasome where it can crosslink to ubiquitinated substrates. The crosslinked substrates form a stalled substrate-holoenzyme, which does not appear to be disassembled in the timescale of the duration of crosslinking and harvesting. Furthermore, stalled substrates appear to have modified ubiquitination. This modification is likely through the action of 26S-associated deubiquitinating enzymes, but it is unclear if the effect seen is due to Rpn11 removal of ubiquitin during translocation or trimming by another associated DUB, such as Ubp6. However, the co-purification of many ubiquitinated proteins as seen by blotting and by MS analysis demonstrates that a more stringent approach to purifying Rpt1-substrate crosslinks must be used.

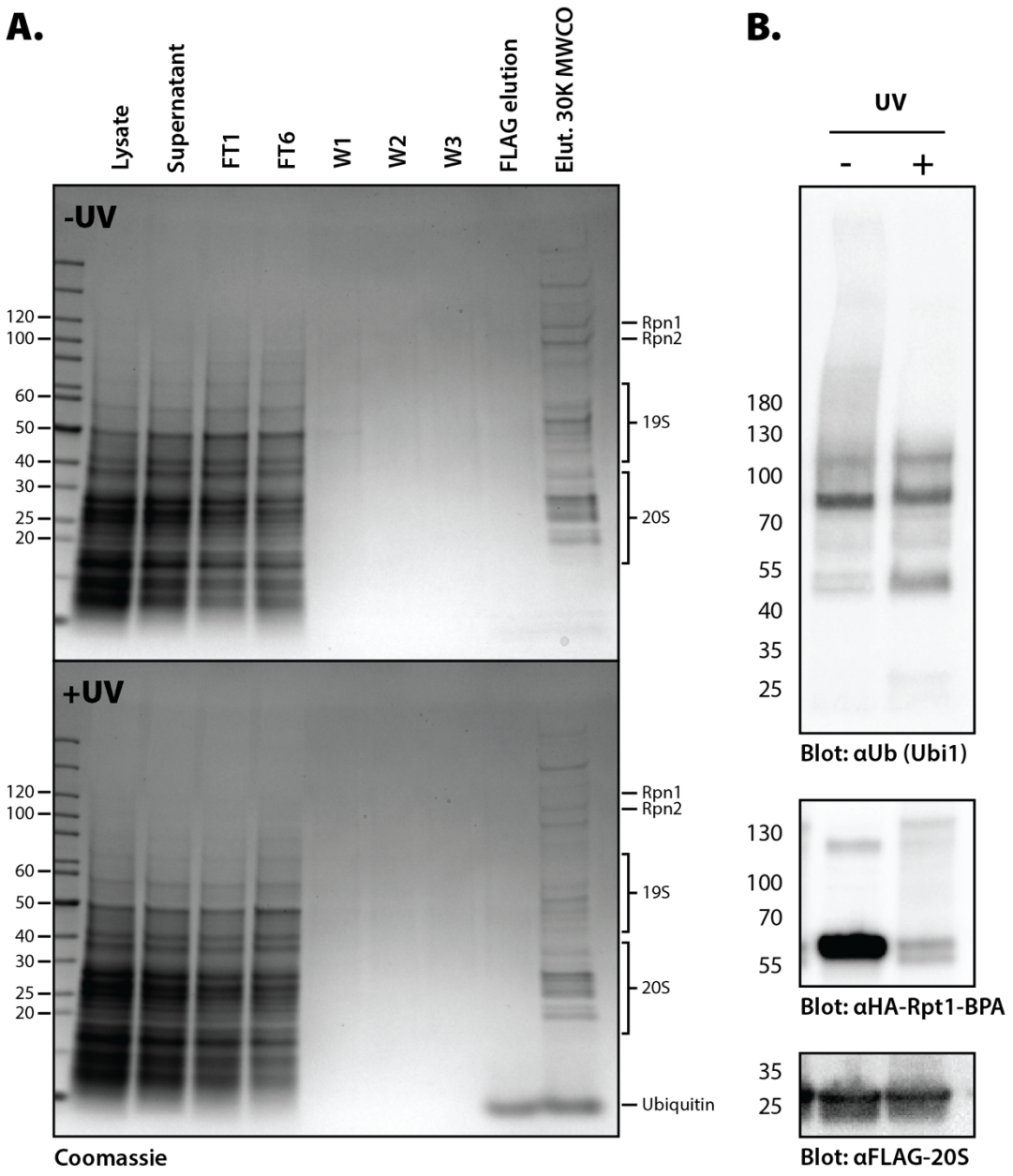

Figure 3.1: FLAG purification of crosslinked 26S holoenzyme reveals multiple co-purifying ubiquitinated species.

A. FLAG purification of 26S from crosslinked yeast shows that cross-linking does not promote 26S disassembly. Instead, cross-linking appears to induce the appearance of ubiquitin monomers. **B.** Western blotting of FLAG elution reveals that purified 26S indeed contains crosslinked Rpt1-Bpa. Anti-ubiquitin blotting also reveals that poly-ubiquitinated species co-purify with uncrosslinked holoenzymes despite extensive washing. Crosslinked substrates demonstrate diminished ubiquitination, perhaps due to the activity of a co-purifying deubiquitinase.

3.B.i. Denaturing prep for Rpt1-substrate crosslinks

Given that MS is an inherently concentration-dependent technique, I opted for the purification of Rpt1-substrate crosslinks using a denaturing immobilized metal affinity chromatography (IMAC) approach to remove as many background proteins from the sample as possible and boost the Rpt1-substrate signal. IMAC is a denaturant-compatible purification strategy which relies on separating proteins based on their affinity for metal ions. The most common recombinant IMAC purification approach employs the use of a poly-histidine tag fused to the target protein, which can chelate metal ions and separate the target protein out of a complex mixture. The protein can then be eluted by the addition of excess imidazole.

Denaturing the sample with urea or guanidine hydrochloride (GdnHCl) unfolds proteins and disrupts all protein-protein interactions, including separating all 26S subunits. When the denatured sample is run over an IMAC resin, a 6x histidine-tagged HA-Rpt1 should remain bound to the resin along with any crosslinked proteins. However, working with denaturants in protein preparations adds some caveats which are worth mentioning. First, while urea is commonly used in trypsin digestion prior to MS, both compounds must be removed from the sample prior to injection into the instrument. Secondly, they both complicate sample analysis by SDS-PAGE and therefore western blotting. In particular, guanidinium is incompatible with SDS-containing sample buffers and will precipitate immediately upon its addition, this also precludes certain forms of MS sample-prep, such as S-traps. Urea precipitates at low temperatures, but even without precipitation at low temperatures the high concentration will produce smears on an SDS-PAGE gel, which made searching for an Rpt1-substrates smear difficult.

To find the optimal conditions for purification, I tried several iterations of the typical IMAC binding, wash, and elution buffers looking for the combination that resulted in a 6x-his Rpt1 band with minimal contamination as determined by SDS-PAGE. It is worth noting that yeast contains many poly-histidine containing proteins, which are going to have to be interpreted as background in the final data analysis (Peng et al., 2003; See below). I grew and crosslinked yeast for these experiments as previously described, and resuspended the ground lysate with a denaturing binding buffer to make sure the lysate was denatured before flowing over Ni-NTA agarose pre-equilibrated with a denaturing binding buffer. My original purification approach utilized 8 M urea throughout the preparation, but I quickly found that from these urea preps the Ni-NTA elution was fairly dirty.

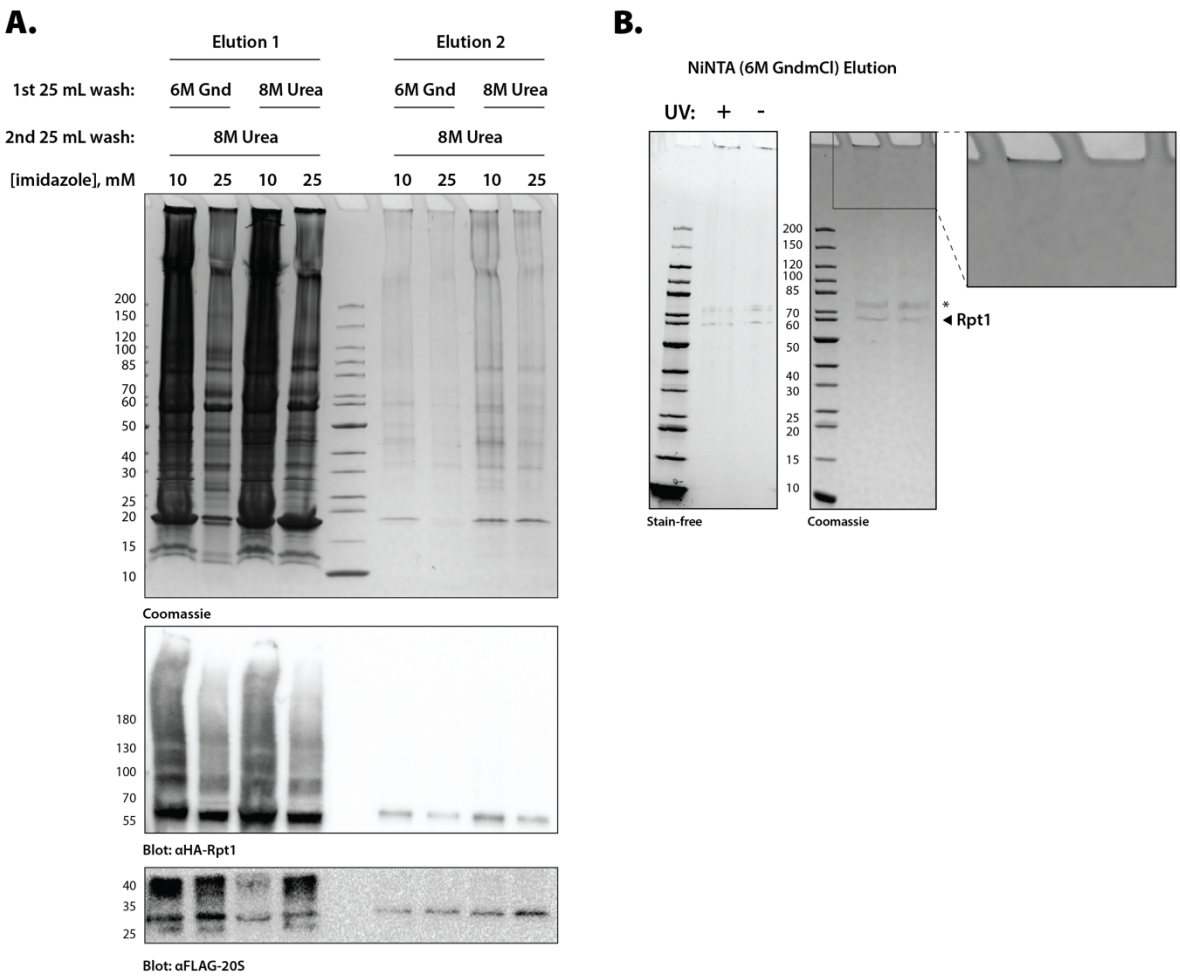

Figure 3.2: Conditions for a denaturing NiNTA preparation of Rpt1-substrate crosslinks.

A. Elutions from denaturing NiNTA purification from yeast expressing HA-6xhis-Rpt1-Bpa. Elution purity is highest when samples are initially denatured in GdnHCl and with 25 mM imidazole wash steps. Second elution samples show that most his-tagged Rpt1 has eluted in the first volume. **B.** Stain-free and coomassie stain gels of elution from denaturing prep of *in vivo* crosslinked samples. Elution is relatively clean and Rpt1 band at 56 kDa is shown. Elutions from +UV samples show smearing and species caught in the gel well. *Denotes a contaminant band from a histidine-rich yeast protein.

With the hypothesis that the urea was not completely separating interacting proteins, I switched to using 6 M guanidine for the initial binding buffer. I sought to measure the difference between urea and guanidinium and the effect of the concentration of imidazole in the washes on the cleanliness of the elution. To do this, I carried out four separate IMAC preps with two washes: an initial wash in either 6 M Gnd or 8 M urea followed by a second wash in 8M urea. For each of these two conditions, I also varied the concentration of imidazole at either 10 or 25 mM to reduce background binding to the Ni-NTA. From this test purification it was clear that an initial wash in 6 M Gdn and 25 mM imidazole resulted in the cleanest elution (**Figure 3.2A**).

Seeing that the relative purity of the elution was dependent on guanidine as the denaturant and on the presence of 25 mM imidazole in the washes, I then carried out a purification of an *in vivo* crosslinked sample. Crosslinked yeast was flash frozen in liquid nitrogen and lysed by cryo-milling. The subsequent lysate powder was resuspended in 8 M Gnd HCl binding buffer containing 10 mM imidazole, to a final concentration of 6 M Gnd. The lysate was run over Ni-NTA resin pre-equilibrated with binding buffer, washed first with 6 M Gnd, 10 mM imidazole wash buffer, followed by a 6 M Gnd, 25 mM imidazole wash, and then eluted using an elution buffer containing 6 M Gnd, 250 mM imidazole. The samples were concentrated using a spin concentrator and run on an SDS-PAGE gel to visualize the elution. Visualization of the gel showed relatively pure samples with a 56 kDa band corresponding to Rpt1-Bpa (**Figure 3.2B**). While there were some contaminant bands visible, it was encouraging to see that the elution from the +UV sample had a smear and additionally had what appeared to be high-molecular weight species which struggled to migrate from the well into the stacking section of the gel. With these results, I then proceeded to prepare these samples for mass spectroscopy.

3.C. Mass spectrometry identification of proteasome substrates

After optimizing the purification of Rpt1-substrate crosslinks, the next steps were to analyze those elutions using mass spectrometry. My original thought process for this approach assumed that the elution from a denaturing Ni-NTA clean up would result in clear identification by MS analysis and database searching of the measured spectra of proteasome substrates which would only be present in the +UV sample. It became clear both from the original FLAG purification of crosslinked holoenzymes, as well as the optimization of the Ni-NTA step, that identification of nonspecifically interacting proteins would convolute the data analysis and the -UV sample would contain more than just uncrosslinked 6xhisRpt1. This meant that sample analysis would not only be as binary as previously thought and that I might have to factor in relative abundances of proteins across the +UV and -UV treatments. The rationale was that non-specific binders will elute in relatively equal amounts in both conditions while cross linked substrates will be relatively enriched in the +UV conditions.

3.C.i. Timing of crosslinking in cells

One concern with using UV light as an initiator of crosslinking is the effect that the light itself will have on the cell and how that might induce changes in proteasome substrates. In order to determine the length of time needed for crosslinking, a crosslinking time course experiment was carried out to measure the dynamics of crosslinking and the viability of cells after crosslinking. Four liters of cells were grown as described previously to OD_{600} of 0.7. Cells were harvested, washed with sterile water, resuspended in PBS, and equally divided into four 150 x 25 mm tissue culture dishes. An uncrosslinked sample was taken and they were then crosslinked under 365 nm light for 2.5, 5, 15, and 30 minutes. A sample of each crosslinking condition was taken for blotting and for spotting assays.

While cells exposed to all lengths of time were still viable when regrown on a YPD plate, as shown by spotting assay, there was a 10-fold reduction in the number of cells between the 15- and 30-minute time point (**Figure 3.3A**). Western blotting for HA-Rpt1 showed that crosslinking to substrates occurs within 2.5 minutes of exposure to light. crosslinking increases in a time-dependent manner and appears to peak at 15 minutes, with a slight decrease after 30 minutes (**Figure 3.3B**). SDS-PAGE and Coomassie stain of the total protein lysate suggests that by 30 minutes there is a decrease in total protein content. Taken together these results suggest that the Bpa in

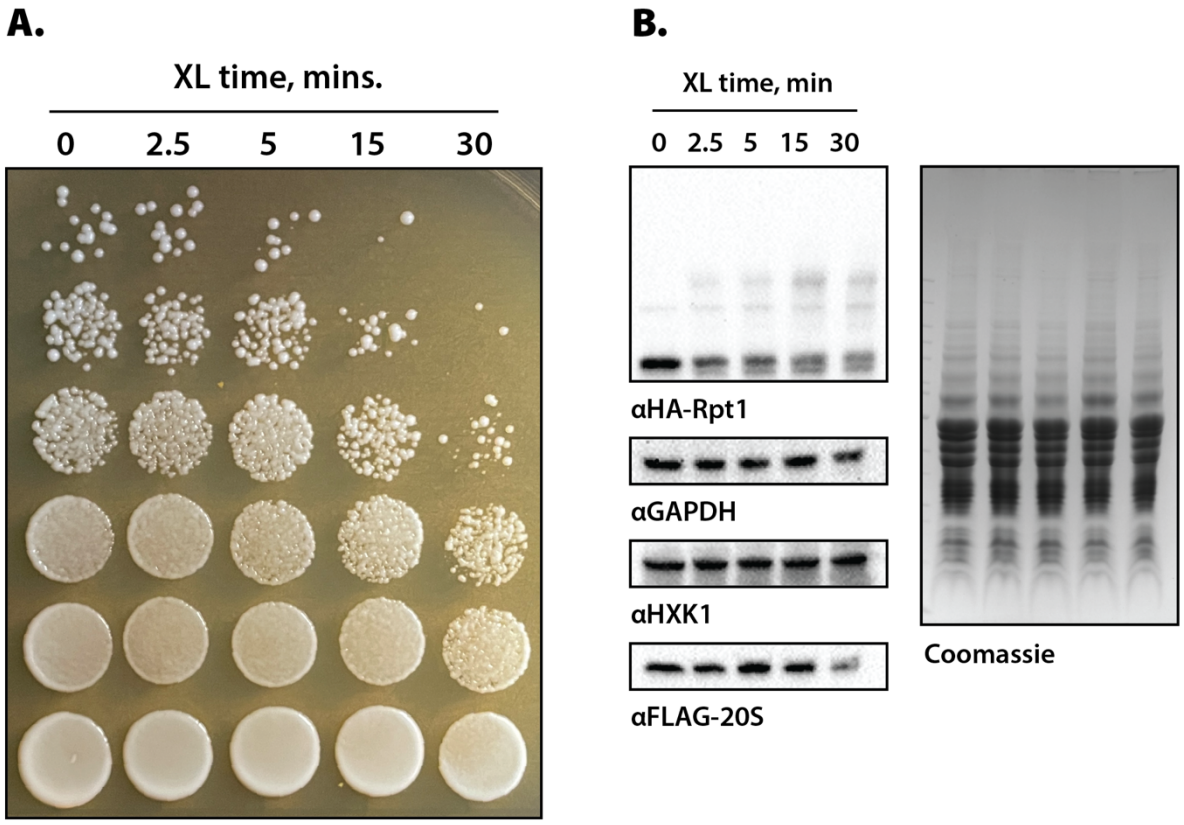

Figure 3.3: Optimization of *in vivo* UV exposure time.

A. Yeast were grown in complete synthetic media minus tryptophan (CSM-Trp) in the presence of 2 mM BPA and 50 nM progesterone until before late log phase, harvested, and exposed to 365 nm light at the indicated time points. A spot assay shows that yeast growth is unaffected up until 30 minutes of exposure. **B.** Western blot analysis of the cells from the same experiment shows that HA-Rpt1-Bpa crosslinking occurs within minutes and appears to peak after 15 minutes.

Rpt1 reacts quickly when exposed to 365 nm light. The crosslinking peaks at 15 minutes, after which the cell might begin to initiate a damage response to either DNA damage from the UV light or from the consequence of depletion of functional proteasomes. For the purpose of my proteasome substrate profiling experiments, I opted to continue with a crosslinking time of 15 minutes.

3.C.ii. Label-free quantification (LFQ) of proteins enriched in crosslinked samples

Preliminary mass spectroscopy experiments showed that indeed that, while there was more signal in the crosslinked +UV elution, there was a substantial amount of signal in the uncrosslinked -UV samples as well. Since there was overlap in the proteins found between the +UV and -UV conditions, I turned to label-free quantification (LFQ) of the proteins on a high-resolution Thermo Lumos MS instrument and, to achieve deeper coverage of low-abundance species, the samples were off-line high-pH (HpH) fractionated into eight fractions which were run as independent MS runs.

Yeast was grown as previously described in three biological replicates, with the only modification being that the cells were crosslinked for 15 minutes instead of 30 given the crosslinking time course data. Proteins eluted from Ni-NTA purification under denaturing conditions were methanol precipitated and digested with trypsin prior to HpH fractionation into 8 runs per condition (+/-UV) for three biological replicates resulting in a total of 48 nLC-MS/MS runs. For analysis, each replicate was treated as a comparison between pairs of +UV and -UV experimental conditions. First, the resulting spectra were searched against a database for the *S. cerevisiae* proteome using a 5% false discovery rate (FDR) cutoff for peptide-spectral matches (PSMs) and filtered to remove common contaminants, which resulted in the identification of over 3000 proteins in each of the replicates (**Figure 3.4A**). For a protein to be considered a putative proteasome substrate, it must have either been present exclusively in the +UV samples or be at least 2-fold enriched in the UV samples in all three biological replicates, when compared to the -UV control. The nature of the Bpa crosslinking chemistry and its position in an actively translocating motor meant that proteins could be crosslinked anywhere along the length of their primary sequences. This, in addition to the upstream affinity purification step, meant that standard LFQ methods, which use the same number of “top” peptides from a given protein to quantify and normalize across runs, were not optimal. Instead, the data was analyzed in two ways: first by comparing the total area from the nLC chromatogram for each identified protein across

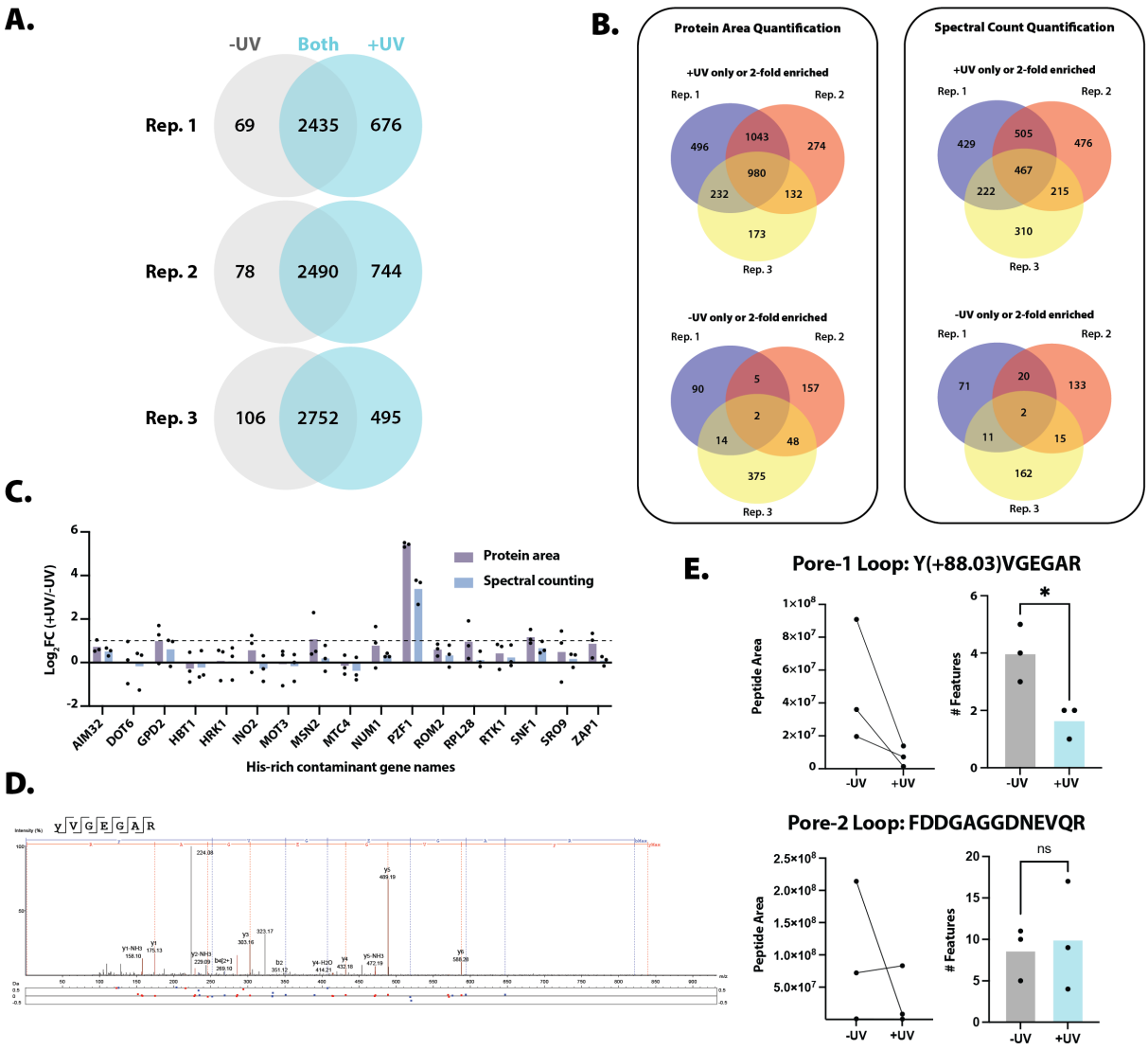

Figure 3.4: Label-free quantification approaches for determining putative substrate cut-off.

A. Protein identification overlaps across +/-UV pairs for each experimental replicate. **B.** Comparison of quantity of putative proteasome substrates based on two methods of quantification. **C.** 16 out of 17 established histidine-rich “contaminating” proteins used as internal standards show no relative enrichment with both quantification methods. **D.** Representative spectrum of Bpa-containing pore-1 loop peptide. The UAA y represents Bpa, or Tyrosine with a mass shift of 88.03 Da (Y+88.03). **E.** Quantification of pore-1 loop peptide (left) shows UV-dependent depletion of Bpa-containing peptide not seen in pore-2 loop peptide from the same data set (right).

the -UV and +UV conditions and in parallel by counting the peptide-spectral matches (spectral counting) for each protein. For each analysis, proteins which were either found only in the +UV sample or were enriched 2-fold over the -UV sample were labeled as putative proteasome substrates. The same analysis was also carried out for proteins which were seen only in the -UV samples or were 2-fold enriched in the -UV condition. Using these criteria, 980 proteins were identified as proteasome substrates using the area and 467 using spectral counting (**Figure 3.4B**). Conversely when the same analysis was carried out for proteins enriched or exclusively found in the -UV condition, only two proteins fit the criteria.

As mentioned before, the yeast proteome contains approximately 17 histidine-rich contaminant proteins which were identified along with other proposed contaminant proteins by the Gygi lab in their studies of the yeast ubiquitinome (Peng et al., 2003). To compare both methods of quantitation (Total area vs. spectral counting), the fold-change of these contaminants was compared under the assumption that, under the conditions of a denaturing Ni-NTA prep, the relative abundance of these histidine-rich contaminant proteins should be approximately equal in both the +UV and -UV denaturing preparations. Under both quantitation methods, 16 out of the 17 his-rich proteins failed to meet the criteria for 2-fold enrichment across all three replicates (**Figure 3.4C**). The only significantly enriched histidine-rich protein was PZF1, or transcription factor IIIA (TFIIIA), which demonstrated an enrichment (8- and 16-fold by spectral counting and total protein intensity, respectively) in crosslinked over uncrosslinked cells and may represent a bona fide putative proteasome substrate.

I was curious about the Bpa-containing peptides derived from Rpt1-Bpa, so the database search was modified to include a +88.03 Da variable modification on Tyrosine, representing the mass difference of the Bpa UAA. With this variable modification, spectral matches were made in the data containing the modification. From these spectral matches I identified two tryptic peptides from Rpt1 were a match: the Bpa-containing pore-1 loop sequence, and the same pore-1 loop region but with one missed tryptic cleavage. Interestingly, when inspecting the Bpa-containing Rpt1 peptide there was a marked decrease in the peptide abundance in the +UV condition as measured by both the chromatographic area, but especially by the number of spectral features (**Figure 3.4E**). I interpreted this difference as corresponding to the loss of the pore-1 loop Bpa peptide spectra as it became convolved with the spectra of the substrate peptides and thus becoming unmatchable to a standard database search. To verify this, I carried out the same analysis for the pore-2 loop peptide from the same data and no significant UV-dependent depletion was observed.

To understand what types of proteins were being identified as substrates, the hits from quantification methods were analyzed using the STRING database of known and predicted protein-protein interactions by showing only the highest confidence physical interactions and clustering the results by k-means clustering into 90 and 40 clusters for the chromatographic and spectral counting hits, respectively (Szklarczyk et al., 2023). The analysis of the physical interactome of the protein hits from both quantification methods revealed that the largest pool of substrates is involved in protein translation (**Figure 3.5A**). Amongst the other highly sampled categories were DNA replication and histone remodeler complexes involved in transcriptional regulation, such as the SAGA complex. Many protein hits, while not part of a larger complex, were involved in general metabolism including lipid and amino acid metabolism and the TCA cycle. Analysis of Gene Ontology enrichment of cellular compartment terms over the yeast proteome showed significant enrichment for various compartments with the highest being the cytoplasm (**Figure 3.5B**). Organelle-localized, nuclear, and even mitochondrial proteins were enriched. There was good agreement on the cellular compartment agreement between hits across the two quantification methods.

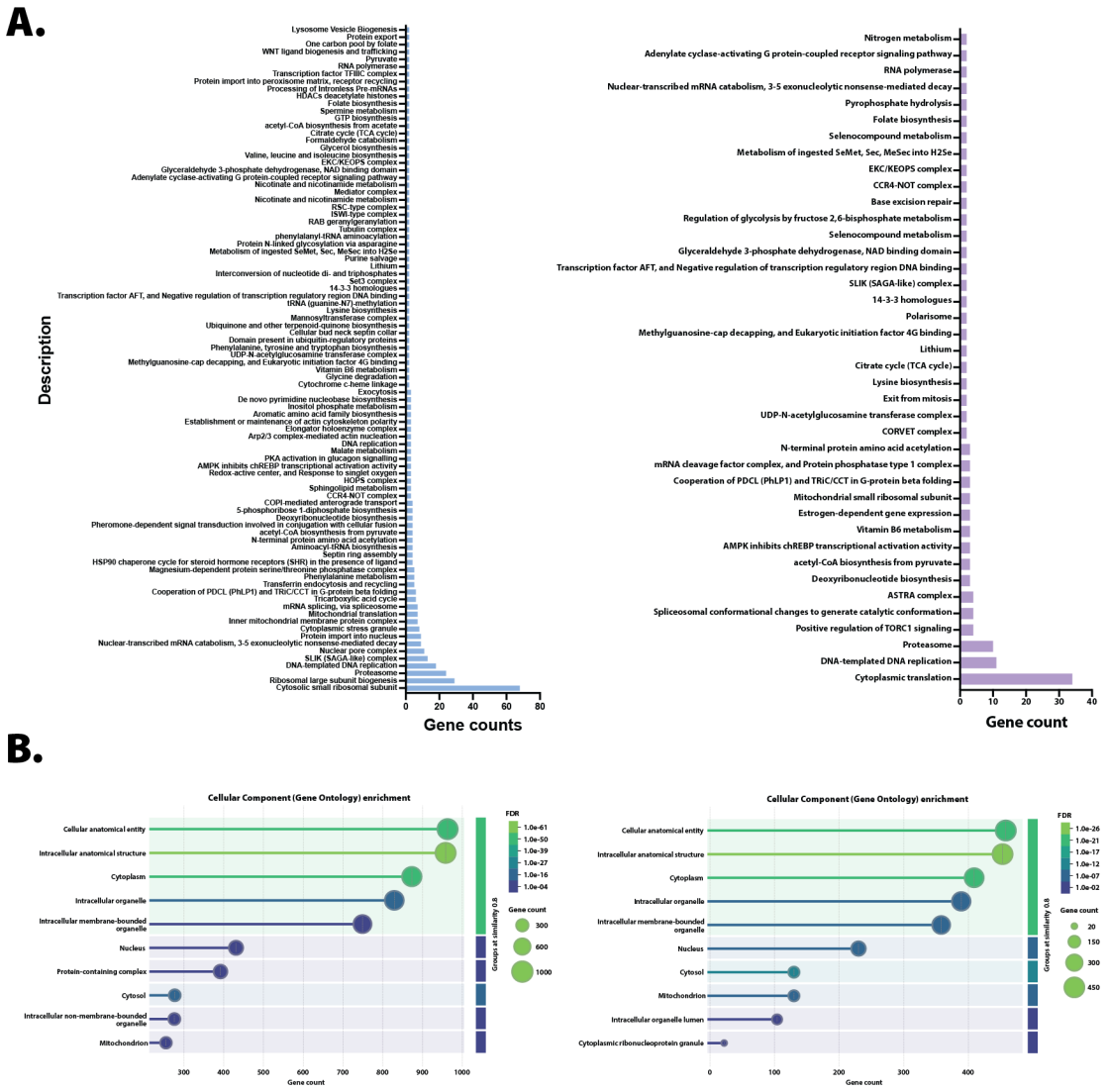

Figure 3.5: Biological context of identified putative proteasome substrates.

A. STRING PPI clusters of genes identified by both MS quantification methods, with protein area on the left and spectral counts on the right. For both the major annotation is proteins involved in translation. **B.** GO enrichment for terms related to the cellular localization for putative substrates.

3.D. Discussion

Trapping and isolating proteasome substrates posed a significant challenge. First, unlike other profiling strategies such as ribosome profiling, the signal that one is trying to measure is destined for degradation and inhibition of this function of the proteasome leads to major cell defects. Additionally, given that the proteasome is a large multi-protein complex, measuring the signal becomes difficult. Mass spectrometry is the gold-standard technique for sequencing and identifying proteins from a complex mixture, but it is concentration-dependent analysis. Given that the proteasome proteins outnumber the substrates by at least 33:1, the analysis is already skewed against the ID of the substrate. Unlike sequencing of nucleic acids, which by the very nature of the biology of the molecule makes amplification of signals easy, this is not so straightforward with protein samples.

To work around these obstacles I, as previously described in Chapter 2, aimed to trap substrates upstream of degradation, but still during engagement. To work around the issue of concentration, I employed a denaturing purification approach which should strip apart protein complexes. Since the substrate is covalently added to the crosslinking Rpt1, the signal has already been captured and all other interactions should be washed away and only Ni-interactors, such as the histidine-tagged crosslinking Rpt1 should remain. Optimization of the purification conditions resulted in purification of Rpt1-substrate crosslinks which could then be analyzed by mass spectrometry.

However, even with denaturing conditions and stringent washes, mass spectrometry analysis of my samples showed significant overlap between the crosslinked and control conditions. This required the use of label-free quantification to determine which proteins were significantly enriched across all three crosslinked biological replicates. In the end, I settled on analyzing my putative substrate hits in two different ways, which I verified by using common contaminants as surrogate internal standards. Altogether I was able to identify between 467 and 980 putative proteasome substrates. These substrates, as expected, span a wide range of biological functions across the various compartments of the cell, but functional enrichments can be seen. From these initial proteasome profiling experiments, we can see that the major function of the proteasome, by number of substrates, in actively dividing cells is degradation of translation components. This is interesting considering that the proteasome is already implicated in both the degradation of ribosome subunits and in quality control of translation at the ribosome.

The mass spectrometry identification of these substrates still leaves many open questions and experimental avenues regarding this approach for proteasome substrate identification. Firstly, diving into the putative substrates to find interesting complexes to generate yeast strains with tagged versions of these proteins to verify protein ubiquitination or stabilization with the addition of proteasome inhibitors. A recent paper employing the same technique to find interactors of Hsp90 was able to use the list of protein hits to then generate a smaller database to narrow their search space and computationally identify crosslinked peptide pairs to find the exact positions of Bpa crosslinking (Kolhe et al., 2023). A preliminary analysis, not included in this thesis, has shown me that I should be able to do the same thing with my own MS datasets and I have already begun to find crosslinked peptide pairs, although only on subsets of my data set. I think the biggest information will be gained when comparing proteasome substrate pools across different conditions, such as adding stressors or inducing heat shock and comparing the enriched proteins. I am currently carrying out some follow up experiments on this to check ERAD via the addition of the glycoprotein synthesis inhibitor tunicamycin. Taken together, this work represents a new tool with which to probe the complex workings of regulated protein degradation in the cell.

References

An, H., & Harper, J. W. (2020). Ribosome Abundance Control Via the Ubiquitin–Proteasome System and Autophagy. *Journal of Molecular Biology*, *432*(1), 170–184. https://doi.org/10.1016/j.jmb.2019.06.001

Aranda-Díaz, A., Mace, K., Zuleta, I., Harrigan, P., & El-Samad, H. (2017). Robust Synthetic Circuits for Two-Dimensional Control of Gene Expression in Yeast. *ACS Synthetic Biology*, *6*(3), 545–554. https://doi.org/10.1021/acssynbio.6b00251

Arkinson, C., Dong, K. C., Gee, C. L., Costello, S. M., Marqusee, S., & Martin, A. (2024). *Nub1 traps unfolded FAT10 for ubiquitin-independent degradation by the 26S proteasome* (p. 2024.06.12.598715). bioRxiv. https://doi.org/10.1101/2024.06.12.598715

Bard, J. A. M., Bashore, C., Dong, K. C., & Martin, A. (2019). The 26S Proteasome Utilizes a Kinetic Gateway to Prioritize Substrate Degradation. *Cell*, *177*(2), 286-298.e15. https://doi.org/10.1016/j.cell.2019.02.031

Bard, J. A. M., & Martin, A. (2018). Recombinant Expression, Unnatural Amino Acid Incorporation, and Site-Specific Labeling of 26S Proteasomal Subcomplexes. In T. Mayor & G. Kleiger (Eds.), *The Ubiquitin Proteasome System: Methods and Protocols* (pp. 219–236). Springer. https://doi.org/10.1007/978-1-4939-8706-1_15

Bashore, C., Dambacher, C. M., Goodall, E. A., Matyskiela, M. E., Lander, G. C., & Martin, A. (2015). Ubp6 deubiquitinase controls conformational dynamics and substrate degradation of the 26S proteasome. *Nature Structural & Molecular Biology*, *22*(9), 712–719. https://doi.org/10.1038/nsmb.3075

Beck, M., Schmidt, A., Malmstroem, J., Claassen, M., Ori, A., Szymborska, A., Herzog, F., Rinner, O., Ellenberg, J., & Aebersold, R. (2011). The quantitative proteome of a human cell line. *Molecular Systems Biology*, *7*(1), 549. https://doi.org/10.1038/msb.2011.82

Beckwith, R., Estrin, E., Worden, E. J., & Martin, A. (2013). Reconstitution of the 26S proteasome reveals functional asymmetries in its AAA+ unfoldase. *Nature Structural & Molecular Biology*, *20*(10), 1164. https://doi.org/10.1038/nsmb.2659

Bodnar, N., & Rapoport, T. (2017). *Toward an understanding of the Cdc48/p97 ATPase* (No. 6:1318). F1000Research. https://doi.org/10.12688/f1000research.11683.1

Brandman, O., & Hegde, R. S. (2016). Ribosome-associated protein quality control. *Nature Structural & Molecular Biology*, *23*(1), 7–15. https://doi.org/10.1038/nsmb.3147

Brandman, O., Stewart-Ornstein, J., Wong, D., Larson, A., Williams, C. C., Li, G.-W., Zhou, S., King, D., Shen, P. S., Weibezahn, J., Dunn, J. G., Rouskin, S., Inada,

T., Frost, A., & Weissman, J. S. (2012). A ribosome-bound quality control complex triggers degradation of nascent peptides and signals translation stress. *Cell*, *151*(5), 1042–1054. https://doi.org/10.1016/j.cell.2012.10.044

Breckel, C. A., Johnson, Z. M., Hickey, C. M., & Hochstrasser, M. (2024). Yeast 26S proteasome nuclear import is coupled to nucleus-specific degradation of the karyopherin adaptor protein Sts1. *Scientific Reports*, *14*(1), 2048. https://doi.org/10.1038/s41598-024-52352-5

Chin, J. W., Cropp, T. A., Anderson, J. C., Mukherji, M., Zhang, Z., & Schultz, P. G. (2003). An Expanded Eukaryotic Genetic Code. *Science*, *301*(5635), 964–967. https://doi.org/10.1126/science.1084772

Chin, J. W., Martin, A. B., King, D. S., Wang, L., & Schultz, P. G. (2002). Addition of a photocrosslinking amino acid to the genetic code of Escherichia coli. *Proceedings of the National Academy of Sciences*, *99*(17), 11020–11024. https://doi.org/10.1073/pnas.172226299

Chin, J. W., Santoro, S. W., Martin, A. B., King, D. S., Wang, L., & Schultz, P. G. (2002). Addition of p-Azido-l-phenylalanine to the Genetic Code of Escherichia coli. *Journal of the American Chemical Society*, *124*(31), 9026–9027. https://doi.org/10.1021/ja027007w

Chin, J. W., & Schultz, P. G. (2002). In Vivo Photocrosslinking with Unnatural Amino Acid Mutagenesis. *ChemBioChem*, *3*(11), 1135–1137. https://doi.org/10.1002/1439-7633(20021104)3:11<1135::AID-CBIC1135>3.0.CO;2-M

Ciechanover, A. (2005). Intracellular protein degradation: From a vague idea thru the lysosome and the ubiquitin–proteasome system and onto human diseases and drug targeting. *Cell Death & Differentiation*, *12*(9), 1178–1190. https://doi.org/10.1038/sj.cdd.4401692

Ciechanover, A., Heller, H., Elias, S., Haas, A. L., & Hershko, A. (1980). ATP-dependent conjugation of reticulocyte proteins with the polypeptide required for protein degradation. *Proceedings of the National Academy of Sciences of the United States of America*, *77*(3), 1365–1368. https://doi.org/10.1073/pnas.77.3.1365

Ciehanover, A., Hod, Y., & Hershko, A. (1978). A heat-stable polypeptide component of an ATP-dependent proteolytic system from reticulocytes. *Biochemical and Biophysical Research Communications*, *81*(4), 1100–1105. https://doi.org/10.1016/0006-291x(78)91249-4

Cohen, M. M. J., Leboucher, G. P., Livnat-Levanon, N., Glickman, M. H., & Weissman, A. M. (2008). Ubiquitin–Proteasome-dependent Degradation of a Mitofusin, a Critical Regulator of Mitochondrial Fusion. *Molecular Biology of the Cell*, *19*(6), 2457–2464. https://doi.org/10.1091/mbc.e08-02-0227

Dang, F., Nie, L., & Wei, W. (2021). Ubiquitin signaling in cell cycle control and tumorigenesis. *Cell Death & Differentiation*, *28*(2), 427–438. https://doi.org/10.1038/s41418-020-00648-0

de Almeida, M., Hinterndorfer, M., Brunner, H., Grishkovskaya, I., Singh, K., Schleiffer, A., Jude, J., Deswal, S., Kalis, R., Vunjak, M., Lendl, T., Imre, R., Roitinger, E., Neumann, T., Kandolf, S., Schutzbier, M., Mechtler, K., Versteeg, G. A., Haselbach, D., & Zuber, J. (2021). AKIRIN2 controls the nuclear import of proteasomes in vertebrates. *Nature*, *599*(7885), 491–496. https://doi.org/10.1038/s41586-021-04035-8

De Duve, C., & Wattiaux, R. (1966). Functions of lysosomes. *Annual Review of Physiology*, *28*, 435–492. https://doi.org/10.1146/annurev.ph.28.030166.002251

de la Peña, A. H., Goodall, E. A., Gates, S. N., Lander, G. C., & Martin, A. (2018). Substrate-engaged 26S proteasome structures reveal mechanisms for ATP-hydrolysis–driven translocation. *Science*, *362*(6418), eaav0725. https://doi.org/10.1126/science.aav0725

Doma, M. K., & Parker, R. (2006). Endonucleolytic cleavage of eukaryotic mRNAs with stalls in translation elongation. *Nature*, *440*(7083), 561–564. https://doi.org/10.1038/nature04530

Dorman, G., & Prestwich, G. D. (1994). Benzophenone Photophores in Biochemistry. *Biochemistry*, *33*(19), 5661–5673. https://doi.org/10.1021/bi00185a001

Duttler, S., Pechmann, S., & Frydman, J. (2013). Principles of Cotranslational Ubiquitination and Quality Control at the Ribosome. *Molecular Cell*, *50*(3), 379–393. https://doi.org/10.1016/j.molcel.2013.03.010

Eshof, B. L. van den, Medfai, L., Nolfi, E., Wawrzyniuk, M., & Sijts, A. J. A. M. (2021). The Function of Immunoproteasomes—An Immunologists' Perspective. *Cells*, *10*(12), 3360. https://doi.org/10.3390/cells10123360

Fatima, A., Irmak, D., Noormohammadi, A., Rinschen, M. M., Das, A., Leidecker, O., Schindler, C., Sánchez-Gaya, V., Wagle, P., Pokrzywa, W., Hoppe, T., Rada-Iglesias, A., & Vilchez, D. (2020). The ubiquitin-conjugating enzyme UBE2K determines neurogenic potential through histone H3 in human embryonic stem cells. *Communications Biology*, *3*(1), 1–19. https://doi.org/10.1038/s42003-020-0984-3

Frottin, F., Schueder, F., Tiwary, S., Gupta, R., Körner, R., Schlichthaerle, T., Cox, J., Jungmann, R., Hartl, F. U., & Hipp, M. S. (2019). The nucleolus functions as a phase-separated protein quality control compartment. *Science (New York, N.Y.)*, *365*(6451), 342–347. https://doi.org/10.1126/science.aaw9157

Galardy, R. E., Craig, L. C., & Printz, M. P. (1973). Benzophenone Triplet: A New Photochemical Probe of Biological Ligand-Receptor Interactions. *Nature New Biology*, *242*(117), 127–128. https://doi.org/10.1038/newbio242127a0

Gardner, R. G., Nelson, Z. W., & Gottschling, D. E. (2005). Degradation-Mediated Protein Quality Control in the Nucleus. *Cell*, *120*(6), 803–815. https://doi.org/10.1016/j.cell.2005.01.016

Giansanti, P., Tsiatsiani, L., Low, T. Y., & Heck, A. J. R. (2016). Six alternative proteases for mass spectrometry–based proteomics beyond trypsin. *Nature Protocols*, *11*(5), 993–1006. https://doi.org/10.1038/nprot.2016.057

Gil, G., Faust, J. R., Chin, D. J., Goldstein, J. L., & Brown, M. S. (1985). Membrane-bound domain of HMG CoA reductase is required for sterol-enhanced degradation of the enzyme. *Cell*, *41*(1), 249–258. https://doi.org/10.1016/0092-8674(85)90078-9

Glotzer, M., Murray, A. W., & Kirschner, M. W. (1991). Cyclin is degraded by the ubiquitin pathway. *Nature*, *349*(6305), 132–138. https://doi.org/10.1038/349132a0

Gödderz, D., Schäfer, E., Palanimurugan, R., & Dohmen, R. J. (2011). The N-Terminal Unstructured Domain of Yeast ODC Functions as a Transplantable and Replaceable Ubiquitin-Independent Degron. *Journal of Molecular Biology*, *407*(3), 354–367. https://doi.org/10.1016/j.jmb.2011.01.051

Groll, M., Ditzel, L., Löwe, J., Stock, D., Bochtler, M., Bartunik, H. D., & Huber, R. (1997). Structure of 20S proteasome from yeast at 2.4Å resolution. *Nature*, *386*(6624), 463–471. https://doi.org/10.1038/386463a0

Gu, X., Nardone, C., Kamitaki, N., Mao, A., Elledge, S. J., & Greenberg, M. E. (2023). The midnolin-proteasome pathway catches proteins for ubiquitination-independent degradation. *Science*, *381*(6660), eadh5021. https://doi.org/10.1126/science.adh5021

Hampton, R. Y., Gardner, R. G., & Rine, J. (1996). Role of 26S proteasome and HRD genes in the degradation of 3-hydroxy-3-methylglutaryl-CoA reductase, an integral endoplasmic reticulum membrane protein. *Molecular Biology of the Cell*, *7*(12), 2029–2044. https://doi.org/10.1091/mbc.7.12.2029

Heo, J.-M., Livnat-Levanon, N., Taylor, E. B., Jones, K. T., Dephoure, N., Ring, J., Xie, J., Brodsky, J. L., Madeo, F., Gygi, S. P., Ashrafi, K., Glickman, M. H., & Rutter, J. (2010). A stress-responsive system for mitochondrial protein degradation. *Molecular Cell*, *40*(3), 465–480. https://doi.org/10.1016/j.molcel.2010.10.021

Hershko, A., Ciechanover, A., Heller, H., Haas, A. L., & Rose, I. A. (1980). Proposed role of ATP in protein breakdown: Conjugation of protein with multiple chains of the polypeptide of ATP-dependent proteolysis. *Proceedings of the National Academy of Sciences of the United States of America*, *77*(4), 1783. https://doi.org/10.1073/pnas.77.4.1783

Hirsch, C., Gauss, R., Horn, S. C., Neuber, O., & Sommer, T. (2009). The ubiquitylation machinery of the endoplasmic reticulum. *Nature*, *458*(7237), 453–460. https://doi.org/10.1038/nature07962

Hoffman, L., Pratt, G., & Rechsteiner, M. (1992). Multiple forms of the 20 S multicatalytic and the 26 S ubiquitin/ATP-dependent proteases from rabbit reticulocyte lysate. *Journal of Biological Chemistry*, *267*(31), 22362–22368. https://doi.org/10.1016/S0021-9258(18)41680-8

Hough, R., Pratt, G., & Rechsteiner, M. (1986). Ubiquitin-lysozyme conjugates. Identification and characterization of an ATP-dependent protease from rabbit reticulocyte lysates. *Journal of Biological Chemistry*, *261*(5), 2400–2408. https://doi.org/10.1016/S0021-9258(17)35950-1

Htet, Z. M., Dong, K. C., & Martin, A. (2024). *The deubiquitinase Rpn11 functions as an allosteric ubiquitin sensor to promote substrate engagement by the 26S proteasome* (p. 2024.10.24.620116). bioRxiv. https://doi.org/10.1101/2024.10.24.620116

Huh, W.-K., Falvo, J. V., Gerke, L. C., Carroll, A. S., Howson, R. W., Weissman, J. S., & O'Shea, E. K. (2003). Global analysis of protein localization in budding yeast. *Nature*, *425*(6959), 686–691. https://doi.org/10.1038/nature02026

Husnjak, K., Elsasser, S., Zhang, N., Chen, X., Randles, L., Shi, Y., Hofmann, K., Walters, K. J., Finley, D., & Dikic, I. (2008). Proteasome subunit Rpn13 is a novel ubiquitin receptor. *Nature*, *453*(7194), 481–488. https://doi.org/10.1038/nature06926

Inobe, T., Fishbain, S., Prakash, S., & Matouschek, A. (2011). Defining the geometry of the two-component proteasome degron. *Nature Chemical Biology*, *7*(3), 161–167. https://doi.org/10.1038/nchembio.521

Jonsson, E., Htet, Z. M., Bard, J. A. M., Dong, K. C., & Martin, A. (2022). Ubiquitin modulates 26S proteasome conformational dynamics and promotes substrate degradation. *Science Advances*, *8*(51), eadd9520. https://doi.org/10.1126/sciadv.add9520

Juszkiewicz, S., Chandrasekaran, V., Lin, Z., Kraatz, S., Ramakrishnan, V., & Hegde, R. S. (2018). ZNF598 Is a Quality Control Sensor of Collided Ribosomes. *Molecular Cell*, *72*(3), 469-481.e7. https://doi.org/10.1016/j.molcel.2018.08.037

Kauer, J. C., Erickson-Viitanen, S., Wolfe, H. R., & DeGrado, W. F. (1986). p-Benzoyl-L-phenylalanine, a new photoreactive amino acid. Photolabeling of calmodulin with a synthetic calmodulin-binding peptide. *Journal of Biological Chemistry*, *261*(23), 10695–10700. https://doi.org/10.1016/S0021-9258(18)67441-1

Koch, B., & Yu, H.-G. (2019). Regulation of inner nuclear membrane associated protein degradation. *Nucleus*, *10*(1), 169–180. https://doi.org/10.1080/19491034.2019.1644593

Kochańczyk, T., Hann, Z. S., Lux, M. C., Delos Reyes, A. M. V., Ji, C., Tan, D. S., & Lima, C. D. (2024). Structural basis for transthiolation intermediates in the ubiquitin pathway. *Nature*, *633*(8028), 216–223. https://doi.org/10.1038/s41586-024-07828-9

Kolhe, J. A., Babu, N. L., & Freeman, B. C. (2023). The Hsp90 molecular chaperone governs client proteins by targeting intrinsically disordered regions. *Molecular Cell*, *83*(12), 2035-2044.e7. https://doi.org/10.1016/j.molcel.2023.05.021

Komander, D., & Rape, M. (2012). The Ubiquitin Code. *Annual Review of Biochemistry*, *81*(Volume 81, 2012), 203–229. https://doi.org/10.1146/annurev-biochem-060310-170328

Krshnan, L., Weijer, M. L. van de, & Carvalho, P. (2022). Endoplasmic Reticulum–Associated Protein Degradation. *Cold Spring Harbor Perspectives in Biology*, *14*(12), a041247. https://doi.org/10.1101/cshperspect.a041247

Lam, Y. W., Lamond, A. I., Mann, M., & Andersen, J. S. (2007). Analysis of nucleolar protein dynamics reveals the nuclear degradation of ribosomal proteins. *Current Biology: CB*, *17*(9), 749–760. https://doi.org/10.1016/j.cub.2007.03.064

Lander, G. C., Estrin, E., Matyskiela, M. E., Bashore, C., Nogales, E., & Martin, A. (2012). Complete subunit architecture of the proteasome regulatory particle. *Nature*, *482*(7384), 186–191. https://doi.org/10.1038/nature10774

Lewis, J. D., & Tollervey, D. (2000). Like attracts like: Getting RNA processing together in the nucleus. *Science (New York, N.Y.)*, *288*(5470), 1385–1389. https://doi.org/10.1126/science.288.5470.1385

Livnat-Levanon, N., & Glickman, M. H. (2011). Ubiquitin-proteasome system and mitochondria—Reciprocity. *Biochimica Et Biophysica Acta*, *1809*(2), 80–87. https://doi.org/10.1016/j.bbagrm.2010.07.005

Livneh, I., Cohen-Kaplan, V., Cohen-Rosenzweig, C., Avni, N., & Ciechanover, A. (2016). The life cycle of the 26S proteasome: From birth, through regulation and function, and onto its death. *Cell Research*, *26*(8), 869–885. https://doi.org/10.1038/cr.2016.86

López-Alfonzo, E. M., Saurabh, A., Zarafshan, S., Pressé, S., & Martin, A. (2023). *Substrate-interacting pore loops of two ATPase subunits determine the degradation efficiency of the 26S proteasome* (p. 2023.12.14.571752). bioRxiv. https://doi.org/10.1101/2023.12.14.571752

Löwe, J., Stock, D., Jap, B., Zwickl, P., Baumeister, W., & Huber, R. (1995). Crystal Structure of the 20S Proteasome from the Archaeon T. acidophilum at 3.4 Å Resolution. *Science*, *268*(5210), 533–539. https://doi.org/10.1126/science.7725097

Luan, B., Huang, X., Wu, J., Mei, Z., Wang, Y., Xue, X., Yan, C., Wang, J., Finley, D. J., Shi, Y., & Wang, F. (2016). Structure of an endogenous yeast 26S proteasome reveals two major conformational states. *Proceedings of the National Academy of Sciences*, *113*(10), 2642–2647. https://doi.org/10.1073/pnas.1601561113

Mandelstam, J. (1957). Turnover of Protein in Starved Bacteria and its Relationship to the Induced Synthesis of Enzyme. *Nature*, *179*(4571), 1179–1181. https://doi.org/10.1038/1791179a0

Matsumoto, M. L., Wickliffe, K. E., Dong, K. C., Yu, C., Bosanac, I., Bustos, D., Phu, L., Kirkpatrick, D. S., Hymowitz, S. G., Rape, M., Kelley, R. F., & Dixit, V. M. (2010). K11-Linked Polyubiquitination in Cell Cycle Control Revealed by a K11 Linkage-Specific Antibody. *Molecular Cell*, *39*(3), 477–484. https://doi.org/10.1016/j.molcel.2010.07.001

Matyskiela, M. E., Lander, G. C., & Martin, A. (2013). Conformational switching of the 26S proteasome enables substrate degradation. *Nature Structural & Molecular Biology*, *20*(7), 781. https://doi.org/10.1038/nsmb.2616

Mayor, T., Graumann, J., Bryan, J., MacCoss, M. J., & Deshaies, R. J. (2007). Quantitative Profiling of Ubiquitylated Proteins Reveals Proteasome Substrates and the Substrate Repertoire Influenced by the Rpn10 Receptor Pathway*. *Molecular & Cellular Proteomics*, *6*(11), 1885–1895. https://doi.org/10.1074/mcp.M700264-MCP200

Mayor, T., Lipford, J. R., Graumann, J., Smith, G. T., & Deshaies, R. J. (2005). Analysis of Polyubiquitin Conjugates Reveals That the Rpn10 Substrate Receptor Contributes to the Turnover of Multiple Proteasome Targets*S. *Molecular & Cellular Proteomics*, *4*(6), 741–751. https://doi.org/10.1074/mcp.M400220-MCP200

Murakami, Y., Matsufuji, S., Kameji, T., Hayashi, S., Igarashi, K., Tamura, T., Tanaka, K., & Ichihara, A. (1992). Ornithine decarboxylase is degraded by the 26S proteasome without ubiquitination. *Nature*, *360*(6404), 597–599. https://doi.org/10.1038/360597a0

Nguyen, A. T., Prado, M. A., Schmidt, P. J., Sendamarai, A. K., Wilson-Grady, J. T., Min, M., Campagna, D. R., Tian, G., Shi, Y., Dederer, V., Kawan, M., Kuehnle, N., Paulo, J. A., Yao, Y., Weiss, M. J., Justice, M. J., Gygi, S. P., Fleming, M. D., & Finley, D. (2017). UBE2O remodels the proteome during terminal erythroid differentiation. *Science*, *357*(6350), eaan0218. https://doi.org/10.1126/science.aan0218

Nollen, E. A., Salomons, F. A., Brunsting, J. F., van der Want, J. J., Sibon, O. C., & Kampinga, H. H. (2001). Dynamic changes in the localization of thermally unfolded nuclear proteins associated with chaperone-dependent protection. *Proceedings of the National Academy of Sciences of the United States of America*, *98*(21), 12038–12043. https://doi.org/10.1073/pnas.201112398

Northrop, A., Byers, H. A., & Radhakrishnan, S. K. (2020). Regulation of NRF1, a master transcription factor of proteasome genes: Implications for cancer and neurodegeneration. *Molecular Biology of the Cell*, *31*(20), 2158–2163. https://doi.org/10.1091/mbc.E20-04-0238

Oh, E., Mark, K. G., Mocciaro, A., Watson, E. R., Prabu, J. R., Cha, D. D., Kampmann, M., Gamarra, N., Zhou, C. Y., & Rape, M. (2020). Gene expression and cell

identity controlled by anaphase-promoting complex. *Nature*, *579*(7797), 136–140. https://doi.org/10.1038/s41586-020-2034-1

Olshina, M. A., & Sharon, M. (2016). Mass Spectrometry: A Technique of Many Faces. *Quarterly Reviews of Biophysics*, *49*, e18. https://doi.org/10.1017/S0033583516000160

Olszewski, M. M., Williams, C., Dong, K. C., & Martin, A. (2019). The Cdc48 unfoldase prepares well-folded protein substrates for degradation by the 26S proteasome. *Communications Biology*, *2*(1), 1–8. https://doi.org/10.1038/s42003-019-0283-z

Pack, C.-G., Yukii, H., Toh-e, A., Kudo, T., Tsuchiya, H., Kaiho, A., Sakata, E., Murata, S., Yokosawa, H., Sako, Y., Baumeister, W., Tanaka, K., & Saeki, Y. (2014). Quantitative live-cell imaging reveals spatio-temporal dynamics and cytoplasmic assembly of the 26S proteasome. *Nature Communications*, *5*(1), 3396. https://doi.org/10.1038/ncomms4396

Parrish, A. R., She, X., Xiang, Z., Coin, I., Shen, Z., Briggs, S. P., Dillin, A., & Wang, L. (2012). Expanding the Genetic Code of Caenorhabditis elegans Using Bacterial Aminoacyl-tRNA Synthetase/tRNA Pairs. *ACS Chemical Biology*, *7*(7), 1292–1302. https://doi.org/10.1021/cb200542j

Peng, J., Schwartz, D., Elias, J. E., Thoreen, C. C., Cheng, D., Marsischky, G., Roelofs, J., Finley, D., & Gygi, S. P. (2003). A proteomics approach to understanding protein ubiquitination. *Nature Biotechnology*, *21*(8), 921–926. https://doi.org/10.1038/nbt849

Pisareva, V. P., Skabkin, M. A., Hellen, C. U. T., Pestova, T. V., & Pisarev, A. V. (2011). Dissociation by Pelota, Hbs1 and ABCE1 of mammalian vacant 80S ribosomes and stalled elongation complexes. *The EMBO Journal*, *30*(9), 1804–1817. https://doi.org/10.1038/emboj.2011.93

Rock, K. L., Farfán-Arribas, D. J., Colbert, J. D., & Goldberg, A. L. (2014). Re-examining class-I presentation and the DRiP hypothesis. *Trends in Immunology*, *35*(4), 144–152. https://doi.org/10.1016/j.it.2014.01.002

Rock, K. L., Gramm, C., Rothstein, L., Clark, K., Stein, R., Dick, L., Hwang, D., & Goldberg, A. L. (1994). Inhibitors of the proteasome block the degradation of most cell proteins and the generation of peptides presented on MHC class I molecules. *Cell*, *78*(5), 761–771. https://doi.org/10.1016/S0092-8674(94)90462-6

Ruskowitz, E. R., & DeForest, C. A. (2019). Proteome-wide Analysis of Cellular Response to Ultraviolet Light for Biomaterial Synthesis and Modification. *ACS Biomaterials Science & Engineering*, *5*(5), 2111–2116. https://doi.org/10.1021/acsbiomaterials.9b00177

Sahu, I., Mali, S. M., Sulkshane, P., Xu, C., Rozenberg, A., Morag, R., Sahoo, M. P., Singh, S. K., Ding, Z., Wang, Y., Day, S., Cong, Y., Kleifeld, O., Brik, A., & Glickman, M. H. (2021). The 20S as a stand-alone proteasome in cells can

degrade the ubiquitin tag. *Nature Communications*, *12*(1), 6173. https://doi.org/10.1038/s41467-021-26427-0

Schmidt, O., Weyer, Y., Baumann, V., Widerin, M. A., Eising, S., Angelova, M., Schleiffer, A., Kremser, L., Lindner, H., Peter, M., Fröhlich, F., & Teis, D. (2019). Endosome and Golgi-associated degradation (EGAD) of membrane proteins regulates sphingolipid metabolism. *The EMBO Journal*, *38*(15), e101433. https://doi.org/10.15252/embj.2018101433

Schoenheimer, R., Ratner, S., & Rittenberg, D. (1939). STUDIES IN PROTEIN METABOLISM: VII. THE METABOLISM OF TYROSINE. *Journal of Biological Chemistry*, *127*(1), 333–344. https://doi.org/10.1016/S0021-9258(18)73846-5

Schubert, U., Antón, L. C., Gibbs, J., Norbury, C. C., Yewdell, J. W., & Bennink, J. R. (2000). Rapid degradation of a large fraction of newly synthesized proteins by proteasomes. *Nature*, *404*(6779), 770–774. https://doi.org/10.1038/35008096

Shao, N., Singh, N. S., Slade, S. E., Jones, A. M. E., & Balasubramanian, M. K. (2015). Site Specific Genetic Incorporation of Azidophenylalanine in Schizosaccharomyces pombe. *Scientific Reports*, *5*(1), 17196. https://doi.org/10.1038/srep17196

Shao, S., von der Malsburg, K., & Hegde, R. S. (2013). Listerin-dependent nascent protein ubiquitination relies on ribosome subunit dissociation. *Molecular Cell*, *50*(5), 637–648. https://doi.org/10.1016/j.molcel.2013.04.015

Shen, B., Xiang, Z., Miller, B., Louie, G., Wang, W., Noel, J. P., Gage, F. H., & Wang, L. (2011). Genetically Encoding Unnatural Amino Acids in Neural Stem Cells and Optically Reporting Voltage-Sensitive Domain Changes in Differentiated Neurons. *Stem Cells*, *29*(8), 1231–1240. https://doi.org/10.1002/stem.679

Shen, P. S., Park, J., Qin, Y., Li, X., Parsawar, K., Larson, M. H., Cox, J., Cheng, Y., Lambowitz, A. M., Weissman, J. S., Brandman, O., & Frost, A. (2015). Rqc2p and 60S ribosomal subunits mediate mRNA-independent elongation of nascent chains. *Science (New York, N.Y.)*, *347*(6217), 75. https://doi.org/10.1126/science.1259724

Shi, Y., Chen, X., Elsasser, S., Stocks, B. B., Tian, G., Lee, B.-H., Shi, Y., Zhang, N., de Poot, S. A. H., Tuebing, F., Sun, S., Vannoy, J., Tarasov, S. G., Engen, J. R., Finley, D., & Walters, K. J. (2016). Rpn1 provides adjacent receptor sites for substrate binding and deubiquitination by the proteasome. *Science*, *351*(6275), aad9421. https://doi.org/10.1126/science.aad9421

Shmueli, M. D., Sheban, D., Eisenberg-Lerner, A., & Merbl, Y. (2022). Histone degradation by the proteasome regulates chromatin and cellular plasticity. *The FEBS Journal*, *289*(12), 3304–3316. https://doi.org/10.1111/febs.15903

Shoemaker, C. J., Eyler, D. E., & Green, R. (2010). Dom34:Hbs1 Promotes Subunit Dissociation and Peptidyl-tRNA Drop-Off to Initiate No-Go Decay. *Science*, *330*(6002), 369–372. https://doi.org/10.1126/science.1192430

Shoemaker, C. J., & Green, R. (2011). Kinetic analysis reveals the ordered coupling of translation termination and ribosome recycling in yeast. *Proceedings of the National Academy of Sciences*, *108*(51), E1392–E1398. https://doi.org/10.1073/pnas.1113956108

Simoni, R. D., Hill, R. L., & Vaughan, M. (2002). The Use of Isotope Tracers to Study Intermediary Metabolism: Rudolf Schoenheimer. *Journal of Biological Chemistry*, *277*(43), e1–e3. https://doi.org/10.1016/S0021-9258(19)72251-0

Singh, R. K., Liang, D., Gajjalaiahvari, U. R., Kabbaj, M.-H. M., Paik, J., & Gunjan, A. (2010). Excess histone levels mediate cytotoxicity via multiple mechanisms. *Cell Cycle*, *9*(20), 4236–4244. https://doi.org/10.4161/cc.9.20.13636

Sivamaruthi, B. S., Raghani, N., Chorawala, M., Bhattacharya, S., Prajapati, B. G., Elossaily, G. M., & Chaiyasut, C. (2023). NF-κB Pathway and Its Inhibitors: A Promising Frontier in the Management of Alzheimer's Disease. *Biomedicines*, *11*(9), 2587. https://doi.org/10.3390/biomedicines11092587

Sung, M.-K., Porras-Yakushi, T. R., Reitsma, J. M., Huber, F. M., Sweredoski, M. J., Hoelz, A., Hess, S., & Deshaies, R. J. (2016). A conserved quality-control pathway that mediates degradation of unassembled ribosomal proteins. *eLife*, *5*, e19105. https://doi.org/10.7554/eLife.19105

Sung, M.-K., Reitsma, J. M., Sweredoski, M. J., Hess, S., & Deshaies, R. J. (2016). Ribosomal proteins produced in excess are degraded by the ubiquitin–proteasome system. *Molecular Biology of the Cell*, *27*(17), 2642. https://doi.org/10.1091/mbc.E16-05-0290

Szklarczyk, D., Kirsch, R., Koutrouli, M., Nastou, K., Mehryary, F., Hachilif, R., Gable, A. L., Fang, T., Doncheva, N. T., Pyysalo, S., Bork, P., Jensen, L. J., & von Mering, C. (2023). The STRING database in 2023: Protein-protein association networks and functional enrichment analyses for any sequenced genome of interest. *Nucleic Acids Research*, *51*(D1), D638–D646. https://doi.org/10.1093/nar/gkac1000

Taniguchi, K., & Karin, M. (2018). NF-κB, inflammation, immunity and cancer: Coming of age. *Nature Reviews Immunology*, *18*(5), 309–324. https://doi.org/10.1038/nri.2017.142

Turner, G. C., & Varshavsky, A. (2000). Detecting and Measuring Cotranslational Protein Degradation in Vivo. *Science*, *289*(5487), 2117–2120. https://doi.org/10.1126/science.289.5487.2117

Twomey, E. C., Ji, Z., Wales, T. E., Bodnar, N. O., Ficarro, S. B., Marto, J. A., Engen, J. R., & Rapoport, T. A. (2019). Substrate processing by the Cdc48 ATPase complex is initiated by ubiquitin unfolding. *Science*, *365*(6452), eaax1033. https://doi.org/10.1126/science.aax1033

Unno, M., Mizushima, T., Morimoto, Y., Tomisugi, Y., Tanaka, K., Yasuoka, N., & Tsukihara, T. (2002). The Structure of the Mammalian 20S Proteasome at 2.75 Å

Resolution. *Structure*, *10*(5), 609–618. https://doi.org/10.1016/S0969-2126(02)00748-7

Verma, R., Aravind, L., Oania, R., McDonald, W. H., Yates, J. R., Koonin, E. V., & Deshaies, R. J. (2002). Role of Rpn11 Metalloprotease in Deubiquitination and Degradation by the 26S Proteasome. *Science*, *298*(5593), 611–615. https://doi.org/10.1126/science.1075898

Wang, F., Durfee, L. A., & Huibregtse, J. M. (2013). A Cotranslational Ubiquitination Pathway for Quality Control of Misfolded Proteins. *Molecular Cell*, *50*(3), 368–378. https://doi.org/10.1016/j.molcel.2013.03.009

Wang, L., Brock, A., Herberich, B., & Schultz, P. G. (2001). Expanding the genetic code of Escherichia coli. *Science (New York, N.Y.)*, *292*(5516), 498–500. https://doi.org/10.1126/science.1060077

Wang, Q., & Wang, L. (2008). New Methods Enabling Efficient Incorporation of Unnatural Amino Acids in Yeast. *Journal of the American Chemical Society*, *130*(19), 6066–6067. https://doi.org/10.1021/ja800894n

Wang, W., Takimoto, J. K., Louie, G. V., Baiga, T. J., Noel, J. P., Lee, K.-F., Slesinger, P. A., & Wang, L. (2007). Genetically encoding unnatural amino acids for cellular and neuronal studies. *Nature Neuroscience*, *10*(8), 1063–1072. https://doi.org/10.1038/nn1932

Wehmer, M., Rudack, T., Beck, F., Aufderheide, A., Pfeifer, G., Plitzko, J. M., Förster, F., Schulten, K., Baumeister, W., & Sakata, E. (2017). Structural insights into the functional cycle of the ATPase module of the 26S proteasome. *Proceedings of the National Academy of Sciences*, *114*(6), 1305–1310. https://doi.org/10.1073/pnas.1621129114

Wolf-Levy, H., Javitt, A., Eisenberg-Lerner, A., Kacen, A., Ulman, A., Sheban, D., Dassa, B., Fishbain-Yoskovitz, V., Carmona-Rivera, C., Kramer, M. P., Nudel, N., Regev, I., Zahavi, L., Elinger, D., Kaplan, M. J., Morgenstern, D., Levin, Y., & Merbl, Y. (2018). Revealing the cellular degradome by mass spectrometry analysis of proteasome-cleaved peptides. *Nature Biotechnology*. https://doi.org/10.1038/nbt.4279

Worden, E. J., Dong, K. C., & Martin, A. (2017). An AAA Motor-Driven Mechanical Switch in Rpn11 Controls Deubiquitination at the 26S Proteasome. *Molecular Cell*, *67*(5), 799-811.e8. https://doi.org/10.1016/j.molcel.2017.07.023

Xie, Z., Zhao, S., Tu, Y., Liu, E., Li, Y., Wang, X., Chen, C., Zhai, S., Qi, J., Wu, C., Wu, H., Zhou, M., & Wang, W. (2024). Proteasome resides in and dismantles plant heat stress granules constitutively. *Molecular Cell*, *84*(17), 3320-3335.e7. https://doi.org/10.1016/j.molcel.2024.07.033

Xu, S., Gierisch, M. E., Schellhaus, A. K., Poser, I., Alberti, S., Salomons, F. A., & Dantuma, N. P. (2023). Cytosolic stress granules relieve the ubiquitin-

proteasome system in the nuclear compartment. *The EMBO Journal*, *42*(3), e111802. https://doi.org/10.15252/embj.2022111802

Yanagitani, K., Juszkiewicz, S., & Hegde, R. S. (2017). UBE2O is a quality control factor for orphans of multiprotein complexes. *Science*, *357*(6350), 472–475. https://doi.org/10.1126/science.aan0178

Yao, T., & Cohen, R. E. (2002). A cryptic protease couples deubiquitination and degradation by the proteasome. *Nature*, *419*(6905), 403–407. https://doi.org/10.1038/nature01071

Appendix

Table of Contents

Protocol 2.1: Expression & purification of recombinant 19S base subcomplex

Description:

This protocol is for the expression & purification of recombinant 19S base subcomplexes.

Materials:

Media

1. Luria Broth (LB) agar (1L): 10 g tryptone, 5 g yeast extract, 10 g NaCl, 15 grams agar.
2. dYT Media (1 L): 16 g tryptone, 10 g yeast extract, 5 g NaCl, add 20 g agar for plates.
3. TB Media (1 L, Unbuffered): 12 g tryptone, 24 g yeast extract, 4 mL glycerol.

Reagents

4. 1000X ampicillin: 300 mg/mL ampicillin sodium in 50% EtOH.
5. 1000X kanamycin: 50 mg/mL kanamycin monosulfate in water.
6. 1000X chloramphenicol: 25 mg/mL chloramphenicol in 100% EtOH.
7. 1 M Isopropyl β-D-1-thiogalactopyranoside (IPTG)
8. 1000X Aprotinin: 1 mg/mL in 25% methanol.
9. 1000X Pepstatin: 1 mg/mL in 90% methanol, 10% acetic acid.
10. 1000X Leupeptin: 1 mg/mL in water.
11. 100X AEBSF: 100 mM in water.
12. Benzonase nuclease.
13. Lysozyme
14. 2 M imidazole: 68.08 g in water, adjust pH to 7.6, top to 500 mL, filter sterilize.
15. 1 M HEPES: 119.15 g in water, adjust pH to 7.6, top to 500 mL, filter sterilize.
16. 1 M Tris HCl: 60.57 g in water, adjust pH to 7.5, top to 500 mL, filter sterilize.
17. 2 M $MgCl_2$: 101.65 in water, top to 250 mL, autoclave.
18. 0.5 M ATP: Dissolve 23 grams in 60 mL water. Adjust pH dropwise until 7.0-7.4 with NaOH, bring the final volume to 75 mL, make 1 mL aliquots and store at -80 °C.

19. 0.5 M TCEP: Add 5.73 g tris(2-carboxyethyl)phosphine-HCl to 30 mL of water. Adjust pH to 7.0 with 5 M NaOH, and then adjust final volume to 40 mL with water. Aliquot and store at −20 °C.
20. 3X FLAG (MDYKDHDGDYKDHDIDYKDDDDK) peptide (Genscript): Dissolve peptide in TBS, adjust pH to 7.6 using NaOH.
21. Bradford Reagent.

Buffers

22. NiA Buffer: 60 mM HEPES, 100 mM NaCl, 100 mM KCl, 10 mM $MgCl_2$, 20 mM imidazole, 5% glycerol, adjust pH to 7.6.
23. NiB Buffer: NiA with 250 mM imidazole, re-adjust pH to 7.6.
24. FLAG Regeneration Buffer: 0.1 M glycine, pH to 3.5.
25. Tris-Buffered Saline (TBS): 50 mM Tris HCl, 150 mM NaCl, pH to 7.5.
26. Gel-filtration (GF) buffer: 30 mM HEPES, 50 mM NaCl, 50 mM KCl, 10 mM $MgCl_2$, 5% glycerol, adjust pH to 7.6, filter sterilize and de-gas prior to use.

Resins

27. Ni-NTA agarose (Sigma).
28. Anti-FLAG M2 agarose (Sigma).

Other materials

29. Bio-Rad Micropulser Electroporator.
30. Bio-Rad 0.2 cm electroporation cuvettes.
31. Probe-tip sonicator.
32. Stainless steel beaker.
33. Superose 6 Increase 10/300 SEC chromatography column (Cytiva).
34. Bio-Rad Mini-PROTEAN TGX 4-20% polyacrylamide gel.
35. 2X sample buffer (Bio-Rad).

Methods:

Growth and Expression of 19S Base

1. Electroporate the pULTRA-Bpa plasmid into electrocompetent BL21(DE3) containing the three 19S base expression plasmids. Plate on an LB plate containing 1X each of ampicillin, kanamycin, chloramphenicol, and spectinomycin.

2. Grow overnight at 37 °C.
3. From the plate, pick a single colony, and start a 5 mL overnight in dYT with 1X of all four antibiotics.
4. Make two overnights by adding 1 mL of the 5 mL overnight to 50 mL of dYT with 1X antibiotics and grow overnight at 37 °C.
5. The following day, transfer the 50 mL cultures into 50 mL conicals and spin down at 4,000xg for 10 minutes.
6. Wash the cell pellets by resuspending each in 30 mL of fresh dYT.
7. Centrifuge and repeat the wash step once more.
8. Inoculate 6L of dYT in 1L with 0.5X antibiotics in baffled growing flasks by adding 10 mL of the cell suspension to each flask.
9. Grow at 37 °C and monitor the OD_{600}.
10. While the cells are growing or prior to growth, autoclave and cool down 1 L centrifuge bottles.
11. Once the cells reach an OD_{600} of 0.6, harvest the cells by centrifuging at 4000xg for 15 minutes.
12. Resuspend the cells in 1 L of unbuffered TB to maximize the exposure of cells for a given concentration of Bpa, and split into two flasks to maximize oxygenation of the media.
13. Dissolve 538.6 mg of Bpa in 300 µL of 1 M NaOH and divide into the two flasks.
14. Allow the cells to shake for 30 minutes to allow the cells to uptake the Bpa and monitor the OD_{600} to make sure the cells are growing.
15. After the incubation, induce expression of the 19S and the UAA tRNA and synthetase pair by adding 0.5 mL of 1 M IPTG (1 mM final) to each flask.
16. Express protein for 5 hours at 30 °C followed by 16 °C overnight.
17. Harvest the cells by centrifuging at 4,000xg for 15 minutes.
18. Resuspend the pellets with cold NiA buffer with added 1X protease inhibitors and 50 U of benzonase so that the final volume is approximately 75 mL.
19. Transfer the cell suspension into two 50 mL conical tubes, flash-freeze in liquid nitrogen and store at -80 °C.

Thawing

1. Take the covered 50 mL conicals containing the cell pellets out of the -80° C freezer and place them in water to thaw.
2. As the frozen pellet thaws and becomes liquid, add **1X AEBSF, 1X Aprotinin, 1X Pepstatin, 1X Leupeptin and 5uL of Benzonase** to each conical.
3. You should also add some lysozyme to the slurry—no need to measure, just add a small scoopful.

4. Take conical out of the water and place on a rotator in the cold room and allow to mix, while prepping the centrifuge.
5. **While cells are thawing:** turn on the ultracentrifuge and begin cooling it to 4º C, grab a metal 125 mL beaker and cool it in the cold room, and also grab 4 round-bottom centrifuge tubes and cool to 4ºC.

Lysis

1. Fill a container with ice and pack it in super well.
2. Push the 125mL metal beaker into the ice and pack the ice around it tightly.

   Note: Sonication can cause the ice to melt around the beaker and the beaker to move/sink. This can fuck up your sonication, so by packing the ice in keeps the beaker from moving and keeps it colder.

3. Pour the thawed cell suspension into the beaker.
4. Sonicate for 3 minutes at 75% power with a cycle of 15 sec. on and 59 sec. off.
5. Transfer the cleared lysate into the cooled round-bottom tubes and balance them as best possible without exposing the lysate to light.
6. Spin lysate in centrifuge at 26,000 xg for 30 - 45 minutes.

   Note: You can also do longer if you want/need more time. (Like if you're in need of lunch!!)

FLAG Regeneration

1. Grab four 1st-step FLAG columns, attach stopcocks, and put them on clamp stands in the cold room.
2. Open the stopcocks to allow the liquid to flow out of the columns and into a waste container, **but do not let the columns run dry.**
3. Add 5 mLs of TBS to each column and allow it to flow until just above the resin.
4. Add another 5 mLs of TBS to each column and using a pipette **gently** resuspend the FLAG resin. Open the stopcock to allow the resin to drain, **again without letting the columns run dry.**
5. Once the resin has settled, add another 10 mLs of TBS and allow it to pass through until just above the resin.
6. Add 5 mLs of 0.1 M glycine pH 3.5 three times, consecutively. It is very important that you keep an eye on the columns during this step, you don't want the columns to run dry or to sit in glycine for more than 20 minutes.
7. Wash once more with 10 mLs of TBS.
8. Wash into NiA + 1 mM ATP. Now the FLAG resin is ready for the Ni elution.

NiNTA Steps

1. For a base prep, you're going to want to use 5 mLs of Ni resin per 50 mL conical. The NiNTA slurry is 50% resin and 50% EtOH solution, so you're going to want to add **10 mLs of slurry to each conical.**
2. Wash the NiNTA resin by adding 2 volumes of NiA buffer per volume of resin, rotating, and spinning down for 2 mins at 700xg in the cold room centrifuge.
3. Repeat **Step 2** once more for a total of two washes.
4. Once the lysate has finished spinning, pour the cleared lysate into the conical containing the Ni resin. Top off with NiA buffer to leave as little air as possible in the conical.
5. Batch bind the lysate and resin while rotating in the cold room for **at least 1 hour.**
6. In the meantime, prepare a clean, wide glass column by washing it with cold mQ H_2O. Then wash it with NiA and leave it in NiA.
7. Using a pipette, transfer the resin-buffer solution to the column and open the stopcock to allow the FT to begin dripping out.

   Note: Don't open the stopcock all the way at first, because the flow will be too fast. Let it drip slowly first, once the Ni resin has settled, you can open the stopcock all the way.

8. Collect the FT in a beaker.
9. Once the liquid is right above the resin, wash with 25 mLs of NiA + 1mM ATP.
10. Repeat **Step 28** for one more wash.
11. While washing, prepare 40 mLs of NiB by adding ATP to 1mM final.

    Note: It ends up being 80 uL of 0.5M ATP.

12. Add 40 mLs of NiB + 1mM ATP to elute the base and collect in the same 50 mL conical.

FLAG Steps

1. Split the NiB elution evenly across the four FLAG columns.
2. Allow the NiB elution to flow through the FLAG columns and collect the flow-through in 15 mL conicals.
3. As the columns are getting low, close the stopcock and top them off with the FT (see diagram).
4. Top the columns off 4-5 times, allowing the FLAG resin to be in contact with FT for at least 30 minutes.

5. Wash each FLAG column with 25 mLs of NiA + 1mM ATP.
6. Repeat **Step 36** for a total of two 25 mL washes.
7. While the columns are washing, prepare four conicals with 15 mLs of NiA + 1mM ATP + 0.15mg/mL FLAG peptide. Add 15 mLs of the elution buffer to each column.
8. Flow the elution buffer through the column and collect the elution.
9. You can now move on to concentrating your protein.

Concentrating

1. Equilibrate a 30K MWCO concentrator by pre-spinning it with cold NiA + 1mM ATP.
2. Concentrate your FLAG elutions by spinning them at 4 °C at 2,000 rcf.
3. Stop when you have concentrated to ~400uL.
4. At this point, you can stop the prep and flash-freeze your concentrated protein or move forward with size-exclusion chromatography (aka sizing or gel filtration).

Size-exclusion clean up & buffer exchange

1. Begin by equilibrating the Sup6i column into a gel filtration (GF) buffer with 0.5 mM ATP and 0.5 mM TCEP.
2. Pre-chill the tabletop centrifuge to 4° C.

   Note: a good way to do this is by using the "fast temp" button on the 'fuge.

3. Equilibrate a 0.22 um spin filter by adding cold NiA + 1 mM ATP.
4. Add your concentrated FLAG eluate to the spin filter and spin at max speed for 5 minutes.
5. Run the protein on the pre-equilibrated Sup6i.

Post-sizing (Concentration by Bradford)

1. Pre-equilibrate a small 30K MWCO concentrator by spinning it with just GF + 0.5 mM ATP.
2. Collect the fractions that correspond with the base elution (see example below).
3. Concentrate the fractions to ideally less than 100 uL.
4. Make 2uL aliquots and flash freeze in LN_2.
5. Store at -80 °C.

Protocol 2.2: Expression & purification of recombinant 19S base subcomplex with Bpa incorporation

Description:

This protocol is for the expression & purification of recombinant 19S base subcomplexes containing Bpa.

Materials:

Media

1. Luria Broth (LB) agar (1L): 10 g tryptone, 5 g yeast extract, 10 g NaCl, 15 grams agar.
2. dYT Media (1 L): 16 g tryptone, 10 g yeast extract, 5 g NaCl, add 20 g agar for plates.
3. TB Media (1 L, Unbuffered): 12 g tryptone, 24 g yeast extract, 4 mL glycerol.

Reagents

4. 1000X ampicillin: 300 mg/mL ampicillin sodium in 50% EtOH.
5. 1000X kanamycin: 50 mg/mL kanamycin monosulfate in water.
6. 1000X chloramphenicol: 25 mg/mL chloramphenicol in 100% EtOH.
7. 1000X spectinomycin: 100 mg/mL spectinomycin dihydrochloride pentahydrate in water.
8. 1 M Isopropyl β-D-1-thiogalactopyranoside (IPTG)
9. 1 M NaOH: 20 g in 500 mL, filter sterilize.
10. 4-benzoyl-L-phenylalanine (Amatek).
11. 1000X Aprotinin: 1 mg/mL in 25% methanol.
12. 1000X Pepstatin: 1 mg/mL in 90% methanol, 10% acetic acid.
13. 1000X Leupeptin: 1 mg/mL in water.
14. 100X AEBSF: 100 mM in water.
15. Benzonase nuclease.
16. Lysozyme
17. 2 M imidazole: 68.08 g in water, adjust pH to 7.6, top to 500 mL, filter sterilize.
18. 1 M HEPES: 119.15 g in water, adjust pH to 7.6, top to 500 mL, filter sterilize.
19. 1 M Tris HCl: 60.57 g in water, adjust pH to 7.5, top to 500 mL, filter sterilize.
20. 2 M $MgCl_2$: 101.65 in water, top to 250 mL, autoclave.
21. 0.5 M ATP: Dissolve 23 grams in 60 mL water. Adjust pH dropwise until 7.0-7.4 with NaOH, bring the final volume to 75 mL, make 1 mL aliquots and store at -80 °C.

22. 0.5 M TCEP: Add 5.73 g tris(2-carboxyethyl)phosphine-HCl to 30 mL of water. Adjust pH to 7.0 with 5 M NaOH, and then adjust final volume to 40 mL with water. Aliquot and store at −20 °C.
23. 3X FLAG (MDYKDHDGDYKDHDIDYKDDDDK) peptide (Genscript): Dissolve peptide in TBS, adjust pH to 7.6 using NaOH.
24. Bradford Reagent.
25. 20X ATPase Assay Mix: 3750 U/mL pyruvate kinase, 4290 U/mL lactate dehydrogenase, 200 mM NADH, 1 M phosphoenolpyruvate, 200 mM ATP in water.

Buffers

26. NiA Buffer: 60 mM HEPES, 100 mM NaCl, 100 mM KCl, 10 mM $MgCl_2$, 20 mM imidazole, 5% glycerol, adjust pH to 7.6.
27. NiB Buffer: NiA with 250 mM imidazole, re-adjust pH to 7.6.
28. FLAG Regeneration Buffer: 0.1 M glycine, pH to 3.5.
29. Tris-Buffered Saline (TBS): 50 mM Tris HCl, 150 mM NaCl, pH to 7.5.
30. Gel-filtration (GF) buffer: 30 mM HEPES, 50 mM NaCl, 50 mM KCl, 10 mM $MgCl_2$, 5% glycerol, adjust pH to 7.6, filter sterilize and de-gas prior to use.

Resins

31. Ni-NTA agarose (Sigma).
32. Anti-FLAG M2 agarose (Sigma).

Other materials

33. Bio-Rad Micropulser Electroporator.
34. Bio-Rad 0.2 cm electroporation cuvettes.
35. pULTRA-Bpa plasmid.
36. Probe-tip sonicator.
37. Stainless steel beaker.
38. Corning 384-well low-volume clear bottom plate.
39. Superose 6 Increase 10/300 SEC chromatography column (Cytiva).
40. Blak-Ray B-100AP 365 nm lamp (Fisher).
41. Bio-Rad Mini-PROTEAN TGX 4-20% polyacrylamide gel.
42. 2X sample buffer (Bio-Rad).

Methods:

Growth and Expression of Bpa Cross-linking 19S Base

1. Electroporate the pULTRA-Bpa plasmid into electrocompetent BL21(DE3) containing the three 19S base expression plasmids. Plate on an LB plate containing 1X each of ampicillin, kanamycin, chloramphenicol, and spectinomycin.
2. Grow overnight at 37 °C.
3. From the plate, pick a single colony, and start a 5 mL overnight in dYT with 1X of all four antibiotics.
4. Make two overnights by adding 1 mL of the 5 mL overnight to 50 mL of dYT with 1X antibiotics and grow overnight at 37 °C.
5. The following day, transfer the 50 mL cultures into 50 mL conicals and spin down at 4,000xg for 10 minutes.
6. Wash the cell pellets by resuspending each in 30 mL of fresh dYT.
7. Centrifuge and repeat the wash step once more.
8. Inoculate 6L of dYT in 1L with 0.5X antibiotics in baffled growing flasks by adding 10 mL of the cell suspension to each flask.
9. Grow at 37 °C and monitor the OD_{600}.
10. While the cells are growing or prior to growth, autoclave and cool down 1 L centrifuge bottles.
11. Once the cells reach an OD_{600} of 0.6, harvest the cells by centrifuging at 4000xg for 15 minutes.
12. Resuspend the cells in 1 L of unbuffered TB to maximize the exposure of cells for a given concentration of Bpa, and split into two flasks to maximize oxygenation of the media.
13. Dissolve 538.6 mg of Bpa in 300 µL of 1 M NaOH and divide into the two flasks.
14. Allow the cells to shake for 30 minutes to allow the cells to uptake the Bpa and monitor the OD_{600} to make sure the cells are growing.
15. After the incubation, induce expression of the 19S and the UAA tRNA and synthetase pair by adding 0.5 mL of 1 M IPTG (1 mM final) to each flask.
16. Express protein for 5 hours at 30 °C followed by 16 °C overnight.
17. Harvest the cells by centrifuging at 4,000xg for 15 minutes.
18. Resuspend the pellets with cold NiA buffer with added 1X protease inhibitors and 50 U of benzonase so that the final volume is approximately 75 mL.
19. Transfer the cell suspension into two 50 mL conical tubes, flash-freeze in liquid nitrogen and store at -80 °C.

Purification of Cross-linking 19S Base Subcomplex

1. Thaw the tubes in water and transfer the contents to a 250 mL stainless steel beaker. Add a small scoop of lysozyme.
2. Sonicate the lysate on ice using a probe-tip sonicator set to 70% amplitude, with a cycle of 3 seconds on and 59 seconds off.
3. Clarify the lysate by centrifugation at 26,000xg for 30 minutes at 4 °C. **All subsequent steps should be carried out in a 4 °C cold room.**
4. While the lysate is centrifuging, measure 10 mL of 50% NiNTA agarose slurry and add to a 50 mL conical tube. Spin the slurry at 700xg for 3 minutes to settle the agarose.
5. Resuspend the resin by topping off the conical with water to wash off the storage solution, spin to settle.
6. Repeat the wash step once more.
7. Carefully decant the water and resuspend the agarose with NiA buffer to 20 mL.
8. Spin to settle and repeat the resuspension.
9. Transfer the clarified lysate to two clean 50 mL conicals. Add 10 mL of NiNTA agarose in NiA to each conical.
10. Batch bind the lysate to the NiNTA, at 4 °C with rotation, for up to one hour.
11. Prepare a glass gravity chromatography column by washing with water and then NiA. Transfer the batch bound mixture to the column and allow the resin to settle.
12. Open the valve and allow the lysate to flow through.
13. Wash the resin with 25 mL of NiA + 1 mM ATP.
14. Repeat the wash step for a total of two washes.
15. Elute the base complex by adding 20 mL of NiB + 1 mM ATP. Collect the elution in a 50 mL conical.
16. Regenerate two 5 mL FLAG columns:
    a. Add 10 mL of TBS and gently resuspend the resin, open the column valve and allow the buffer to flow and the resin to re-pack.
    b. Wash once more with 10 mL of TBS, close the valve when the buffer is just above the resin. **Do not let the resin run dry**.
    c. Regenerate the resin by flowing three sequential 5 mL volumes of 0.1 M glycine regeneration buffer. It is important to monitor the resin at this step so it does not run dry or sit in the glycine buffer for more than 20 minutes.
    d. Wash the resin once more with 10 mL TBS.
    e. Equilibrate the resin with 10 mL of NiA + 1 mM ATP. The resin is now ready for the NiNTA elution.
17. Split the NiNTA elution across the two FLAG columns. Allow the elution to flow through the FLAG resin and collect the flowthrough in 15 mL conicals.

18. When the volume approaches the resin bed, close the valve and top off the resin with the flowthrough. Repeat this binding step 4 times, ensuring the elution has been in contact with the resin for at least 30 minutes.
19. Wash each FLAG column with 25 mL of NiA + 1 mM ATP.
20. Repeat the wash for a total of two washes.
21. While the columns are washing, prepare two conicals with 15 mL of NiA with 1 mM ATP and 0.15 mg/mL 3X FLAG peptide.
22. Add the elution buffer to the column, allow it to flow through, and collect the elution.
23. Pre-equilibrate a 15 mL 100K MWCO concentrator by adding NiA + 1 mM ATP and spinning at 4 °C.
24. Concentrate the elution at 4 °C to approximately 500 µL by spinning at 2,000xg in 5 minute increments.
25. Filter the concentrated protein with a pre-equilibrated 0.22 µm spin filter.
26. Equilibrate a Superose 6 Increase 10/300 size-exclusion chromatography column with GF buffer with 0.5 mM ATP and 0.5 mM TCEP.
27. Inject the protein concentrate into the FPLC using a 0.5 mL loop and run, making sure to collect 0.5 mL fractions. The base subcomplex should elute at an elution volume of approximately 13 mL. Collect the fractions corresponding to the eluted base subcomplex.
28. Concentrate using a 500 µL 100K MWCO concentrator to approximately 100 µL.
29. Take a small sample for SDS-PAGE and for measuring protein concentration by the Bradford method.
30. Aliquot and flash freeze samples in liquid nitrogen. They can be stored at -80 °C, but will not tolerate subsequent freeze-thaw cycles.

Protocol 2.3: Expression & purification of titin model proteasome substrates

Description:

This protocol is for the expression & purification of titin substrates for assaying 26S proteasome degradation.

Materials:

Media

1. dYT Media, 1 L: 16 g tryptone, 10 g yeast extract, 5 g NaCl, add 20 g agar for plates.
2. M9 Minimal Media, 1 L: 0.2407 g $MgSO_4$, 200uL of $CaCl_2$, 875 mL mQ H_2O, combine and autoclave, then add 20mL of 20% glucose and 100mL of 10X M9 salts to complete the media.
3. 20% Glucose, 500 mL: 100 g of D-glucose, top to 500 mL with mQ H_2O, filter sterilize.
4. 10X M9 Salts, 500 mL: 35 g $Na_2HPO_4 \cdot 7\ H_2O$, 15 g KH_2PO_4, 2.5 g NaCl, 5 g NH_4Cl, combine and autoclave.

Buffers

5. Chitin Buffer, 500 mL: 60 mM HEPES, pH 7.6, 150 mM NaCl, 2 mM EDTA, 5% glycerol.
6. Chitin Wash Buffer 1, 250mL: 60 mM HEPES, pH 7.6, 750 mM NaCl, 2 mM EDTA, 5% glycerol, 0.1% Triton X-100, 1X Protease inhibitors
7. Chitin Wash Buffer 2, 250mL: 60 mM HEPES, pH 7.6, 100 mM NaCl, 2 mM EDTA, 5% glycerol, 1X Protease inhibitors
8. Chitin Elution Buffer, 250mL: 30 mM HEPES, pH 8.5, 100 mM NaCl, 2mM EDTA, 5% glycerol
9. Chitin Elution Buffer +DTT - Recommended: 50 mL per column: Add 385.26 g of powdered DTT to 50 mL of Chitin Elution buffer.
    a. **Note**: You will have to re-adjust the pH back to 8.5.
10. S75 16/600 GF buffer, 150 mL for equilibration & 150 mL per run: 30 mM HEPES, pH 7.6, 150 mM NaCl, 1 mM EDTA, 5% glycerol, 0.5 mM TCEP (add right before)
11. Sortase labelling buffer: 30 mM HEPES, pH 7.6, 300 mM NaCl, 20 mM imidazole, 5% glycerol

12. S75 10/300 GF buffer: 30 mM HEPES, pH 7.6, 250 mM NaCl, 50 mM KCl, 10 mM $MgCl_2$, 5% glycerol, 0.5 mM TCEP (add right before)
13. 0.3M NaOH, for regenerating chitin resin: 6 g in 500 mL.
14. 20% ethanol, for storing chitin resin: 20mL ethanol per 100 mL

Methods:

Growth

1. Start a 50 mL overnight of your substrate(s) growing at 30ºC with shaking.
2. Prepare 3 L of M9 Minimal media per substrate that you're going to prep.
3. On the day of growth: add the M9 salts to 1X, the filtered glucose, and 1X kanamycin.
4. Warm the media for at least 30 mins.
5. While warming the media, wash the starter cells with dYT twice.
6. Add starter to the complete M9 media to a starting OD of 0.05.
7. Grow at 30ºC until they reach an OD of 0.7.
8. Induce protein expression with 0.5 mM IPTG for 3hrs at 30ºC.
9. Harvest cells the same day by spinning them at 3,500 rpm for 15 minutes.
10. Resuspend the pellet in Chitin Buffer and add 1mM AEBSF, 1X leupeptin, 1X pepstatin.
11. Flash freeze and store at -80ºC.
12. and 1uL benzonase/25mL of lysate.

Purification - Day 1

13. Thaw pellets in a room temperature water bath.
14. Add 1 uL of benzonase per 25 mL lysate.
15. In a metal beaker, sonicate lysate at 75% amplitude for 3 minutes with cycles of 15 seconds off and 59 seconds on.
16. Spin the lysate at 15,000rpm for 25 to 30 mins.
17. In a gravity column, prepare the 10 mL chitin resin per 1 L of cells grown by washing it with 5 CV's of Chitin Buffer.
18. Take the resin from the column and place in a 50 mL conical and batch bind lysate to resin for 1hr.
19. Place the bound mixture back in a column. Wash with 50mLs of Chitin Wash Buffer 1
    a. **Note**: Add the protease inhibitors to the wash buffers day of and usually right before using.

20. Wash with 50mLs of Chitin Wash Buffer 2.
21. Buffer exchange the column into Chitin Elution Buffer +DTT and let it sit overnight at 4ºC.
22. **Optional**: Equilibrate the S75 16/600 overnight, this HiLoad column takes ~2hrs to equilibrate. This will save you two hours the next day.

Purification - Day 2

23. In the morning, collect off the column with Chitin Elution Buffer with no DTT (around 15-20 mL total).
24. Take the eluent and flow over 2 mL of fresh chitin resin to remove any uncleaved intein.

Concentration & size-exclusion (S75 16/600)

25. Concentrate substrate in a 10K MWCO concentrator to >2mLs.
    a. **Note**: Spin at 4000 rpm for 15 min intervals.
26. Use two spin filters to filter at ~13,000 rpm. Each spin filter can hold a max of ~700 uL.
27. Run on S75 16/600 into a Substrate Storage Buffer.
    a. **Note**: Peak should be around 70mL of elution volume.

Resin regeneration

28. To regenerate the resin, wash with 1 CV of 0.3 M NaOH.
29. Let the resin sit in 0.3 M NaOH for 30 minutes.
30. Wash with another 2-3 CV's of 0.3 M NaOH.
31. Wash back into water.
32. Store resin in 20% ethanol.

Protocol 2.4: Labeling of titin model substrates

Description:

This protocol is for the labeling of titin substrates for assaying 26S proteasome degradation with a peptide via a sortase reaction mediated by the SrtA protein. This protocol can be carried out with whatever peptide you want to add to the substrate, but this one is written with a fluorescein-6x-histidine peptide.

Materials:

Buffers

1. NiA Binding Buffer: 60 mM HEPES, 100 mM NaCl, 100 mM KCl, 10 mM $MgCl_2$, 20 mM imidazole, 5% glycerol, adjust pH to 7.6.
2. NiB Elution Buffer: NiA with 250 mM imidazole, re-adjust pH to 7.6.
3. GF Buffer: 30 mM HEPES, 50 mM NaCl, 50 mM KCl, 10 mM $MgCl_2$, 5% glycerol, adjust pH to 7.6, filter sterilize and de-gas prior to use.

Reagents

1. FAM-Sortase Peptide (Genscript).
2. 1 mL NiNTA cartridge (Sigma).
3. Peristaltic pump.
4. 10K MWCO concentrator.

Methods:

Setting up SrtA reaction

1. In a 1.5 mL Eppendorf tube, set up a 500 uL reaction with the following concentrations in plain GF buffer: 10 mM $CaCl_2$, 0.5 mM sortase peptide, 20 uM SrtA, 100 uM titin substrate, 1 mM DTT.
2. Incubate for an hour at RT on a bench-top covered in aluminum foil to prevent dye photobleaching.
3. After 1 hr. dilute with 1 mL of NiA binding buffer to prepare for clean up.

Reaction clean up

1. Using a peristaltic pump, load the diluted reaction onto a 1 mL column, at a flow rate of 1 mL/min.

2. Wash with binding buffer until you have collected approximately 10 mL of flow through in a 15mL conical tube.
3. Wash with an extra 5 mL of binding buffer but no need to collect.
4. Elute with elution buffer. Collect at least 10 mL of elution or until the column is not green anymore.
5. Concentrate the FT and elution in separate 10K MWCO concentrators to ~500uL each by spinning at 3500 rpm in 10 minute intervals at 4 °C..
    a. Note: Take a 2uL sample to run on a gel of the concentrated elution and FT.
6. You can freeze the sample here or go on to sizing using the S75i 10/300 column on the FPLC.

Size exclusion clean up

1. Equilibrate the S75i 10/300 with S75i GF buffer with 0.5 mM TCEP.
2. Use a 0.22 um spin filter to filter the elution before sizing.
3. Load onto the FPLC using a 500 uL loop.
4. The sizing trace should show you a peak corresponding to FAM-substrate dimer, FAM-substrate, and then any leftover peptide that didn't react.
5. Take 10uL samples from a couple of fractions of each peak for a gel.
6. Collect the FAM-substrate fractions, which should elute around 13 mL.
7. Concentrate using a small 10K MWCO concentrator to about 100 uL.
8. Make 5uL aliquots in labelled tubes and snap freeze them in LN_2.

Protocol 2.5: *In vivo* crosslinking of Bpa-proteasome in yeast

Description:

This protocol is for growing yeast expressing Bpa-containing proteasome for crosslinking to substrates in live cells. This protocol dovetails nicely with the denaturing Ni-NTA prep protocol.

Materials:

Media

1. 10X Yeast nitrogen base without amino acids: 67 g/L in water. Filter sterilize.
2. 40% dextrose: 200 g in 500 mL. Filter sterilize.
3. Complete synthetic media without tryptophan (Csm-Trp, Sunrise Science Products): 0.74 g/L in water. Autoclave, cool down and then add 100 mL of 10X YNB and 50 mL of 40% dextrose.

Buffers

4. 1X Phosphate-buffered saline (PBS): Dilute 10X PBS (Thermo) to 1X in water, adjust the pH to 7.4, autoclave to sterilize.

Chemicals

5. 1,000X ampicillin
6. Bpa: p-benzoyl-L-phenylalanine (Amatek).
7. 1000X progesterone solution (Sigma): 157 mg in 100% ethanol for a 1000000X solution then do three subsequent 1/10 dilutions to get to 1,000X (See Methods below).
8. 1 M NaOH.
9. 100% ethanol.
10. 1000X Aprotinin: 1 mg/mL in 25% methanol.
11. 1000X Pepstatin: 1 mg/mL in 90% methanol, 10% acetic acid.
12. 1000X Leupeptin: 1 mg/mL in water.
13. 100X AEBSF: 100 mM in water.

Other reagents

14. Plastic cuvettes.
15. OD_{600} meter.
16. 150 mm Tissue Culture Dish (Corning)

17. 365 nm LED lamp (Amazon).
18. 16 oz. polypropylene containers with lids (Amazon).

Methods:

Day 1 - Overnight

1. From a Csm-Trp streak plate, pick a single colony and inoculate a 5 mL starter of Csm-Trp media with 0.5X ampicillin.
2. Grow overnight at 30 °C with rotation.

Day 2 - 50 mL starter culture

3. Inoculate four 50 mL starter cultures in Csm-Trp + 0.5X ampicillin with 1 mL of overnight culture.
4. Grow overnight at 30 °C with rotation.

Day 3 - Growth & Expression of Bpa-base

5. Prepare 8 L of Csm-Trp media.
6. Right before starting growth, add 100 mL 10X YNB (1X final) and 50 mL 40% dextrose (2% final) to each flask.
7. Dissolve 4.3 grams of Bpa in 48 mL of 1 M NaOH. Filter sterilize.
8. Divide the Bpa solution evenly amongst the media. Allow to shake to mix.
9. Measure the OD_{600} of the 50 mL starter cultures and add cells to each flask to a starting OD_{600} of 0.1.
10. Shake for 30 minutes to allow the cells to uptake the Bpa.
11. To prepare a 1000X progesterone solution:
    a. Measure 157 mg of progesterone and dissolve in 10 mL of 100% ethanol.
    b. Dilute by adding 1 mL of solution to 9 mL of 100% ethanol for 100000X.
    c. Dilute 100,000X solution by adding 1 mL to 9 mL 100% ethanol for 10000X.
    d. Dilute 10,000X solution by adding 1 mL to 9 mL of sterile water for a final solution of 1000X progesterone in 10% ethanol.
12. Add 1 mL of the progesterone solution to each flask.
13. Grow for approximately 13 hours, until cells reach an OD_{600} of 0.7.

Day 4 - Cell Harvesting and Cross-linking

14. Clean and autoclave four 1 L centrifuge bottles and 2 L of water.
15. When the cells have reached the appropriate OD_{600}, transfer to the centrifuge bottles and pellet by spinning at 3,500rpm for 15 minutes.
16. Pour off the media and repeat Step 15 with the other 4 L of cultures.

17. Wash the cells by resuspending with the 2L of sterile water.
18. Turn on the LED lamps in the cold room to allow them to warm up.
19. Spin the cells again to pellet and resuspend with 400 mL of 1X PBS.
20. Add 50 mL of cell suspension into eight 150 mm tissue culture dishes.
21. Place four of the dishes under a 365 nm LED lamp in the cold room. Keep the other four dishes in the dark at room temperature.
22. Allow to crosslink for 15 minutes.
23. Harvest the +UV and -UV cells from each dish into labelled 50 mL conicals, spin for 15 minutes at 4,000rpm at 4 °C.
24. Resuspend the pellets in 1X PBS + 1X protease inhibitors. You want the final volume to be at or less than 20 mL. You may take a sample of the cells here for western blotting to confirm crosslinking.
25. Flash freeze by dripping into a labeled plastic storage container filled with liquid nitrogen.

Protocol 2.6: Monitoring yeast strain growth via plate reader

Description:

This protocol is for measuring the growth of yeast in a plate reader. This experiment can be done to check conditions for any growth defects in generated strains.

Materials:

Media

1. 10X Yeast nitrogen base without amino acids: 67 g/L in water. Filter sterilize.
2. 40% dextrose: 200 g in 500 mL. Filter sterilize.
3. Complete synthetic media without tryptophan (Csm-Trp, Sunrise Science Products): 0.74 g/L in water. Autoclave, cool down and then add 100 mL of 10X YNB and 50 mL of 40% dextrose.

Other

1. Plastic cuvettes.
2. OD_{600} meter.
3. 96-well flat bottom plate (Corning).
4. Breathe-Easy sealing membrane (Sigma).
5. Plate reader.

Methods:

Day 1 - Initial overnight

1. Pick a single colony and inoculate 10 mL of Csm-Trp media.
2. Grow overnight to saturation.

Day 2 - Day-of pre-culture

1. Measure the OD of the initial overnight.
2. Dilute to OD_{600} = 0.1 in the desired conditions (media, etc.) you want to test growth in.
3. Grow for several divisions.

Day 2 - Making a plate

1. Dilute day-of culture to OD_{600} = 0.05 in an Eppendorf tube.
2. Add in triplicate, to the wells of a clear, 96-well flat-bottom plate. Be sure to add a media-only control for background subtraction.
3. Cover with Breathe-Easy sealing membrane.

Day 2 - Reading the plate

1. Grow with shaking, at 30 °C for 24 hours. Measure the OD_{600} every 10 minutes.

Day 3 - Plotting and calculating using Growthcurver

1. Plot the data using the R package Growthcurver with background subtraction from a media-only control.

Protocol 3.1: Purification of endogenous proteasome complexes from yeast

Description:

This protocol is for the purification of FLAG-tagged endogenous proteasome holoenzyme (26S) or subcomplexes (19S or 20S) from *Saccharomyces cerevisiae*. My yeast strains all have an endogenous 3xFLAG tag on the genomic locus of the 20S subunit PRE1. This allows for a simple, one-step purification of the proteasome fraction from yeast cells. This protocol can also be used for the purification of holoenzymes containing Rpt1-substrate crosslinks after UV exposure.

Materials:

Media

1. YPD**:** 20 g peptone, 10 g yeast extract, top to 950 mL and autoclave. Add 50 mL of 40% glucose before using (2% final).

   Note: YP is yeast extract and peptone and YPD is YP with 2% dextrose.

Buffers

1. High-salt Gel-Filtration (hsGF) Buffer (1L): 60 mM HEPES, pH 7.6, 400 mM NaCl, 100 mM KCl, 1 mM EDTA.
2. Yeast GF Buffer (yGF, 1L): 60 mM HEPES, pH 7.6, 50 mM NaCl, 50 mM KCl, 5 mM $MgCl_2$, 10% glycerol, 1 mM DTT (Added right before size-exclusion).

Methods

Day 1 - Streak

1. Using a sterile wooden dowel or inoculation loop, streak from a cell stock onto a YP plate.
2. Grow at 30 ºC for two days.

Day 3 - Starter culture

1. Check plate(s) for single colonies.
2. Under a flame and ~very~ aseptically inoculate a 50mL culture of YPD.

Optional: You can add 0.5X ampicillin too to prevent bacterial growth.

3. Grow at 30ºC for two days.

Note: If you forget to add glucose to the starter it should be okay, you can just let it grow an additional day.

Day 4 - Making media

1. Make however many liters of YP you need.
2. Autoclave. Let cool.
3. Make a stock of 40% glucose and filter sterilize into a sterile container. Keep in mind you will need 50mL glucose/L of YP.

Day 5 - Expression

1. Add 50 mL of glucose to each liter of YP.

Note: For other yeast strains we would add 1.6mg/mL adenine(ade) and tryptophan(trp) to each flask of YPD, but not for the ySY11 strain.

2. Under a flame and using sterile pipettes, inoculate each flask with 5mL of starter culture.

Optional: You can add 0.5X ampicillin too to prevent bacterial growth.

Note: I would 100% recommend doing this, actually.

3. Grow at 30ºC for 2-3 days.

Day 7 - Harvest

1. Look at the yeast under the microscope. Make sure that they are confluent, and that there is no bacterial contamination which should look like black spots.
2. Harvest yeast in a centrifuge at 4,000 rpm for 15 minutes.
3. Resuspend cells in the minimum amount of buffer. In the past, this has been around 5 mL per liter, but can be as high as 10mL per liter.

Day 7 - Freezing aka "Popcorning" & Cryomilling

1. Label a tupperware container with name, date, and strain.
2. In a wide styrofoam cooler, place the tupperware container and fill it with liquid nitrogen (LN_2).

3. Fill the area around the tupperware with liquid nitrogen but not higher than the LN_2 in the tupperware.
4. Create popcorn by slowly dripping cells into the liquid nitrogen, make sure to drip it in so it forms granules and not big clumps. This will make the cryomilling better later on.
5. Store popcorned yeast at -80ºC. It's better to let the popcorned yeast sit for at least a day before moving onto cryomilling.
6. After cryo-milling store powdered yeast at -80ºC.

Purification

1. Calculate how much mass (grams) yeast powder you want to use.
2. You're going to measure 1.5X the mass of yeast in mLs of normal yeast GF.

    Example: I used 50 g of yeast powder—and resuspended in 75 mLs of yGF.

3. Bring the yGF to room temp and add 1mL of NP-40 10% per 50 mLs of yGF (0.2% NP-40 final) and ATP to a final concentration of 0.5 mM.

    Note: I also added 2 tubes of ATP regen to each lysis.

4. Thaw the cell powder on the bench top in a water bath.
5. Add the yGF (+ NP-40 + ATP) once the edges of the powder begin to melt.
6. Once you add the buffer, stir with a spatula until no more ice remains—stir slowly and try to minimize foaming.

    Note: The solution will be chunky because of lipids, but there should not be any ice crystals.

7. Spin at 26,000 rcf for 40-45 mins at 4 °C.
8. Equilibrate four **1st step FLAG** columns by:
    a. Wash with 2 C.V.s of TBS.
    b. Wash with 3 consecutive C.V.s of 0.1M glycine pH 3.5.
    c. Wash with 2 C.V.s of TBS again.
    d. 2 consecutive C.V.s of yGF + NP-40.
9. Gently re-suspend the FLAG resin and distribute amongst 50mL falcon tubes.
10. Batch bind lysate to the resin for 1hr at 4 °C.
11. Pour the mixture back into a glass column, allow to drain until right before resin is exposed.
    a. Wash with 20 mL per column of yGF + 0.2% NP-40 + 0.5 mM ATP.

b. Wash with 20 mL per column of yGF + 0.1% NP-40 + 0.5 mM ATP.
c. Wash with 20 mL per column of yGF + 0.5 mM ATP.
d. Elute with 15 mL of yGF + 0.5mM ATP + 0.15 mg/mL FLAG peptide.

12. **If wanting to purify 20S only**:
    a. Carry out an additional wash with 20 mL of high-salt GF prior to elution to dissociate the 19S from bound 20S.
13. Concentrate to 500 uL using a 30K MWCO cartridge at 4 , 2000 rcf in 5-10 minute increments.
14. Run on a Superose 6i column pre-equilibrated with yGF with 0.5 mM ATP and 0.5 mM TCEP. **If only purifying 20S**: omit the ATP from the buffer during gel-filtration as it will interfere with determining the concentration downstream. **If purifying substrate-crosslinked Bpa holoenzyme:** you can skip the size-exclusion step and proceed directly into the next application.

Determining concentrations

1. For complexes containing 19S, calculate the concentration with a Bradford assay using a standard curve of known BSA concentrations.
2. For 20S-only complexes, use a spectrophotometer to measure the absorbance at 280 nm of a dilution of the eluted protein.

Protocol 3.2: Denaturing Ni-NTA purification of 6xHis-Rpt1-substrate crosslinks

Description:

This protocol is for the purification of 6xhis-tagged Rpt1 (or any his-tagged protein) under denaturing conditions. The downstream application of this protocol is for a relatively clean sample going into mass spectrometry analysis.

Materials:

Buffer Stocks

1. 0.5 M sodium phosphate: 35.49 grams of Na_2HPO_4 in 500 mL of water. Filter sterilized.
2. 4 M NaCl: Dissolve 233.76 grams of NaCl in 1 liter of water. Filter sterilize.
3. 2 M imidazole: 68.08 g in water, adjust pH to 7.6, top to 500 mL, filter sterilize.

Buffers

1. Gnd HCl Binding Buffer (500 mL): 20 mM Na_2HPO_4, 150 mM NaCl, 10 mM imidazole, 8M Gnd HCl, pH to 7.4.
2. Gnd HCl Wash Buffer 1 (500 mL): 20 mM Na_2HPO_4, 300 mM NaCl, 10 mM imidazole, 6M Gnd HCl, pH to 7.4.
3. Gnd HCl Wash Buffer 2 (500 mL): 20 mM Na_2HPO_4, 300 mM NaCl, 25 mM imidazole, 6M Gnd HCl, pH to 7.4.
4. Gnd HCl Elution Buffer(250 mL): 20 mM Na_2HPO_4, 300 mM NaCl, 250 mM imidazole, 6M Gnd HCl, pH to 7.4.
5. Sodium phosphate Buffer (250 mL): 20 mM Na_2HPO_4, 300 mM NaCl, pH to 7.4

Reagents

1. Ni-NTA agarose (Sigma).
2. SPEX SamplePrep cryogenic mill.
3. Large cryo-mill canisters.
4. Liquid nitrogen.
5. Probe-tip sonicator.
6. Econo-Pac disposable 10 mL chromatography columns (Bio-Rad).
7. 10K MWCO spin concentrators.

Methods:

Cell lysis by cryo-milling

1. Pre-chill two cryo-milling canisters (+UV/-UV) in the cryo-mill using the autofill program.
2. Once chilled to liquid nitrogen temperatures, open the canisters and add the frozen yeast pellets to each canister.
3. Lyse the yeast by grinding using the two-barrel protocol (15 cycles of 2 minutes of grinding time and 1 minute of cooling time).
4. Transfer the lysate powder to a plastic container and store at -80 °C or proceed with the purification.

Denaturing Ni-NTA purification

Note: this method is carried out for each +UV and -UV pair.

1. Resuspend the powder with Gnd HCl Binding Buffer so that the final concentration of Gnd HCl is approximately 6 M. Typically, there is 20 mL of lysate so add 60 mL of Binding Buffer.
2. Incubate the lysate at room temperature with stirring to denature the lysate and prevent the formation of ice crystals.
3. Once the lysate appears homogeneous, transfer to labeled stainless-steel beakers and sonicate using 70% amplitude with a cycle of 3 seconds on and 59 seconds off.
4. Clarify the lysate by transferring to centrifuge tubes and spinning at 26,000xg for 30 minutes.
5. While the lysate is spinning, prepare 10 mL of NiNTA slurry (5 mL of agarose):
    a. In a 50 mL conical, spin at 700xg for 2 minutes and pour off the storage solution.
    b. Wash twice by resuspending the resin in clean water and spin to collect the agarose.
    c. Wash into 6 M Gnd HCl Binding Buffer by topping off to 10 mL in the conical.
6. Transfer the clarified lysate into 50 mL conicals, divide the NiNTA resin across the lysate. You should have approximately 2.5 mL of NiNTA resin per +UV and -UV prep.
7. Batch bind the resin for up to 1 hour at room temperature with rotation.
8. Transfer the lysate and resin mixture into a disposable chromatography column. Allow the resin to settle for 15 minutes and snap off the plug to allow the liquid to flow.
9. Continually top off the columns until all the liquid has been transferred into the columns.

10. Wash each column with two sequential 25 mL volumes of Wash Buffer 1 for a total of 50 mL per column of Wash 1.
11. Wash each column with two sequential 25 mL volumes of Wash Buffer 2 for a total of 50 mL pero column of Wash 2.
12. Add 25 mL of Elution Buffer to each column and collect the elution.
13. Concentrate the elution using a 10K MWCO concentrator to approximately 500 uL.

Protocol 3.3: Methanol precipitation of proteins for mass spectrometry

Description:

This is a protocol for precipitating and washing the protein samples from denaturing NiNTA preps prior to sample submission for LC-MS/MS.

Materials:

1. 100% Methanol, chilled to -20 °C.
2. Probe-tip sonicator.
3. 50 mL Oak Ridge Style Round Bottom Centrifuge Tube.
4. 2 mL low-retention Eppendorf tubes.

Methods:

Day 1 - Precipitation

1. Chill a bottle of 100% methanol at -20 °C.
2. Transfer your concentrated denaturing prep elution to a 50 mL Oak Ridge style centrifuge tube.
3. Add 9 volumes of ice-cold 100% methanol to the tube and vortex briefly.
4. Incubate at -80 °C overnight.

Day 2 - Wash & Dry Protein Samples

5. Spin at 12,000xg for 10-15 mins at 4 °C. Protein will pellet at bottom.
6. Carefully aspirate supernatant.
7. Add 1 mL of pre-chilled (-20 °C) methanol to each tube.
8. Sonicate using a probe-tip sonicator (3 sec pulse, 20 sec off, 20% amplitude, 2-3 pulses) until protein goes into solution.
9. Transfer to 2 mL low-retention microcentrifuge tube.
10. Spin at 6,500 xg for 5 mins. Carefully aspirate the supernatant.
11. Repeat methanol wash (**Steps 7-10** once more).
12. Allow the pellet to air-dry by covering the tubes with a kimwipe for 10 minutes.
13. Dried pellets can be submitted to the UCB MS facility for LC-MS/MS.

Table 2.1: MS Identified Proteins in +UV FLAG-purified 26S Holoenzyme Preparations

Table 2-1: MS Identified Proteins in +UV FLAG-purified 26S Holoenzymes					Proteasome-associated	
Protein	**Protein ID**	**Entry Name**	**Gene**	**Protein Description**	**Subcomplex**	**Notes**
sp|P38764|RPN1_YEAST	P38764	RPN1_YEAST	RPN1	26S proteasome regulatory subunit RPN1	19S Base	Ub-receptor
sp|P32565|RPN2_YEAST	P32565	RPN2_YEAST	RPN2	26S proteasome regulatory subunit RPN2		
sp|P33299|PRS7_YEAST	P33299	PRS7_YEAST	RPT1	26S proteasome regulatory subunit 7 homolog		AAA+ ATPase
sp|P40327|PRS4_YEAST	P40327	PRS4_YEAST	RPT2	26S proteasome regulatory subunit 4 homolog		
sp|P33298|PRS6B_YEAST	P33298	PRS6B_YEAST	RPT3	26S proteasome regulatory subunit 6B homolog		
sp|P53549|PRS10_YEAST	P53549	PRS10_YEAST	RPT4	26S proteasome subunit RPT4		
sp|P33297|PRS6A_YEAST	P33297	PRS6A_YEAST	RPT5	26S proteasome regulatory subunit 6A		
sp|Q01939|PRS8_YEAST	Q01939	PRS8_YEAST	RPT6	26S proteasome regulatory subunit 8 homolog		
sp|O13563|RPN13_YEAST	O13563	RPN13_YEAST	RPN13	26S proteasome regulatory subunit RPN13		Ub-receptor
sp|P43588|RPN11_YEAST	P43588	RPN11_YEAST	RPN11	Ubiquitin carboxyl-terminal hydrolase RPN11	19S Lid	De-ubiquitinase
sp|P32496|RPN12_YEAST	P32496	RPN12_YEAST	RPN12	26S proteasome regulatory subunit RPN12		
sp|P40016|RPN3_YEAST	P40016	RPN3_YEAST	RPN3	26S proteasome regulatory subunit RPN3		
sp|Q12250|RPN5_YEAST	Q12250	RPN5_YEAST	RPN5	26S proteasome regulatory subunit RPN5		
sp|Q12377|RPN6_YEAST	Q12377	RPN6_YEAST	RPN6	26S proteasome regulatory subunit RPN6		
sp|Q06103|RPN7_YEAST	Q06103	RPN7_YEAST	RPN7	26S proteasome regulatory subunit RPN7		
sp|Q08723|RPN8_YEAST	Q08723	RPN8_YEAST	RPN8	26S proteasome regulatory subunit RPN8		
sp|Q04062|RPN9_YEAST	Q04062	RPN9_YEAST	RPN9	26S proteasome regulatory subunit RPN9		
sp|O94742|SEM1_YEAST	O94742	SEM1_YEAST	SEM1	26S proteasome complex subunit SEM1		
sp|P21242|PSA7_YEAST	P21242	PSA7_YEAST	PRE10	Probable proteasome subunit alpha type-7	20S CP	alpha-ring
sp|P40302|PSA6_YEAST	P40302	PSA6_YEAST	PRE5	Proteasome subunit alpha type-6		
sp|P40303|PSA4_YEAST	P40303	PSA4_YEAST	PRE6	Proteasome subunit alpha type-4		
sp|P23639|PSA2_YEAST	P23639	PSA2_YEAST	PRE8	Proteasome subunit alpha type-2		
sp|P23638|PSA3_YEAST	P23638	PSA3_YEAST	PRE9	Proteasome subunit alpha type-3		
sp|P32379|PSA5_YEAST	P32379	PSA5_YEAST	PUP2	Proteasome subunit alpha type-5		
sp|P21243|PSA1_YEAST	P21243	PSA1_YEAST	SCL1	Proteasome subunit alpha type-1		
sp|P22141|PSB4_YEAST	P22141	PSB4_YEAST	PRE1	Proteasome subunit beta type-4		beta-ring
sp|P30656|PSB5_YEAST	P30656	PSB5_YEAST	PRE2	Proteasome subunit beta type-5		
sp|P38624|PSB1_YEAST	P38624	PSB1_YEAST	PRE3	Proteasome subunit beta type-1		
sp|P30657|PSB7_YEAST	P30657	PSB7_YEAST	PRE4	Proteasome subunit beta type-7		
sp|P23724|PSB6_YEAST	P23724	PSB6_YEAST	PRE7	Proteasome subunit beta type-6		
sp|P25043|PSB2_YEAST	P25043	PSB2_YEAST	PUP1	Proteasome subunit beta type-2		
sp|P25451|PSB3_YEAST	P25451	PSB3_YEAST	PUP3	Proteasome subunit beta type-3		
sp|P38886|RPN10_YEAST	P38886	RPN10_YEAST	RPN10	26S proteasome regulatory subunit RPN10	N/A	Ub-receptor
sp|P36040|POC2_YEAST	P36040	POC2_YEAST	ADD66	Proteasome assembly chaperone 2	N/A	
sp|P43583|BLM10_YEAST	P43583	BLM10_YEAST	BLM10	Proteasome activator BLM10	N/A	
sp|P38779|CIC1_YEAST	P38779	CIC1_YEAST	CIC1	Proteasome-interacting protein CIC1	N/A	
sp|P38737|ECM29_YEAST	P38737	ECM29_YEAST	ECM29	Proteasome component ECM29	N/A	
sp|Q05778|POC1_YEAST	Q05778	POC1_YEAST	PBA1	Proteasome chaperone 1	N/A	
sp|P04710|ADT1_YEAST	P04710	ADT1_YEAST	AAC1	ADP,ATP carrier protein 1		
sp|Q00955|ACAC_YEAST	Q00955	ACAC_YEAST	ACC1	Acetyl-CoA carboxylase		
sp|P52910|ACS2_YEAST	P52910	ACS2_YEAST	ACS2	Acetyl-coenzyme A synthetase 2		
sp|P60010|ACT_YEAST	P60010	ACT_YEAST	ACT1	Actin		
sp|P07245|C1TC_YEAST	P07245	C1TC_YEAST	ADE3	C-1-tetrahydrofolate synthase, cytoplasmic		
sp|P00330|ADH1_YEAST	P00330	ADH1_YEAST	ADH1	Alcohol dehydrogenase 1		
sp|P39925|AFG3_YEAST	P39925	AFG3_YEAST	AFG3	Mitochondrial respiratory chain complexes assembly protein AFG3		
sp|Q99222|AFI1_YEAST	Q99222	AFI1_YEAST	AFI1	ARF3-interacting protein 1		
sp|P25376|AGP1_YEAST	P25376	AGP1_YEAST	AGP1	General amino acid permease AGP1		
sp|Q12449|AHA1_YEAST	Q12449	AHA1_YEAST	AHA1	Hsp90 co-chaperone AHA1		
sp|P40053|AIM9_YEAST	P40053	AIM9_YEAST	AIM9	Altered inheritance of mitochondria protein 9, mitochondrial		
sp|P47019|ALB1_YEAST	P47019	ALB1_YEAST	ALB1	Ribosome biogenesis protein ALB1		
sp|P54115|ALDH6_YEAST	P54115	ALDH6_YEAST	ALD6	Magnesium-activated aldehyde dehydrogenase, cytosolic		
sp|P53868|ALG9_YEAST	P53868	ALG9_YEAST	ALG9	Alpha-1,2-mannosyltransferase ALG9		
sp|P38281|APD1_YEAST	P38281	APD1_YEAST	APD1	Actin patches distal protein 1		
sp|P40024|ARB1_YEAST	P40024	ARB1_YEAST	ARB1	ABC transporter ATP-binding protein ARB1		
sp|P11076|ARF1_YEAST	P11076	ARF1_YEAST	ARF1	ADP-ribosylation factor 1		
sp|P22768|ASSY_YEAST	P22768	ASSY_YEAST	ARG1	Argininosuccinate synthase		
sp|P53090|ARO8_YEAST	P53090	ARO8_YEAST	ARO8	Aromatic/aminoadipate aminotransferase 1		
sp|Q12406|ARP7_YEAST	Q12406	ARP7_YEAST	ARP7	Actin-related protein 7		
sp|Q03862|ARX1_YEAST	Q03862	ARX1_YEAST	ARX1	Probable metalloprotease ARX1		
sp|P38011|GBLP_YEAST	P38011	GBLP_YEAST	ASC1	Guanine nucleotide-binding protein subunit beta-like protein		
sp|P48361|ASK10_YEAST	P48361	ASK10_YEAST	ASK10	Activator of SKN7 protein 10		
sp|P49089|ASNS1_YEAST	P49089	ASNS1_YEAST	ASN1	Asparagine synthetase [glutamine-hydrolyzing] 1		
sp|Q07528|ATG20_YEAST	Q07528	ATG20_YEAST	ATG20	Autophagy-related protein 20		
sp|P47113|BFA1_YEAST	P47113	BFA1_YEAST	BFA1	Mitotic check point protein BFA1		
sp|P38934|BFR1_YEAST	P38934	BFR1_YEAST	BFR1	Nuclear segregation protein BFR1		
sp|Q06631|BFR2_YEAST	Q06631	BFR2_YEAST	BFR2	Protein BFR2		
sp|Q08965|BMS1_YEAST	Q08965	BMS1_YEAST	BMS1	Ribosome biogenesis protein BMS1		
sp|Q08235|BRX1_YEAST	Q08235	BRX1_YEAST	BRX1	Ribosome biogenesis protein BRX1		
sp|Q08492|BUD21_YEAST	Q08492	BUD21_YEAST	BUD21	Bud site selection protein 21		
sp|P29547|EF1G1_YEAST	P29547	EF1G1_YEAST	CAM1	Elongation factor 1-gamma 1		
sp|P33322|CBF5_YEAST	P33322	CBF5_YEAST	CBF5	H/ACA ribonucleoprotein complex subunit CBF5		
sp|P38626|NCB5R_YEAST	P38626	NCB5R_YEAST	CBR1	NADH-cytochrome b5 reductase 1		
sp|P39076|TCPB_YEAST	P39076	TCPB_YEAST	CCT2	T-complex protein 1 subunit beta		
sp|P39077|TCPG_YEAST	P39077	TCPG_YEAST	CCT3	T-complex protein 1 subunit gamma		
sp|P39078|TCPD_YEAST	P39078	TCPD_YEAST	CCT4	T-complex protein 1 subunit delta		
sp|P40413|TCPE_YEAST	P40413	TCPE_YEAST	CCT5	T-complex protein 1 subunit epsilon		
sp|P39079|TCPZ_YEAST	P39079	TCPZ_YEAST	CCT6	T-complex protein 1 subunit zeta		
sp|P47079|TCPQ_YEAST	P47079	TCPQ_YEAST	CCT8	T-complex protein 1 subunit theta		
sp|P40986|CDC1_YEAST	P40986	CDC1_YEAST	CDC1	Cell division control protein 1		
sp|P25342|CDC10_YEAST	P25342	CDC10_YEAST	CDC10	Cell division control protein 10		
sp|P09798|CDC16_YEAST	P09798	CDC16_YEAST	CDC16	Anaphase-promoting complex subunit CDC16		

sp|P00549|KPYK1_YEAST	P00549	KPYK1_YEAST	CDC19	Pyruvate kinase 1
sp|P07260|IF4E_YEAST	P07260	IF4E_YEAST	CDC33	Eukaryotic translation initiation factor 4E
sp|P25694|CDC48_YEAST	P25694	CDC48_YEAST	CDC48	Cell division control protein 48
sp|P26637|SYLC_YEAST	P26637	SYLC_YEAST	CDC60	Leucine--tRNA ligase, cytoplasmic
sp|Q06697|CDC73_YEAST	Q06697	CDC73_YEAST	CDC73	Cell division control protein 73
sp|P43634|CHA4_YEAST	P43634	CHA4_YEAST	CHA4	Activatory protein CHA4
sp|P22137|CLH_YEAST	P22137	CLH_YEAST	CHC1	Clathrin heavy chain
sp|P32657|CHD1_YEAST	P32657	CHD1_YEAST	CHD1	Chromo domain-containing protein 1
sp|P15790|CSK21_YEAST	P15790	CSK21_YEAST	CKA1	Casein kinase II subunit alpha
sp|P19454|CSK22_YEAST	P19454	CSK22_YEAST	CKA2	Casein kinase II subunit alpha'
sp|P43639|CSK2B_YEAST	P43639	CSK2B_YEAST	CKB1	Casein kinase II subunit beta
sp|P38930|CSK2C_YEAST	P38930	CSK2C_YEAST	CKB2	Casein kinase II subunit beta'
sp|Q03690|CLU_YEAST	Q03690	CLU_YEAST	CLU1	Clustered mitochondria protein 1
sp|P53622|COPA_YEAST	P53622	COPA_YEAST	COP1	Coatomer subunit alpha
sp|P03965|CARB_YEAST	P03965	CARB_YEAST	CPA2	Carbamoyl-phosphate synthase arginine-specific large chain
sp|P40442|CSS1_YEAST	P40442	CSS1_YEAST	CSS1	Secreted protein CSS1
sp|P89105|CTR9_YEAST	P89105	CTR9_YEAST	CTR9	RNA polymerase-associated protein CTR9
sp|Q12389|DBP10_YEAST	Q12389	DBP10_YEAST	DBP10	ATP-dependent RNA helicase DBP10
sp|P24783|DBP2_YEAST	P24783	DBP2_YEAST	DBP2	ATP-dependent RNA helicase DBP2
sp|P20447|DBP3_YEAST	P20447	DBP3_YEAST	DBP3	ATP-dependent RNA helicase DBP3
sp|P20449|DBP5_YEAST	P20449	DBP5_YEAST	DBP5	ATP-dependent RNA helicase DBP5
sp|P38719|DBP8_YEAST	P38719	DBP8_YEAST	DBP8	ATP-dependent RNA helicase DBP8
sp|Q06218|DBP9_YEAST	Q06218	DBP9_YEAST	DBP9	ATP-dependent RNA helicase DBP9
sp|P06634|DED1_YEAST	P06634	DED1_YEAST	DED1	ATP-dependent RNA helicase DED1
sp|P38707|SYNC_YEAST	P38707	SYNC_YEAST	DED81	Asparagine--tRNA ligase, cytoplasmic
sp|P41819|DIM1_YEAST	P41819	DIM1_YEAST	DIM1	Dimethyladenosine transferase
sp|Q12220|UTP12_YEAST	Q12220	UTP12_YEAST	DIP2	U3 small nucleolar RNA-associated protein 12
sp|Q08162|RRP44_YEAST	Q08162	RRP44_YEAST	DIS3	Exosome complex exonuclease DIS3
sp|Q03921|DOP1_YEAST	Q03921	DOP1_YEAST	DOP1	Protein dopey
sp|P04802|SYDC_YEAST	P04802	SYDC_YEAST	DPS1	Aspartate--tRNA ligase, cytoplasmic
sp|P32892|DRS1_YEAST	P32892	DRS1_YEAST	DRS1	ATP-dependent RNA helicase DRS1
sp|P48510|DSK2_YEAST	P48510	DSK2_YEAST	DSK2	Ubiquitin domain-containing protein DSK2
sp|P07273|TFS2_YEAST	P07273	TFS2_YEAST	DST1	Transcription elongation factor S-II
sp|P38149|DUG2_YEAST	P38149	DUG2_YEAST	DUG2	Probable di- and tripeptidase DUG2
sp|P53871|DUG3_YEAST	P53871	DUG3_YEAST	DUG3	Probable glutamine amidotransferase DUG3
sp|P39009|DUN1_YEAST	P39009	DUN1_YEAST	DUN1	DNA damage response protein kinase DUN1
sp|P36049|EBP2_YEAST	P36049	EBP2_YEAST	EBP2	rRNA-processing protein EBP2
sp|Q04217|DHR1_YEAST	Q04217	DHR1_YEAST	ECM16	Probable ATP-dependent RNA helicase DHR1
sp|P32471|EF1B_YEAST	P32471	EF1B_YEAST	EFB1	Elongation factor 1-beta
sp|Q3E705|EFG1P_YEAST	Q3E705	EFG1P_YEAST	EFG1	rRNA-processing protein EFG1
sp|P32324|EF2_YEAST	P32324	EF2_YEAST	EFT1	Elongation factor 2
sp|Q03071|ELOC_YEAST	Q03071	ELOC_YEAST	ELC1	Elongin-C
sp|Q06287|NEP1_YEAST	Q06287	NEP1_YEAST	EMG1	Ribosomal RNA small subunit methyltransferase NEP1
sp|P40085|TAPT1_YEAST	P40085	TAPT1_YEAST	EMP65	Endoplasmic reticulum membrane protein 65
sp|P00924|ENO1_YEAST	P00924	ENO1_YEAST	ENO1	Enolase 1
sp|P00925|ENO2_YEAST	P00925	ENO2_YEAST	ENO2	Enolase 2
sp|P38333|ENP1_YEAST	P38333	ENP1_YEAST	ENP1	Essential nuclear protein 1
sp|P48234|NOL10_YEAST	P48234	NOL10_YEAST	ENP2	Ribosome biogenesis protein ENP2
sp|Q04660|ERB1_YEAST	Q04660	ERB1_YEAST	ERB1	Ribosome biogenesis protein ERB1
sp|P41338|ERG10_YEAST	P41338	ERG10_YEAST	ERG10	Acetyl-CoA acetyltransferase
sp|P54781|ERG5_YEAST	P54781	ERG5_YEAST	ERG5	C-22 sterol desaturase ERG5
sp|Q03661|ESC1_YEAST	Q03661	ESC1_YEAST	ESC1	Silent chromatin protein ESC1
sp|Q06344|ESF1_YEAST	Q06344	ESF1_YEAST	ESF1	Pre-rRNA-processing protein ESF1
sp|P53743|ESF2_YEAST	P53743	ESF2_YEAST	ESF2	Pre-rRNA-processing protein ESF2
sp|P39002|LCF3_YEAST	P39002	LCF3_YEAST	FAA3	Long-chain-fatty-acid--CoA ligase 3
sp|P40546|FAF1_YEAST	P40546	FAF1_YEAST	FAF1	Protein FAF1
sp|Q05040|FAR8_YEAST	Q05040	FAR8_YEAST	FAR8	Factor arrest protein 8
sp|P07149|FAS1_YEAST	P07149	FAS1_YEAST	FAS1	Fatty acid synthase subunit beta
sp|P19097|FAS2_YEAST	P19097	FAS2_YEAST	FAS2	Fatty acid synthase subunit alpha
sp|P14540|ALF_YEAST	P14540	ALF_YEAST	FBA1	Fructose-bisphosphate aldolase
sp|Q05498|FCF1_YEAST	Q05498	FCF1_YEAST	FCF1	rRNA-processing protein FCF1
sp|Q12035|FCF2_YEAST	Q12035	FCF2_YEAST	FCF2	rRNA-processing protein FCF2
sp|P40988|FET4_YEAST	P40988	FET4_YEAST	FET4	Low-affinity Fe(2+) transport protein
sp|Q08913|FEX1_YEAST	Q08913	FEX1_YEAST	FEX1	Fluoride export protein 1
sp|P38631|FKS1_YEAST	P38631	FKS1_YEAST	FKS1	1,3-beta-glucan synthase component FKS1
sp|P51601|GCH1_YEAST	P51601	GCH1_YEAST	FOL2	GTP cyclohydrolase 1
sp|P38911|FKBP3_YEAST	P38911	FKBP3_YEAST	FPR3	Peptidyl-prolyl cis-trans isomerase
sp|Q06205|FKBP4_YEAST	Q06205	FKBP4_YEAST	FPR4	FK506-binding protein 4
sp|P23900|FPS1_YEAST	P23900	FPS1_YEAST	FPS1	Glycerol uptake/efflux facilitator protein
sp|P25659|FUB1_YEAST	P25659	FUB1_YEAST	FUB1	Silencing boundary-establishment protein FUB1
sp|P39730|IF2P_YEAST	P39730	IF2P_YEAST	FUN12	Eukaryotic translation initiation factor 5B
sp|P28007|GAR1_YEAST	P28007	GAR1_YEAST	GAR1	H/ACA ribonucleoprotein complex subunit GAR1
sp|P32481|IF2G_YEAST	P32481	IF2G_YEAST	GCD11	Eukaryotic translation initiation factor 2 subunit gamma
sp|Q02979|GDE1_YEAST	Q02979	GDE1_YEAST	GDE1	Glycerophosphocholine phosphodiesterase GDE1
sp|P07262|DHE4_YEAST	P07262	DHE4_YEAST	GDH1	NADP-specific glutamate dehydrogenase 1
sp|P38988|GGC1_YEAST	P38988	GGC1_YEAST	GGC1	Mitochondrial GTP/GDP carrier protein 1
sp|P53900|PFD4_YEAST	P53900	PFD4_YEAST	GIM3	Prefoldin subunit 4
sp|P32288|GLNA_YEAST	P32288	GLNA_YEAST	GLN1	Glutamine synthetase
sp|P38720|6PGD1_YEAST	P38720	6PGD1_YEAST	GND1	6-phosphogluconate dehydrogenase, decarboxylating 1
sp|P06738|PHSG_YEAST	P06738	PHSG_YEAST	GPH1	Glycogen phosphorylase
sp|P00950|PMG1_YEAST	P00950	PMG1_YEAST	GPM1	Phosphoglycerate mutase 1
sp|Q03835|GLRX3_YEAST	Q03835	GLRX3_YEAST	GRX3	Monothiol glutaredoxin-3
sp|P32642|GLRX4_YEAST	P32642	GLRX4_YEAST	GRX4	Monothiol glutaredoxin-4

sp|P46655|SYEC_YEAST	P46655	SYEC_YEAST	GUS1	Glutamate--tRNA ligase, cytoplasmic
sp|Q03532|HAS1_YEAST	Q03532	HAS1_YEAST	HAS1	ATP-dependent RNA helicase HAS1
sp|P20448|DBP4_YEAST	P20448	DBP4_YEAST	HCA4	ATP-dependent RNA helicase HCA4
sp|Q05775|EIF3J_YEAST	Q05775	EIF3J_YEAST	HCR1	Eukaryotic translation initiation factor 3 subunit J
sp|P32347|DCUP_YEAST	P32347	DCUP_YEAST	HEM12	Uroporphyrinogen decarboxylase
sp|P32874|HFA1_YEAST	P32874	HFA1_YEAST	HFA1	Acetyl-CoA carboxylase, mitochondrial
sp|P02309|H4_YEAST	P02309	H4_YEAST	HHF1	Histone H4
sp|P53551|H1_YEAST	P53551	H1_YEAST	HHO1	Histone H1
sp|P61830|H3_YEAST	P61830	H3_YEAST	HHT1	Histone H3
sp|P00498|HIS1_YEAST	P00498	HIS1_YEAST	HIS1	ATP phosphoribosyltransferase
sp|P00815|HIS2_YEAST	P00815	HIS2_YEAST	HIS4	Histidine biosynthesis trifunctional protein
sp|P12683|HMDH1_YEAST	P12683	HMDH1_YEAST	HMG1	3-hydroxy-3-methylglutaryl-coenzyme A reductase 1
sp|P13663|DHAS_YEAST	P13663	DHAS_YEAST	HOM2	Aspartate-semialdehyde dehydrogenase
sp|P29295|HRR25_YEAST	P29295	HRR25_YEAST	HRR25	Casein kinase I homolog HRR25
sp|P15108|HSC82_YEAST	P15108	HSC82_YEAST	HSC82	ATP-dependent molecular chaperone HSC82
sp|P31539|HS104_YEAST	P31539	HS104_YEAST	HSP104	Heat shock protein 104
sp|P15992|HSP26_YEAST	P15992	HSP26_YEAST	HSP26	Heat shock protein 26
sp|P02829|HSP82_YEAST	P02829	HSP82_YEAST	HSP82	ATP-dependent molecular chaperone HSP82
sp|P02293|H2B1_YEAST	P02293	H2B1_YEAST	HTB1	Histone H2B.1
sp|P53119|HUL5_YEAST	P53119	HUL5_YEAST	HUL5	E3 ubiquitin-protein ligase HUL5
sp|P04807|HXKB_YEAST	P04807	HXKB_YEAST	HXK2	Hexokinase-2
sp|P32465|HXT1_YEAST	P32465	HXT1_YEAST	HXT1	Low-affinity glucose transporter HXT1
sp|P32466|HXT3_YEAST	P32466	HXT3_YEAST	HXT3	Low-affinity glucose transporter HXT3
sp|P23301|IF5A1_YEAST	P23301	IF5A1_YEAST	HYP2	Eukaryotic translation initiation factor 5A-1
sp|P09436|SYIC_YEAST	P09436	SYIC_YEAST	ILS1	Isoleucine--tRNA ligase, cytoplasmic
sp|P47170|IML1_YEAST	P47170	IML1_YEAST	IML1	Vacuolar membrane-associated protein IML1
sp|P32899|IMP3_YEAST	P32899	IMP3_YEAST	IMP3	U3 small nucleolar ribonucleoprotein protein IMP3
sp|P53941|IMP4_YEAST	P53941	IMP4_YEAST	IMP4	U3 small nucleolar ribonucleoprotein protein IMP4
sp|P01097|ATIF_YEAST	P01097	ATIF_YEAST	INH1	ATPase inhibitor, mitochondrial
sp|P53877|IPI3_YEAST	P53877	IPI3_YEAST	IPI3	Pre-rRNA-processing protein IPI3
sp|P38217|IMB2_YEAST	P38217	IMB2_YEAST	KAP104	Importin subunit beta-2
sp|P16474|BIP_YEAST	P16474	BIP_YEAST	KAR2	Endoplasmic reticulum chaperone BiP
sp|P47114|KCH1_YEAST	P47114	KCH1_YEAST	KCH1	Low affinity K(+) transporter 1
sp|P50090|KEL2_YEAST	P50090	KEL2_YEAST	KEL2	Kelch repeat-containing protein 2
sp|P20967|ODO1_YEAST	P20967	ODO1_YEAST	KGD1	2-oxoglutarate dehydrogenase, mitochondrial
sp|P53914|NAT10_YEAST	P53914	NAT10_YEAST	KRE33	RNA cytidine acetyltransferase
sp|P22023|KRE5_YEAST	P22023	KRE5_YEAST	KRE5	Killer toxin-resistance protein 5
sp|P42846|KRI1_YEAST	P42846	KRI1_YEAST	KRI1	Protein KRI1
sp|P25586|KRR1_YEAST	P25586	KRR1_YEAST	KRR1	KRR1 small subunit processome component
sp|P15180|SYKC_YEAST	P15180	SYKC_YEAST	KRS1	Lysine--tRNA ligase, cytoplasmic
sp|P38691|KSP1_YEAST	P38691	KSP1_YEAST	KSP1	Serine/threonine-protein kinase KSP1
sp|P14681|KSS1_YEAST	P14681	KSS1_YEAST	KSS1	Mitogen-activated protein kinase KSS1
sp|P38130|KTR3_YEAST	P38130	KTR3_YEAST	KTR3	Probable mannosyltransferase KTR3
sp|Q04377|LCD1_YEAST	Q04377	LCD1_YEAST	LCD1	DNA damage checkpoint protein LCD1
sp|P40079|LCP5_YEAST	P40079	LCP5_YEAST	LCP5	U3 small nucleolar ribonucleoprotein protein LCP5
sp|P38439|LEO1_YEAST	P38439	LEO1_YEAST	LEO1	RNA polymerase-associated protein LEO1
sp|P07264|LEUC_YEAST	P07264	LEUC_YEAST	LEU1	3-isopropylmalate dehydratase
sp|P43586|LOC1_YEAST	P43586	LOC1_YEAST	LOC1	60S ribosomal subunit assembly/export protein LOC1
sp|P35688|LRG1_YEAST	P35688	LRG1_YEAST	LRG1	Rho-GTPase-activating protein LRG1
sp|P53145|LSG1_YEAST	P53145	LSG1_YEAST	LSG1	Large subunit GTPase 1
sp|P47074|MAD3_YEAST	P47074	MAD3_YEAST	MAD3	Spindle assembly checkpoint component MAD3
sp|P20484|MAK11_YEAST	P20484	MAK11_YEAST	MAK11	Protein MAK11
sp|P10962|MAK16_YEAST	P10962	MAK16_YEAST	MAK16	Protein MAK16
sp|Q12176|MAK21_YEAST	Q12176	MAK21_YEAST	MAK21	Ribosome biogenesis protein MAK21
sp|P38112|MAK5_YEAST	P38112	MAK5_YEAST	MAK5	ATP-dependent RNA helicase MAK5
sp|P40513|MAM33_YEAST	P40513	MAM33_YEAST	MAM33	Mitochondrial acidic protein MAM33
sp|P35191|MDJ1_YEAST	P35191	MDJ1_YEAST	MDJ1	DnaJ homolog 1, mitochondrial
sp|P38111|ATR_YEAST	P38111	ATR_YEAST	MEC1	Serine/threonine-protein kinase MEC1
sp|Q12343|MED4_YEAST	Q12343	MED4_YEAST	MED4	Mediator of RNA polymerase II transcription subunit 4
sp|P06106|CYSD_YEAST	P06106	CYSD_YEAST	MET17	Homocysteine/cysteine synthase
sp|P05694|METE_YEAST	P05694	METE_YEAST	MET6	5-methyltetrahydropteroyltriglutamate--homocysteine methyltransferase
sp|Q99257|MEX67_YEAST	Q99257	MEX67_YEAST	MEX67	mRNA export factor MEX67
sp|P32787|MG101_YEAST	P32787	MG101_YEAST	MGM101	Mitochondrial genome maintenance protein MGM101
sp|P09440|C1TM_YEAST	P09440	C1TM_YEAST	MIS1	C-1-tetrahydrofolate synthase, mitochondrial
sp|P46985|MNN11_YEAST	P46985	MNN11_YEAST	MNN11	Probable alpha-1,6-mannosyltransferase MNN11
sp|P39107|MNN9_YEAST	P39107	MNN9_YEAST	MNN9	Mannan polymerase complexes subunit MNN9
sp|P40562|MPH1_YEAST	P40562	MPH1_YEAST	MPH1	ATP-dependent DNA helicase MPH1
sp|P47083|MPP10_YEAST	P47083	MPP10_YEAST	MPP10	U3 small nucleolar RNA-associated protein MPP10
sp|Q06106|MRD1_YEAST	Q06106	MRD1_YEAST	MRD1	Multiple RNA-binding domain-containing protein 1
sp|Q12117|MRH1_YEAST	Q12117	MRH1_YEAST	MRH1	Protein MRH1
sp|P33201|MRT4_YEAST	P33201	MRT4_YEAST	MRT4	Ribosome assembly factor MRT4
sp|Q05648|MRX10_YEAST	Q05648	MRX10_YEAST	MRX10	MIOREX complex component 10
sp|P48564|MRX6_YEAST	P48564	MRX6_YEAST	MRX6	MIOREX complex component 6
sp|P15424|MS116_YEAST	P15424	MS116_YEAST	MSS116	ATP-dependent RNA helicase MSS116, mitochondrial
sp|Q03897|WDR59_YEAST	Q03897	WDR59_YEAST	MTC5	Maintenance of telomere capping protein 5
sp|P25566|MXR2_YEAST	P25566	MXR2_YEAST	MXR2	Peptide methionine sulfoxide reductase 2
sp|Q03735|NAB6_YEAST	Q03735	NAB6_YEAST	NAB6	RNA-binding protein NAB6
sp|Q02931|UTP17_YEAST	Q02931	UTP17_YEAST	NAN1	NET1-associated nuclear protein 1
sp|P25293|NAP1_YEAST	P25293	NAP1_YEAST	NAP1	Nucleosome assembly protein
sp|P12945|NAT1_YEAST	P12945	NAT1_YEAST	NAT1	N-terminal acetyltransferase A complex subunit NAT1
sp|P40215|NDH1_YEAST	P40215	NDH1_YEAST	NDE1	External NADH-ubiquinone oxidoreductase 1, mitochondrial
sp|P32495|NHP2_YEAST	P32495	NHP2_YEAST	NHP2	H/ACA ribonucleoprotein complex subunit NHP2
sp|P32497|EIF3C_YEAST	P32497	EIF3C_YEAST	NIP1	Eukaryotic translation initiation factor 3 subunit C

sp|Q08962|NIP7_YEAST	Q08962	NIP7_YEAST	NIP7	60S ribosome subunit biogenesis protein NIP7
sp|P38861|NMD3_YEAST	P38861	NMD3_YEAST	NMD3	60S ribosomal export protein NMD3
sp|Q08444|NOB1_YEAST	Q08444	NOB1_YEAST	NOB1	20S-pre-rRNA D-site endonuclease NOB1
sp|P39744|NOC2_YEAST	P39744	NOC2_YEAST	NOC2	Nucleolar complex protein 2
sp|Q07896|NOC3_YEAST	Q07896	NOC3_YEAST	NOC3	Nucleolar complex-associated protein 3
sp|Q06512|NOC4_YEAST	Q06512	NOC4_YEAST	NOC4	Nucleolar complex protein 4
sp|Q02892|NOG1_YEAST	Q02892	NOG1_YEAST	NOG1	Nucleolar GTP-binding protein 1
sp|P15646|FBRL_YEAST	P15646	FBRL_YEAST	NOP1	rRNA 2'-O-methyltransferase fibrillarin
sp|Q08208|NOP12_YEAST	Q08208	NOP12_YEAST	NOP12	Nucleolar protein 12
sp|P53883|NOP13_YEAST	P53883	NOP13_YEAST	NOP13	Nucleolar protein 13
sp|Q99207|NOP14_YEAST	Q99207	NOP14_YEAST	NOP14	Nucleolar complex protein 14
sp|P53927|NOP15_YEAST	P53927	NOP15_YEAST	NOP15	Ribosome biogenesis protein 15
sp|P40007|NOP16_YEAST	P40007	NOP16_YEAST	NOP16	Nucleolar protein 16
sp|P40991|NOP2_YEAST	P40991	NOP2_YEAST	NOP2	25S rRNA (cytosine(2870)-C(5))-methyltransferase
sp|P37838|NOP4_YEAST	P37838	NOP4_YEAST	NOP4	Nucleolar protein 4
sp|Q12460|NOP56_YEAST	Q12460	NOP56_YEAST	NOP56	Nucleolar protein 56
sp|Q12499|NOP58_YEAST	Q12499	NOP58_YEAST	NOP58	Nucleolar protein 58
sp|Q07623|NOP6_YEAST	Q07623	NOP6_YEAST	NOP6	Nucleolar protein 6
sp|P53261|PESC_YEAST	P53261	PESC_YEAST	NOP7	Pescadillo homolog
sp|Q01560|NOP3_YEAST	Q01560	NOP3_YEAST	NPL3	Serine/arginine (SR)-type shuttling mRNA binding protein NPL3
sp|P39923|NPR2_YEAST	P39923	NPR2_YEAST	NPR2	Nitrogen permease regulator 2
sp|P38742|NPR3_YEAST	P38742	NPR3_YEAST	NPR3	Nitrogen permease regulator 3
sp|P53136|NSA1_YEAST	P53136	NSA1_YEAST	NSA1	Ribosome biogenesis protein NSA1
sp|P40078|NSA2_YEAST	P40078	NSA2_YEAST	NSA2	Ribosome biogenesis protein NSA2
sp|P27476|NSR1_YEAST	P27476	NSR1_YEAST	NSR1	Nuclear localization sequence-binding protein
sp|P40354|NTA1_YEAST	P40354	NTA1_YEAST	NTA1	Protein N-terminal amidase
sp|P40010|NUG1_YEAST	P40010	NUG1_YEAST	NUG1	Nuclear GTP-binding protein NUG1
sp|P49687|NU145_YEAST	P49687	NU145_YEAST	NUP145	Nucleoporin NUP145
sp|P38219|OLA1_YEAST	P38219	OLA1_YEAST	OLA1	Obg-like ATPase 1
sp|P21147|ACO1_YEAST	P21147	ACO1_YEAST	OLE1	Acyl-CoA desaturase 1
sp|P04147|PABP_YEAST	P04147	PABP_YEAST	PAB1	Polyadenylate-binding protein, cytoplasmic and nuclear
sp|P38351|PAF1_YEAST	P38351	PAF1_YEAST	PAF1	RNA polymerase II-associated protein 1
sp|P38126|PCH2_YEAST	P38126	PCH2_YEAST	PCH2	Pachytene checkpoint protein 2
sp|P32473|ODPB_YEAST	P32473	ODPB_YEAST	PDB1	Pyruvate dehydrogenase E1 component subunit beta, mitochondrial
sp|P06169|PDC1_YEAST	P06169	PDC1_YEAST	PDC1	Pyruvate decarboxylase isozyme 1
sp|P17967|PDI_YEAST	P17967	PDI_YEAST	PDI1	Protein disulfide-isomerase
sp|P33302|PDR5_YEAST	P33302	PDR5_YEAST	PDR5	Pleiotropic ABC efflux transporter of multiple drugs
sp|Q04264|PDS5_YEAST	Q04264	PDS5_YEAST	PDS5	Sister chromatid cohesion protein PDS5
sp|P32606|PT127_YEAST	P32606	PT127_YEAST	PET127	Putative mitochondrial translation system component PET127
sp|Q99373|PET20_YEAST	Q99373	PET20_YEAST	PET20	Protein PET20, mitochondrial
sp|P18239|ADT2_YEAST	P18239	ADT2_YEAST	PET9	ADP,ATP carrier protein 2
sp|P16861|PFKA1_YEAST	P16861	PFKA1_YEAST	PFK1	ATP-dependent 6-phosphofructokinase subunit alpha
sp|P16862|PFKA2_YEAST	P16862	PFKA2_YEAST	PFK2	ATP-dependent 6-phosphofructokinase subunit beta
sp|P40433|6P21_YEAST	P40433	6P21_YEAST	PFK26	6-phosphofructo-2-kinase 1
sp|P00560|PGK_YEAST	P00560	PGK_YEAST	PGK1	Phosphoglycerate kinase
sp|P36775|LONM_YEAST	P36775	LONM_YEAST	PIM1	Lon protease homolog, mitochondrial
sp|P05030|PMA1_YEAST	P05030	PMA1_YEAST	PMA1	Plasma membrane ATPase 1
sp|P38929|ATC2_YEAST	P38929	ATC2_YEAST	PMC1	Calcium-transporting ATPase 2
sp|Q99216|PNO1_YEAST	Q99216	PNO1_YEAST	PNO1	Pre-rRNA-processing protein PNO1
sp|Q04636|POB3_YEAST	Q04636	POB3_YEAST	POB3	FACT complex subunit POB3
sp|P15873|PCNA_YEAST	P15873	PCNA_YEAST	POL30	Proliferating cell nuclear antigen
sp|P39985|DPO5_YEAST	P39985	DPO5_YEAST	POL5	rDNA transcriptional regulator POL5
sp|P06103|EIF3B_YEAST	P06103	EIF3B_YEAST	PRT1	Eukaryotic translation initiation factor 3 subunit B
sp|P41940|MPG1_YEAST	P41940	MPG1_YEAST	PSA1	Mannose-1-phosphate guanyltransferase
sp|Q04373|PUF6_YEAST	Q04373	PUF6_YEAST	PUF6	Pumilio homology domain family member 6
sp|Q08647|PUS7_YEAST	Q08647	PUS7_YEAST	PUS7	Multisubstrate pseudouridine synthase 7
sp|P21304|PWP1_YEAST	P21304	PWP1_YEAST	PWP1	Periodic tryptophan protein 1
sp|P25635|PWP2_YEAST	P25635	PWP2_YEAST	PWP2	Periodic tryptophan protein 2
sp|P32628|RAD23_YEAST	P32628	RAD23_YEAST	RAD23	UV excision repair protein RAD23
sp|P39729|RBG1_YEAST	P39729	RBG1_YEAST	RBG1	Ribosome-interacting GTPase 1
sp|Q08096|RCL1_YEAST	Q08096	RCL1_YEAST	RCL1	RNA 3'-terminal phosphate cyclase-like protein
sp|Q06709|REH1_YEAST	Q06709	REH1_YEAST	REH1	Cytoplasmic 60S subunit biogenesis factor REH1
sp|P38344|REI1_YEAST	P38344	REI1_YEAST	REI1	Cytoplasmic 60S subunit biogenesis factor REI1
sp|P22276|RPC2_YEAST	P22276	RPC2_YEAST	RET1	DNA-directed RNA polymerase III subunit RPC2
sp|P22336|RFA1_YEAST	P22336	RFA1_YEAST	RFA1	Replication factor A protein 1
sp|P38251|RFC5_YEAST	P38251	RFC5_YEAST	RFC5	Replication factor C subunit 5
sp|P32445|RIM1_YEAST	P32445	RIM1_YEAST	RIM1	Single-stranded DNA-binding protein RIM1, mitochondrial
sp|Q04781|LTN1_YEAST	Q04781	LTN1_YEAST	RKR1	E3 ubiquitin-protein ligase listerin
sp|Q07915|RLP24_YEAST	Q07915	RLP24_YEAST	RLP24	Ribosome biogenesis protein RLP24
sp|P40693|RLP7_YEAST	P40693	RLP7_YEAST	RLP7	Ribosome biogenesis protein RLP7
sp|Q05635|RNH2B_YEAST	Q05635	RNH2B_YEAST	RNH202	Ribonuclease H2 subunit B
sp|P09938|RIR2_YEAST	P09938	RIR2_YEAST	RNR2	Ribonucleoside-diphosphate reductase small chain 1
sp|P45818|ROK1_YEAST	P45818	ROK1_YEAST	ROK1	ATP-dependent RNA helicase ROK1
sp|P22138|RPA2_YEAST	P22138	RPA2_YEAST	RPA135	DNA-directed RNA polymerase I subunit RPA135
sp|P10964|RPA1_YEAST	P10964	RPA1_YEAST	RPA190	DNA-directed RNA polymerase I subunit RPA190
sp|P47006|RPA34_YEAST	P47006	RPA34_YEAST	RPA34	DNA-directed RNA polymerase I subunit RPA34
sp|Q01080|RPA49_YEAST	Q01080	RPA49_YEAST	RPA49	DNA-directed RNA polymerase I subunit RPA49
sp|P08518|RPB2_YEAST	P08518	RPB2_YEAST	RPB2	DNA-directed RNA polymerase II subunit RPB2
sp|P16370|RPB3_YEAST	P16370	RPB3_YEAST	RPB3	DNA-directed RNA polymerase II subunit RPB3
sp|P20434|RPAB1_YEAST	P20434	RPAB1_YEAST	RPB5	DNA-directed RNA polymerases I, II, and III subunit RPABC1
sp|P07703|RPAC1_YEAST	P07703	RPAC1_YEAST	RPC40	DNA-directed RNA polymerases I and III subunit RPAC1
sp|P38805|RPF1_YEAST	P38805	RPF1_YEAST	RPF1	Ribosome production factor 1
sp|P36160|RPF2_YEAST	P36160	RPF2_YEAST	RPF2	Ribosome biogenesis protein RPF2

sp|P38249|EIF3A_YEAST	P38249	EIF3A_YEAST	RPG1	Eukaryotic translation initiation factor 3 subunit A
sp|P41805|RL10_YEAST	P41805	RL10_YEAST	RPL10	60S ribosomal protein L10
sp|P0C0W9|RL11A_YEAST	P0C0W9	RL11A_YEAST	RPL11A	60S ribosomal protein L11-A
sp|P0CX53|RL12A_YEAST	P0CX53	RL12A_YEAST	RPL12A	60S ribosomal protein L12-A
sp|P40212|RL13B_YEAST	P40212	RL13B_YEAST	RPL13B	60S ribosomal protein L13-B
sp|P36105|RL14A_YEAST	P36105	RL14A_YEAST	RPL14A	60S ribosomal protein L14-A
sp|P05748|RL15A_YEAST	P05748	RL15A_YEAST	RPL15A	60S ribosomal protein L15-A
sp|P26784|RL16A_YEAST	P26784	RL16A_YEAST	RPL16A	60S ribosomal protein L16-A
sp|P26785|RL16B_YEAST	P26785	RL16B_YEAST	RPL16B	60S ribosomal protein L16-B
sp|P05740|RL17A_YEAST	P05740	RL17A_YEAST	RPL17A	60S ribosomal protein L17-A
sp|P46990|RL17B_YEAST	P46990	RL17B_YEAST	RPL17B	60S ribosomal protein L17-B
sp|P0CX49|RL18A_YEAST	P0CX49	RL18A_YEAST	RPL18A	60S ribosomal protein L18-A
sp|P0CX82|RL19A_YEAST	P0CX82	RL19A_YEAST	RPL19A	60S ribosomal protein L19-A
sp|P0CX43|RL1A_YEAST	P0CX43	RL1A_YEAST	RPL1A	60S ribosomal protein L1-A
sp|P0CX23|RL20A_YEAST	P0CX23	RL20A_YEAST	RPL20A	60S ribosomal protein L20-A
sp|Q02753|RL21A_YEAST	Q02753	RL21A_YEAST	RPL21A	60S ribosomal protein L21-A
sp|Q12672|RL21B_YEAST	Q12672	RL21B_YEAST	RPL21B	60S ribosomal protein L21-B
sp|P05749|RL22A_YEAST	P05749	RL22A_YEAST	RPL22A	60S ribosomal protein L22-A
sp|P0CX41|RL23A_YEAST	P0CX41	RL23A_YEAST	RPL23A	60S ribosomal protein L23-A
sp|P04449|RL24A_YEAST	P04449	RL24A_YEAST	RPL24A	60S ribosomal protein L24-A
sp|P24000|RL24B_YEAST	P24000	RL24B_YEAST	RPL24B	60S ribosomal protein L24-B
sp|P04456|RL25_YEAST	P04456	RL25_YEAST	RPL25	60S ribosomal protein L25
sp|P05743|RL26A_YEAST	P05743	RL26A_YEAST	RPL26A	60S ribosomal protein L26-A
sp|P53221|RL26B_YEAST	P53221	RL26B_YEAST	RPL26B	60S ribosomal protein L26-B
sp|P0C2H6|RL27A_YEAST	P0C2H6	RL27A_YEAST	RPL27A	60S ribosomal protein L27-A
sp|P02406|RL28_YEAST	P02406	RL28_YEAST	RPL28	60S ribosomal protein L28
sp|P05747|RL29_YEAST	P05747	RL29_YEAST	RPL29	60S ribosomal protein L29
sp|P0CX45|RL2A_YEAST	P0CX45	RL2A_YEAST	RPL2A	60S ribosomal protein L2-A
sp|P14126|RL3_YEAST	P14126	RL3_YEAST	RPL3	60S ribosomal protein L3
sp|P14120|RL30_YEAST	P14120	RL30_YEAST	RPL30	60S ribosomal protein L30
sp|P0C2H8|RL31A_YEAST	P0C2H8	RL31A_YEAST	RPL31A	60S ribosomal protein L31-A
sp|P0C2H9|RL31B_YEAST	P0C2H9	RL31B_YEAST	RPL31B	60S ribosomal protein L31-B
sp|P38061|RL32_YEAST	P38061	RL32_YEAST	RPL32	60S ribosomal protein L32
sp|P05744|RL33A_YEAST	P05744	RL33A_YEAST	RPL33A	60S ribosomal protein L33-A
sp|P41056|RL33B_YEAST	P41056	RL33B_YEAST	RPL33B	60S ribosomal protein L33-B
sp|P0CX84|RL35A_YEAST	P0CX84	RL35A_YEAST	RPL35A	60S ribosomal protein L35-A
sp|P05745|RL36A_YEAST	P05745	RL36A_YEAST	RPL36A	60S ribosomal protein L36-A
sp|O14455|RL36B_YEAST	O14455	RL36B_YEAST	RPL36B	60S ribosomal protein L36-B
sp|P49166|RL37A_YEAST	P49166	RL37A_YEAST	RPL37A	60S ribosomal protein L37-A
sp|P51402|RL37B_YEAST	P51402	RL37B_YEAST	RPL37B	60S ribosomal protein L37-B
sp|P49167|RL38_YEAST	P49167	RL38_YEAST	RPL38	60S ribosomal protein L38
sp|P04650|RL39_YEAST	P04650	RL39_YEAST	RPL39	60S ribosomal protein L39
sp|P0CX27|RL44A_YEAST	P0CX27	RL44A_YEAST	RPL42A	60S ribosomal protein L42-A
sp|P0CX25|RL43A_YEAST	P0CX25	RL43A_YEAST	RPL43A	60S ribosomal protein L43-A
sp|P10664|RL4A_YEAST	P10664	RL4A_YEAST	RPL4A	60S ribosomal protein L4-A
sp|P49626|RL4B_YEAST	P49626	RL4B_YEAST	RPL4B	60S ribosomal protein L4-B
sp|P26321|RL5_YEAST	P26321	RL5_YEAST	RPL5	60S ribosomal protein L5
sp|Q02326|RL6A_YEAST	Q02326	RL6A_YEAST	RPL6A	60S ribosomal protein L6-A
sp|P05739|RL6B_YEAST	P05739	RL6B_YEAST	RPL6B	60S ribosomal protein L6-B
sp|P05737|RL7A_YEAST	P05737	RL7A_YEAST	RPL7A	60S ribosomal protein L7-A
sp|Q12213|RL7B_YEAST	Q12213	RL7B_YEAST	RPL7B	60S ribosomal protein L7-B
sp|P17076|RL8A_YEAST	P17076	RL8A_YEAST	RPL8A	60S ribosomal protein L8-A
sp|P29453|RL8B_YEAST	P29453	RL8B_YEAST	RPL8B	60S ribosomal protein L8-B
sp|P05738|RL9A_YEAST	P05738	RL9A_YEAST	RPL9A	60S ribosomal protein L9-A
sp|P04050|RPB1_YEAST	P04050	RPB1_YEAST	RPO21	DNA-directed RNA polymerase II subunit RPB1
sp|P04051|RPC1_YEAST	P04051	RPC1_YEAST	RPO31	DNA-directed RNA polymerase III subunit RPC1
sp|P05317|RLA0_YEAST	P05317	RLA0_YEAST	RPP0	60S acidic ribosomal protein P0
sp|P02400|RLA4_YEAST	P02400	RLA4_YEAST	RPP2B	60S acidic ribosomal protein P2-beta
sp|P32905|RSSA1_YEAST	P32905	RSSA1_YEAST	RPS0A	40S ribosomal protein S0-A
sp|P46654|RSSA2_YEAST	P46654	RSSA2_YEAST	RPS0B	40S ribosomal protein S0-B
sp|P0CX47|RS11A_YEAST	P0CX47	RS11A_YEAST	RPS11A	40S ribosomal protein S11-A
sp|P48589|RS12_YEAST	P48589	RS12_YEAST	RPS12	40S ribosomal protein S12
sp|P05756|RS13_YEAST	P05756	RS13_YEAST	RPS13	40S ribosomal protein S13
sp|P06367|RS14A_YEAST	P06367	RS14A_YEAST	RPS14A	40S ribosomal protein S14-A
sp|Q01855|RS15_YEAST	Q01855	RS15_YEAST	RPS15	40S ribosomal protein S15
sp|P0CX51|RS16A_YEAST	P0CX51	RS16A_YEAST	RPS16A	40S ribosomal protein S16-A
sp|P02407|RS17A_YEAST	P02407	RS17A_YEAST	RPS17A	40S ribosomal protein S17-A
sp|P0CX55|RS18A_YEAST	P0CX55	RS18A_YEAST	RPS18A	40S ribosomal protein S18-A
sp|P07280|RS19A_YEAST	P07280	RS19A_YEAST	RPS19A	40S ribosomal protein S19-A
sp|P33442|RS3A1_YEAST	P33442	RS3A1_YEAST	RPS1A	40S ribosomal protein S1-A
sp|P23248|RS3A2_YEAST	P23248	RS3A2_YEAST	RPS1B	40S ribosomal protein S1-B
sp|P25443|RS2_YEAST	P25443	RS2_YEAST	RPS2	40S ribosomal protein S2
sp|P38701|RS20_YEAST	P38701	RS20_YEAST	RPS20	40S ribosomal protein S20
sp|P0C0V8|RS21A_YEAST	P0C0V8	RS21A_YEAST	RPS21A	40S ribosomal protein S21-A
sp|P0C0W1|RS22A_YEAST	P0C0W1	RS22A_YEAST	RPS22A	40S ribosomal protein S22-A
sp|P0CX29|RS23A_YEAST	P0CX29	RS23A_YEAST	RPS23A	40S ribosomal protein S23-A
sp|P0CX31|RS24A_YEAST	P0CX31	RS24A_YEAST	RPS24A	40S ribosomal protein S24-A
sp|P0C0T4|RS25B_YEAST	P0C0T4	RS25B_YEAST	RPS25B	40S ribosomal protein S25-B
sp|P39938|RS26A_YEAST	P39938	RS26A_YEAST	RPS26A	40S ribosomal protein S26-A
sp|P35997|RS27A_YEAST	P35997	RS27A_YEAST	RPS27A	40S ribosomal protein S27-A
sp|Q3E7X9|RS28A_YEAST	Q3E7X9	RS28A_YEAST	RPS28A	40S ribosomal protein S28-A
sp|P0C0X0|RS28B_YEAST	P0C0X0	RS28B_YEAST	RPS28B	40S ribosomal protein S28-B
sp|P41057|RS29A_YEAST	P41057	RS29A_YEAST	RPS29A	40S ribosomal protein S29-A

sp|P05750|RS3_YEAST	P05750	RS3_YEAST	RPS3	40S ribosomal protein S3
sp|P0CX33|RS30A_YEAST	P0CX33	RS30A_YEAST	RPS30A	40S ribosomal protein S30-A
sp|P05759|RS31_YEAST	P05759	RS31_YEAST	RPS31	Ubiquitin-40S ribosomal protein S31
sp|P0CX35|RS4A_YEAST	P0CX35	RS4A_YEAST	RPS4A	40S ribosomal protein S4-A
sp|P26783|RS5_YEAST	P26783	RS5_YEAST	RPS5	40S ribosomal protein S5
sp|P0CX37|RS6A_YEAST	P0CX37	RS6A_YEAST	RPS6A	40S ribosomal protein S6-A
sp|P26786|RS7A_YEAST	P26786	RS7A_YEAST	RPS7A	40S ribosomal protein S7-A
sp|P48164|RS7B_YEAST	P48164	RS7B_YEAST	RPS7B	40S ribosomal protein S7-B
sp|P0CX39|RS8A_YEAST	P0CX39	RS8A_YEAST	RPS8A	40S ribosomal protein S8-A
sp|O13516|RS9A_YEAST	O13516	RS9A_YEAST	RPS9A	40S ribosomal protein S9-A
sp|Q12532|RQC2_YEAST	Q12532	RQC2_YEAST	RQC2	Ribosome quality control complex subunit 2
sp|P35178|RRP1_YEAST	P35178	RRP1_YEAST	RRP1	Ribosomal RNA-processing protein 1
sp|Q12754|RRP12_YEAST	Q12754	RRP12_YEAST	RRP12	Ribosomal RNA-processing protein 12
sp|Q06511|RRP15_YEAST	Q06511	RRP15_YEAST	RRP15	Ribosomal RNA-processing protein 15
sp|P38712|RRP3_YEAST	P38712	RRP3_YEAST	RRP3	ATP-dependent rRNA helicase RRP3
sp|Q05022|RRP5_YEAST	Q05022	RRP5_YEAST	RRP5	rRNA biogenesis protein RRP5
sp|P25368|RRP7_YEAST	P25368	RRP7_YEAST	RRP7	Ribosomal RNA-processing protein 7
sp|P38961|RRP8_YEAST	P38961	RRP8_YEAST	RRP8	25S rRNA (adenine(645)-N(1))-methyltransferase
sp|Q06506|RRP9_YEAST	Q06506	RRP9_YEAST	RRP9	Ribosomal RNA-processing protein 9
sp|Q08746|RRS1_YEAST	Q08746	RRS1_YEAST	RRS1	Regulator of ribosome biosynthesis
sp|P40470|RRT14_YEAST	P40470	RRT14_YEAST	RRT14	Regulator of rDNA transcription protein 14
sp|Q08281|RTC1_YEAST	Q08281	RTC1_YEAST	RTC1	Restriction of telomere capping protein 1
sp|P53064|RTF1_YEAST	P53064	RTF1_YEAST	RTF1	RNA polymerase-associated protein RTF1
sp|Q03940|RUVB1_YEAST	Q03940	RUVB1_YEAST	RVB1	RuvB-like protein 1
sp|Q12464|RUVB2_YEAST	Q12464	RUVB2_YEAST	RVB2	RuvB-like protein 2
sp|P39954|SAHH_YEAST	P39954	SAHH_YEAST	SAH1	Adenosylhomocysteinase
sp|P10659|METK1_YEAST	P10659	METK1_YEAST	SAM1	S-adenosylmethionine synthase 1
sp|P19358|METK2_YEAST	P19358	METK2_YEAST	SAM2	S-adenosylmethionine synthase 2
sp|Q12136|SAS10_YEAST	Q12136	SAS10_YEAST	SAS10	Something about silencing protein 10
sp|P10080|SSBP1_YEAST	P10080	SSBP1_YEAST	SBP1	Single-stranded nucleic acid-binding protein
sp|P03882|SCE1_YEAST	P03882	SCE1_YEAST	SCEI	Intron-encoded endonuclease I-SceI
sp|P06105|SC160_YEAST	P06105	SC160_YEAST	SCP160	Protein SCP160
sp|P38164|SEA4_YEAST	P38164	SEA4_YEAST	SEA4	SEH-associated protein 4
sp|Q04491|SEC13_YEAST	Q04491	SEC13_YEAST	SEC13	Protein transport protein SEC13
sp|P18759|SEC18_YEAST	P18759	SEC18_YEAST	SEC18	Vesicular-fusion protein SEC18
sp|P15303|SEC23_YEAST	P15303	SEC23_YEAST	SEC23	Protein transport protein SEC23
sp|P07283|PMM_YEAST	P07283	PMM_YEAST	SEC53	Phosphomannomutase
sp|P32915|SC61A_YEAST	P32915	SC61A_YEAST	SEC61	Protein transport protein SEC61
sp|Q01590|SED5_YEAST	Q01590	SED5_YEAST	SED5	Integral membrane protein SED5
sp|P53011|SEH1_YEAST	P53011	SEH1_YEAST	SEH1	Nucleoporin SEH1
sp|Q06132|SGD1_YEAST	Q06132	SGD1_YEAST	SGD1	Suppressor of glycerol defect protein 1
sp|P37292|GLYM_YEAST	P37292	GLYM_YEAST	SHM1	Serine hydroxymethyltransferase, mitochondrial
sp|P25294|SIS1_YEAST	P25294	SIS1_YEAST	SIS1	Protein SIS1
sp|Q03656|SKY1_YEAST	Q03656	SKY1_YEAST	SKY1	Serine/threonine-protein kinase SKY1
sp|Q12232|SLP1_YEAST	Q12232	SLP1_YEAST	SLP1	Uncharacterized protein SLP1
sp|P06782|SNF1_YEAST	P06782	SNF1_YEAST	SNF1	Carbon catabolite-derepressing protein kinase
sp|P12904|AAKG_YEAST	P12904	AAKG_YEAST	SNF4	5'-AMP-activated protein kinase subunit gamma
sp|P43544|SNO3_YEAST	P43544	SNO3_YEAST	SNO3	Probable pyridoxal 5'-phosphate synthase subunit SNO3
sp|P39990|SNU13_YEAST	P39990	SNU13_YEAST	SNU13	13 kDa ribonucleoprotein-associated protein
sp|P47057|SNX4_YEAST	P47057	SNX4_YEAST	SNX4	Sorting nexin-4
sp|P33750|DCA13_YEAST	P33750	DCA13_YEAST	SOF1	Protein SOF1
sp|P25808|SPB4_YEAST	P25808	SPB4_YEAST	SPB4	ATP-dependent rRNA helicase SPB4
sp|P32558|SPT16_YEAST	P32558	SPT16_YEAST	SPT16	FACT complex subunit SPT16
sp|P32914|SPT4_YEAST	P32914	SPT4_YEAST	SPT4	Transcription elongation factor SPT4
sp|P27692|SPT5_YEAST	P27692	SPT5_YEAST	SPT5	Transcription elongation factor SPT5
sp|P23615|SPT6_YEAST	P23615	SPT6_YEAST	SPT6	Transcription elongation factor SPT6
sp|P25567|SRO9_YEAST	P25567	SRO9_YEAST	SRO9	RNA-binding protein SRO9
sp|P17555|CAP_YEAST	P17555	CAP_YEAST	SRV2	Adenylyl cyclase-associated protein
sp|P10591|HSP71_YEAST	P10591	HSP71_YEAST	SSA1	Heat shock protein SSA1
sp|P10592|HSP72_YEAST	P10592	HSP72_YEAST	SSA2	Heat shock protein SSA2
sp|P09435|HSP73_YEAST	P09435	HSP73_YEAST	SSA3	Heat shock protein SSA3
sp|P11484|SSB1_YEAST	P11484	SSB1_YEAST	SSB1	Ribosome-associated molecular chaperone SSB1
sp|P32589|HSP7F_YEAST	P32589	HSP7F_YEAST	SSE1	Heat shock protein homolog SSE1
sp|P53599|SSK2_YEAST	P53599	SSK2_YEAST	SSK2	MAP kinase kinase kinase SSK2
sp|P38788|SSZ1_YEAST	P38788	SSZ1_YEAST	SSZ1	Ribosome-associated complex subunit SSZ1
sp|Q03497|STE20_YEAST	Q03497	STE20_YEAST	STE20	Serine/threonine-protein kinase STE20
sp|P39015|STM1_YEAST	P39015	STM1_YEAST	STM1	Suppressor protein STM1
sp|P20459|IF2A_YEAST	P20459	IF2A_YEAST	SUI2	Eukaryotic translation initiation factor 2 subunit alpha
sp|P09064|IF2B_YEAST	P09064	IF2B_YEAST	SUI3	Eukaryotic translation initiation factor 2 subunit beta
sp|P46677|TAF1_YEAST	P46677	TAF1_YEAST	TAF1	Transcription initiation factor TFIID subunit 1
sp|P53072|TAN1_YEAST	P53072	TAN1_YEAST	TAN1	tRNA acetyltransferase TAN1
sp|P48231|TCB2_YEAST	P48231	TCB2_YEAST	TCB2	Tricalbin-2
sp|P12612|TCPA_YEAST	P12612	TCPA_YEAST	TCP1	T-complex protein 1 subunit alpha
sp|P00360|G3P1_YEAST	P00360	G3P1_YEAST	TDH1	Glyceraldehyde-3-phosphate dehydrogenase 1
sp|P00358|G3P2_YEAST	P00358	G3P2_YEAST	TDH2	Glyceraldehyde-3-phosphate dehydrogenase 2
sp|P00359|G3P3_YEAST	P00359	G3P3_YEAST	TDH3	Glyceraldehyde-3-phosphate dehydrogenase 3
sp|P02994|EF1A_YEAST	P02994	EF1A_YEAST	TEF1	Elongation factor 1-alpha
sp|P36008|EF1G2_YEAST	P36008	EF1G2_YEAST	TEF4	Elongation factor 1-gamma 2
sp|P41895|T2FA_YEAST	P41895	T2FA_YEAST	TFG1	Transcription initiation factor IIF subunit alpha
sp|P04801|SYTC_YEAST	P04801	SYTC_YEAST	THS1	Threonine--tRNA ligase, cytoplasmic
sp|P10081|IF4A_YEAST	P10081	IF4A_YEAST	TIF1	ATP-dependent RNA helicase eIF4A
sp|P40217|EIF3I_YEAST	P40217	EIF3I_YEAST	TIF34	Eukaryotic translation initiation factor 3 subunit I
sp|Q04067|EIF3G_YEAST	Q04067	EIF3G_YEAST	TIF35	Eukaryotic translation initiation factor 3 subunit G

sp|P38431|IF5_YEAST	P38431	IF5_YEAST	TIF5	Eukaryotic translation initiation factor 5
sp|Q12522|IF6_YEAST	Q12522	IF6_YEAST	TIF6	Eukaryotic translation initiation factor 6
sp|Q08687|TMA16_YEAST	Q08687	TMA16_YEAST	TMA16	Translation machinery-associated protein 16
sp|P35691|TCTP_YEAST	P35691	TCTP_YEAST	TMA19	Translationally-controlled tumor protein homolog
sp|P04786|TOP1_YEAST	P04786	TOP1_YEAST	TOP1	DNA topoisomerase 1
sp|P35169|TOR1_YEAST	P35169	TOR1_YEAST	TOR1	Serine/threonine-protein kinase TOR1
sp|P00942|TPIS_YEAST	P00942	TPIS_YEAST	TPI1	Triosephosphate isomerase
sp|Q00764|TPS1_YEAST	Q00764	TPS1_YEAST	TPS1	Alpha,alpha-trehalose-phosphate synthase [UDP-forming] 56 kDa subunit
sp|P38811|TRA1_YEAST	P38811	TRA1_YEAST	TRA1	Transcription-associated protein 1
sp|P00931|TRP_YEAST	P00931	TRP_YEAST	TRP5	Tryptophan synthase
sp|Q99190|TECR_YEAST	Q99190	TECR_YEAST	TSC13	Very-long-chain enoyl-CoA reductase
sp|Q07381|TSR1_YEAST	Q07381	TSR1_YEAST	TSR1	Ribosome biogenesis protein TSR1
sp|P02557|TBB_YEAST	P02557	TBB_YEAST	TUB2	Tubulin beta chain
sp|O13527|YA11B_YEAST	O13527	YA11B_YEAST	TY1B-A	Truncated transposon Ty1-A Gag-Pol polyprotein
sp|O13535|YH11B_YEAST	O13535	YH11B_YEAST	TY1B-H	Transposon Ty1-H Gag-Pol polyprotein
sp|P38820|UBA4_YEAST	P38820	UBA4_YEAST	UBA4	Adenylyltransferase and sulfurtransferase UBA4
sp|P43593|UBP6_YEAST	P43593	UBP6_YEAST	UBP6	Ubiquitin carboxyl-terminal hydrolase 6
sp|Q03327|UGO1_YEAST	Q03327	UGO1_YEAST	UGO1	Mitochondrial fusion and transport protein UGO1
sp|Q05776|UPS1_YEAST	Q05776	UPS1_YEAST	UPS1	Protein UPS1, mitochondrial
sp|P07259|PYR1_YEAST	P07259	PYR1_YEAST	URA2	Protein URA2
sp|P47108|URB2_YEAST	P47108	URB2_YEAST	URB2	Nucleolar pre-ribosomal-associated protein 2
sp|P42945|UTP10_YEAST	P42945	UTP10_YEAST	UTP10	U3 small nucleolar RNA-associated protein 10
sp|P34247|UTP11_YEAST	P34247	UTP11_YEAST	UTP11	U3 small nucleolar RNA-associated protein 11
sp|Q05946|UTP13_YEAST	Q05946	UTP13_YEAST	UTP13	U3 small nucleolar RNA-associated protein 13
sp|Q04500|UTP14_YEAST	Q04500	UTP14_YEAST	UTP14	U3 small nucleolar RNA-associated protein 14
sp|Q04305|UTP15_YEAST	Q04305	UTP15_YEAST	UTP15	U3 small nucleolar RNA-associated protein 15
sp|P40362|UTP18_YEAST	P40362	UTP18_YEAST	UTP18	U3 small nucleolar RNA-associated protein 18
sp|P35194|UTP20_YEAST	P35194	UTP20_YEAST	UTP20	U3 small nucleolar RNA-associated protein 20
sp|Q06078|UTP21_YEAST	Q06078	UTP21_YEAST	UTP21	U3 small nucleolar RNA-associated protein 21
sp|P53254|UTP22_YEAST	P53254	UTP22_YEAST	UTP22	U3 small nucleolar RNA-associated protein 22
sp|Q06679|UTP4_YEAST	Q06679	UTP4_YEAST	UTP4	U3 small nucleolar RNA-associated protein 4
sp|Q04177|UTP5_YEAST	Q04177	UTP5_YEAST	UTP5	U3 small nucleolar RNA-associated protein 5
sp|Q02354|UTP6_YEAST	Q02354	UTP6_YEAST	UTP6	U3 small nucleolar RNA-associated protein 6
sp|P40055|UTP7_YEAST	P40055	UTP7_YEAST	UTP7	U3 small nucleolar RNA-associated protein 7
sp|P53276|UTP8_YEAST	P53276	UTP8_YEAST	UTP8	U3 small nucleolar RNA-associated protein 8
sp|P38882|UTP9_YEAST	P38882	UTP9_YEAST	UTP9	U3 small nucleolar RNA-associated protein 9
sp|Q12045|VIK1_YEAST	Q12045	VIK1_YEAST	VIK1	Spindle pole body-associated protein VIK1
sp|P17255|VATA_YEAST	P17255	VATA_YEAST	VMA1	V-type proton ATPase catalytic subunit A
sp|P32842|VATL2_YEAST	P32842	VATL2_YEAST	VMA11	V-type proton ATPase subunit c'
sp|P16140|VATB_YEAST	P16140	VATB_YEAST	VMA2	V-type proton ATPase subunit B
sp|P32563|VPP1_YEAST	P32563	VPP1_YEAST	VPH1	V-type proton ATPase subunit a, vacuolar isoform
sp|Q07878|VPS13_YEAST	Q07878	VPS13_YEAST	VPS13	Intermembrane lipid transfer protein VPS13
sp|P39904|VPS52_YEAST	P39904	VPS52_YEAST	VPS52	Vacuolar protein sorting-associated protein 52
sp|P33767|OSTB_YEAST	P33767	OSTB_YEAST	WBP1	Dolichyl-diphosphooligosaccharide--protein glycosyltransferase subunit WBP1
sp|Q12109|SYWC_YEAST	Q12109	SYWC_YEAST	WRS1	Tryptophan--tRNA ligase, cytoplasmic
sp|P22147|XRN1_YEAST	P22147	XRN1_YEAST	XRN1	5'-3' exoribonuclease 1
sp|P38202|YBC8_YEAST	P38202	YBC8_YEAST	YBL028C	UPF0642 protein YBL028C
sp|P25491|MAS5_YEAST	P25491	MAS5_YEAST	YDJ1	Mitochondrial protein import protein MAS5
sp|Q05506|SYRC_YEAST	Q05506	SYRC_YEAST	YDR341C	Arginine--tRNA ligase, cytoplasmic
sp|P16521|EF3A_YEAST	P16521	EF3A_YEAST	YEF3	Elongation factor 3A
sp|P38616|YGP1_YEAST	P38616	YGP1_YEAST	YGP1	Protein YGP1
sp|P39676|FHP_YEAST	P39676	FHP_YEAST	YHB1	Flavohemoprotein
sp|P38708|YHI0_YEAST	P38708	YHI0_YEAST	YHR020W	Putative proline--tRNA ligase YHR020W
sp|P36015|YKT6_YEAST	P36015	YKT6_YEAST	YKT6	Synaptobrevin homolog YKT6
sp|P53723|YN8B_YEAST	P53723	YN8B_YEAST	YNR021W	UPF0674 endoplasmic reticulum membrane protein YNR021W
sp|Q12159|YRA1_YEAST	Q12159	YRA1_YEAST	YRA1	RNA annealing protein YRA1
sp|P38079|YRO2_YEAST	P38079	YRO2_YEAST	YRO2	Protein YRO2
sp|P40341|YTA12_YEAST	P40341	YTA12_YEAST	YTA12	Mitochondrial respiratory chain complexes assembly protein YTA12
sp|Q12024|YTM1_YEAST	Q12024	YTM1_YEAST	YTM1	Ribosome biogenesis protein YTM1
sp|Q02256|PVH1_YEAST	Q02256	PVH1_YEAST	YVH1	Tyrosine-protein phosphatase YVH1
sp|P32527|ZUO1_YEAST	P32527	ZUO1_YEAST	ZUO1	Zuotin

Table 2.2: MS Identified Proteins in -UV FLAG-purified 26S Holoenzyme Preparations

Table 2-2: MS Identified Proteins in -UV FLAG-purified 26S Holoenzymes					Proteasome-associated	
Protein	**Protein ID**	**Entry Name**	**Gene**	**Protein Description**	**Subcomplex**	**Notes**
sp|P38764|RPN1_YEAST	P38764	RPN1_YEAST	RPN1	26S proteasome regulatory subunit RPN1	19S Base	Ub-receptor
sp|O13563|RPN13_YEAST	O13563	RPN13_YEAST	RPN13	26S proteasome regulatory subunit RPN13		Ub-receptor
sp|P32565|RPN2_YEAST	P32565	RPN2_YEAST	RPN2	26S proteasome regulatory subunit RPN2		
sp|P33299|PRS7_YEAST	P33299	PRS7_YEAST	RPT1	26S proteasome regulatory subunit 7 homolog		AAA+ ATPase
sp|P40327|PRS4_YEAST	P40327	PRS4_YEAST	RPT2	26S proteasome regulatory subunit 4 homolog		
sp|P33298|PRS6B_YEAST	P33298	PRS6B_YEAST	RPT3	26S proteasome regulatory subunit 6B homolog		
sp|P53549|PRS10_YEAST	P53549	PRS10_YEAST	RPT4	26S proteasome subunit RPT4		
sp|P33297|PRS6A_YEAST	P33297	PRS6A_YEAST	RPT5	26S proteasome regulatory subunit 6A		
sp|Q01939|PRS8_YEAST	Q01939	PRS8_YEAST	RPT6	26S proteasome regulatory subunit 8 homolog		
sp|P43588|RPN11_YEAST	P43588	RPN11_YEAST	RPN11	Ubiquitin carboxyl-terminal hydrolase RPN11	19S Lid	De-ubiquitinase
sp|P32496|RPN12_YEAST	P32496	RPN12_YEAST	RPN12	26S proteasome regulatory subunit RPN12		
sp|P40016|RPN3_YEAST	P40016	RPN3_YEAST	RPN3	26S proteasome regulatory subunit RPN3		
sp|Q12250|RPN5_YEAST	Q12250	RPN5_YEAST	RPN5	26S proteasome regulatory subunit RPN5		
sp|Q12377|RPN6_YEAST	Q12377	RPN6_YEAST	RPN6	26S proteasome regulatory subunit RPN6		
sp|Q06103|RPN7_YEAST	Q06103	RPN7_YEAST	RPN7	26S proteasome regulatory subunit RPN7		
sp|Q08723|RPN8_YEAST	Q08723	RPN8_YEAST	RPN8	26S proteasome regulatory subunit RPN8		
sp|Q04062|RPN9_YEAST	Q04062	RPN9_YEAST	RPN9	26S proteasome regulatory subunit RPN9		
sp|O94742|SEM1_YEAST	O94742	SEM1_YEAST	SEM1	26S proteasome complex subunit SEM1		
sp|P21242|PSA7_YEAST	P21242	PSA7_YEAST	PRE10	Probable proteasome subunit alpha type-7	20S CP	alpha ring
sp|P40302|PSA6_YEAST	P40302	PSA6_YEAST	PRE5	Proteasome subunit alpha type-6		
sp|P40303|PSA4_YEAST	P40303	PSA4_YEAST	PRE6	Proteasome subunit alpha type-4		
sp|P23639|PSA2_YEAST	P23639	PSA2_YEAST	PRE8	Proteasome subunit alpha type-2		
sp|P23638|PSA3_YEAST	P23638	PSA3_YEAST	PRE9	Proteasome subunit alpha type-3		
sp|P32379|PSA5_YEAST	P32379	PSA5_YEAST	PUP2	Proteasome subunit alpha type-5		
sp|P21243|PSA1_YEAST	P21243	PSA1_YEAST	SCL1	Proteasome subunit alpha type-1		
sp|P22141|PSB4_YEAST	P22141	PSB4_YEAST	PRE1	Proteasome subunit beta type-4		beta ring
sp|P30656|PSB5_YEAST	P30656	PSB5_YEAST	PRE2	Proteasome subunit beta type-5		
sp|P38624|PSB1_YEAST	P38624	PSB1_YEAST	PRE3	Proteasome subunit beta type-1		
sp|P30657|PSB7_YEAST	P30657	PSB7_YEAST	PRE4	Proteasome subunit beta type-7		
sp|P23724|PSB6_YEAST	P23724	PSB6_YEAST	PRE7	Proteasome subunit beta type-6		
sp|P25043|PSB2_YEAST	P25043	PSB2_YEAST	PUP1	Proteasome subunit beta type-2		
sp|P25451|PSB3_YEAST	P25451	PSB3_YEAST	PUP3	Proteasome subunit beta type-3		
sp|P38886|RPN10_YEAST	P38886	RPN10_YEAST	RPN10	26S proteasome regulatory subunit RPN10	N/A	Ub-receptor
sp|P36040|POC2_YEAST	P36040	POC2_YEAST	ADD66	Proteasome assembly chaperone 2	N/A	
sp|P43583|BLM10_YEAST	P43583	BLM10_YEAST	BLM10	Proteasome activator BLM10	N/A	
sp|P38779|CIC1_YEAST	P38779	CIC1_YEAST	CIC1	Proteasome-interacting protein CIC1	N/A	
sp|P38737|ECM29_YEAST	P38737	ECM29_YEAST	ECM29	Proteasome component ECM29	N/A	
sp|Q05778|POC1_YEAST	Q05778	POC1_YEAST	PBA1	Proteasome chaperone 1	N/A	
sp|P04710|ADT1_YEAST	P04710	ADT1_YEAST	AAC1	ADP,ATP carrier protein 1		
sp|P15891|ABP1_YEAST	P15891	ABP1_YEAST	ABP1	Actin-binding protein		
sp|Q00955|ACAC_YEAST	Q00955	ACAC_YEAST	ACC1	Acetyl-CoA carboxylase		
sp|P52910|ACS2_YEAST	P52910	ACS2_YEAST	ACS2	Acetyl-coenzyme A synthetase 2		
sp|P60010|ACT_YEAST	P60010	ACT_YEAST	ACT1	Actin		
sp|Q02336|ADA2_YEAST	Q02336	ADA2_YEAST	ADA2	Transcriptional adapter 2		
sp|P07245|C1TC_YEAST	P07245	C1TC_YEAST	ADE3	C-1-tetrahydrofolate synthase, cytoplasmic		
sp|P07244|PUR2_YEAST	P07244	PUR2_YEAST	ADE57	Bifunctional purine biosynthetic protein ADE5,7		
sp|P00330|ADH1_YEAST	P00330	ADH1_YEAST	ADH1	Alcohol dehydrogenase 1		
sp|Q12449|AHA1_YEAST	Q12449	AHA1_YEAST	AHA1	Hsp90 co-chaperone AHA1		
sp|P40053|AIM9_YEAST	P40053	AIM9_YEAST	AIM9	Altered inheritance of mitochondria protein 9, mitochondrial		
sp|P40825|SYA_YEAST	P40825	SYA_YEAST	ALA1	Alanine--tRNA ligase, mitochondrial		
sp|P47019|ALB1_YEAST	P47019	ALB1_YEAST	ALB1	Ribosome biogenesis protein ALB1		
sp|P54115|ALDH6_YEAST	P54115	ALDH6_YEAST	ALD6	Magnesium-activated aldehyde dehydrogenase, cytosolic		
sp|P32629|ANP1_YEAST	P32629	ANP1_YEAST	ANP1	Mannan polymerase II complex ANP1 subunit		
sp|P38281|APD1_YEAST	P38281	APD1_YEAST	APD1	Actin patches distal protein 1		
sp|P14904|AMPL_YEAST	P14904	AMPL_YEAST	APE1	Vacuolar aminopeptidase 1		
sp|P36000|AP1B1_YEAST	P36000	AP1B1_YEAST	APL2	AP-1 complex subunit beta-1		
sp|P35181|AP1S1_YEAST	P35181	AP1S1_YEAST	APS1	AP-1 complex subunit sigma-1		
sp|P40024|ARB1_YEAST	P40024	ARB1_YEAST	ARB1	ABC transporter ATP-binding protein ARB1		
sp|P53731|ARPC2_YEAST	P53731	ARPC2_YEAST	ARC35	Actin-related protein 2/3 complex subunit 2		
sp|P11076|ARF1_YEAST	P11076	ARF1_YEAST	ARF1	ADP-ribosylation factor 1		
sp|P22768|ASSY_YEAST	P22768	ASSY_YEAST	ARG1	Argininosuccinate synthase		
sp|P08566|ARO1_YEAST	P08566	ARO1_YEAST	ARO1	Pentafunctional AROM polypeptide		
sp|P53090|ARO8_YEAST	P53090	ARO8_YEAST	ARO8	Aromatic/aminoadipate aminotransferase 1		
sp|Q05123|ARP9_YEAST	Q05123	ARP9_YEAST	ARP9	Actin-like protein ARP9		
sp|Q03862|ARX1_YEAST	Q03862	ARX1_YEAST	ARX1	Probable metalloprotease ARX1		
sp|P38011|GBLP_YEAST	P38011	GBLP_YEAST	ASC1	Guanine nucleotide-binding protein subunit beta-like protein		
sp|P48361|ASK10_YEAST	P48361	ASK10_YEAST	ASK10	Activator of SKN7 protein 10		
sp|P49089|ASNS1_YEAST	P49089	ASNS1_YEAST	ASN1	Asparagine synthetase [glutamine-hydrolyzing] 1		
sp|Q07528|ATG20_YEAST	Q07528	ATG20_YEAST	ATG20	Autophagy-related protein 20		
sp|P47113|BFA1_YEAST	P47113	BFA1_YEAST	BFA1	Mitotic check point protein BFA1		
sp|P38934|BFR1_YEAST	P38934	BFR1_YEAST	BFR1	Nuclear segregation protein BFR1		
sp|Q06631|BFR2_YEAST	Q06631	BFR2_YEAST	BFR2	Protein BFR2		
sp|Q08965|BMS1_YEAST	Q08965	BMS1_YEAST	BMS1	Ribosome biogenesis protein BMS1		
sp|Q08235|BRX1_YEAST	Q08235	BRX1_YEAST	BRX1	Ribosome biogenesis protein BRX1		
sp|Q08492|BUD21_YEAST	Q08492	BUD21_YEAST	BUD21	Bud site selection protein 21		
sp|P29547|EF1G1_YEAST	P29547	EF1G1_YEAST	CAM1	Elongation factor 1-gamma 1		
sp|P33322|CBF5_YEAST	P33322	CBF5_YEAST	CBF5	H/ACA ribonucleoprotein complex subunit CBF5		
sp|P38626|NCB5R_YEAST	P38626	NCB5R_YEAST	CBR1	NADH-cytochrome b5 reductase 1		
sp|P39077|TCPG_YEAST	P39077	TCPG_YEAST	CCT3	T-complex protein 1 subunit gamma		
sp|P39078|TCPD_YEAST	P39078	TCPD_YEAST	CCT4	T-complex protein 1 subunit delta		
sp|P40413|TCPE_YEAST	P40413	TCPE_YEAST	CCT5	T-complex protein 1 subunit epsilon		
sp|P39079|TCPZ_YEAST	P39079	TCPZ_YEAST	CCT6	T-complex protein 1 subunit zeta		
sp|P47079|TCPQ_YEAST	P47079	TCPQ_YEAST	CCT8	T-complex protein 1 subunit theta		
sp|P40986|CDC1_YEAST	P40986	CDC1_YEAST	CDC1	Cell division control protein 1		

sp|P25342|CDC10_YEAST	P25342	CDC10_YEAST	CDC10	Cell division control protein 10
sp|P09798|CDC16_YEAST	P09798	CDC16_YEAST	CDC16	Anaphase-promoting complex subunit CDC16
sp|P00549|KPYK1_YEAST	P00549	KPYK1_YEAST	CDC19	Pyruvate kinase 1
sp|P07260|IF4E_YEAST	P07260	IF4E_YEAST	CDC33	Eukaryotic translation initiation factor 4E
sp|P25694|CDC48_YEAST	P25694	CDC48_YEAST	CDC48	Cell division control protein 48
sp|P26637|SYLC_YEAST	P26637	SYLC_YEAST	CDC60	Leucine--tRNA ligase, cytoplasmic
sp|Q06697|CDC73_YEAST	Q06697	CDC73_YEAST	CDC73	Cell division control protein 73
sp|P43634|CHA4_YEAST	P43634	CHA4_YEAST	CHA4	Activatory protein CHA4
sp|P22137|CLH_YEAST	P22137	CLH_YEAST	CHC1	Clathrin heavy chain
sp|P32657|CHD1_YEAST	P32657	CHD1_YEAST	CHD1	Chromo domain-containing protein 1
sp|P38907|CENPN_YEAST	P38907	CENPN_YEAST	CHL4	Inner kinetochore subunit CHL4
sp|P15790|CSK21_YEAST	P15790	CSK21_YEAST	CKA1	Casein kinase II subunit alpha
sp|P19454|CSK22_YEAST	P19454	CSK22_YEAST	CKA2	Casein kinase II subunit alpha'
sp|P43639|CSK2B_YEAST	P43639	CSK2B_YEAST	CKB1	Casein kinase II subunit beta
sp|P38930|CSK2C_YEAST	P38930	CSK2C_YEAST	CKB2	Casein kinase II subunit beta'
sp|P48562|CLA4_YEAST	P48562	CLA4_YEAST	CLA4	Serine/threonine-protein kinase CLA4
sp|Q03690|CLU_YEAST	Q03690	CLU_YEAST	CLU1	Clustered mitochondria protein 1
sp|Q07897|CMS1_YEAST	Q07897	CMS1_YEAST	CMS1	Protein CMS1
sp|P53622|COPA_YEAST	P53622	COPA_YEAST	COP1	Coatomer subunit alpha
sp|P03965|CARB_YEAST	P03965	CARB_YEAST	CPA2	Carbamoyl-phosphate synthase arginine-specific large chain
sp|P38845|CRP1_YEAST	P38845	CRP1_YEAST	CRP1	Cruciform DNA-recognizing protein 1
sp|P40442|CSS1_YEAST	P40442	CSS1_YEAST	CSS1	Secreted protein CSS1
sp|P89105|CTR9_YEAST	P89105	CTR9_YEAST	CTR9	RNA polymerase-associated protein CTR9
sp|Q08412|CUE5_YEAST	Q08412	CUE5_YEAST	CUE5	Ubiquitin-binding protein CUE5
sp|Q12389|DBP10_YEAST	Q12389	DBP10_YEAST	DBP10	ATP-dependent RNA helicase DBP10
sp|P24783|DBP2_YEAST	P24783	DBP2_YEAST	DBP2	ATP-dependent RNA helicase DBP2
sp|P20447|DBP3_YEAST	P20447	DBP3_YEAST	DBP3	ATP-dependent RNA helicase DBP3
sp|P20449|DBP5_YEAST	P20449	DBP5_YEAST	DBP5	ATP-dependent RNA helicase DBP5
sp|P36120|DBP7_YEAST	P36120	DBP7_YEAST	DBP7	ATP-dependent RNA helicase DBP7
sp|P38719|DBP8_YEAST	P38719	DBP8_YEAST	DBP8	ATP-dependent RNA helicase DBP8
sp|Q06218|DBP9_YEAST	Q06218	DBP9_YEAST	DBP9	ATP-dependent RNA helicase DBP9
sp|P06634|DED1_YEAST	P06634	DED1_YEAST	DED1	ATP-dependent RNA helicase DED1
sp|P38707|SYNC_YEAST	P38707	SYNC_YEAST	DED81	Asparagine--tRNA ligase, cytoplasmic
sp|P39517|DHH1_YEAST	P39517	DHH1_YEAST	DHH1	ATP-dependent RNA helicase DHH1
sp|P41819|DIM1_YEAST	P41819	DIM1_YEAST	DIM1	Dimethyladenosine transferase
sp|Q12220|UTP12_YEAST	Q12220	UTP12_YEAST	DIP2	U3 small nucleolar RNA-associated protein 12
sp|Q08162|RRP44_YEAST	Q08162	RRP44_YEAST	DIS3	Exosome complex exonuclease DIS3
sp|P04802|SYDC_YEAST	P04802	SYDC_YEAST	DPS1	Aspartate--tRNA ligase, cytoplasmic
sp|P32892|DRS1_YEAST	P32892	DRS1_YEAST	DRS1	ATP-dependent RNA helicase DRS1
sp|P38149|DUG2_YEAST	P38149	DUG2_YEAST	DUG2	Probable di- and tripeptidase DUG2
sp|P53871|DUG3_YEAST	P53871	DUG3_YEAST	DUG3	Probable glutamine amidotransferase DUG3
sp|P39009|DUN1_YEAST	P39009	DUN1_YEAST	DUN1	DNA damage response protein kinase DUN1
sp|P36049|EBP2_YEAST	P36049	EBP2_YEAST	EBP2	rRNA-processing protein EBP2
sp|P39715|ECM1_YEAST	P39715	ECM1_YEAST	ECM1	Shuttling pre-60S factor ECM1
sp|Q04217|DHR1_YEAST	Q04217	DHR1_YEAST	ECM16	Probable ATP-dependent RNA helicase DHR1
sp|P34216|EDE1_YEAST	P34216	EDE1_YEAST	EDE1	EH domain-containing and endocytosis protein 1
sp|Q3E705|EFG1P_YEAST	Q3E705	EFG1P_YEAST	EFG1	rRNA-processing protein EFG1
sp|P32324|EF2_YEAST	P32324	EF2_YEAST	EFT1	Elongation factor 2
sp|Q03071|ELOC_YEAST	Q03071	ELOC_YEAST	ELC1	Elongin-C
sp|P25358|ELO2_YEAST	P25358	ELO2_YEAST	ELO2	Elongation of fatty acids protein 2
sp|Q02884|ELP4_YEAST	Q02884	ELP4_YEAST	ELP4	Elongator complex protein 4
sp|Q06287|NEP1_YEAST	Q06287	NEP1_YEAST	EMG1	Ribosomal RNA small subunit methyltransferase NEP1
sp|P40085|TAPT1_YEAST	P40085	TAPT1_YEAST	EMP65	Endoplasmic reticulum membrane protein 65
sp|P00924|ENO1_YEAST	P00924	ENO1_YEAST	ENO1	Enolase 1
sp|P00925|ENO2_YEAST	P00925	ENO2_YEAST	ENO2	Enolase 2
sp|P38333|ENP1_YEAST	P38333	ENP1_YEAST	ENP1	Essential nuclear protein 1
sp|P48234|NOL10_YEAST	P48234	NOL10_YEAST	ENP2	Ribosome biogenesis protein ENP2
sp|Q04660|ERB1_YEAST	Q04660	ERB1_YEAST	ERB1	Ribosome biogenesis protein ERB1
sp|P25340|ERG4_YEAST	P25340	ERG4_YEAST	ERG4	Delta(24(24(1)))-sterol reductase ERG4
sp|P54781|ERG5_YEAST	P54781	ERG5_YEAST	ERG5	C-22 sterol desaturase ERG5
sp|Q03661|ESC1_YEAST	Q03661	ESC1_YEAST	ESC1	Silent chromatin protein ESC1
sp|Q06344|ESF1_YEAST	Q06344	ESF1_YEAST	ESF1	Pre-rRNA-processing protein ESF1
sp|P53743|ESF2_YEAST	P53743	ESF2_YEAST	ESF2	Pre-rRNA-processing protein ESF2
sp|P30624|LCF1_YEAST	P30624	LCF1_YEAST	FAA1	Long-chain-fatty-acid--CoA ligase 1
sp|P40546|FAF1_YEAST	P40546	FAF1_YEAST	FAF1	Protein FAF1
sp|Q12099|FAL1_YEAST	Q12099	FAL1_YEAST	FAL1	ATP-dependent RNA helicase FAL1
sp|Q05040|FAR8_YEAST	Q05040	FAR8_YEAST	FAR8	Factor arrest protein 8
sp|P07149|FAS1_YEAST	P07149	FAS1_YEAST	FAS1	Fatty acid synthase subunit beta
sp|P19097|FAS2_YEAST	P19097	FAS2_YEAST	FAS2	Fatty acid synthase subunit alpha
sp|P14540|ALF_YEAST	P14540	ALF_YEAST	FBA1	Fructose-bisphosphate aldolase
sp|Q05498|FCF1_YEAST	Q05498	FCF1_YEAST	FCF1	rRNA-processing protein FCF1
sp|Q12035|FCF2_YEAST	Q12035	FCF2_YEAST	FCF2	rRNA-processing protein FCF2
sp|P40988|FET4_YEAST	P40988	FET4_YEAST	FET4	Low-affinity Fe(2+) transport protein
sp|P38631|FKS1_YEAST	P38631	FKS1_YEAST	FKS1	1,3-beta-glucan synthase component FKS1
sp|P51601|GCH1_YEAST	P51601	GCH1_YEAST	FOL2	GTP cyclohydrolase 1
sp|P38911|FKBP3_YEAST	P38911	FKBP3_YEAST	FPR3	Peptidyl-prolyl cis-trans isomerase
sp|Q06205|FKBP4_YEAST	Q06205	FKBP4_YEAST	FPR4	FK506-binding protein 4
sp|P23900|FPS1_YEAST	P23900	FPS1_YEAST	FPS1	Glycerol uptake/efflux facilitator protein
sp|P25659|FUB1_YEAST	P25659	FUB1_YEAST	FUB1	Silencing boundary-establishment protein FUB1
sp|P39730|IF2P_YEAST	P39730	IF2P_YEAST	FUN12	Eukaryotic translation initiation factor 5B
sp|Q04739|GAL83_YEAST	Q04739	GAL83_YEAST	GAL83	SNF1 protein kinase subunit beta-3
sp|P28007|GAR1_YEAST	P28007	GAR1_YEAST	GAR1	H/ACA ribonucleoprotein complex subunit GAR1
sp|P32481|IF2G_YEAST	P32481	IF2G_YEAST	GCD11	Eukaryotic translation initiation factor 2 subunit gamma
sp|P32502|EI2BB_YEAST	P32502	EI2BB_YEAST	GCD7	Translation initiation factor eIF-2B subunit beta
sp|P33892|GCN1_YEAST	P33892	GCN1_YEAST	GCN1	eIF-2-alpha kinase activator GCN1
sp|Q02979|GDE1_YEAST	Q02979	GDE1_YEAST	GDE1	Glycerophosphocholine phosphodiesterase GDE1

sp|P07262|DHE4_YEAST	P07262	DHE4_YEAST	GDH1	NADP-specific glutamate dehydrogenase 1
sp|Q08622|GEP3_YEAST	Q08622	GEP3_YEAST	GEP3	Genetic interactor of prohibitins 3, mitochondrial
sp|P38988|GGC1_YEAST	P38988	GGC1_YEAST	GGC1	Mitochondrial GTP/GDP carrier protein 1
sp|P32598|PP12_YEAST	P32598	PP12_YEAST	GLC7	Serine/threonine-protein phosphatase PP1-2
sp|Q12680|GLT1_YEAST	Q12680	GLT1_YEAST	GLT1	Glutamate synthase [NADH]
sp|P37303|GLY1_YEAST	P37303	GLY1_YEAST	GLY1	Low specificity L-threonine aldolase
sp|P38720|6PGD1_YEAST	P38720	6PGD1_YEAST	GND1	6-phosphogluconate dehydrogenase, decarboxylating 1
sp|P41911|GPD2_YEAST	P41911	GPD2_YEAST	GPD2	Glycerol-3-phosphate dehydrogenase [NAD(+)] 2, mitochondrial
sp|P06738|PHSG_YEAST	P06738	PHSG_YEAST	GPH1	Glycogen phosphorylase
sp|P00950|PMG1_YEAST	P00950	PMG1_YEAST	GPM1	Phosphoglycerate mutase 1
sp|P41277|GPP1_YEAST	P41277	GPP1_YEAST	GPP1	Glycerol-1-phosphate phosphohydrolase 1
sp|Q03835|GLRX3_YEAST	Q03835	GLRX3_YEAST	GRX3	Monothiol glutaredoxin-3
sp|P32642|GLRX4_YEAST	P32642	GLRX4_YEAST	GRX4	Monothiol glutaredoxin-4
sp|P46655|SYEC_YEAST	P46655	SYEC_YEAST	GUS1	Glutamate--tRNA ligase, cytoplasmic
sp|Q03532|HAS1_YEAST	Q03532	HAS1_YEAST	HAS1	ATP-dependent RNA helicase HAS1
sp|P20448|DBP4_YEAST	P20448	DBP4_YEAST	HCA4	ATP-dependent RNA helicase HCA4
sp|Q05775|EIF3J_YEAST	Q05775	EIF3J_YEAST	HCR1	Eukaryotic translation initiation factor 3 subunit J
sp|Q06629|HDA2_YEAST	Q06629	HDA2_YEAST	HDA2	HDA1 complex subunit 2
sp|P32874|HFA1_YEAST	P32874	HFA1_YEAST	HFA1	Acetyl-CoA carboxylase, mitochondrial
sp|P02309|H4_YEAST	P02309	H4_YEAST	HHF1	Histone H4
sp|P53551|H1_YEAST	P53551	H1_YEAST	HHO1	Histone H1
sp|P61830|H3_YEAST	P61830	H3_YEAST	HHT1	Histone H3
sp|P00498|HIS1_YEAST	P00498	HIS1_YEAST	HIS1	ATP phosphoribosyltransferase
sp|P00815|HIS2_YEAST	P00815	HIS2_YEAST	HIS4	Histidine biosynthesis trifunctional protein
sp|P12683|HMDH1_YEAST	P12683	HMDH1_YEAST	HMG1	3-hydroxy-3-methylglutaryl-coenzyme A reductase 1
sp|P13663|DHAS_YEAST	P13663	DHAS_YEAST	HOM2	Aspartate-semialdehyde dehydrogenase
sp|P29295|HRR25_YEAST	P29295	HRR25_YEAST	HRR25	Casein kinase I homolog HRR25
sp|P15108|HSC82_YEAST	P15108	HSC82_YEAST	HSC82	ATP-dependent molecular chaperone HSC82
sp|P15992|HSP26_YEAST	P15992	HSP26_YEAST	HSP26	Heat shock protein 26
sp|P19882|HSP60_YEAST	P19882	HSP60_YEAST	HSP60	Heat shock protein 60, mitochondrial
sp|P02829|HSP82_YEAST	P02829	HSP82_YEAST	HSP82	ATP-dependent molecular chaperone HSP82
sp|P02293|H2B1_YEAST	P02293	H2B1_YEAST	HTB1	Histone H2B.1
sp|Q12692|H2AZ_YEAST	Q12692	H2AZ_YEAST	HTZ1	Histone H2A.Z
sp|P53119|HUL5_YEAST	P53119	HUL5_YEAST	HUL5	E3 ubiquitin-protein ligase HUL5
sp|P32465|HXT1_YEAST	P32465	HXT1_YEAST	HXT1	Low-affinity glucose transporter HXT1
sp|P32466|HXT3_YEAST	P32466	HXT3_YEAST	HXT3	Low-affinity glucose transporter HXT3
sp|P21954|IDHP_YEAST	P21954	IDHP_YEAST	IDP1	Isocitrate dehydrogenase [NADP], mitochondrial
sp|P09436|SYIC_YEAST	P09436	SYIC_YEAST	ILS1	Isoleucine--tRNA ligase, cytoplasmic
sp|P06168|ILV5_YEAST	P06168	ILV5_YEAST	ILV5	Ketol-acid reductoisomerase, mitochondrial
sp|P47170|IML1_YEAST	P47170	IML1_YEAST	IML1	Vacuolar membrane-associated protein IML1
sp|P32899|IMP3_YEAST	P32899	IMP3_YEAST	IMP3	U3 small nucleolar ribonucleoprotein protein IMP3
sp|P53941|IMP4_YEAST	P53941	IMP4_YEAST	IMP4	U3 small nucleolar ribonucleoprotein protein IMP4
sp|P53877|IPI3_YEAST	P53877	IPI3_YEAST	IPI3	Pre-rRNA-processing protein IPI3
sp|Q06683|IRC3_YEAST	Q06683	IRC3_YEAST	IRC3	Putative ATP-dependent helicase IRC3
sp|Q08773|ISW2_YEAST	Q08773	ISW2_YEAST	ISW2	ISWI chromatin-remodeling complex ATPase ISW2
sp|P30605|ITR1_YEAST	P30605	ITR1_YEAST	ITR1	Myo-inositol transporter 1
sp|P38217|IMB2_YEAST	P38217	IMB2_YEAST	KAP104	Importin subunit beta-2
sp|P40069|IMB4_YEAST	P40069	IMB4_YEAST	KAP123	Importin subunit beta-4
sp|P16474|BIP_YEAST	P16474	BIP_YEAST	KAR2	Endoplasmic reticulum chaperone BiP
sp|P50090|KEL2_YEAST	P50090	KEL2_YEAST	KEL2	Kelch repeat-containing protein 2
sp|P38873|KOG1_YEAST	P38873	KOG1_YEAST	KOG1	Target of rapamycin complex 1 subunit KOG1
sp|P53914|NAT10_YEAST	P53914	NAT10_YEAST	KRE33	RNA cytidine acetyltransferase
sp|P42846|KRI1_YEAST	P42846	KRI1_YEAST	KRI1	Protein KRI1
sp|P25586|KRR1_YEAST	P25586	KRR1_YEAST	KRR1	KRR1 small subunit processome component
sp|P15180|SYKC_YEAST	P15180	SYKC_YEAST	KRS1	Lysine--tRNA ligase, cytoplasmic
sp|P38691|KSP1_YEAST	P38691	KSP1_YEAST	KSP1	Serine/threonine-protein kinase KSP1
sp|P38130|KTR3_YEAST	P38130	KTR3_YEAST	KTR3	Probable mannosyltransferase KTR3
sp|Q04377|LCD1_YEAST	Q04377	LCD1_YEAST	LCD1	DNA damage checkpoint protein LCD1
sp|P40079|LCP5_YEAST	P40079	LCP5_YEAST	LCP5	U3 small nucleolar ribonucleoprotein protein LCP5
sp|P38439|LEO1_YEAST	P38439	LEO1_YEAST	LEO1	RNA polymerase-associated protein LEO1
sp|P07264|LEUC_YEAST	P07264	LEUC_YEAST	LEU1	3-isopropylmalate dehydratase
sp|P43586|LOC1_YEAST	P43586	LOC1_YEAST	LOC1	60S ribosomal subunit assembly/export protein LOC1
sp|P53145|LSG1_YEAST	P53145	LSG1_YEAST	LSG1	Large subunit GTPase 1
sp|P20484|MAK11_YEAST	P20484	MAK11_YEAST	MAK11	Protein MAK11
sp|P10962|MAK16_YEAST	P10962	MAK16_YEAST	MAK16	Protein MAK16
sp|Q12176|MAK21_YEAST	Q12176	MAK21_YEAST	MAK21	Ribosome biogenesis protein MAK21
sp|P38112|MAK5_YEAST	P38112	MAK5_YEAST	MAK5	ATP-dependent RNA helicase MAK5
sp|P40513|MAM33_YEAST	P40513	MAM33_YEAST	MAM33	Mitochondrial acidic protein MAM33
sp|P35191|MDJ1_YEAST	P35191	MDJ1_YEAST	MDJ1	DnaJ homolog 1, mitochondrial
sp|P38111|ATR_YEAST	P38111	ATR_YEAST	MEC1	Serine/threonine-protein kinase MEC1
sp|P53128|MTHR2_YEAST	P53128	MTHR2_YEAST	MET13	Methylenetetrahydrofolate reductase 2
sp|P06106|CYSD_YEAST	P06106	CYSD_YEAST	MET17	Homocysteine/cysteine synthase
sp|P05694|METE_YEAST	P05694	METE_YEAST	MET6	5-methyltetrahydropteroyltriglutamate--homocysteine methyltransferase
sp|Q99257|MEX67_YEAST	Q99257	MEX67_YEAST	MEX67	mRNA export factor MEX67
sp|P32787|MG101_YEAST	P32787	MG101_YEAST	MGM101	Mitochondrial genome maintenance protein MGM101
sp|P09440|C1TM_YEAST	P09440	C1TM_YEAST	MIS1	C-1-tetrahydrofolate synthase, mitochondrial
sp|P53141|MLC1_YEAST	P53141	MLC1_YEAST	MLC1	Myosin light chain 1
sp|P46985|MNN11_YEAST	P46985	MNN11_YEAST	MNN11	Probable alpha-1,6-mannosyltransferase MNN11
sp|P39107|MNN9_YEAST	P39107	MNN9_YEAST	MNN9	Mannan polymerase complexes subunit MNN9
sp|P40562|MPH1_YEAST	P40562	MPH1_YEAST	MPH1	ATP-dependent DNA helicase MPH1
sp|P47083|MPP10_YEAST	P47083	MPP10_YEAST	MPP10	U3 small nucleolar RNA-associated protein MPP10
sp|Q06106|MRD1_YEAST	Q06106	MRD1_YEAST	MRD1	Multiple RNA-binding domain-containing protein 1
sp|Q12117|MRH1_YEAST	Q12117	MRH1_YEAST	MRH1	Protein MRH1
sp|Q02204|RM13_YEAST	Q02204	RM13_YEAST	MRPL13	54S ribosomal protein L13, mitochondrial
sp|P36525|RM24_YEAST	P36525	RM24_YEAST	MRPL24	54S ribosomal protein L24, mitochondrial
sp|P33201|MRT4_YEAST	P33201	MRT4_YEAST	MRT4	Ribosome assembly factor MRT4

sp|Q05648|MRX10_YEAST	Q05648	MRX10_YEAST	MRX10	MIOREX complex component 10
sp|Q03079|MRX11_YEAST	Q03079	MRX11_YEAST	MRX11	MIOREX complex component 11
sp|P48564|MRX6_YEAST	P48564	MRX6_YEAST	MRX6	MIOREX complex component 6
sp|P38714|SYRM_YEAST	P38714	SYRM_YEAST	MSR1	Arginine--tRNA ligase, mitochondrial
sp|P15424|MS116_YEAST	P15424	MS116_YEAST	MSS116	ATP-dependent RNA helicase MSS116, mitochondrial
sp|Q03897|WDR59_YEAST	Q03897	WDR59_YEAST	MTC5	Maintenance of telomere capping protein 5
sp|Q03735|NAB6_YEAST	Q03735	NAB6_YEAST	NAB6	RNA-binding protein NAB6
sp|Q02931|UTP17_YEAST	Q02931	UTP17_YEAST	NAN1	NET1-associated nuclear protein 1
sp|P25293|NAP1_YEAST	P25293	NAP1_YEAST	NAP1	Nucleosome assembly protein
sp|P12945|NAT1_YEAST	P12945	NAT1_YEAST	NAT1	N-terminal acetyltransferase A complex subunit NAT1
sp|P40215|NDH1_YEAST	P40215	NDH1_YEAST	NDE1	External NADH-ubiquinone oxidoreductase 1, mitochondrial
sp|Q08972|NEW1_YEAST	Q08972	NEW1_YEAST	NEW1	[NU+] prion formation protein 1
sp|P32495|NHP2_YEAST	P32495	NHP2_YEAST	NHP2	H/ACA ribonucleoprotein complex subunit NHP2
sp|P32497|EIF3C_YEAST	P32497	EIF3C_YEAST	NIP1	Eukaryotic translation initiation factor 3 subunit C
sp|Q08962|NIP7_YEAST	Q08962	NIP7_YEAST	NIP7	60S ribosome subunit biogenesis protein NIP7
sp|P38861|NMD3_YEAST	P38861	NMD3_YEAST	NMD3	60S ribosomal export protein NMD3
sp|Q08444|NOB1_YEAST	Q08444	NOB1_YEAST	NOB1	20S-pre-rRNA D-site endonuclease NOB1
sp|P39744|NOC2_YEAST	P39744	NOC2_YEAST	NOC2	Nucleolar complex protein 2
sp|Q07896|NOC3_YEAST	Q07896	NOC3_YEAST	NOC3	Nucleolar complex-associated protein 3
sp|Q06512|NOC4_YEAST	Q06512	NOC4_YEAST	NOC4	Nucleolar complex protein 4
sp|Q02892|NOG1_YEAST	Q02892	NOG1_YEAST	NOG1	Nucleolar GTP-binding protein 1
sp|P53742|NOG2_YEAST	P53742	NOG2_YEAST	NOG2	Nucleolar GTP-binding protein 2
sp|P15646|FBRL_YEAST	P15646	FBRL_YEAST	NOP1	rRNA 2'-O-methyltransferase fibrillarin
sp|Q08208|NOP12_YEAST	Q08208	NOP12_YEAST	NOP12	Nucleolar protein 12
sp|P53883|NOP13_YEAST	P53883	NOP13_YEAST	NOP13	Nucleolar protein 13
sp|Q99207|NOP14_YEAST	Q99207	NOP14_YEAST	NOP14	Nucleolar complex protein 14
sp|P53927|NOP15_YEAST	P53927	NOP15_YEAST	NOP15	Ribosome biogenesis protein 15
sp|P40991|NOP2_YEAST	P40991	NOP2_YEAST	NOP2	25S rRNA (cytosine(2870)-C(5))-methyltransferase
sp|P37838|NOP4_YEAST	P37838	NOP4_YEAST	NOP4	Nucleolar protein 4
sp|Q12460|NOP56_YEAST	Q12460	NOP56_YEAST	NOP56	Nucleolar protein 56
sp|Q12499|NOP58_YEAST	Q12499	NOP58_YEAST	NOP58	Nucleolar protein 58
sp|Q07623|NOP6_YEAST	Q07623	NOP6_YEAST	NOP6	Nucleolar protein 6
sp|P53261|PESC_YEAST	P53261	PESC_YEAST	NOP7	Pescadillo homolog
sp|P47077|NOP9_YEAST	P47077	NOP9_YEAST	NOP9	Nucleolar protein 9
sp|Q01560|NOP3_YEAST	Q01560	NOP3_YEAST	NPL3	Serine/arginine (SR)-type shuttling mRNA binding protein NPL3
sp|P39923|NPR2_YEAST	P39923	NPR2_YEAST	NPR2	Nitrogen permease regulator 2
sp|P38742|NPR3_YEAST	P38742	NPR3_YEAST	NPR3	Nitrogen permease regulator 3
sp|P53136|NSA1_YEAST	P53136	NSA1_YEAST	NSA1	Ribosome biogenesis protein NSA1
sp|P40078|NSA2_YEAST	P40078	NSA2_YEAST	NSA2	Ribosome biogenesis protein NSA2
sp|P27476|NSR1_YEAST	P27476	NSR1_YEAST	NSR1	Nuclear localization sequence-binding protein
sp|P40354|NTA1_YEAST	P40354	NTA1_YEAST	NTA1	Protein N-terminal amidase
sp|P40010|NUG1_YEAST	P40010	NUG1_YEAST	NUG1	Nuclear GTP-binding protein NUG1
sp|P49687|NU145_YEAST	P49687	NU145_YEAST	NUP145	Nucleoporin NUP145
sp|P32332|OAC1_YEAST	P32332	OAC1_YEAST	OAC1	Mitochondrial oxaloacetate transport protein
sp|P38219|OLA1_YEAST	P38219	OLA1_YEAST	OLA1	Obg-like ATPase 1
sp|P21147|ACO1_YEAST	P21147	ACO1_YEAST	OLE1	Acyl-CoA desaturase 1
sp|P54791|ORC4_YEAST	P54791	ORC4_YEAST	ORC4	Origin recognition complex subunit 4
sp|P04147|PABP_YEAST	P04147	PABP_YEAST	PAB1	Polyadenylate-binding protein, cytoplasmic and nuclear
sp|P38351|PAF1_YEAST	P38351	PAF1_YEAST	PAF1	RNA polymerase II-associated protein 1
sp|P38126|PCH2_YEAST	P38126	PCH2_YEAST	PCH2	Pachytene checkpoint protein 2
sp|P16387|ODPA_YEAST	P16387	ODPA_YEAST	PDA1	Pyruvate dehydrogenase E1 component subunit alpha, mitochondrial
sp|P32473|ODPB_YEAST	P32473	ODPB_YEAST	PDB1	Pyruvate dehydrogenase E1 component subunit beta, mitochondrial
sp|P06169|PDC1_YEAST	P06169	PDC1_YEAST	PDC1	Pyruvate decarboxylase isozyme 1
sp|P17967|PDI_YEAST	P17967	PDI_YEAST	PDI1	Protein disulfide-isomerase
sp|P33302|PDR5_YEAST	P33302	PDR5_YEAST	PDR5	Pleiotropic ABC efflux transporter of multiple drugs
sp|Q04264|PDS5_YEAST	Q04264	PDS5_YEAST	PDS5	Sister chromatid cohesion protein PDS5
sp|P12868|PEP5_YEAST	P12868	PEP5_YEAST	PEP5	E3 ubiquitin-protein ligase PEP5
sp|Q99373|PET20_YEAST	Q99373	PET20_YEAST	PET20	Protein PET20, mitochondrial
sp|P16861|PFKA1_YEAST	P16861	PFKA1_YEAST	PFK1	ATP-dependent 6-phosphofructokinase subunit alpha
sp|P16862|PFKA2_YEAST	P16862	PFKA2_YEAST	PFK2	ATP-dependent 6-phosphofructokinase subunit beta
sp|P40433|6P21_YEAST	P40433	6P21_YEAST	PFK26	6-phosphofructo-2-kinase 1
sp|P00560|PGK_YEAST	P00560	PGK_YEAST	PGK1	Phosphoglycerate kinase
sp|P33401|PGM1_YEAST	P33401	PGM1_YEAST	PGM1	Phosphoglucomutase 1
sp|P46956|PHO86_YEAST	P46956	PHO86_YEAST	PHO86	Inorganic phosphate transporter PHO86
sp|P36775|LONM_YEAST	P36775	LONM_YEAST	PIM1	Lon protease homolog, mitochondrial
sp|P05030|PMA1_YEAST	P05030	PMA1_YEAST	PMA1	Plasma membrane ATPase 1
sp|P38929|ATC2_YEAST	P38929	ATC2_YEAST	PMC1	Calcium-transporting ATPase 2
sp|Q99216|PNO1_YEAST	Q99216	PNO1_YEAST	PNO1	Pre-rRNA-processing protein PNO1
sp|Q04636|POB3_YEAST	Q04636	POB3_YEAST	POB3	FACT complex subunit POB3
sp|P15873|PCNA_YEAST	P15873	PCNA_YEAST	POL30	Proliferating cell nuclear antigen
sp|P39985|DPO5_YEAST	P39985	DPO5_YEAST	POL5	rDNA transcriptional regulator POL5
sp|P04840|VDAC1_YEAST	P04840	VDAC1_YEAST	POR1	Mitochondrial outer membrane protein porin 1
sp|P40478|VDAC2_YEAST	P40478	VDAC2_YEAST	POR2	Mitochondrial outer membrane protein porin 2
sp|P26570|PPZ1_YEAST	P26570	PPZ1_YEAST	PPZ1	Serine/threonine-protein phosphatase PP-Z1
sp|P53131|PRP43_YEAST	P53131	PRP43_YEAST	PRP43	Pre-mRNA-splicing factor ATP-dependent RNA helicase PRP43
sp|P32895|KPR1_YEAST	P32895	KPR1_YEAST	PRS1	Ribose-phosphate pyrophosphokinase 1
sp|P38063|KPR4_YEAST	P38063	KPR4_YEAST	PRS4	Ribose-phosphate pyrophosphokinase 4
sp|P06103|EIF3B_YEAST	P06103	EIF3B_YEAST	PRT1	Eukaryotic translation initiation factor 3 subunit B
sp|P41940|MPG1_YEAST	P41940	MPG1_YEAST	PSA1	Mannose-1-phosphate guanyltransferase
sp|P36081|PSG1_YEAST	P36081	PSG1_YEAST	PSG1	PMA1 stabilization in the Golgi protein 1
sp|Q04373|PUF6_YEAST	Q04373	PUF6_YEAST	PUF6	Pumilio homology domain family member 6
sp|P21304|PWP1_YEAST	P21304	PWP1_YEAST	PWP1	Periodic tryptophan protein 1
sp|P25635|PWP2_YEAST	P25635	PWP2_YEAST	PWP2	Periodic tryptophan protein 2
sp|P11154|PYC1_YEAST	P11154	PYC1_YEAST	PYC1	Pyruvate carboxylase 1
sp|P32628|RAD23_YEAST	P32628	RAD23_YEAST	RAD23	UV excision repair protein RAD23
sp|P32863|RAD54_YEAST	P32863	RAD54_YEAST	RAD54	DNA repair and recombination protein RAD54

sp|P39729|RBG1_YEAST	P39729	RBG1_YEAST	RBG1	Ribosome-interacting GTPase 1
sp|P53721|RCF2_YEAST	P53721	RCF2_YEAST	RCF2	Respiratory supercomplex factor 2, mitochondrial
sp|Q08096|RCL1_YEAST	Q08096	RCL1_YEAST	RCL1	RNA 3'-terminal phosphate cyclase-like protein
sp|Q06709|REH1_YEAST	Q06709	REH1_YEAST	REH1	Cytoplasmic 60S subunit biogenesis factor REH1
sp|P38344|REI1_YEAST	P38344	REI1_YEAST	REI1	Cytoplasmic 60S subunit biogenesis factor REI1
sp|P03871|REP1_YEAST	P03871	REP1_YEAST	REP1	Partitioning protein REP1
sp|P22276|RPC2_YEAST	P22276	RPC2_YEAST	RET1	DNA-directed RNA polymerase III subunit RPC2
sp|P22336|RFA1_YEAST	P22336	RFA1_YEAST	RFA1	Replication factor A protein 1
sp|P38251|RFC5_YEAST	P38251	RFC5_YEAST	RFC5	Replication factor C subunit 5
sp|Q07844|RIX7_YEAST	Q07844	RIX7_YEAST	RIX7	Ribosome biogenesis ATPase RIX7
sp|Q04781|LTN1_YEAST	Q04781	LTN1_YEAST	RKR1	E3 ubiquitin-protein ligase listerin
sp|Q07915|RLP24_YEAST	Q07915	RLP24_YEAST	RLP24	Ribosome biogenesis protein RLP24
sp|P40693|RLP7_YEAST	P40693	RLP7_YEAST	RLP7	Ribosome biogenesis protein RLP7
sp|P11745|RNA1_YEAST	P11745	RNA1_YEAST	RNA1	Ran GTPase-activating protein 1
sp|Q05635|RNH2B_YEAST	Q05635	RNH2B_YEAST	RNH202	Ribonuclease H2 subunit B
sp|P09938|RIR2_YEAST	P09938	RIR2_YEAST	RNR2	Ribonucleoside-diphosphate reductase small chain 1
sp|P45818|ROK1_YEAST	P45818	ROK1_YEAST	ROK1	ATP-dependent RNA helicase ROK1
sp|P22138|RPA2_YEAST	P22138	RPA2_YEAST	RPA135	DNA-directed RNA polymerase I subunit RPA135
sp|P10964|RPA1_YEAST	P10964	RPA1_YEAST	RPA190	DNA-directed RNA polymerase I subunit RPA190
sp|P47006|RPA34_YEAST	P47006	RPA34_YEAST	RPA34	DNA-directed RNA polymerase I subunit RPA34
sp|Q01080|RPA49_YEAST	Q01080	RPA49_YEAST	RPA49	DNA-directed RNA polymerase I subunit RPA49
sp|P08518|RPB2_YEAST	P08518	RPB2_YEAST	RPB2	DNA-directed RNA polymerase II subunit RPB2
sp|P16370|RPB3_YEAST	P16370	RPB3_YEAST	RPB3	DNA-directed RNA polymerase II subunit RPB3
sp|P20433|RPB4_YEAST	P20433	RPB4_YEAST	RPB4	DNA-directed RNA polymerase II subunit RPB4
sp|P20434|RPAB1_YEAST	P20434	RPAB1_YEAST	RPB5	DNA-directed RNA polymerases I, II, and III subunit RPABC1
sp|P27999|RPB9_YEAST	P27999	RPB9_YEAST	RPB9	DNA-directed RNA polymerase II subunit RPB9
sp|P07703|RPAC1_YEAST	P07703	RPAC1_YEAST	RPC40	DNA-directed RNA polymerases I and III subunit RPAC1
sp|P38805|RPF1_YEAST	P38805	RPF1_YEAST	RPF1	Ribosome production factor 1
sp|P36160|RPF2_YEAST	P36160	RPF2_YEAST	RPF2	Ribosome biogenesis protein RPF2
sp|P38249|EIF3A_YEAST	P38249	EIF3A_YEAST	RPG1	Eukaryotic translation initiation factor 3 subunit A
sp|P41805|RL10_YEAST	P41805	RL10_YEAST	RPL10	60S ribosomal protein L10
sp|P0C0W9|RL11A_YEAST	P0C0W9	RL11A_YEAST	RPL11A	60S ribosomal protein L11-A
sp|P0CX53|RL12A_YEAST	P0CX53	RL12A_YEAST	RPL12A	60S ribosomal protein L12-A
sp|P40212|RL13B_YEAST	P40212	RL13B_YEAST	RPL13B	60S ribosomal protein L13-B
sp|P36105|RL14A_YEAST	P36105	RL14A_YEAST	RPL14A	60S ribosomal protein L14-A
sp|P38754|RL14B_YEAST	P38754	RL14B_YEAST	RPL14B	60S ribosomal protein L14-B
sp|P05748|RL15A_YEAST	P05748	RL15A_YEAST	RPL15A	60S ribosomal protein L15-A
sp|P26784|RL16A_YEAST	P26784	RL16A_YEAST	RPL16A	60S ribosomal protein L16-A
sp|P26785|RL16B_YEAST	P26785	RL16B_YEAST	RPL16B	60S ribosomal protein L16-B
sp|P05740|RL17A_YEAST	P05740	RL17A_YEAST	RPL17A	60S ribosomal protein L17-A
sp|P46990|RL17B_YEAST	P46990	RL17B_YEAST	RPL17B	60S ribosomal protein L17-B
sp|P0CX49|RL18A_YEAST	P0CX49	RL18A_YEAST	RPL18A	60S ribosomal protein L18-A
sp|P0CX82|RL19A_YEAST	P0CX82	RL19A_YEAST	RPL19A	60S ribosomal protein L19-A
sp|P0CX43|RL1A_YEAST	P0CX43	RL1A_YEAST	RPL1A	60S ribosomal protein L1-A
sp|P0CX23|RL20A_YEAST	P0CX23	RL20A_YEAST	RPL20A	60S ribosomal protein L20-A
sp|Q02753|RL21A_YEAST	Q02753	RL21A_YEAST	RPL21A	60S ribosomal protein L21-A
sp|Q12672|RL21B_YEAST	Q12672	RL21B_YEAST	RPL21B	60S ribosomal protein L21-B
sp|P05749|RL22A_YEAST	P05749	RL22A_YEAST	RPL22A	60S ribosomal protein L22-A
sp|P0CX41|RL23A_YEAST	P0CX41	RL23A_YEAST	RPL23A	60S ribosomal protein L23-A
sp|P04449|RL24A_YEAST	P04449	RL24A_YEAST	RPL24A	60S ribosomal protein L24-A
sp|P24000|RL24B_YEAST	P24000	RL24B_YEAST	RPL24B	60S ribosomal protein L24-B
sp|P04456|RL25_YEAST	P04456	RL25_YEAST	RPL25	60S ribosomal protein L25
sp|P05743|RL26A_YEAST	P05743	RL26A_YEAST	RPL26A	60S ribosomal protein L26-A
sp|P53221|RL26B_YEAST	P53221	RL26B_YEAST	RPL26B	60S ribosomal protein L26-B
sp|P0C2H6|RL27A_YEAST	P0C2H6	RL27A_YEAST	RPL27A	60S ribosomal protein L27-A
sp|P02406|RL28_YEAST	P02406	RL28_YEAST	RPL28	60S ribosomal protein L28
sp|P05747|RL29_YEAST	P05747	RL29_YEAST	RPL29	60S ribosomal protein L29
sp|P0CX45|RL2A_YEAST	P0CX45	RL2A_YEAST	RPL2A	60S ribosomal protein L2-A
sp|P14126|RL3_YEAST	P14126	RL3_YEAST	RPL3	60S ribosomal protein L3
sp|P14120|RL30_YEAST	P14120	RL30_YEAST	RPL30	60S ribosomal protein L30
sp|P0C2H8|RL31A_YEAST	P0C2H8	RL31A_YEAST	RPL31A	60S ribosomal protein L31-A
sp|P0C2H9|RL31B_YEAST	P0C2H9	RL31B_YEAST	RPL31B	60S ribosomal protein L31-B
sp|P38061|RL32_YEAST	P38061	RL32_YEAST	RPL32	60S ribosomal protein L32
sp|P05744|RL33A_YEAST	P05744	RL33A_YEAST	RPL33A	60S ribosomal protein L33-A
sp|P41056|RL33B_YEAST	P41056	RL33B_YEAST	RPL33B	60S ribosomal protein L33-B
sp|P40525|RL34B_YEAST	P40525	RL34B_YEAST	RPL34B	60S ribosomal protein L34-B
sp|P0CX84|RL35A_YEAST	P0CX84	RL35A_YEAST	RPL35A	60S ribosomal protein L35-A
sp|P05745|RL36A_YEAST	P05745	RL36A_YEAST	RPL36A	60S ribosomal protein L36-A
sp|O14455|RL36B_YEAST	O14455	RL36B_YEAST	RPL36B	60S ribosomal protein L36-B
sp|P49166|RL37A_YEAST	P49166	RL37A_YEAST	RPL37A	60S ribosomal protein L37-A
sp|P51402|RL37B_YEAST	P51402	RL37B_YEAST	RPL37B	60S ribosomal protein L37-B
sp|P49167|RL38_YEAST	P49167	RL38_YEAST	RPL38	60S ribosomal protein L38
sp|P04650|RL39_YEAST	P04650	RL39_YEAST	RPL39	60S ribosomal protein L39
sp|P0CX27|RL44A_YEAST	P0CX27	RL44A_YEAST	RPL42A	60S ribosomal protein L42-A
sp|P0CX25|RL43A_YEAST	P0CX25	RL43A_YEAST	RPL43A	60S ribosomal protein L43-A
sp|P10664|RL4A_YEAST	P10664	RL4A_YEAST	RPL4A	60S ribosomal protein L4-A
sp|P49626|RL4B_YEAST	P49626	RL4B_YEAST	RPL4B	60S ribosomal protein L4-B
sp|P26321|RL5_YEAST	P26321	RL5_YEAST	RPL5	60S ribosomal protein L5
sp|Q02326|RL6A_YEAST	Q02326	RL6A_YEAST	RPL6A	60S ribosomal protein L6-A
sp|P05739|RL6B_YEAST	P05739	RL6B_YEAST	RPL6B	60S ribosomal protein L6-B
sp|P05737|RL7A_YEAST	P05737	RL7A_YEAST	RPL7A	60S ribosomal protein L7-A
sp|Q12213|RL7B_YEAST	Q12213	RL7B_YEAST	RPL7B	60S ribosomal protein L7-B
sp|P17076|RL8A_YEAST	P17076	RL8A_YEAST	RPL8A	60S ribosomal protein L8-A
sp|P29453|RL8B_YEAST	P29453	RL8B_YEAST	RPL8B	60S ribosomal protein L8-B
sp|P05738|RL9A_YEAST	P05738	RL9A_YEAST	RPL9A	60S ribosomal protein L9-A
sp|P04050|RPB1_YEAST	P04050	RPB1_YEAST	RPO21	DNA-directed RNA polymerase II subunit RPB1

sp|P04051|RPC1_YEAST	P04051	RPC1_YEAST	RPO31	DNA-directed RNA polymerase III subunit RPC1
sp|P05317|RLA0_YEAST	P05317	RLA0_YEAST	RPP0	60S acidic ribosomal protein P0
sp|P02400|RLA4_YEAST	P02400	RLA4_YEAST	RPP2B	60S acidic ribosomal protein P2-beta
sp|P32905|RSSA1_YEAST	P32905	RSSA1_YEAST	RPS0A	40S ribosomal protein S0-A
sp|P46654|RSSA2_YEAST	P46654	RSSA2_YEAST	RPS0B	40S ribosomal protein S0-B
sp|P0CX47|RS11A_YEAST	P0CX47	RS11A_YEAST	RPS11A	40S ribosomal protein S11-A
sp|P48589|RS12_YEAST	P48589	RS12_YEAST	RPS12	40S ribosomal protein S12
sp|P05756|RS13_YEAST	P05756	RS13_YEAST	RPS13	40S ribosomal protein S13
sp|P06367|RS14A_YEAST	P06367	RS14A_YEAST	RPS14A	40S ribosomal protein S14-A
sp|Q01855|RS15_YEAST	Q01855	RS15_YEAST	RPS15	40S ribosomal protein S15
sp|P0CX51|RS16A_YEAST	P0CX51	RS16A_YEAST	RPS16A	40S ribosomal protein S16-A
sp|P02407|RS17A_YEAST	P02407	RS17A_YEAST	RPS17A	40S ribosomal protein S17-A
sp|P0CX55|RS18A_YEAST	P0CX55	RS18A_YEAST	RPS18A	40S ribosomal protein S18-A
sp|P07280|RS19A_YEAST	P07280	RS19A_YEAST	RPS19A	40S ribosomal protein S19-A
sp|P33442|RS3A1_YEAST	P33442	RS3A1_YEAST	RPS1A	40S ribosomal protein S1-A
sp|P23248|RS3A2_YEAST	P23248	RS3A2_YEAST	RPS1B	40S ribosomal protein S1-B
sp|P25443|RS2_YEAST	P25443	RS2_YEAST	RPS2	40S ribosomal protein S2
sp|P38701|RS20_YEAST	P38701	RS20_YEAST	RPS20	40S ribosomal protein S20
sp|P0C0V8|RS21A_YEAST	P0C0V8	RS21A_YEAST	RPS21A	40S ribosomal protein S21-A
sp|P0C0W1|RS22A_YEAST	P0C0W1	RS22A_YEAST	RPS22A	40S ribosomal protein S22-A
sp|P0CX29|RS23A_YEAST	P0CX29	RS23A_YEAST	RPS23A	40S ribosomal protein S23-A
sp|P0CX31|RS24A_YEAST	P0CX31	RS24A_YEAST	RPS24A	40S ribosomal protein S24-A
sp|P0C0T4|RS25B_YEAST	P0C0T4	RS25B_YEAST	RPS25B	40S ribosomal protein S25-B
sp|P39938|RS26A_YEAST	P39938	RS26A_YEAST	RPS26A	40S ribosomal protein S26-A
sp|P35997|RS27A_YEAST	P35997	RS27A_YEAST	RPS27A	40S ribosomal protein S27-A
sp|P41057|RS29A_YEAST	P41057	RS29A_YEAST	RPS29A	40S ribosomal protein S29-A
sp|P41058|RS29B_YEAST	P41058	RS29B_YEAST	RPS29B	40S ribosomal protein S29-B
sp|P05750|RS3_YEAST	P05750	RS3_YEAST	RPS3	40S ribosomal protein S3
sp|P0CX33|RS30A_YEAST	P0CX33	RS30A_YEAST	RPS30A	40S ribosomal protein S30-A
sp|P05759|RS31_YEAST	P05759	RS31_YEAST	RPS31	Ubiquitin-40S ribosomal protein S31
sp|P0CX35|RS4A_YEAST	P0CX35	RS4A_YEAST	RPS4A	40S ribosomal protein S4-A
sp|P26783|RS5_YEAST	P26783	RS5_YEAST	RPS5	40S ribosomal protein S5
sp|P0CX37|RS6A_YEAST	P0CX37	RS6A_YEAST	RPS6A	40S ribosomal protein S6-A
sp|P26786|RS7A_YEAST	P26786	RS7A_YEAST	RPS7A	40S ribosomal protein S7-A
sp|P48164|RS7B_YEAST	P48164	RS7B_YEAST	RPS7B	40S ribosomal protein S7-B
sp|P0CX39|RS8A_YEAST	P0CX39	RS8A_YEAST	RPS8A	40S ribosomal protein S8-A
sp|O13516|RS9A_YEAST	O13516	RS9A_YEAST	RPS9A	40S ribosomal protein S9-A
sp|Q12532|RQC2_YEAST	Q12532	RQC2_YEAST	RQC2	Ribosome quality control complex subunit 2
sp|Q04225|RRB1_YEAST	Q04225	RRB1_YEAST	RRB1	Ribosome assembly protein RRB1
sp|P35178|RRP1_YEAST	P35178	RRP1_YEAST	RRP1	Ribosomal RNA-processing protein 1
sp|Q12754|RRP12_YEAST	Q12754	RRP12_YEAST	RRP12	Ribosomal RNA-processing protein 12
sp|Q06511|RRP15_YEAST	Q06511	RRP15_YEAST	RRP15	Ribosomal RNA-processing protein 15
sp|P38712|RRP3_YEAST	P38712	RRP3_YEAST	RRP3	ATP-dependent rRNA helicase RRP3
sp|Q05022|RRP5_YEAST	Q05022	RRP5_YEAST	RRP5	rRNA biogenesis protein RRP5
sp|P25368|RRP7_YEAST	P25368	RRP7_YEAST	RRP7	Ribosomal RNA-processing protein 7
sp|P38961|RRP8_YEAST	P38961	RRP8_YEAST	RRP8	25S rRNA (adenine(645)-N(1))-methyltransferase
sp|Q06506|RRP9_YEAST	Q06506	RRP9_YEAST	RRP9	Ribosomal RNA-processing protein 9
sp|P40470|RRT14_YEAST	P40470	RRT14_YEAST	RRT14	Regulator of rDNA transcription protein 14
sp|Q03430|RSM28_YEAST	Q03430	RSM28_YEAST	RSM28	37S ribosomal protein RSM28, mitochondrial
sp|Q08281|RTC1_YEAST	Q08281	RTC1_YEAST	RTC1	Restriction of telomere capping protein 1
sp|P53064|RTF1_YEAST	P53064	RTF1_YEAST	RTF1	RNA polymerase-associated protein RTF1
sp|Q03940|RUVB1_YEAST	Q03940	RUVB1_YEAST	RVB1	RuvB-like protein 1
sp|Q12464|RUVB2_YEAST	Q12464	RUVB2_YEAST	RVB2	RuvB-like protein 2
sp|P39954|SAHH_YEAST	P39954	SAHH_YEAST	SAH1	Adenosylhomocysteinase
sp|P10659|METK1_YEAST	P10659	METK1_YEAST	SAM1	S-adenosylmethionine synthase 1
sp|P19358|METK2_YEAST	P19358	METK2_YEAST	SAM2	S-adenosylmethionine synthase 2
sp|Q12136|SAS10_YEAST	Q12136	SAS10_YEAST	SAS10	Something about silencing protein 10
sp|P10080|SSBP1_YEAST	P10080	SSBP1_YEAST	SBP1	Single-stranded nucleic acid-binding protein
sp|P06105|SC160_YEAST	P06105	SC160_YEAST	SCP160	Protein SCP160
sp|P38164|SEA4_YEAST	P38164	SEA4_YEAST	SEA4	SEH-associated protein 4
sp|Q04491|SEC13_YEAST	Q04491	SEC13_YEAST	SEC13	Protein transport protein SEC13
sp|P18759|SEC18_YEAST	P18759	SEC18_YEAST	SEC18	Vesicular-fusion protein SEC18
sp|P15303|SEC23_YEAST	P15303	SEC23_YEAST	SEC23	Protein transport protein SEC23
sp|P41811|COPB2_YEAST	P41811	COPB2_YEAST	SEC27	Coatomer subunit beta'
sp|Q01590|SED5_YEAST	Q01590	SED5_YEAST	SED5	Integral membrane protein SED5
sp|P53011|SEH1_YEAST	P53011	SEH1_YEAST	SEH1	Nucleoporin SEH1
sp|Q00416|SEN1_YEAST	Q00416	SEN1_YEAST	SEN1	Helicase SEN1
sp|P40054|SERA_YEAST	P40054	SERA_YEAST	SER3	D-3-phosphoglycerate dehydrogenase 1
sp|Q06132|SGD1_YEAST	Q06132	SGD1_YEAST	SGD1	Suppressor of glycerol defect protein 1
sp|P37292|GLYM_YEAST	P37292	GLYM_YEAST	SHM1	Serine hydroxymethyltransferase, mitochondrial
sp|P25294|SIS1_YEAST	P25294	SIS1_YEAST	SIS1	Protein SIS1
sp|P33333|PLSC_YEAST	P33333	PLSC_YEAST	SLC1	1-acyl-sn-glycerol-3-phosphate acyltransferase
sp|Q12232|SLP1_YEAST	Q12232	SLP1_YEAST	SLP1	Uncharacterized protein SLP1
sp|P32908|SMC1_YEAST	P32908	SMC1_YEAST	SMC1	Structural maintenance of chromosomes protein 1
sp|P06782|SNF1_YEAST	P06782	SNF1_YEAST	SNF1	Carbon catabolite-derepressing protein kinase
sp|P12904|AAKG_YEAST	P12904	AAKG_YEAST	SNF4	5'-AMP-activated protein kinase subunit gamma
sp|P32568|SNQ2_YEAST	P32568	SNQ2_YEAST	SNQ2	Protein SNQ2
sp|P39990|SNU13_YEAST	P39990	SNU13_YEAST	SNU13	13 kDa ribonucleoprotein-associated protein
sp|P47057|SNX4_YEAST	P47057	SNX4_YEAST	SNX4	Sorting nexin-4
sp|P33750|DCA13_YEAST	P33750	DCA13_YEAST	SOF1	Protein SOF1
sp|P25808|SPB4_YEAST	P25808	SPB4_YEAST	SPB4	ATP-dependent rRNA helicase SPB4
sp|P32558|SPT16_YEAST	P32558	SPT16_YEAST	SPT16	FACT complex subunit SPT16
sp|P32914|SPT4_YEAST	P32914	SPT4_YEAST	SPT4	Transcription elongation factor SPT4
sp|P27692|SPT5_YEAST	P27692	SPT5_YEAST	SPT5	Transcription elongation factor SPT5
sp|P23615|SPT6_YEAST	P23615	SPT6_YEAST	SPT6	Transcription elongation factor SPT6
sp|P35177|SPT7_YEAST	P35177	SPT7_YEAST	SPT7	Transcriptional activator SPT7

sp|Q02821|IMA1_YEAST	Q02821	IMA1_YEAST	SRP1	Importin subunit alpha
sp|P38688|SRP72_YEAST	P38688	SRP72_YEAST	SRP72	Signal recognition particle subunit SRP72
sp|P17555|CAP_YEAST	P17555	CAP_YEAST	SRV2	Adenylyl cyclase-associated protein
sp|P10591|HSP71_YEAST	P10591	HSP71_YEAST	SSA1	Heat shock protein SSA1
sp|P10592|HSP72_YEAST	P10592	HSP72_YEAST	SSA2	Heat shock protein SSA2
sp|P09435|HSP73_YEAST	P09435	HSP73_YEAST	SSA3	Heat shock protein SSA3
sp|P11484|SSB1_YEAST	P11484	SSB1_YEAST	SSB1	Ribosome-associated molecular chaperone SSB1
sp|P32589|HSP7F_YEAST	P32589	HSP7F_YEAST	SSE1	Heat shock protein homolog SSE1
sp|P53599|SSK2_YEAST	P53599	SSK2_YEAST	SSK2	MAP kinase kinase kinase SSK2
sp|P38788|SSZ1_YEAST	P38788	SSZ1_YEAST	SSZ1	Ribosome-associated complex subunit SSZ1
sp|Q03497|STE20_YEAST	Q03497	STE20_YEAST	STE20	Serine/threonine-protein kinase STE20
sp|P39015|STM1_YEAST	P39015	STM1_YEAST	STM1	Suppressor protein STM1
sp|Q07478|SUB2_YEAST	Q07478	SUB2_YEAST	SUB2	ATP-dependent RNA helicase SUB2
sp|P20459|IF2A_YEAST	P20459	IF2A_YEAST	SUI2	Eukaryotic translation initiation factor 2 subunit alpha
sp|P09064|IF2B_YEAST	P09064	IF2B_YEAST	SUI3	Eukaryotic translation initiation factor 2 subunit beta
sp|P12385|ERF1_YEAST	P12385	ERF1_YEAST	SUP45	Eukaryotic peptide chain release factor subunit 1
sp|P43554|SWP82_YEAST	P43554	SWP82_YEAST	SWP82	SWI/SNF global transcription activator complex subunit SWP82
sp|P31377|STX8_YEAST	P31377	STX8_YEAST	SYN8	Syntaxin-8
sp|P48231|TCB2_YEAST	P48231	TCB2_YEAST	TCB2	Tricalbin-2
sp|Q03640|TCB3_YEAST	Q03640	TCB3_YEAST	TCB3	Tricalbin-3
sp|P12612|TCPA_YEAST	P12612	TCPA_YEAST	TCP1	T-complex protein 1 subunit alpha
sp|P00360|G3P1_YEAST	P00360	G3P1_YEAST	TDH1	Glyceraldehyde-3-phosphate dehydrogenase 1
sp|P00358|G3P2_YEAST	P00358	G3P2_YEAST	TDH2	Glyceraldehyde-3-phosphate dehydrogenase 2
sp|P00359|G3P3_YEAST	P00359	G3P3_YEAST	TDH3	Glyceraldehyde-3-phosphate dehydrogenase 3
sp|P02994|EF1A_YEAST	P02994	EF1A_YEAST	TEF1	Elongation factor 1-alpha
sp|P36008|EF1G2_YEAST	P36008	EF1G2_YEAST	TEF4	Elongation factor 1-gamma 2
sp|P04801|SYTC_YEAST	P04801	SYTC_YEAST	THS1	Threonine--tRNA ligase, cytoplasmic
sp|P10081|IF4A_YEAST	P10081	IF4A_YEAST	TIF1	ATP-dependent RNA helicase eIF4A
sp|P38912|IF1A_YEAST	P38912	IF1A_YEAST	TIF11	Eukaryotic translation initiation factor 1A
sp|P40217|EIF3I_YEAST	P40217	EIF3I_YEAST	TIF34	Eukaryotic translation initiation factor 3 subunit I
sp|Q04067|EIF3G_YEAST	Q04067	EIF3G_YEAST	TIF35	Eukaryotic translation initiation factor 3 subunit G
sp|P38431|IF5_YEAST	P38431	IF5_YEAST	TIF5	Eukaryotic translation initiation factor 5
sp|Q12522|IF6_YEAST	Q12522	IF6_YEAST	TIF6	Eukaryotic translation initiation factor 6
sp|Q08687|TMA16_YEAST	Q08687	TMA16_YEAST	TMA16	Translation machinery-associated protein 16
sp|P35691|TCTP_YEAST	P35691	TCTP_YEAST	TMA19	Translationally-controlled tumor protein homolog
sp|Q12000|TMA46_YEAST	Q12000	TMA46_YEAST	TMA46	Translation machinery-associated protein 46
sp|P04786|TOP1_YEAST	P04786	TOP1_YEAST	TOP1	DNA topoisomerase 1
sp|P35169|TOR1_YEAST	P35169	TOR1_YEAST	TOR1	Serine/threonine-protein kinase TOR1
sp|P00942|TPIS_YEAST	P00942	TPIS_YEAST	TPI1	Triosephosphate isomerase
sp|P53283|TPO2_YEAST	P53283	TPO2_YEAST	TPO2	Polyamine transporter 2
sp|P38811|TRA1_YEAST	P38811	TRA1_YEAST	TRA1	Transcription-associated protein 1
sp|P00899|TRPE_YEAST	P00899	TRPE_YEAST	TRP2	Anthranilate synthase component 1
sp|P00937|TRPG_YEAST	P00937	TRPG_YEAST	TRP3	Multifunctional tryptophan biosynthesis protein
sp|P00931|TRP_YEAST	P00931	TRP_YEAST	TRP5	Tryptophan synthase
sp|P34760|TSA1_YEAST	P34760	TSA1_YEAST	TSA1	Peroxiredoxin TSA1
sp|Q99190|TECR_YEAST	Q99190	TECR_YEAST	TSC13	Very-long-chain enoyl-CoA reductase
sp|Q07381|TSR1_YEAST	Q07381	TSR1_YEAST	TSR1	Ribosome biogenesis protein TSR1
sp|P02557|TBB_YEAST	P02557	TBB_YEAST	TUB2	Tubulin beta chain
sp|O13527|YA11B_YEAST	O13527	YA11B_YEAST	TY1B-A	Truncated transposon Ty1-A Gag-Pol polyprotein
sp|O13535|YH11B_YEAST	O13535	YH11B_YEAST	TY1B-H	Transposon Ty1-H Gag-Pol polyprotein
sp|P38820|UBA4_YEAST	P38820	UBA4_YEAST	UBA4	Adenylyltransferase and sulfurtransferase UBA4
sp|P43593|UBP6_YEAST	P43593	UBP6_YEAST	UBP6	Ubiquitin carboxyl-terminal hydrolase 6
sp|Q03327|UGO1_YEAST	Q03327	UGO1_YEAST	UGO1	Mitochondrial fusion and transport protein UGO1
sp|P07259|PYR1_YEAST	P07259	PYR1_YEAST	URA2	Protein URA2
sp|P47108|URB2_YEAST	P47108	URB2_YEAST	URB2	Nucleolar pre-ribosomal-associated protein 2
sp|P42945|UTP10_YEAST	P42945	UTP10_YEAST	UTP10	U3 small nucleolar RNA-associated protein 10
sp|P34247|UTP11_YEAST	P34247	UTP11_YEAST	UTP11	U3 small nucleolar RNA-associated protein 11
sp|Q05946|UTP13_YEAST	Q05946	UTP13_YEAST	UTP13	U3 small nucleolar RNA-associated protein 13
sp|Q04500|UTP14_YEAST	Q04500	UTP14_YEAST	UTP14	U3 small nucleolar RNA-associated protein 14
sp|Q04305|UTP15_YEAST	Q04305	UTP15_YEAST	UTP15	U3 small nucleolar RNA-associated protein 15
sp|P40362|UTP18_YEAST	P40362	UTP18_YEAST	UTP18	U3 small nucleolar RNA-associated protein 18
sp|P35194|UTP20_YEAST	P35194	UTP20_YEAST	UTP20	U3 small nucleolar RNA-associated protein 20
sp|Q06078|UTP21_YEAST	Q06078	UTP21_YEAST	UTP21	U3 small nucleolar RNA-associated protein 21
sp|P53254|UTP22_YEAST	P53254	UTP22_YEAST	UTP22	U3 small nucleolar RNA-associated protein 22
sp|P36144|RL1D1_YEAST	P36144	RL1D1_YEAST	UTP30	Ribosome biogenesis protein UTP30
sp|Q06679|UTP4_YEAST	Q06679	UTP4_YEAST	UTP4	U3 small nucleolar RNA-associated protein 4
sp|Q04177|UTP5_YEAST	Q04177	UTP5_YEAST	UTP5	U3 small nucleolar RNA-associated protein 5
sp|Q02354|UTP6_YEAST	Q02354	UTP6_YEAST	UTP6	U3 small nucleolar RNA-associated protein 6
sp|P40055|UTP7_YEAST	P40055	UTP7_YEAST	UTP7	U3 small nucleolar RNA-associated protein 7
sp|P53276|UTP8_YEAST	P53276	UTP8_YEAST	UTP8	U3 small nucleolar RNA-associated protein 8
sp|P38882|UTP9_YEAST	P38882	UTP9_YEAST	UTP9	U3 small nucleolar RNA-associated protein 9
sp|P07806|SYV_YEAST	P07806	SYV_YEAST	VAS1	Valine--tRNA ligase, mitochondrial
sp|P17255|VATA_YEAST	P17255	VATA_YEAST	VMA1	V-type proton ATPase catalytic subunit A
sp|P32842|VATL2_YEAST	P32842	VATL2_YEAST	VMA11	V-type proton ATPase subunit c'
sp|P16140|VATB_YEAST	P16140	VATB_YEAST	VMA2	V-type proton ATPase subunit B
sp|P32563|VPP1_YEAST	P32563	VPP1_YEAST	VPH1	V-type proton ATPase subunit a, vacuolar isoform
sp|P21576|VPS1_YEAST	P21576	VPS1_YEAST	VPS1	Vacuolar protein sorting-associated protein 1
sp|Q07878|VPS13_YEAST	Q07878	VPS13_YEAST	VPS13	Intermembrane lipid transfer protein VPS13
sp|Q03944|VPS64_YEAST	Q03944	VPS64_YEAST	VPS64	Vacuolar protein sorting-associated protein 64
sp|P33767|OSTB_YEAST	P33767	OSTB_YEAST	WBP1	Dolichyl-diphosphooligosaccharide--protein glycosyltransferase subunit WBP1
sp|P38202|YBC8_YEAST	P38202	YBC8_YEAST	YBL028C	UPF0642 protein YBL028C
sp|P25491|MAS5_YEAST	P25491	MAS5_YEAST	YDJ1	Mitochondrial protein import protein MAS5
sp|Q05506|SYRC_YEAST	Q05506	SYRC_YEAST	YDR341C	Arginine--tRNA ligase, cytoplasmic
sp|P16521|EF3A_YEAST	P16521	EF3A_YEAST	YEF3	Elongation factor 3A
sp|P53156|YGI1_YEAST	P53156	YGI1_YEAST	YGL081W	Uncharacterized protein YGL081W
sp|P38616|YGP1_YEAST	P38616	YGP1_YEAST	YGP1	Protein YGP1

sp|P53278|YG3A_YEAST	P53278	YG3A_YEAST	YGR130C	Uncharacterized protein YGR130C
sp|P39676|FHP_YEAST	P39676	FHP_YEAST	YHB1	Flavohemoprotein
sp|P38708|YHI0_YEAST	P38708	YHI0_YEAST	YHR020W	Putative proline--tRNA ligase YHR020W
sp|P36015|YKT6_YEAST	P36015	YKT6_YEAST	YKT6	Synaptobrevin homolog YKT6
sp|Q03559|YM8V_YEAST	Q03559	YM8V_YEAST	YMR295C	Uncharacterized protein YMR295C
sp|P53723|YN8B_YEAST	P53723	YN8B_YEAST	YNR021W	UPF0674 endoplasmic reticulum membrane protein YNR021W
sp|Q12010|YPQ1_YEAST	Q12010	YPQ1_YEAST	YPQ1	Probable vacuolar amino acid transporter YPQ1
sp|Q12159|YRA1_YEAST	Q12159	YRA1_YEAST	YRA1	RNA annealing protein YRA1
sp|P38079|YRO2_YEAST	P38079	YRO2_YEAST	YRO2	Protein YRO2
sp|P40341|YTA12_YEAST	P40341	YTA12_YEAST	YTA12	Mitochondrial respiratory chain complexes assembly protein YTA12
sp|Q12024|YTM1_YEAST	Q12024	YTM1_YEAST	YTM1	Ribosome biogenesis protein YTM1
sp|Q02256|PVH1_YEAST	Q02256	PVH1_YEAST	YVH1	Tyrosine-protein phosphatase YVH1
sp|P32804|ZRT1_YEAST	P32804	ZRT1_YEAST	ZRT1	Zinc-regulated transporter 1
sp|P32527|ZUO1_YEAST	P32527	ZUO1_YEAST	ZUO1	Zuotin